Methods for Stability and Noise Analysis of Coupled Oscillating Systems

Djurhuus, Torsten

Publication date:
2008

Document Version
Early version, also known as pre-print

Methods for Stability and Noise Analysis of Coupled Oscillating Systems.

Torsten Djurhuus

September 28, 2007

Contents

Introduction **6**

1 Basic Theory **13**
1.1 Equivalence Theory 13
1.1.1 Single Oscillators - The Andronov-Hopf Normal-Form 14
1.1.2 Coupled Oscillators - The Synchronized State 23
1.2 Averaging Theory 28
1.3 Symmetry Considerations 31

2 Single Oscillators Perturbed by White Noise - Inhomogeneous Phase Diffusion **36**
2.1 A Linear Response Theory for Noise Forced Limit Cycle Solutions 37
2.1.1 Deriving the Oscillator Phase Stochastic Differential Equation . . . 38
2.1.2 Deriving the Oscillator Phase Asymptotic Statistics - the Fokker-Planck Equation 43
2.1.3 Calculating the Oscillator Spectrum 46
2.1.4 An Alternative Model of the Asymptotic Phase Statistics of a Free-Running Oscillator. 48
2.2 Review of 3 Popular Oscillator Phase Noise Methodologies 50
2.2.1 Demir's Phase Macro Model 52
2.2.2 Hajimiri's Impulse Sensitivity Function 54
2.2.3 Kurokawa's Model - Harmonic Oscillators 54

3 A Phase Macro Model for Coupled Oscillator Systems **57**
3.1 The General Model Formulation 59
3.2 A Phase Macro Model for the Sub-Harmonic Injection Locked Oscillator (S-ILO) 63
3.2.1 Deriving the Torus Projection Operators for the S-ILO 64
3.2.2 The Stochastic Differential Equations 69
3.2.3 Characterizing the Self-Referenced S-OSC Phase 71
3.2.4 The Spectrum of a Noise Perturbed Injection locked oscillator . . . 73
3.2.5 Verification of the Developed Model 76

4 n Unilaterally Ring-Coupled Harmonic Oscillators Perturbed by White Noise **80**
4.1 Modes of n Unidirectional Ring Coupled Identical Harmonic Oscillators . 82
4.1.1 Ashwins's Symmetry Approach 82
4.1.2 Rogge's Method 85
4.1.3 Discussion 88
4.2 Practical Applications of the Unidirectional Ring 89

4.3 A Quasi-Sinusoidal Model of the Unilateral Ring 90
4.4 Linear Start-Up and Stability Analysis 95
4.4.1 Linear Stability of In-Phase Mode for the Unidirectional Ring with $\beta = 0$ 99
4.4.2 n=2, $\beta = \pi$: The Cross Coupled Quadrature Oscillator 100
4.5 Linear Response Noise Analysis - Coupling Induced AM to PM Noise Conversion 103
4.5.1 Deriving the Dynamics of the Diagonal Flow 105
4.5.2 Calculating $\bar{D}_{\phi\phi}$ (Method #1) : Rotating the Averaged Phase Equation 107
4.5.3 Calculating $\bar{D}_{\phi\phi}$ (Method #2) : A PLTV Impulse Response Characterization 108
4.5.4 Calculating $\bar{D}_{\phi\phi}$ (Method #3) : the Stochastic Integration Approach 110
4.6 A new Definition of Oscillator Q 113
4.7 The Cross-Coupled Harmonic Quadrature Oscillator 113
4.7.1 Deriving the CCQO Amplitude/Phase Equations 114
4.7.2 Asymmetry Considerations 116
4.7.3 Linear Response Noise Analysis 120

Conclusion **126**

A The Noise Appendix : Narrow-band Noise / Stochastic Integration / The Fokker-Planck Equation **130**
A.1 Narowband Noise 131
A.1.1 The Noise Admittance $Y_n = G_n + jB_n$ 134
A.1.2 A Pulse Train Noise Model 135
A.2 Stochastic Integration 137
A.3 The Fokker-Planck Equation 140

B Deriving the Averaged Stochastic Differential Equations for a General Class of Second Order Oscillators **142**
B.1 A van der Pol Oscillator with a Varactor 143
B.1.1 A Phasor Approach 146

C Various Derivations **148**
C.1 Section 1.1.1 : Normal-Form Calculations 148
C.2 Calculating the Eigenvalues of the Matrix J_{11} on page 98 150
C.3 Calculating the Eigenvalues of the Matrix J_{22} on page 99 151
C.4 Calculations Used in the Proof of Theorem 3.3 on page 68 153
C.5 The ILO Monodromy Matrix 156
C.6 Computing the Spectrum of the Noise Perturbed ILO 158

D Floquet Theory **159**
D.1 Deriving the Monodromy Matrix $\Phi(2\pi, 0)$ 163

Abstract

In this thesis a study of analytical and numerical models of coupled oscillating systems, perturbed by delta-correlated noise sources, is undertaken. These models are important for the attainment of a qualitative understanding of the complex dynamics seen in various physical, biological, electronic systems and for the derivation of fast and computationally efficient CAD routines. The text concentrates on developing models for coupled electronic oscillators. These circuit blocks find use in RF/microwave and optical communication systems as coherent multi-phase signal generators, power combiners and phase-noise filters; to name but a few of the possible applications areas.

Taking outset in the established single-oscillator phase-macro model, a novel numerical algorithm for the automated phase-noise characterization of coupled oscillators, perturbed by noise, is developed. The algorithm, which is based on stochastic integration and Floquet theory and is independent of circuit topology and parameters, proceeds by deriving the invariant manifold projection operators. This formulation is easily integrated into commercial CAD environments, such as SPICE™ and SPECTRE™. The algorithm improves the computational efficiency, compared to brute-force Monte-Carlo techniques, by several orders of magnitude.

Unilateral ring-coupled oscillators have proven a reliable and power efficient way to create coherent multi-phase signal generators in the RF/microwave frequency range. A complete and self-contained study of this complex multi-mode system is undertaken. The developed model explains the existence of a so-called dominant mode, ensuring a consistent signal phase pattern following start-up. A linear response model is derived to investigate linear stability and noise properties. It is shown that a linear coupling transconductor will cancel the coupling induced noise contribution in the single-side band phase-noise spectrum. This phenomena was not discussed in any of the previous publications considering this circuit. The model gives a general insight into the qualitative properties of unilateral ring-coupled oscillators, perturbed by white noise.

Resumé

I denne afhandling vil der blive udført et studie af mulige analytiske og numeriske modeller af koblede oscillerende systemer. Disse modeller er vigtige med henblik på at opnå et kvalitativt overblik, *mht.* den komplekse dynamik der observeres i diverse fysiske, biologiske, elektroniske systemer og for udviklingen af hurtige, beregnings-effektive simulerings-routiner. Teksten koncentrerer sig om modellering af elektroniske koblede systemer. Disse kredsløbs-blokke finder anvendelse i RF/mikrobølge og optiske kommunikations systemer som multi-fase signal-kilder, power combiners og fase-støjs filtre; for bare at nævne nogle få eksempler.

Med udgangspunkt i den allerede eksisterende enkelt-oscillator phase-macro model vil der blive udviklet en ny algoritme med henblik på at finde en automatiseret, topologi og parameter uafhængig fase-støjs beskrivelse af koblede oscillatorer. Denne algoritme, som bygger på stokastisk integration og Floquet teori, er baseret på udledningen af ortogonale projektions operatorer, der afbilder støj-responsen ned på den invariante manifold. På denne form er algoritmen meget velegnet til at blive integreret i kommercielle kredsløbs simulations-platforme, så som SPICE™ og SPECTRE™. Algoritmen er flere størrelsesordner hurtigere *ift.* en simple Monte-Carlo fremgangsmåde.

Unilateral ring-kobling af oscillatorer har vist sig at være en pålidlig og effektiv måde at frembringe multi-fase signaler i RF/mikrobølge frekvens-området. Et komplet studie af dette komplekse multi-mode system vil blive udført. Den udviklede model forklarer eksistensen af en såkaldt dominant mode, der sikre at et konsistent fase-mønster altid følger efter opstart. En linear respons model er udviklet med henblik på at undersøge linær stabillitet og støj egenskaber. Det vil blive vist, hvordan linær kobling vil resultere i, at det ekstra koblings inducerede bidrag til enkelt-sidebånd fase-støj spektrumet vil blive fjernet. Dette fænomen er ikke nævnt i nogle af de tidligere publikationer på dette felt. Den udviklede model giver et generelt indblik i de kvalitative støj-egenskaber af unilateralle ring-koblede oscillatorer.

Preface

This PhD study was carried out from 01/07/2004 to 30/09/2007 at the section of Electromagnetic systems (EMI)/ElectroScience (ES), Ørsted•DTU, Technical University of Denmark. The effective study period was 39 months, including a 3 months extension. The financial support for this PhD study was provided by EMI-Ørsted•DTU internal funding. Professor Viktor Krozer was supervisor for the project together with co-supervisor Associate Professor Jens Vidkjær.

Acknowledgements

I would first of all like to thank Professor Viktor Krozer, Associate Professor Jens Vidkjær and Professor Erik Lintz Christensen. I am grateful for all their help, support and advice.

I should also like to thank Assistant Professor Tom Keinicke Johansen for many interesting conversations and for taking the time to teach me about transistor modelling.

During the past three years I have been working together with Viktor, Jens and Tom and I have benefitted from their significant experience in the field of nonlinear dynamics and RF/microwave oscillator design. I would like to thank them for always finding time to discuss oscillator theory with me and for their many suggestions during our discussions.

I would also like to thank the whole Microwave group at Oersted•DTU and especially PhD students Dzenan Hadziabdic and Chenhui Jiang.

Technical University of Denmark
Kgs. Lyngby, September 28, 2007

Introduction

The physical phenomena of synchronization, also known as frequency locking or just locking [1], was discovered by Dutch scientist Christian Huygens in the year 1665. Huygens was onboard a ship, conducting longitude measurement [2] sea-trials of the pendulum-clocks which he had invented, when he fell sick. From his sick-bed he had plenty of time to observe two pendulum clocks suspended from a wooden beam in the room in which he lay. The two clocks seemed to always swing in tune and always with a 180^o phase difference between the swings, also known as *anti-phase* swing. Even if prepared in an arbitrary asymmetric initial state, (*i.e.* different swing period and initial phase), the system would return to this equilibrium state after a short transient interval. Huygens surmised that the two clocks interacted though the wooden beam, onto which they were both attached, even though this interaction was imperceptible! This discovery was, to say the least, revolutionary; a model explaining how such a weak, almost non-existing, cause could provoke this clearly visible effect would escape science for more than two centuries. Even to this day, this concept probably seems very strange to many people. It is not impossible to imagine a person, without a scientific background, who, when confronted with a scenario whereby two mechanical systems seem to communicate with each-other through some invisible channel, would suggest some-kind of magic trick.

Although it is claimed that the Huygens's problem was only recently solved by Kurt Wiesenfeld and his co-workers [2], a mathematical model explaining the qualitative traits of oscillator synchronization has been around for some time. The branch of applied mathematics, known as dynamical systems theory, was pioneered by people like Jules Henri Poincaré who in the late part of the 19'th century worked on solving different problems in celestial mechanics. This framework was then developed throughout the 20'th century and, with the introduction of chaos theory in the early 1960's, remains a very active area of research to this day. The theory explains how some systems are situated on a border-line in parameter-space where any small persistent perturbation leads to a so-called *bifurcation*; a term used to describe a qualitative, sometimes dramatic, change in the dynamics. The canonical model of an oscillator is a rotation in the complex plane

[1] in this report we shall sometimes refer to synchronization as just *locking* which is then used in sentences like : "the two systems are locked ...". This syntax is not strictly correct since locking can refer to both *phase locking* and *frequency locking*. However, in this report we only consider frequency locking thus, hopefully, removing any confusion.

[2] at the time when Huygens lived there did not exist an exact method of sea navigation; something which prevented safe long distance travel and resulted in many lost lives due to shipwrecks. While the latitude was relatively easy to determine from measurements of the pole star elevation, the only real way of determining longitude was by a procedure known as *dead reckoning*; which was highly unreliable. It had long been known that the longitude could be calculated by reading the time off a very reliable clock. Say you started out in London at noon, then by measuring the time at noon locally (*i.e.* the time when the sun is highest in the sky) the clock would always tell you how far away from London noon you were. If *e.g.* the clock read midnight, then you would know that you were half way around the earth. Several prominent scientist like Huygens and Newton had a go at solving this problem which was considered one of the most important of its time. It was solved by English clockmaker John Harrison around 1761 [1].

where the oscillator state is referenced by an amplitude and a phase. While the amplitude is a stable state variable, corresponding to a negative Floquet characteristic exponent, the oscillator phase is by definition a so-called neutrally stable variable. By this we take to mean that the phase will follow any perturbation passively; that is, without reacting to it. Neutrally stable variables are special since they lie on the above mentioned bifurcation borders and are hence susceptible to the slightest changes in the environment caused by external influences. Considering a scenario whereby two oscillators are bilaterally [3] coupled; for zero coupling the two sub-systems swing with different periods/frequency and hence also without any specific phase relation. As we now introduce a small coupling, the neutrally stable phase variables bifurcate in a so-called *saddle-node bifurcation* creating a new synchronized system where the two oscillators/clocks move with a common rhythm. Actually, two new solutions, also called *modes*, are created, the *anti-phase* and the *in-phase* modes, however, baring some-kind of multi-mode oscillation, only one of these will survive. Although the bilaterally coupled oscillators may seem to behave in similar fashion to what was described for the coupled pendulum system above, we should be careful to make comparisons. In this report we study the coupling of asymptotically stable oscillators, implying that the systems to be coupled are *dissipative*. However, Huygens original pendulum setup is a so-called Hamiltonian system where dissipation is so weak that it's almost non-existent. The analysis of these systems lies well beyond the scope of this report [4] and we instead refer the interested reader to [2] and it's references.

Had Huygens lived today he would most certainly be in awe when confronted with the scope of his invention and range of application that it has found. Basically, the concept is used to explain any kind of scenario whereby several autonomous distinct parts come together an act as a single entity. Such behavior is surprisingly abundant in nature and new examples are continually being discovered. Situations can be observed in social gatherings where the applause after a (classical) concert or theater play will start completely incoherent and then move into synchronicity or in a crowd crossing a bridge [5]. In biology and physiology synchronization, plays a role in connection with the concept of *biological clocks*, possessed by many plants and most animals allowing them to synchronize their rhythm to the 24 hour Earth cycle, pacemaker cells responsible for the regular beating of the heart and many other examples too numerous to mention. Finally, we also note that synchronization is key to understanding the neurological processes in the most autonomous dynamical system known to man : the human brain.

In electrical engineering the benefits of synchronization were being developed in the 1920's by people like W.H. Eccels, J.H Vincent, Nobel prize laureate E. Appleton and the famous electrical engineer B. van der Pol. Besides his celebrated work on oscillator theory and it's application to physiological systems, Balthasar van der Pol was also one of the pioneers in the applications of synchronized signal generators. He showed how one could stabilize high power triode signal generators by injecting a weak but precise reference at some appropriate circuit node. Stabilized, high power signal sources was, and is, one of the main design challenges of wireless communication systems. Most

[3] bilateral coupling means that the coupling from port 1 to port 2 is equal to the coupling in the other direction (port 2 to port 1). The opposite of bilateral coupling is *unilateral coupling*; a subject which we shall study in detain in chapter 4.

[4] a short discussion is however included in section 1.2, on page 28, where we consider averaging applied to single and coupled oscillators.

[5] people crossing a bridge will in general try to synchronize their footfalls. When the London Millennium Bridge opened in June of 2000 people nicknamed it the "Wobbly Bridge" due to swaying motion of the structure when loaded to its full capacity. Initial small resonances in the construction were being amplified by the crowd on the bridge who seemed to be encouraged to synchronize their gait with the sway [3].

people probably remember van der Pol for his iconic oscillator model which is ubiquitous in various different areas of science, such as applied mathematics, electrical engineering, biology *etc.*, where modelling of periodic behavior is considered. Almost all new proposed oscillator models can in some way be traced back to his original work; the ones in this report being no exception to that rule.

Today coupled/injection locked oscillators / lasers find various applications within wireless / fiber-optic communication systems, radar and satellite equipment *etc.* Often these circuits are employed in order to achieve one of the following objectives

1. *the creation of a coherent multi-phase pattern.*
2. *analog frequency multiplication and division.*
3. *stabilization of a noise-corrupted carrier signal.*
4. *coherent power combining of several signal generators.*

Modern wireless receivers such as the zero-IF, the Low-IF and image-reject architectures such as the Hartley and Weaver all rely on quadrature, also known as I/Q, signals [4]. The quadrature signals are also used at the transmitter side in *e.g. direct conversion transmitters*. In optical communication systems these signals are used in the implementation of data clock recovery (DRC) circuit blocks. The I/Q constellation can be generated very effectively by coupling two oscillator unilaterally in ring configuration, with a 180^o explicit phase shift in one of the coupling branches [5], [6], [7], [8]. This circuit structure, known here as the *cross-coupled quadrature oscillator* (CCQO), was invented in 1996 by Rofougaran *et al.* [5] and it will receive detailed attention in section 4.7 of this report. Multi-phase modes are used in phased array antenna systems [9], in beam scanning antenna arrays [10], fractional-N synthesizers [11], high speed samplers and sub-harmonic mixers. In the past such signals where often produced by ring oscillators or by using poly-phase filters, however, as is well known, these designs suffer from a very poor noise-to-power ratio [8]. As will be discussed in chapter 4, ring-coupled oscillators have been proven to be an attractive and reliable alternative.

By locking the carrier to the sub/super harmonic of the reference, analog frequency multiplication/division can be achieved. Compared to digital division/multiplication, this is a very compact and low-power alternative which is often used in modern PLL structures [12].

Since the pioneering work of van der Pol and co-workers, it has been known that we can stabilize the phase of a high-power, noise-corrupted carrier signal by injecting a weak but precise reference signal. The slave/carrier oscillator is forced to follow the phase of the master/refference oscillator to maintain the equilibrium condition of oscillation, also known as Barkhausen's criterion. This then implies that the high stability of the master is to a certain degree *inherited* by the slave. In practical applications, such a *phase filter* is often implemented by injecting a weak signal from a quartz oscillator operating at some subharmonic of the carrier oscillator. The unilateral injection locked configuration is however not the only kind of locked system exhibiting this phase-filtering behavior. When coupled sub-systems/oscillators synchronize it means that they have decided on a common frequency which is some function of the individual oscillator frequencies. As a noise pulse then arrives and disturbs this steady-state frequency, the oscillators will "work together" to regain the equilibrium condition of synchrony. In the case of n all-to-all coupled oscillators, this means that the oscillator, perturbed by a noise pulse, will not fell the full brunt the disturbance but instead only a factor $1/n$. Since the noise

sources of the different oscillators are uncorrelated this leads to the well known factor $1/n$ multiplying the noise-to-power ratio, corresponding to a $10\log(n)$ decrease, in dBc, in the single sideband (SSB) phase-noise spectrum [6]; a phenomena seen in many other coupled oscillator structures as well [13]. In this report we shall develop models which will help us understand this cooperative behavior of coupled, noise-forced oscillators. The analysis considers the asymptotic or steady-state dynamics perturbed by delta-correlated noise sources and hence only pays attention to the state of the system *after* synchronization has been achieved. The interesting, but challenging, topic of locking transient analysis is not considered in this report. Noise calculations are made relatively easy by the fact that one considers the response to small perturbations. We are then allowed to linearize the inherent oscillator non-linearities since the state of the system is never driven very far away from equilibrium conditions. This type of analysis is known as *linear response theory*, a topic which is tightly linked with the core-purpose of this report. In fact, if asked to introduce the text in the next four chapters, a fitting description wold be : "linear response theory applied to autonomous single and coupled oscillating systems perturbed by delta-correlated stochastic sources".

This report documents the introduction of two novel models considering coupled oscillators perturbed by noise; with the aim of characterizing the phase-noise performance and asymmetry response of these systems. In chapter 3 we shall consider the *phase macro-model*, which is a projection methodology originally devised for the single oscillator phase-noise characterization; applied here to general coupled oscillator structures. Then in chapter 4 we describe a canonical normal-form formulation pertaining to n unilaterally ring-coupled harmonic oscillators.

The search for faster, less memory consuming and increasingly rigorous *circuit aided design* (CAD) routines for the simulation of nonlinear electric circuits is an ongoing effort and a very active area of research. With regard to phase-noise characterization of single/free-running oscillators, many people, including this author, believe that this search ended with the introduction of the phase macro-model by Demir *et al.* [14], [15], [16]. The method is based on a projection formalism, originally proposed by Kaertner in [17], with the projection operators being numerically derived using a Floquet theoretic decomposition. The algorithm only requires a numerically derived steady-state and the circuit *monodromy matrix* (MM), which is a special *state-transition-matrix* (STM), to work and is hence completely independent of circuit topology and parameters. After numerically integrating the linear response equations for a single oscillator period and with the correct initial conditions, the phase-noise characterization is complete. The formulation is very rigorous, being based on stochastic integration techniques and Floquet theory. It is very hard to imagine a more rigorous or computational efficient routine for the simulation of single oscillator phase-noise and it is, without a doubt, a "near-optimum" formulation, considering the problem it is trying to solve. With regard to a possible algorithm for the numerical phase-noise characterization of coupled oscillators it then seems only natural to turn to the solid foundation offered by the Demir model and try to extend it to encompass coupled systems. Chapter 3 hence documents the attempt of this author towards the derivation of a novel coupled oscillator model, based on the above mentioned projection formalism. Essentially, the procedure consists of defining n projection operators corresponding to the n-dimensional invariant manifold on which the

[6] since the response to the perturbation is multiplied by a factor $1/n$ the output noise power will multiplied by a factor $1/n^2$. This then has to multiplied by a factor n to account for n uncorrelated noise sources (uncorrelated noise add in power), thus leading to the factor $1/n$. Note that a decrease in *dB below the carrier* (dBc), refers to a increase in the stability of the signal and that this improvement is a *close-to-carrier* effect [6].

solution resides.

By re-using the work of Demir *et. al* we of course get all the computational effectiveness of their model for "free" and we furthermore save a lot of time since we do not have to re-invent the wheel, so to speak. At present time, most noise simulations of coupled oscillator and phase-locked systems are done using brute-force Monte Carlo techniques. The computational savings gained by switching to a projection formalism, like the one described in chapter 3, would be several orders of magnitude. Other schemes exist, like the *mixing method*, used in *e.g.* Advanced Design Systems (ADS), which is based on conversion matrix calculations and the *sensitivity method* where the response at each node is calculated based on a numerically estimated sensitivity. The paper [18] documents a projection formalism for the calculation of oscillator phase noise based on a *harmonic balance* (HB) steady-state techniques. Both the mixing, sensitivity and the projection formalism in [18] are frequency domain models which do not consider stochastic integration techniques for solving the oscillator ODE forced by noise. This in turn implies that a SSB phase-noise spectrum proportional to $1/f_m^x$ will result, where f_m is the offset frequency away from the carrier and x is a number between 1 and 3, depending on the power-density spectrum of the noise sources. The singular behavior of this spectrum, for offset frequencies close to zero, of-course has nothing to do with the physical situation. Methods based on stochastic integration correctly prescribe a Lorentzian spectrum which is everywhere finite. Finally, we note that Kaertner's original proposal in [17] lies very close to the phase-macro model formulation in [14]. However, in this report we have chosen to only consider the Demir method since the algorithm is much simpler to implement in program-code, while being based on just as rigorous theory.

Applied mathematical models can very coarsely be divided into two main constituents : qualitative and quantitative. While a quantitative model aims to emulate the physical system to as high a degree as possible, a qualitative model makes several approximations in order to simplify the system by considering only parameters and degrees-of-freedom which are "vital" in the quest to capture the "essential" behavior of the system. Certainly, the projection formalism described in chapter 3 is of a quantitative nature and this is then followed in chapter 4 by an example of a qualitative model. Here we consider the derivation of the canonical amplitude/phase state-equations describing the dynamics of a system of n unilaterally ring-coupled harmonic oscillators; with the aim of investigating stability, phase-noise performance and asymmetry response of this complex multi-mode system. As discussed above, an I/Q signal constellation, as is generated by the CCQO, is used in many modern transceiver architectures to remove any spurious image signal and as part of the modulation scheme. However, unavoidable asymmetry between the two oscillator blocks, or in the coupling network, will cause the output to deviate from quadrature. This, in-turn, will limit the image rejection properties of the receiver. At the transmitter such imbalance would reduce the dynamic range and decrease the bit-error-rate (BER). In a phased array antenna system, imbalance in the phase relation would lead to spurious effects in radiation pattern. The phase-noise of the sources are specified to maintain receiver sensitivity and avoid reciprocal mixing and transmitter interference. Often these very strict phase-noise specifications will make the design of low-noise signal sources the bottleneck of the overall transceiver architecture. The need for models explaining how the different circuit parameters affect the noise and asymmetry performance should be obvious to everyone. As we shall explain in chapter 4 the design of optimum ring-coupled signal generators are complicated by the fact that there seems to exist a trade-off between optimum noise and asymmetry operation in these circuit structures.

We end this introduction with a short overview of the different chapters and appen-

dices found in this report.

Chapter 1 "Basic Theory" : a detailed introduction to the concepts of equivalence theory, averaging methods and the symmetry formalism. The methods and techniques developed in this chapter will be used throughout the rest of the report.

Chapter 2 "Single Oscillators Perturbed by White Noise - Inhomogeneous Phase Diffusion" : a thorough description of the single oscillator phase noise problem and a review of three popular models from the literature. The text tries to simplify the complex notation found in the original solution to problem, posed by Demir *et al* in [14]. A new, intuitive, less mathematical explanation regarding the asymptotic statistics of a free-running oscillator, perturbed by delta-correlated noise sources, is included.

Chapter 3 "A Phase Macro Model for Coupled Systems with $\Gamma \times \mathbb{S}^1$ *Symmetry" :* this chapter describes the development of a novel projection based formalism used to characterize the phase-noise of coupled oscillators, numerically. A model prescribing the phase-noise spectrum of a sub-harmonic injection locked oscillator perturbed by white noise is developed. Given so-called *normally hyperbolic* conditions, it is possible to identify 2 Floquet projection operators from the n possible choices which are then used to set up the stochastic differential equations defining the noise-forced system, tangentially to the invariant manifold. These equations are solved using stochastic integration techniques.

Chapter 4 "n Unilaterally Ring-Coupled Harmonic Oscillators Perturbed by White Noise" : this chapter contains a complete and self-contained text discussing every aspect regarding the steady-state analysis of the unilateral ring-coupled oscillator system. We explain why the system always chooses the same mode, known here as the *dominant mode*, at startup and we investigate linear stability and noise response. Starting from the linear response equations and using the concepts of *diagonal phase* and *effective diffusion constant*, which was introduced in chapter 2, we are able to derive a novel qualitative expression for the close-to-carrier phase-noise of this coupled structure. Special attention is paid to the special CCQO configuration which has been the subject of three papers [6],[19],[20] written by the author during the course of this project.

Appendix A "The Noise Appendix - Narrow-band Noise / Stochastic Integration / The Fokker-Planck Equation" : this report considers the effects of noise forcing on autonomous ordinary differential equations (ODE). The solution is then formulated through stochastic integration techniques. This appendix includes an easy to read introduction to the concept of stochastic integration and the Fokker-Planck equation.

Appendix B "Deriving the Averaged Stochastic Differential Equations for a General Class of Second Order Oscillators" : this is a easily readable introduction to field of averaged stochastic differential equations, also known here as *Kurokawa theory*.

Appendix C "Various Derivations" : as the name suggest, this appendix contains derivations, to large to be included in the main text.

Appendix D "Floquet Theory" : Floquet theory is used in the model formulation in chapter 3 and in the original phase macro model in [14]. Using this theory we can define a *monodromy matrix* (MM), which is a special *state-transition matrix* (STM), mapping the oscillator state one period forward in time. This map is returned by the CAD program's steady-state routine and hence contains all the information available to us about the

solution. A detailed understanding of this matrix is therefore very important. It will be shown that we can approximated the MM map by considering the averaged state equations.

Chapter 1

Basic Theory

This chapter reviews analytical tools and techniques that will be used in the models described throughout the next 3 chapters. The procedures generally allow for a significant simplification and classification of the, often, complex and diverse dynamical systems; with the aim of extracting qualitative behavioral models of coupled oscillators perturbed by noise. We shall investigate three main methodologies

- equivalence theory
- averaging methods
- the symmetry formalism/group theory

The generalized theoretic discussion will become clearer when applied to an example. We consider the prototype electrical oscillator [1]

$$L\frac{\partial i_L}{\partial t} = -v_C \tag{1.1}$$

$$C\frac{\partial v_C}{\partial t} = i_L - \frac{v_C}{R} + G_{mo}(v_C)v_C \tag{1.2}$$

where v_C is the voltage across the capacitor C, i_L is the current through the inductor L, $R = 1/G$ is the resistive loss and $G_{mo}(v_C) = g_0 + g_1 v_C + g_2 v_C^2$ is the nonlinear energy restoring circuit element. Equations (1.1)-(1.2) are often referred to as a *van der Pol unit*. It will be shown that this system contains sufficient degrees-of-freedom (2) to capture any qualitative behavior of an arbitrary higher dimensional harmonic oscillator without inherent frequency control (*i.e. varactors*).

1.1 Equivalence Theory

Equivalence theory considers asymptotic dynamics as the orbits have settled on an invariant manifold; expressed in a "rotated" coordinate system, constructed to reduced the complexity of the manifold equations as much as possible. Equivalence theory naturally divides into two main constituents

[1] the oscillator in (1.1)-(1.2) is used several places throughout this report. For a schematic of this circuit see figure 4.1, on page 80, or figure B.1 in appendix B.

- *center-manifold reduction* : this procedure projects the state equations onto the invariant manifold; the so-called *center-manifold*. Considering only the center-manifold dynamics allows for a significant reduction in the dimensionality of the system under investigation.
- *normal form transformation* : applying a nonlinear rotation to the state-space coordinate system we can achieve a coordinate frame where all nonlinearities, except the "essentials", are removed. The rotated equations are thus written on a *standard/normal form* implying that the qualitative behavior of a whole class of dynamical systems can be treated by considering only a single set of *normal* equations.

Two standard textbooks on the above subjects are [21] and [22]. The general results on the center-manifold theory and the normal-form methods included in this chapter are all taken from [21]. The review paper by Crawford [23] is a popular reference with many authors. The books by Goloubitsky *et al.* [24], [25] are also very educational, but we should caution that they use a different, slightly more complex, notation compared to what will be included in this report. Finally, the book by Hoppensteadt *et al.* [26] considers equivalence theory with special attention being paid to the analysis of coupled oscillators.

We proceed in section 1.1.1 below by considering equivalence theory as it applies to single oscillators and then, in section 1.1.2, we move on to investigate coupled structures.

1.1.1 Single Oscillators - The Andronov-Hopf Normal-Form

The free-running oscillator is described by a $k \geq 2$ dimensional autonomous ODE

$$\dot{x} = f(x, \mu) \tag{1.3}$$

where $x(t) : \mathbb{R} \to \mathbb{R}^k$ is the state vector, $f(\cdot, \cdot) : \mathbb{R}^k \times \mathbb{R} \to \mathbb{R}^k$ is the vector field and μ is a *dedicated bifurcation parameter* [2]. We assume that $x = 0$ is a stable equilibrium/fixed point [3] of (1.3) for $\mu < 0$ which becomes unstable as μ becomes greater than zero. As μ crosses the bifurcation boundary $\mu = 0$, a so-called *Andronov-Hopf bifurcation* will take place whereby two imaginary eigenvalues of the Jacobian matrix, $J \in \mathbb{R}^{k \times k}$, where

$$J_{ij} = \left. \frac{\partial f_i}{\partial x_j} \right|_{x_j = 0} \tag{1.4}$$

will cross the imaginary axis with finite speed. All other eigenvalues of the Jacobian are assumed to have real parts less than zero.

The Center-Manifold Theorem

At $\mu = 0$ the state space is hence split into a *center subspace* $\mathbb{E}^c$ and a *stable subspace* $\mathbb{E}^s$ as $\mathbb{R}^k = \mathbb{E}^c \oplus \mathbb{E}^s$. By this division we can write (1.3) as

$$\dot{v} = Av + f_c(v, y, \mu) \tag{1.5}$$

$$\dot{y} = By + f_s(v, y, \mu) \tag{1.6}$$

$$\dot{\mu} = 0 \tag{1.7}$$

[2] this section describes the Andronov Hopf bifurcation which is a *co-dimension 1 bifurcation* [21]. This means that only one parameter is needed to unfold the equations.

[3] an arbitrary fixed point $x = a$ is easily brought back to zero by the linear transformation $x \to x - a$.

where $v \in \mathbb{E}^c$, $y \in \mathbb{E}^s$, A is 2×2 matrix with imaginary eigenvalues and B is a $(k-2) \times (k-2)$ matrix having only eigenvalues with negative real parts. The functions f_c and f_s contain all the nonlinear terms of the original state equations [4]. Using simple similarity transformations we can write the two matrices in (1.5)-(1.6) as

$$A = \begin{bmatrix} 0 & -\omega \\ \omega & 0 \end{bmatrix} \tag{1.8}$$

$$B = \begin{bmatrix} \lambda_{1s} & 0 & \cdots & 0 \\ 0 & \lambda_{2s} & \cdots & 0 \\ \vdots & \vdots & \ddots & \vdots \\ 0 & 0 & \cdots & \lambda_{(k-2)s} \end{bmatrix} \tag{1.9}$$

where $\omega \in \mathbb{R}$ and $\Re\{\lambda_{is} < 0\}$ for all $i \in [1; k-2]$. The following statements can now be made [21]

- there will exist a smooth center-manifold given by $v + y_c$ where $y_c = h(v, \mu)$ and h is a smooth function which satisfies $h(0,0) = 0$, $dh(0,0)/dx = 0$.
- this manifold is invariant and will contain all bifurcating solutions.
- all orbits in phase space will approach this invariant manifold exponentially with time.

Thus in order to study the qualitative dynamics we can restrict our attention to the two dimensional (for a fixed μ) center-manifold $v+h(v,\mu)$. The derivation of the function $y_c = h(v,\mu)$ is a standard procedure explained in many of the references mentioned in the beginning of this chapter [5]. We will not go into specifics here but simply assume that this map has been derived somehow.

Since the center-manifold for an Andronov-Hopf bifurcation is 2-dimensional, the equations are most naturally described using complex variables. Introducing the notation $v = [v_1\, v_2]^T$, we then define the $z \in \mathbb{C}$ as

$$z = v_1 + jv_2 \tag{1.10}$$

The v and z representations are related through the linear transformation

$$\begin{bmatrix} v_1 \\ v_2 \end{bmatrix} = \frac{1}{2} \begin{bmatrix} 1 & 1 \\ -j & j \end{bmatrix} \begin{bmatrix} z \\ \overline{z} \end{bmatrix} \tag{1.11}$$

where the $\overline{z}$ refers to the complex conjugate of z. Inserting $y = h(v,\mu)$ into (1.5) and using the above transformation, we can then write the center-manifold dynamics as

$$\dot{z} = \lambda(\mu) z + F(z, \overline{z}, \mu) \tag{1.12}$$

$$\dot{\overline{z}} = \overline{\lambda}(\mu)\overline{z} + \overline{F}(z, \overline{z}, \mu) \tag{1.13}$$

where the eigenvalue λ is defined through

[4] note that according to (1.7) μ should now be consider as a state variable which means that terms of the form μv, $\mu^2 v$ *etc.* are no longer linear, but non-linear terms.

[5] see *e.g.* [23, *pp.* 1009-1014].

$$\lambda = \rho(\mu) + j\omega = \rho_r(\mu) + j\rho_i(\mu) + j\omega \tag{1.14}$$

$$\lambda(0) = j\omega \tag{1.15}$$

$$\frac{d\rho_r}{d\mu} > 0 \tag{1.16}$$

with ω being defined in (1.8) and the functions F and $\overline{F}$ are complex conjugates which hold all the nonlinear terms.

At this point we return to our example oscillator in (1.1)-(1.2). The system is two dimensional and can therefore be consider the result of a k dimensional oscillator, as defined in (1.3), projected onto the center-manifold, with $v_1 = i_L$ and $v_2 = v_C$. The Jacobian of the vector field in (1.1)-(1.2) is found, using (1.4), as

$$J = \begin{bmatrix} 0 & -\frac{1}{L} \\ \frac{1}{C} & g_0 - G \end{bmatrix} \tag{1.17}$$

The two complex conjugate eigenvalues are found to be

$$\begin{aligned} \lambda = \frac{1}{2C}(g_0 - G) \pm \frac{j}{2}\sqrt{4\omega_0^2 - \left(\frac{g_0 - G}{C}\right)^2} \approx \\ \frac{(g_0 - G)}{2C} \mp j\frac{(g_0 - G)}{8C}\frac{(g_0 - G)}{G} \pm j\omega_0 \end{aligned} \tag{1.18}$$

Comparing with (1.14) we see that we can make the identification

$$\rho_r = \frac{(g_0 - G)}{2C} \tag{1.19}$$

$$\rho_i = -\frac{(g_0 - G)}{8C}\frac{(g_0 - G)}{G} \tag{1.20}$$

$$\omega = \omega_0 \tag{1.21}$$

$$\mu \propto g_0 - G \tag{1.22}$$

where

$$\omega_0 = \frac{1}{\sqrt{LC}} \tag{1.23}$$

Using the substitutions

$$c_1 = \frac{g_0 - G}{C} \tag{1.24}$$

$$c_2 = \sqrt{4\omega_0^2 - c_1^2} \tag{1.25}$$

the eigenvectors of the matrix in (1.17) are written as columns in the transformation matrix T

$$T = \begin{bmatrix} -\frac{2}{L}\frac{1}{c_1 + jc_2} & -\frac{2}{L}\frac{1}{c_1 - jc_2} \\ 1 & 1 \end{bmatrix} \tag{1.26}$$

$$T^{-1} = \frac{1}{2c_2}\begin{bmatrix} -j2\omega_0^2 L & c_2 - jc_1 \\ j2\omega_0^2 L & c_2 + jc_1 \end{bmatrix} \tag{1.27}$$

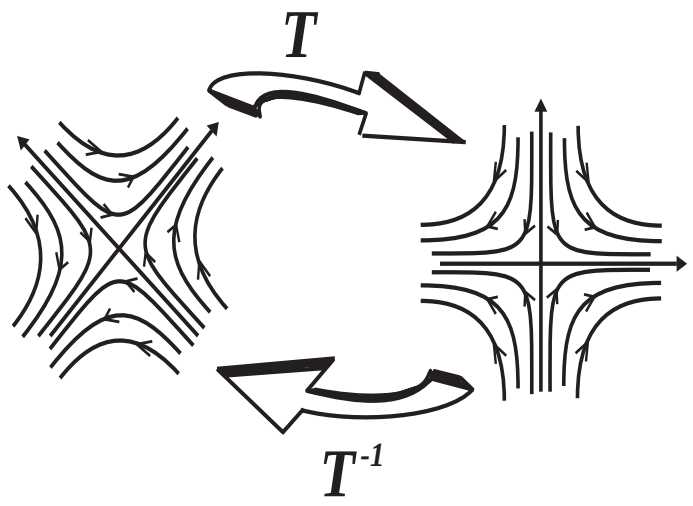

Figure 1.1: the normal form method in the linear domain. T rotates the coordinates to produce the simplest possible representation of the dynamical system. For the linear *saddle* system shown here, this simply corresponds changing the basis vectors. We hence see that all saddle systems are equivalent and we a free to study the least complex representation, which is clearly given by the system in the right part of the figure.

We can then define the new complex parameters z as

$$\begin{bmatrix} i_L \\ v_C \end{bmatrix} = T \begin{bmatrix} z \\ \overline{z} \end{bmatrix} \tag{1.28}$$

Using this transformation, (1.1)-(1.2) are written as

$$\begin{aligned} \begin{bmatrix} \dot{z} \\ \dot{\overline{z}} \end{bmatrix} =& \frac{1}{2c_2} \begin{bmatrix} -j2\omega_0^2 L & c_2 - jc_1 \\ j2\omega_0^2 L & c_2 + jc_1 \end{bmatrix} \begin{bmatrix} 0 & -\frac{1}{L} \\ \frac{1}{C} & g_0 - G \end{bmatrix} \begin{bmatrix} -\frac{2}{L}\frac{1}{c_1+jc_2} & -\frac{2}{L}\frac{1}{c_1-jc_2} \\ 1 & 1 \end{bmatrix} \begin{bmatrix} z \\ \overline{z} \end{bmatrix} + \\ & \frac{1}{2c_2} \begin{bmatrix} -j2\omega_0^2 L & c_2 - jc_1 \\ j2\omega_0^2 L & c_2 + jc_1 \end{bmatrix} \begin{bmatrix} 0 \\ \frac{g_1}{C} v_C(z,\overline{z})^2 + \frac{g_2}{C} v_C(z,\overline{z})^3 \end{bmatrix} = \\ & \begin{bmatrix} \lambda & 0 \\ 0 & \overline{\lambda} \end{bmatrix} \begin{bmatrix} z \\ \overline{z} \end{bmatrix} + \frac{1}{2c_2} \begin{bmatrix} (c_2 - jc_1)\{\frac{g_1}{C}(z^2 + \overline{z}^2 - 2z\overline{z}) - \frac{g_2}{C}(z^3 - \overline{z}^3 + 3z\overline{z}^2 - 3z^2\overline{z})\} \\ (c_2 + jc_1)\{\frac{g_1}{C}(z^2 + \overline{z}^2 - 2z\overline{z}) - \frac{g_2}{C}(z^3 - \overline{z}^3 + 3z\overline{z}^2 - 3z^2\overline{z})\} \end{bmatrix} \end{aligned} \tag{1.29}$$

which is on the form (1.12)-(1.13). As (1.29) stands, we are really no better off compared to the original state equations in (1.1)-(1.2). After having reduced the dimensionality from k to 2 with the center manifold theorem, we now need a tool that will reduce the complexity/non-linearity of these center manifold equations.

The Normal-Form Method.

The normal form method describes a non-linear transformation that will "rotate" the coordinate system, in such a way that the state equations in the rotated frame will contain the fewest possible non-linear terms. The linear equivalent of this operation is represented by a change of basis vectors as illustrated by the operation T in figure 1.1. One only needs to study the clean/standard form on the right side of figure 1.1. The results obtained in this coordinate system are then transformed back to the original *skewed*

coordinate system, on the left, by the inverse transformation T^{-1}. More importantly, letting T represent an arbitrary rotation in the plane $\mathbb{R}^2$, we can study the whole system class [6] simultaneously while considering only the simple normal form on the right side of figure 1.1. When introducing nonlinearity into the formulation, the eigenvectors are no-longer represented by simple Euclidian basis vectors but are instead constructed from homogeneous polynomials named *monomials* [7], which span the infinite dimensional space of nonlinear vector functions. We should, however, keep the linear representation in figure 1.1 in mind, when we try to understand the *non-linear* transformations. Firstly, it provides a good mental picture of what the normal-form method "does"; namely, some kind of rotation of the coordinate system. Secondly, it illustrates, very effectively, what we are trying to achieve by this exercise; that being, a clean/simple representation which is equivalent to all other *skewed/complex* members within the system class.

In this section we shall discuss the so-called *Elphick-Tirapegui-Brachet-Coullet-Iooss normal form* which is formulated in terms of system symmetry. The first step in the procedure consist of writing (1.12)-(1.13) as

$$\dot{z} = Jz + F_2(z) + F_3(z) + \cdots F_{r-1}(z) + O(|z|^r) \tag{1.30}$$

where $r > 3$ is an arbitrary integer and we have introduced the compact notation $z = [z\ \overline{z}]^T$. The terms F_k contain *monomials* of order k

$$F_k = z^{m_1}\overline{z}^{m_2} \tag{1.31}$$

where $m_1 + m_2 = k$. We also write $F_k \in \mathbb{H}_k$, with $\mathbb{H}_k$ being the vector space of k'th order monomials in z and $\overline{z}$.

As shown in appendix C.1, by introducing a close to unity change of coordinates

$$z = w + h_k(w) \tag{1.32}$$

where $w \in \mathbb{C}$ and $h_k(\cdot) : \mathbb{C} \to \mathbb{H}_k$, we can write (1.30) as

$$\begin{aligned} \dot{w} = & \underbrace{Jw}_{\text{first order term}} + \underbrace{F_2(w)}_{\text{second order term}} + \cdots + \underbrace{L_J^{(k)}(h_k) + F_k(w)}_{\text{k'th order term}} + \\ & \underbrace{\tilde{F}_{k+1}(w)}_{\text{k+1 order term}} + \cdots + \underbrace{\tilde{F}_{r-1}(w)}_{\text{r-1 order term}} + \underbrace{O(|w|^r)}_{\text{r order term}} \end{aligned} \tag{1.33}$$

where we have defined the *Lie bracket* $L_J^{(k)}(\cdot) : \mathbb{H}_k \to \mathbb{H}_k$

$$L_J^{(k)}(h_k) = [h_k(z), Jz] = -\big(Dh_k(z)Jz - Jh_k(z)\big) \tag{1.34}$$

In (1.33), the *tilde* symbol $\tilde{F}_{k+1}$ illustrates that the coordinate change in (1.32) has affected the higher order monomials in some unspecified way. More importantly, the operation has left the lower order terms untouched. Referring to equation (1.33), the k'th order monomial in (1.30), F_k, can be removed if we can find a transformation, h_k, in (1.32), such that $L_J^{(k)}(h_k) = -F_k(w)$. Since the transformation has no impact on the lower order terms we can work our way through (1.30), term by term, without destroying earlier obtained results. Considering the j'th term, $F_j(w)$, in (1.30), the Lie bracket in

[6] in figure 1.1 the orbits represent solutions of a linear *saddle system* where one of eigenvalues have positive real part while the other is negative. It follows that all linear saddle systems are equivalent.

[7] where a k'th order polynomial has the form $a_k x^k + a_{k-1}x^{k-1} + \cdots a_1 x + a_0$, a k'th order monomial is written ax^k.

(1.34) can only remove the monomials which lie in it's *image*, $\mathrm{Im}L_J^{(j)}(h_j)$, also called it's *range*, while it is forced to leave the terms residing in the complement space, $\mathrm{Ker}L_{J^*}^{(k)}$ [8], behind, since it cannot reach them. Here, $\mathrm{Ker}L_{J^*}^{(k)}$, refers to the *kernel* of the Lie bracket $L_{J^*}^{(k)}$ and J^* is the Hermitian (transposed + complex conjugated) of the system Jacobian, J, in (1.30). The normal-form equations are hence made up of k'th order monomials residing within the vector space $\mathrm{Ker}L_{J^*}^{(k)}$, for an arbitrary $k < r$. One refers to the terms which can be removed by the operator in (1.34) as *non-resonant monomials* while those that are left behind are termed *resonant monomials* [21].

As shown in appendix C.1, the terms contained in $\mathrm{Ker}L_{J^*}^{(k)}$ are equivariant with regard to the group actions of the one parameter group e^{J^*s}. A vector field, $f(x)$, is equivariant with respect to operations of a group, Γ, if

$$\gamma f(\gamma x) = f(x) \quad \forall \gamma \in \Gamma \tag{1.35}$$

applies. Assuming that $x(t)$ is a solution to

$$\dot{x} = f(x) \tag{1.36}$$

then γx is also a solution [9]. The normal-form solution of an ODE with the Jacobian J will hence possess a symmetry defined by the one parameter continues group e^{J^*s} (s is the parameter).

In this chapter we consider harmonic oscillators as represented by the Andronov-Hopf bifurcation. From (1.12)-(1.13), (1.14)-(1.16) on page 16 and footnote 4, on page 15, we see that we can write the Hermitian Jacobian as

$$J^* = \begin{bmatrix} -j\omega & 0 \\ 0 & j\omega \end{bmatrix} \tag{1.37}$$

The one parameter group from the above discussion then gets the form

$$e^{J^*s} = \begin{bmatrix} \exp(-j\omega s) & 0 \\ 0 & \exp(j\omega s) \end{bmatrix} \tag{1.38}$$

As an example, consider the two vectors $z\overline{z}$ and $z^2\overline{z}$; performing the above discussed rotation we get

$$\exp(j\theta)\big(z\exp(-j\theta)\overline{z}\exp(j\theta)\big) = z\overline{z}\exp(j\theta) \neq z\overline{z} \tag{1.39}$$

$$\exp(j\theta)\big(z\exp(-j\theta)\overline{z}\exp(j\theta)\big)z\exp(-j\theta) = z^2\overline{z} \tag{1.40}$$

where $\theta = \omega s$ is now a arbitrary angle. From the above equations we see that while $z^2\overline{z}$ is equivariant with regard to the operation in (1.38), the term $z\overline{z}$ is not; implying that $z\overline{z}$ can be removed (non-resonant monomial) while the term $z^2\overline{z}$ stays (resonant monomial). From the above discussion and examples we can summarize the results as follows

[8] this is discussed in appendix C.1.

[9] this is seen by inserting γx into (1.36) and the subsequently using (1.35).

note 1.1 *In order for a monomial in* (1.12)-(1.13) *to remain in the Andronov-Hopf normal-form (resonance) it has to be equivariant with regard to a rotation in the complex plane; hence, the orbits, corresponding to solutions of the normal-form equations, are angular symmetric. This rotational symmetry of the equations, and the corresponding solutions, is represented by the continuous one parameter group* $e^{J^* s}$ *which is equivalent to* $\mathbb{S}^1$*, where* $\mathbb{S}^1$ *is known as the circle group.*

A thorough investigation of all terms up to order 4 would show that all second and fourth order terms are resonant and hence removable. All third order terms can also be removed, except the non-resonant term $z^2\overline{z}$. We can therefore write the Andronov-Hopf normal form of the system in (1.12)-(1.13) up to fifth order

$$\dot{z} = (\rho_r(\mu) + j\rho_i(\mu) + j\omega)z + c(\mu)z^2\overline{z} + O(|z|^5) \tag{1.41}$$

$$\dot{\overline{z}} = (\rho_r(\mu) - j\rho_i(\mu) - j\omega)\overline{z} + \overline{c}(\mu)\overline{z}^2 z + O(|z|^5) \tag{1.42}$$

where we have used (1.14)-(1.15) and $c(\mu)$ is some unspecified complex parameter resulting from the normal-form transformations. Often these equations are written on polar form with $z = A\exp(j\phi)$. Setting $c(\mu) = d(\mu) - jb(\mu)$, dropping the explicit dependence on μ and ignoring the $O(|z|^5)$ terms, we can write for the amplitude

$$\frac{dA^2}{dt} = 2A\dot{A} = \frac{d}{dt}z\overline{z} = \dot{z}\overline{z} + z\dot{\overline{z}} = 2\rho_r z\overline{z} + 2d(z\overline{z})^2 \tag{1.43}$$

and for the phase

$$\begin{aligned}\dot{\phi} = \frac{d}{dt}\arctan\left(-j\frac{z-\overline{z}}{z+\overline{z}}\right) = \frac{-j}{1-\left(\frac{z-\overline{z}}{z+\overline{z}}\right)^2}\frac{(z+\overline{z})(\dot{z}-\dot{\overline{z}}) - (z-\overline{z})(\dot{z}+\dot{\overline{z}})}{(z+\overline{z})^2} = \\ \frac{-j}{2z\overline{z}}(\dot{z}\overline{z} - z\dot{\overline{z}}) = \omega + \rho_i - bz\overline{z}\end{aligned} \tag{1.44}$$

Using $z\overline{z} = A^2$ we get the final form of the *third order Adronov-Hopf normal form equations*

$$\frac{dA}{dt} = \rho_r A - dA^3 = \rho_r\left[1 - \left(\frac{d}{\rho_r}\right)A^2\right]A \tag{1.45}$$

$$\frac{d\phi}{dt} = \omega + \rho_i - bA^2 \tag{1.46}$$

We now return to the complex state equations for the van der Pol oscillator which were written in (1.29). Repeating the above procedure which led to (1.45)-(1.46) on this set of equations, we find the following parameters

$$\omega = \omega_0 \tag{1.47}$$

$$\rho_r = \frac{(g_0 - G)}{2C} \tag{1.48}$$

$$\rho_i = -\frac{(g_0 - G)}{8C}\frac{(g_0 - G)}{G} \tag{1.49}$$

$$b = \frac{3g_2}{C}\frac{c_1}{2c_2} = \frac{3g_2}{C}\frac{g_0 - G}{2\left[\omega_0 - \frac{(g_0-G)}{8C}\frac{(g_0-G)}{G}\right]} \approx 3g_2\frac{(g_0 - G)}{G} \tag{1.50}$$

$$d = \frac{3g_2}{2C} \tag{1.51}$$

where we have used the definitions from (1.19)-(1.21).

Substituting these parameters in (1.45)-(1.46) we find the *van der Pol normal form equations*

$$\boxed{\begin{aligned} \frac{dA}{d\tau} &= \mu_o\left[1 - \left(\frac{A}{\alpha}\right)^2\right]A \qquad (1.52)\\ \frac{d\phi}{d\tau} &= 2Q - \frac{1}{4}\mu_o^2 - 3g_2\mu_o A^2 \qquad (1.53) \end{aligned}}$$

where we have introduced the slow time

$$\tau = \frac{\omega_0}{2Q} \tag{1.54}$$

and the definitions

$$Q = \omega_0 CR = R\sqrt{\frac{C}{L}} = \frac{R}{\omega_0 L} \tag{1.55}$$

$$\mu_o = \frac{g_0 - G}{G} \tag{1.56}$$

$$\alpha = \sqrt{\frac{g_0 - G}{3g_2}} \tag{1.57}$$

In the above definitions, Q is the oscillator Q-factor, $2\mu_o$ is the absolute value of the second Floquet characteristic exponent [10] of the limit cycle solution and α is the stable amplitude of the oscillator. The parameter b in (1.50) describes how the oscillator frequency depends on the amplitude. We see that this parameter is controlled by μ_o and g_2 together. For a moderately non-linear characteristic G_{mo} in (1.2), on page 13, both of these parameters are small. In this case we can approximate $b \approx 0$ and we say that (1.52)-(1.53) represents an *isochronous oscillator*. The parameter μ_0 in (1.56) and (1.52)-(1.53) will play an important role for the derivations in the next section, as well as in the model of the unilateral ring coupled oscillators described in chapter 4. From (1.48), (1.55) and (1.56) we see that we can write

[10] the second Floquet characteristic exponent controls the relaxation time of the amplitude. We refer to appendix D for an introduction to Floquet theory.

$$\mu_o = \rho_r \frac{2Q}{\omega_0} \tag{1.58}$$

Since μ_o is proportional to the bifurcation parameter ρ_r (see equation (1.14)) we see that oscillations are initialized by μ_o crossing the boundary $\mu_o = 0$. Furthermore, taking the derivative around the solution branch $A = \alpha$ in (1.52) we see that the *Floquet characteristic exponent*, which describes the relaxation time-constant of orbits approaching the limit cycle, is given by $-2\mu_o$. Finally, we note that μ_o can be seen as indicatory of *oscillator dissipation*. For a fixed *overdrive* $g_0 - G > 0$ we see that $\mu_0 \propto 1/G = R$ which means that the larger the dissipation the larger μ_o and the smaller the limit cycle amplitude relaxation time constant

note 1.2 *The oscillator dissipation as represented by the parameter μ_o controls the amplitude relaxation time-constant of the stable limit cycle. The larger the dissipation the tighter orbits are locked to this limit set.*

The above derivations illustrated how the qualitative dynamics of an arbitrary k-dimensional ($k \geq 2$) harmonic oscillator could be represented by a simple 2 dimensional system with rotational symmetry. When we say that the center manifold normal form equations *represents* the dynamics of the more complex "real" oscillator, what is meant is that any qualitative behavior which one would expect to observe in the original k dimensional system can be captured by (1.45)-(1.46). Another way of saying this is that (1.45)-(1.46) contains the minimum number of parameters needed to fit all qualitative dynamics in the original system to a rotation in the complex plane. The important conclusion is therefore that by studying the normal form (1.45)-(1.46) we simultaneous investigate all sinusoidal oscillators. Hence, there is no need to study systems more complex than (1.45)-(1.46) since no new information would be gained. This is an extremely powerful result which allows us to keep the analysis general while keeping the algebra manageable.

With respect to the van der Pol unit in (1.52)-(1.53), we can therefore draw the following important conclusion

note 1.3 *the van der Pol normal-form in* (1.52)-(1.53) *describe the simplest possible representation of a harmonic limit cycle. This model will hence be representative of the qualitative behavior generated by the system class of harmonic oscillators with no internal frequency control (i.e. varactors).*

which is a result that we shall use many times in this report.

There exist a connection between stable sub-manifolds and the symmetry of the governing the equations. As explained above in note 1.1, on page 20, the fact that the solutions have symmetry represented by the group $\mathbb{S}^1$ implies, that if $x(t)$ is a solution, then $x(t+\theta)$, where $\theta \in [0; 2\pi]$, is also a solution; illustrating that we are dealing with an oscillator (periodic solution). The limit cycle which all orbits approach asymptotically

with time will then constitute a stable sub-manifold[11] inside the center-manifold. This sub-manifold is also known as a *ω-limit set* [21]. Since this set is invariant under the operation $\mathbb{S}^1$ it must be a circle. That this is the case is easily seen from (1.45)-(1.46) where the amplitude of the circle is seen to be $\hat{A} = \sqrt{\rho/d} = \alpha$.

In the limit $\mu_o \to \infty$ the amplitude can be adiabatically removed [12] from normal form equations in (1.52)-(1.53) and we hence get the *phase-only* representation of the van der Pol oscillator

$$\frac{d\phi}{d\tau} = 2Q - \frac{1}{4}\mu_o^2 - 3g_2\mu_o\alpha^2 \tag{1.59}$$

Hence, for large dissipation [13] the oscillator is modelled by a single angular coordinate, the *oscillator phase*, moving with a uniform speed on the sub-manifold $\mathbb{S}^1$.

1.1.2 Coupled Oscillators - The Synchronized State

In the previous section it was shown how normal form theory allowed us to reduce the dimension of the autonomous system in (1.3) from k to 2. Based on this result, one could make the obvious conjecture that the same procedure applied on n coupled oscillators would reduce the dimension from nk to $2n$. As we shall continue to show, this will indeed be the case provided we consider *weakly coupled* units. What exactly constitutes a weak coupling is of-course not immediately obvious and much of the text in this section will be concerned with clarifying this concept. In the following we shall draw on the derivations made in the previous section which dealt with equivalence theory of single oscillators. The center manifold theorem was thoroughly discussed here. The analytical machinery involved in the derivation of a center manifold of coupled units does not differ from what was shown for single oscillators in the previous section. We shall therefore not include a separate discussion of this subject.

Let us write dynamic equations for the n coupled k-dimensional oscillators as

$$\dot{x} = f(x, \lambda) + \underline{\underline{\kappa}} x \tag{1.60}$$

where $x(\cdot) : \mathbb{R} \to \mathbb{R}^{nk}$ and $f(\cdot,\cdot) : \mathbb{R}^{nk} \times \mathbb{R}^n \to \mathbb{R}^{nk}$ is the vector field, $\lambda \in \mathbb{R}^n$ is vector containing n bifurcation parameters $\lambda = [\lambda_1\ \lambda_2\ \cdots\ \lambda_n]^T$ and $\underline{\underline{\kappa}} \in \mathbb{R}^{n\times n}$ is the coupling matrix

$$\underline{\underline{\kappa}} = \begin{bmatrix} \kappa_{11} & \kappa_{12} & \cdots & \kappa_{1n} \\ \kappa_{21} & \kappa_{22} & \cdots & \kappa_{2n} \\ \vdots & \vdots & \ddots & \vdots \\ \kappa_{n1} & \kappa_{n2} & \cdots & \kappa_{nn} \end{bmatrix} \tag{1.61}$$

where κ_{ij} describes the coupling from the j'th to the i'th oscillator. Although we only consider linear coupling here, the scope could easily be extended to include non-linear coupling functions [14]. We consider a scenario where the units are uncoupled ($\kappa_{ij} = 0$) and

[11] by this we simply mean a set of points which all orbits, corresponding to any initial condition, will approach asymptotically with time. For a more technical definition see [21].

[12] in the limit $\mu_o \to \infty$ we will have $A = \hat{A} = \alpha$ on all time scales, as is seen from (1.52).

[13] obviously, (1.59) has problems with the limit $\mu_o \to \infty$, since this would imply an infinite oscillator frequency. Instead we simply use the term "large" without specifying the exact size.

[14] the effects of non-linear coupling are examined in chapter 4 where we investigate the dynamics of a unilateral ring of n harmonic oscillators.

let λ cross the border $\lambda = 0$ [15]. As explained above in connection with the single oscillator, the Jacobian of each of the oscillators will have 2 eigenvalues crossing the imaginary axis with finite speed. Since the units are uncoupled, the Jacobian J, corresponding to the vector field in (1.60), will then have n pairs of complex conjugate eigenvalues, simultaneously crossing the imaginary axis with finite speed. This is known as a *multiple Andronov-Hopf bifurcation* [21]. As discussed above for the single oscillator, using center manifold reductions and normal-form transformations we can reduce the dynamics of the each oscillator to the form [16]

$$\frac{dA_j}{dt} = \rho_{r,j}\left[1 - \left(\frac{d_j}{\rho_{r,j}}\right)A_j^2\right]A_j \qquad j = 1, 2, \cdots n \tag{1.62}$$

$$\frac{d\phi_j}{dt} = \omega_j + \rho_{i,j} - b_j A_j^2 \qquad j = 1, 2, \cdots n \tag{1.63}$$

The symmetry of (1.62)-(1.63) is described by the n parameter group $\mathbb{T}^n = \underbrace{\mathbb{S}^1 \times \mathbb{S}^1 \cdots \times \mathbb{S}^1}_{n \text{ times}}$ which is known as the *n-torus group*. This is easily explained since the symmetry of the single units were $\mathbb{S}^1$ [17], then because the units are uncoupled, the symmetry group for the whole system is found by multiplying the groups of the individual systems. Another way of saying this is as follows

note 1.4 *for the case of the single harmonic oscillator, as described through the Andronov-Hopf bifurcation, we were free to rotate the coordinate system in the complex plane through an arbitrary angle. With the Multiple Andronov-Hopf bifurcation we consider n coordinate systems and since they are all uncoupled we can rotate each of them independently of the rest. We can therefore describe the symmetry using a n parameter group which rotates each of the n coordinate systems independent of the rest. This group is the n-torus group* $\mathbb{T}^n$.

As was the case with the limit cycle of the single oscillator, the stable sub-manifold must be invariant to the operations contained in system symmetry group; this implies that all orbits approach the n-torus $\mathbb{T}^n$, asymptotically with time. The sub-manifold $\mathbb{T}^n$ is *hyperbolic* [18] for $\kappa_{ij} = 0$ and will therefore persist if perturbed. However, as seen from (1.63), with $b_i = 0$ [19], the phase variables are neutrally stable and a perturbation will hence cause a bifurcation in these variables. The manifold will persists perturbations because it is defined in terms of the oscillator amplitudes in (1.62), which are stable state variables. Hence, the vector field *normal* to the surface of the invariant center manifold, which specifies the amplitude dynamics, will remain unaffected while the tangential dynamics (phase dynamics) will simply follow any perturbation.

[15] we assume here that all n bifurcation parameters λ_i are identical which implies that they cross the border $\lambda_i = 0$ simultaneously, for all i.

[16] see (1.45)-(1.46) on page 20.

[17] see discussion in 1.1.1.

[18] the n-torus is hyperbolic because the individual oscillator solutions are represented by a hyperbolic limit cycle, as seen from (1.62). The persistence towards perturbations follow directly from this hyperbolic property[21].

[19] if $b_i \neq 0$ we have to define a new phase variable which is then neutrally stable. See discussion in section 2.2.3, on page 54, for an example of this.

The Synchronized State

We now introduce very weak coupling $|\kappa_{ij}| \ll 1$ between the units. As explained above, the solution will stay on $\mathbb{T}^n$, however, under the correct circumstances [20] a *frequency-locked* or *synchronized* solution will bifurcate creating a new one-dimensional sub-manifold/ω-limit set on the n-torus. The first thing we note about this bifurcation is that it must be a *saddle-node* type bifurcation since it is a co-dimension 1 steady-state bifurcation in the phase variables in (1.63). Secondly, the bifurcation must change the symmetry of the solution. With $\kappa_{ij} = 0$ the oscillators where uncoupled and the symmetry was given by $\mathbb{T}^n = \underbrace{\mathbb{S}^1 \times \mathbb{S}^1 \cdots \times \mathbb{S}^1}_{n \text{ times}}$ representing the fact that the phases of the different oscillators were independent; implying that a rotation in one plane did not affect the dynamics in the other planes. After the locking bifurcation the oscillators are all synchronized and we can therefore not rotate in one plane without performing the same rotation in the remaining $n-1$ planes. Assuming that the coupling network is symmetric as prescribed by the group Γ we therefore have the result

note 1.5 *the symmetry of the uncoupled normal form equations on the n-torus is $\mathbb{T}^n$. When coupled through a Γ symmetric network, and assuming the creation of a synchronized solution through a saddle-node bifurcation, the symmetry of the normal form equations are given by the group $\Gamma \times \mathbb{S}^1$.*

When we say that the coupling network has symmetry Γ we mean that the units in (1.62)-(1.63) can be permuted according to the operations/actions contained in this group [21]. For the linear coupling scheme in (1.60) this implies that the coupling matrix *commutes* with the operations in Γ

$$\gamma \underline{\underline{\kappa}} = \underline{\underline{\kappa}} \gamma \quad \forall \gamma \in \Gamma \tag{1.64}$$

According to the above note the normal form equations of the n coupled units will take the form [22]

$$\frac{dA_i}{d\tau_i} = \mu_{o,i}\left[1 - \left(\frac{A_i}{\alpha_i}\right)^2\right]A_i + \Lambda_i(A_1, \cdots, A_n, \phi_1, \cdots, \phi_n; \kappa_{ij}) \qquad i = 1, 2, \cdots n \tag{1.65}$$

$$\frac{d\phi_i}{d\tau_i} = \frac{2Q_i}{\omega_i}\Delta\omega_i + \Phi_i(A_1, \cdots, A_n, \phi_1, \cdots, \phi_n; \kappa_{ij}) \qquad i = 1, 2, \cdots n \tag{1.66}$$

where $\Delta\omega_i = \omega_i - \omega_1$, with $T_1 = 2\pi/\omega_1$ representing the period of the solution, and we have time normalized the equations as explained in connection with (1.52)-(1.53) in the previous section. The coupling parameter κ_{ij} includes all the non-zero terms from

[20] the oscillators will only synchronize if the deviation in the oscillator frequency distribution is on the same order as the coupling strength [27].

[21] some possible coupling structures include the *symmetric group* $\Gamma = \mathbb{S}_n$ which corresponds to identical all-all coupling, $\Gamma = \mathbb{D}_n$, the *Dihedral group*, which corresponds to bilateral ring coupling and $\Gamma = \mathbb{Z}_n$, the *cyclic group*, which represents unilateral ring coupling. We refer to the discussion in section 1.3 for thorough discussion of symmetry as it finds application in the analysis of coupled oscillators.

[22] in the following we consider the special case of *isochronous* oscillators ($b_i = 0$), in order to simplify the expressions as much as possible without loosing sight of the main qualitative points of the analysis. Non-isochronous oscillators are easily included in the formulation as explained in footnote 19.

the i'th row of the coupling matrix in (1.61). In the following we shall assume symmetric oscillators (*i.e.* $\rho_{r,i} = \rho$, $d_i = d$ *etc.*) and symmetric coupling which implies that $\kappa_{ij} = \kappa$ for all i, j which involve non-zero contributions. Which terms are non-zero depends on the coupling symmetry Γ. It then follows from the above discussion that A_i and Φ_i are both $\Gamma \times \mathbb{S}^1$-equivariant [23].

It is important to understand that the functions, $\Lambda_i(\cdot)$, $\Phi_i(\cdot)$, in (1.65)-(1.66) are not derived from the uncoupled system (1.62)-(1.63) by simply adding them to the righthand-side of the equations. Instead, they are the result of a nonlinear mixing process which initiates the synchronized state. The multiple Andronov-Hopf normal-form considers the loss of stability at a fixed point in state space whereafter the oscillators settle on $\mathbb{T}^n$. At this point there is no phase relation between the individual oscillators. We then introduce a small coupling $|\kappa| \ll 1$; the different tones will mix in the oscillator nonlinear energy restoring circuit component; modelled here by the first term on the righthand side of (1.62). Eventually, if the coupling is weak, and if the asymmetry of the oscillators is even weaker, this system will find an equilibrium synchronized state represented by the symmetry $\mathbb{S}$. This system is then modelled by (1.65)-(1.66). In order to illustrate this let us consider the multiple Andronov-Hopf normal-form in (1.62)-(1.63) where the *resonant monomials*, for the i'th equation, had the form

$$z_i \quad z_i^2\overline{z}_i \quad z_i^3\overline{z}_i^2 \quad ect. \tag{1.67}$$

The normal-form equations of the synchronized system in (1.65)-(1.66) will also contain these terms. However, because of the $\mathbb{S}^1$ symmetry, caused by the frequency-lock, this normal form will also have terms on the form

$$\kappa z_j \quad \kappa z_i^2\overline{z}_j \quad \kappa^2 z_i z_j \overline{z}_j \quad \kappa^2 z_i^3\overline{z}_j^2 \quad ect. \tag{1.68}$$

where the subscript i again refers to the oscillator under consideration and j represents an oscillator unit that is coupled to this cell. Let us consider the first term in (1.68), κz_j. We now add the new coupled oscillator resonant terms to (1.65)-(1.66), written on complex form [24], which then gets the form

$$\dot{z}_i = \cdots + \kappa z_j \tag{1.69}$$
$$\dot{\overline{z}}_i = \cdots + \kappa \overline{z}_j \tag{1.70}$$

by copying the procedure which led to the single oscillator amplitude/phase equations in (1.43)-(1.44) we can find the two coupling functions in (1.65)-(1.66) as follows

$$\Lambda_i = \frac{1}{2A_i}\big\{\dot{z}_i\overline{z}_i + z_i\dot{\overline{z}}_i\big\} =$$
$$\frac{1}{2A_i}\big\{\kappa z_j\overline{z}_i + z_i\kappa\overline{z}_j\big\} = \frac{\kappa A_j}{2}\big\{\exp\big(j[\phi_j - \phi_i]\big) + \exp\big(j[\phi_i - \phi_j]\big)\big\} \Rightarrow$$

$$\boxed{\Lambda_i = \kappa A_j \cos(\phi_j - \phi_i)} \tag{1.71}$$

$$\Phi_i = \frac{-j}{2A_i^2}\big\{\dot{z}_i\overline{z}_i - z_i\dot{\overline{z}}_i\big\} =$$
$$\frac{-j}{2A_i^2}\big\{\kappa z_j\overline{z}_i - z_i\kappa z_j\big\} = \frac{\kappa A_j}{2A_i}\big\{\exp\big(j[\phi_j - \phi_i]\big) - \exp\big(j[\phi_i - \phi_j]\big)\big\} \Rightarrow$$

[23] see (1.35) on page 19 for a definition of vector field equivariance.

[24] see discussion in connection with the derivation of (1.12)-(1.13), on page 15.

$$\Phi_i = \kappa \frac{A_j}{A_i} \sin(\phi_j - \phi_i) \qquad (1.72)$$

where we have set $z_i = A_i \exp(j\phi_i)$ and $z_j = A_j \exp(j\phi_j)$. The expressions in (1.71)-(1.72) should look familiar to anyone acquainted with qualitative coupled oscillator analysis. In particular, (1.72) constitutes the functional form of the famous Kuramoto model [27], which considers *all-to-all* coupled ($\Gamma = \mathbb{S}_n$) harmonic oscillators. Often the expressions in (1.71)-(1.72) are derived through averaging procedures [6], [28], illustrating that averaging is a "short-cut" to deriving the normal-form equations; an issue we shall discuss further in the next section of this chapter. However, normal-form calculations supplies us with something that a simple averaging procedure could never bring - a clear view of the "big picture" of qualitative coupled oscillator behavior.

At this point we return to the subject of *weak coupling* which was introduced in the introduction to this section. Throughout the development, which eventually lead to the statements in note 1.5, we were assuming a persisting n-torus $\mathbb{T}^n$, which were connected to the hyperbolic amplitude state equations in (1.65). However, the hyperbolic amplitude equations can of-course only be ensured if the perturbing term (*i.e.* the coupling) is smaller than the eigenvalue determining the linear stability of the amplitude branch $A = \alpha$. This eigenvalue is also know as the *Floquet characteristic component*, and from note 1.2 on page 22 we know that this is equal to $2\mu_o$. If $|\kappa| > 2\mu_o$ then the coupling function A_i will potentially control the amplitude dynamics in (1.65) which means that the n-torus could possibly be destroyed. Alternatively, the strong coupling could lead to *amplitude death* [27]. Let us just for a brief moment consider the general case where the oscillators have different parameters in (1.65)-(1.66). If the condition

$$\mu_o = \min_i\{\mu_{o,i}\} \gg \max_j\{\kappa_{ij}/2\} \qquad (1.73)$$

is upheld for the normal form equations (1.65)-(1.66), then we say that the invariant manifold of the solutions is the *normally hyperbolic n-torus* $\mathbb{T}^n$. The term "normally hyperbolic" refers to the time-constants governing the tangent-space dynamics. If (1.73) applies, then the dynamics normal to the torus are characterized by the fast time-constant $2\mu_o$. The dynamics tangential to the torus, which represent the phase orbits, is seen from (1.66) to be characterized by a slow time-constant on the order $O(|\kappa|)$.

Imagine that we create N initial values, off the torus, in the laboratory. If (1.73) is fulfilled the orbits corresponding to each of these initial values will do a very quick approach onto $\mathbb{T}^n$ and once on the torus they will be governed by the slow dynamics of (1.66). On the observable time scales it will then look as if the orbits where initially on the manifold. We therefore almost only observe the *slow tangent phase dynamics* in (1.66). A good mental picture would be to imagine the points in state-space as *sticking* to the n-torus. We summarize the above discussion as

note 1.6 *the n-torus $\mathbb{T}^n$ and the state equations describing the synchronized solution are normally hyperbolic if* (1.73) *is fulfilled. Weak coupling implies normal hyperbolicity and hence refers to a scenario where the slow phase orbits dominate the fast amplitude dynamics on all time scales of practical importance. A normal hyperbolic manifold implies that the coupling is weaker than the dissipation.*

In the above note we used the notation from note 1.2 on page 22 to link μ_o in (1.73) with the concept of *dissipation*. Normal hyperbolicity will play a significant role in the construction of a projection formalism for the numerical characterization of coupled oscillators perturbed by noise, as described in chapter 3.

This section concludes with a brief discussion of what is known as the *phase-only* representation of n coupled oscillators. Let us consider the theoretic limit $\mu_o \to \infty$ in (1.65)-(1.66). No matter how strong coupling we introduce : on all observable time scales, we will only be able to observe the phase dynamics while the amplitude will be unobservable. We can therefore *adiabatically* remove the amplitude equations in (1.65) from the system [25]. We hence arrive at the following *phase-only*, representation of n coupled harmonic oscillators [29]

$$\frac{d\phi_i}{d\tau_i} = \frac{2Q_i}{\omega_i}\Delta\omega_i + \Phi_i(\alpha_1, \cdots, \alpha_n, \phi_1, \cdots, \phi_n; \kappa_{ij}) \quad i = 1, 2, \cdots n \tag{1.74}$$

where $\Phi = [\Phi_1 \cdots \Phi_n]$ is $\Gamma \times \mathbb{S}^1$ equivariant. Note that (1.74) is "approximately" representative of the full system dynamics if the normally hyperbolic condition in (1.73) is fulfilled.

1.2 Averaging Theory

The classical formulation of oscillator averaging theory is discussed in the paper [30], which was written by Peter Ashwin. Here we consider the general second order lossless system perturbed by a weak dissipative force

$$\ddot{x} + \frac{dU}{dx} = \varepsilon F(x, \dot{x}) \tag{1.75}$$

where $x \in \mathbb{R}$ is the state variable, $U(x) : \mathbb{R} \to \mathbb{R}$ is the circuit potential, $|\varepsilon| \ll 1$ is a small parameter representing the weakness of the dissipation as given by $F(x, \dot{x})$. For zero dissipation ($\varepsilon = 0$), the solutions of (1.75), $z(\alpha, \psi)$, represents *constant energy orbits*

$$\underbrace{\frac{\omega}{2}\left(\frac{\partial z}{\partial \psi}\right)^2}_{\text{kinetic energy}} + \underbrace{U(z)}_{\text{potential energy}} = \underbrace{\alpha}_{\text{total energy}} \tag{1.76}$$

where α is the energy of the solution, $z(\alpha, \psi)$, which is 2π periodic in ψ, and ω is the period of the solution before time-normalization. Equation (1.76) is also known as the *Hamiltonian* [26] of the system and an analytic solution, for a given set of initial conditions, can be found by integrating this expression [27].

The introduction of a small dissipative perturbation suggests that the total energy of the system will no longer be constant on the orbits corresponding to the solutions of (1.75), which then instead take the form

$$x(t) = z(\alpha(t), \psi(t)) \tag{1.77}$$

[25] by which we mean that we set each variable A_i equal to its steady-state value α_i.

[26] in the introduction to this report we considered the coupled pendulum scenario which originally led Huygens to discover the phenomena of synchronization (see discussion on page 6). As mentioned, this system was almost loss-free and could hence be described as an Hamiltonian system.

[27] this requires the use of so-called *Jacobian integrals*; a topic well beyond the scope of this report. We refer the interested reader to [30].

where the energy α and the phase ψ are now *slowly varying* functions of time. This slowness follows directly from (1.75) and the smallness of ε. In [30] it shown how the energy and phase variables obey the equations

$$\dot{\alpha} = \varepsilon\omega\left(\frac{\partial z}{\partial \psi}\right)F(\alpha,\psi) \tag{1.78}$$

$$\dot{\psi} = \omega - \varepsilon\omega\left(\frac{\partial z}{\partial \alpha}\right)F(\alpha,\psi) \tag{1.79}$$

where we have set $F(\alpha,\psi) \equiv F(z(\alpha,\psi),\dot{z}(\alpha,\psi))$. The solution of (1.78)-(1.79) can be expanded in powers of ε

$$\alpha(\varphi) = \alpha^{(0)} + \varepsilon\big(\alpha^{(1)} + \beta^{(1)}(\varphi)\big) + O(\varepsilon^2) \tag{1.80}$$

$$\psi(\varphi) = \varphi + \varepsilon\phi^{(1)}(\varphi) + O(\epsilon^2) \tag{1.81}$$

where φ is the linear phase of the unperturbed solution of (1.76) and both $\beta^{(1)}$ and $\phi^{(1)}$ are 2π periodic functions of their arguments. Inserting (1.80)-(1.81) into (1.78)-(1.79), equating terms of same power of ε, and averaging the resulting equations, we get the so-called *persistence conditions* [31], from which we can find the unknown parameters and functions in (1.80)-(1.81). The procedure is easily extended to coupled oscillators by introducing a new perturbing function, $\varepsilon^2 G(x,\dot{x})$, in (1.75), where x now represents the vector $x = [x_1\ x_2\ \cdots\ x_n]$ and we have assumed that the coupling is one order weaker than the dissipation [28].

Although the above method is very general and mathematical rigorous, this comes at a price; in order to reach any kind of usable results one has to go through several lengthy and tedious calculations. In this report we shall therefore opt for a more user-friendly formulation which only deals potentials of the form

$$U(x) \propto x^2 \tag{1.82}$$

implying a harmonic solution. We shall refer to the methods and techniques connected with averaging of harmonic oscillators as *Kurokawa theory*, since K. Kurokawa introduced this formulation in [32]. This particular averaging approach has become a standard for qualitative analysis of electrical coupled harmonic oscillators [6],[10],[13],[32]. The publications [32], [33] contain the original work of Kurokawa. Another, more recent, contribution can be found in the work of Vanassche *et al.* [34],[35]. In appendix B, on page 142, we have included thorough and easy-to-read introduction to Kurokawa theory. This text is recommended as good introduction for persons unfamiliar with the subject.

Assume that the state equations have been projected onto the center-manifold, as described in section 1.1.1. We then consider the general second order system [29]

$$L\frac{\partial i_L}{\partial t} = -v_C \tag{1.83}$$

$$C(v_C)\frac{\partial v_C}{\partial t} = i_L - \frac{v_C}{R} + G_{mo}(v_C)v_C \tag{1.84}$$

[28] this is necessary to ensure a normally hyperbolic n-torus $\mathbb{T}^n$. See discussion in section 1.1.2 and note 1.6 on page 27 for an explanation.

[29] the physical circuit represented by these equations is depicted in figure B.1 on page 142.

where the different parameters and variables were discussed in connection (1.1)-(1.2), on page 13, and we have included a *nonlinear capacitance/varactor* $C(v_C) = c_0 + c_1 v_C + c_2 v_C^2$. As was shown in (1.77), the solution can be written as the constant energy solution, which for the potential in (1.82) implies a sinusoid $\cos(\omega_0 t)$, with a slow modulation of the energy/amplitude and phase. We therefore write the following *quasi-sinusoidal solution* of (1.83)-(1.84)

$$v_C(t) = A(t)\cos(\omega_0 t + \phi(t)) \tag{1.85}$$

where A and and ϕ are the slow *envelope* and *phase* of the *quasi-sinusoidal* solution. Equation (1.85) can only be a good approximation of the true solution if the higher order harmonics are sufficiently suppressed This must mean that the frequency discriminator/resonator [30] must be high-Q , [4], [36]. We put these observations into a note

note 1.7 *the Kurokawa method assumes a quasi-sinusoidal / harmonic solution of the center-manifold equations. This, in-turn, implies a high-Q oscillator.*

This statement should come as no surprise, as weak dissipation was also implied in the more general formulation which led to the perturbed solution in (1.77).

The actually averaging procedure, applied to the system in (1.83)-(1.84), is rather extensive and is therefore referred to appendix B, where the noise forced oscillator is investigated. Ignoring the noise forcing current source i_n, and re-defining the oscillator phase as $\phi \to \phi + \omega_0 t$, we can write (B.36)-(B.37), on page 146 in appendix B, as

$$\frac{1}{\hat{A}}\frac{dA}{d\tau} = s\left[1 - \left(\frac{A}{\alpha}\right)^2\right]\frac{A}{\hat{A}} \tag{1.86}$$

$$\frac{d\phi}{d\tau} = 2Q + rA^2 \tag{1.87}$$

where the different parameters are listed in (B.38)-(B.39) on page 146. If we, furthermore, assume a constant capacitance $C(v_C) = c_0$ then we get $r = 0$ and $s = \mu_o$. Comparing the above system with normal-form equations in (1.52)-(1.53), on page 21, we see that they are similar in form. However, from (B.43) we get the following amplitude for the averaging method $\alpha_{avr} = \sqrt{4(g_0 - G)/(3g_2)}$, while the normal-form method gives the result $\alpha_{nf} = \sqrt{(g_0 - G)/(3g_2)}$. We see that $\alpha_{avr}/\alpha_{nf} = 2$.

In section 4.3, on page 90, we derive the averaged equations n oscillators coupled in a unilateral ring with an implicit phase shift β. The synchronized state is represented mathematically by the group $\mathbb{Z}_n^\beta \times \mathbb{S}^1$. Assuming linear coupling [31], the equations take the form

$$\frac{dA_i}{d\tau_i} = \mu_{o,i}\left[1 - \left(\frac{A_i}{\alpha_i}\right)^2\right]A_i + \frac{g_{c0}}{G_{Li}}\cos\big(\phi_{i-1} - \phi_i + \beta\delta_{1i}\big)A_{i-1} \tag{1.88}$$

$$\frac{d\phi_i}{d\tau_i} = \frac{2Q_i}{\omega_{0i}}\Delta\omega_i + \frac{g_{c0}}{G_{Li}}\sin\big(\phi_{i-1} - \phi_i + \beta\delta_{1i}\big)\frac{A_{i-1}}{A_i} \tag{1.89}$$

$$i \in \{1, 2, \cdots, n | i = 1 \Rightarrow i - 1 = n\}$$

[30] see figure B.1 on page 142.

[31] this means that we set $G_{mc,i}(A_{i-1}) = g_{c0,i} - \frac{3}{4}g_{c2,i}A_i^2$ in (4.47), on page 93, equal to g_{c0}.

By comparing (1.88) and (1.89) with the normal form results in (1.71) and (1.72), respectively, we see that (1.88)-(1.89) has the same form as the normal-form equations in (1.65)-(1.66) on page 25 [32].

Based on the above derivations in (1.86)-(1.87) and (1.88)-(1.89), we can state the following observation

note 1.8 *the averaging method can be seen as short-cut to deriving the normal-form state equations. The two procedures will lead to equations which are similar in form, while the specific parameter expressions may differ.*

1.3 Symmetry Considerations

The theory of symmetrically coupled Adronov-Hopf bifurcations was developed by Golubitsky *et al.* in the book [25] [33]. Later, in the paper [29], Ashwin simplified the formulation, by investigating the problem using the *phase-only representation* of n coupled oscillators, which was derived in (1.74) on page 28.

Apart from being an introduction to group theory, as it applies to the analysis of coupled oscillators, this section is concerned with answering the question

Given n identical oscillators and a symmetric coupling network, which possible frequency-locked solutions, also known as modes, exist.

and although we shall not derive the actual analytical expressions we do intend to review some of the general results from [29] which will allow us to calculate the modes for a given coupling structure. These results are then used in chapter 4, where we set out to investigate the possible modes of an unilateral ring of n coupled oscillators with an explicit phase shift.

Before we start, let us address a concern often voiced when it comes to symmetry calculations. Briefly, the argument goes as follows

Since the concept of perfect symmetry, i.e. identical oscillators, coupling etc., are mathematical thought-experiments, the calculations made using such definitions have no physical relevance.

While it is certainly true that perfect symmetry does not exist in nature, it is however quite reasonable to argue in favor of the benefits of symmetry calculations applied to the analysis of *nearly* symmetric systems. We suppose that the Jacobian of the state equations, with regard to the system parameters, is non-singular. The *implicit function theorem*[34] then guarantees that the solution curves, as a function of these parameters,

[32] the explicit phase shift β is not important here and can be ignored. Comparing with the normal-form in (1.65)-(1.66) it is seen that we have defined the coupling strength as $\kappa_i = g_{c0}/G_{Li}$ and, furthermore, that we have chosen the non-resonant monomial z_j as $z_j = z_{i-1}$ which follows from the symmetry $\Gamma = \mathbb{Z}_n$.

[33] as far as this author can tell; see also [37].

[34] the implicit function theorem, in 1 dimension, states that if the derivative of a function $f(x, \epsilon) : \mathbb{R} \times \mathbb{R} \to \mathbb{R}$, with respect to the parameter ϵ, is different from zero then there exist a branch of solution curves $x(\epsilon)$ to the equation $f(x, \epsilon) = 0$ (we assume that $f(x, 0) = 0$ has a solution), in a small region around $\epsilon = 0$. This also holds for higher dimensional systems where the derivative should now be substituted for the vector field Jacobian [25], [37].

will be *continuous*. Thus, as the parameters disperse around their symmetric mean, the solution curves will disperse in a similar fashion; *continuously* away from perfect symmetry. However, since we assume that the variance of the parameter dispersion is small, it follows that the solution will stay *close* to the original symmetric solutions. In the words of Golubitsky *et al.* [37]

note 1.9 *the nearly symmetric solutions still have much more in common with the perfectly symmetric orbits, than they do a solution from a system with no symmetry.*

The phase-only equations of n coupled oscillators were derived in (1.74) in section 1.1.2. For symmetric oscillators we get

$$\frac{d\phi_i}{d\tau_i} = \Phi_i(\phi_1, \cdots \phi_n; \kappa_{ij}) \quad i = 1, 2, \cdots n \tag{1.90}$$

As discussed in section 1.1.2, the phase vector function $\Phi = [\Phi_1 \cdots \Phi_n]$ is $\Gamma \times \mathbb{S}^1$ equivariant. By normalizing the oscillator amplitudes α_i in (1.74), we can write the *normally hyperbolic n-torus*, on which the orbits descibed by (1.90) live, as

$$\mathbb{T}^n = \underbrace{\mathbb{S}^1 \times \mathbb{S}^1 \cdots \times \mathbb{S}^1}_{n \text{ times}} = \{z \in \mathbb{C}^n \mid |z_i| = 1\} \tag{1.91}$$

On $\mathbb{T}^n$, as it is defined above, the individual oscillators are represented by a unit amplitude phasor $z_i = e^{j\phi_i}$ in the complex plane $\mathbb{C}$.

The symmetry of a solution is given by its *isotropy subgroup*, which is a selection of operations/actions, contained in $\Gamma \times \mathbb{S}^1$, which preserve the synchronized phase configuration in question. As shown in [29], these subgroups will inherit the structure of the original coupled oscillator symmetry $\Gamma \times \mathbb{S}^1$. This group has a *spatial part*, Γ, which concerns the permutation of the n identical oscillators, and a *temporal part*, $\mathbb{S}^1$, which concerns the combined phase shift of the synchronized solution[35]. Any subgroup Σ can hence also be divided into a spatial part $\pi_s(\Sigma)$ and a temporal part $\pi_t(\Sigma)$. We then write any action, contained in this group, as

$$(\sigma, w) \in \Sigma \quad ; \ \sigma \in \pi_s(\Sigma) \quad ; \ w \in \pi_t(\Sigma) \tag{1.92}$$

Since the states, by definition, are fixed by an action contained in the isotropy subgroup, we get

$$z_i = (\sigma, w) z_i = w z_{\sigma(i)} \tag{1.93}$$

As an example of an action $\sigma \in \pi_s(\Sigma)$, consider 4 coupled oscillators and the operation $\sigma = (12)(34)$ which states *"switch oscillator 1 and 2 and switch oscillator 3 and 4"*

$$\sigma(z_1, z_2, z_3, z_4) = (z_{\sigma(1)}, z_{\sigma(2)}, z_{\sigma(3)}, z_{\sigma(4)}) = (z_2, z_1, z_4, z_3) \tag{1.94}$$

We can also define σ^{-1} which refer to the inverse mapping

[35] and autonomous dynamical system is independent of a constant phase-shift. For the coupled oscillator configuration studied here, this means that all n oscillators should be shifted an equal amount. This combined phase-shift is also known as the *diagonal phase* (see discussion in section 4.5.1).

$$(z_1, z_2, z_3, z_4) = \sigma^{-1}(z_2, z_1, z_4, z_3) = \big(z_{\sigma^{-1}(2)}, z_{\sigma^{-1}(1)}, z_{\sigma^{-1}(4)}, z_{\sigma^{-1}(3)}\big) \tag{1.95}$$

and we therefore see that $\sigma \in \pi_s\big(\Sigma\big)$ must be a *isomorphism* [36]. Another example is given by the *n-cycle*

$$\sigma = (1, 2, \cdots, n) \tag{1.96}$$

which works by permuting the n oscillators in a cyclic fashion. For this group we can also define σ^k as

$$\begin{aligned}
&\sigma^0 = I \\
&\sigma^1 = (1, 2, 3 \cdots, n) \\
&\sigma^2 = (n, 1, 2, \cdots, n-1) \\
&\vdots \\
&\sigma^{n-1} = (2, 3, 4 \cdots, 1)
\end{aligned} \tag{1.97}$$

This action has special importance to this report since it serves as generator for the *cyclic group* $\mathbb{Z}_n$. In chapter 4 we shall consider the analysis of a system of harmonic oscillators with coupling symmetry $\Gamma = \mathbb{Z}_n$.

Any action $\sigma \in \pi_s\big(\Sigma\big)$ will divide the n oscillators into l disjoint partitions of lengths k_j , $j = 1, 2 \cdots, l$. As an example, consider 9 coupled oscillators and the operation

$$\sigma = (1 \to 3, 2 \to 1, 3 \to 4, 4 \to 2)(5, 6, 7)(89) \tag{1.98}$$

where $(5, 6, 7)$ refers to the 3-cycle as defined in (1.96)-(1.97) and (89) refers to the switching of oscillators 8 and 9 (see discussion in connection with (1.94)). As illustrated in figure 1.2, this action divides the 9 oscillators into 3 disjoint sets with $k_1 = 4$, $k_2 = 3$ and $k_3 = 2$. The figure illustrates, that if z_i is member of partition j, then we have

$$\sigma^{k_j} z_i = z_i \tag{1.99}$$

Using the result in (1.99), we can write (1.93) as

$$z_i = w^{k_j} z_{\sigma^{k_j}(i)} = w^{k_j} z_i \tag{1.100}$$

which means that we must have

$$w^{k_j} = 1 \quad ; \; w \in \pi_t\big(\Sigma\big) \tag{1.101}$$

However, since $\sum_j k_j = n$ (see figure 1.2) we can derive the important result

$$w^n = w^{\sum k_j} = \prod w^{k_j} = 1 \tag{1.102}$$

This is interpreted to mean that the temporal projection of Σ is represented by subgroup of $\mathbb{Z}_n$ [29]. We can therefore write $\pi_t\big(\Sigma\big) \equiv \mathbb{Z}_m$ for some m which divides n.

We summarize the above results as follows

[36] a map f is an *isomorphism* if it is bijective *i.e.* one-to-one (injective) and onto (surjective) and if both f and f^{-1} are structure-preserving (homeomorphisms).

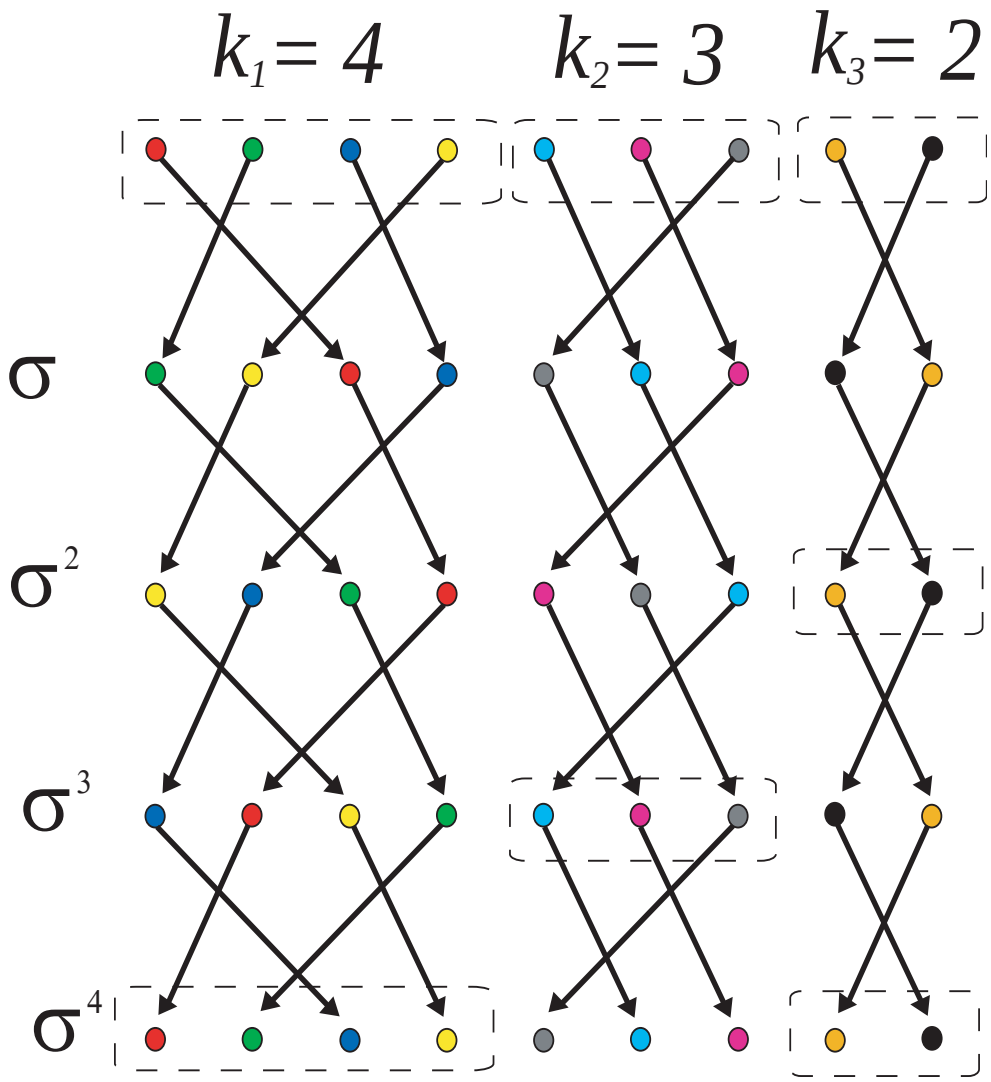

Figure 1.2: The 9 coupled oscillators are divided into 3 disjoint sets by the action σ defined in (1.98). The sets have lengths $k_1 = 4$, $k_2 = 3$ and $k_3 = 2$. The individual oscillators are represented by colored dots : $\#1 =$ •, $\#2 =$ •, $\#3 =$ • *etc.* The dotted boxes encapsulates the original configuration of the 3 sets and also signal the return to this state after a certain number of operations. Set number 1, consisting of oscillators $\#1 - \#4$, returns to the original state after 4 operations, set number 2 ($\#5 - \#7$) after 3 operations and set number 3 ($\#8 - \#9$) after 2 and 4 operations. From the above example it is seen that if oscillator $\#i$, as represented by the phasor z_i (see (1.91)), belongs set j, then we have that $\sigma^{k_j} z_i = z_i$ [29].

note 1.10 *The modes of the $\Gamma \times \mathbb{S}^1$ symmetric system of n coupled oscillators constitute spatio-temporal symmetries which represent the fixed spaces of the isotropy subgroups Σ. The actions contained in these subgroups are written (σ, w) where $\sigma \in \pi_s(\Sigma)$ and $w \in \pi_t(\Sigma)$. The spatial projection $\pi_s(\Sigma)$ must be a subgroup of the coupling symmetry Γ and the temporal projection $\pi_t(\Sigma)$ must be a subgroup of $\mathbb{Z}_n$*

From the above text we see that we can write $w \in \pi_t(\Sigma)$ as

$$w = \omega^m = e^{j2\pi\frac{m}{n}} \tag{1.103}$$

where m divides n and we have used the notation

$$\omega = e^{j\frac{2\pi}{n}} \tag{1.104}$$

Chapter 2

Single Oscillators Perturbed by White Noise - Inhomogeneous Phase Diffusion

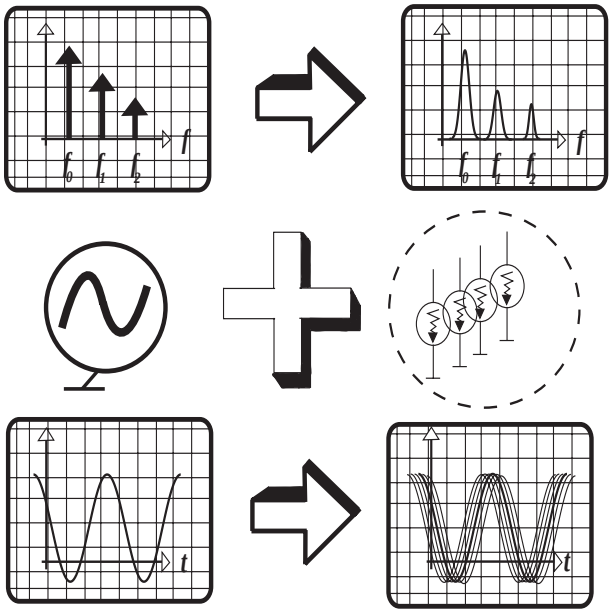

Figure 2.1: Illustrating the effects of oscillator noise in the frequency and time domains. The oscillator spectrum, as measured with a spectrum analyzer, is shown in the two top screens of the figure. Without noise (left screen), the spectrum consist of a series of impulses at the harmonics of the solution. With noise (right screen), the spectrum spreads out, resulting in a Lorentzian characteristic [38], [14]. The time domain waveform, as measured with an oscilloscope, is shown in the two lower screens. Without noise (left screen), the waveform has DC (zero) crossing with perfect timing. With noise (right screen), the uncertainty in timing of the zero crossings increases linearly with time [14].

The subject of this chapter concerns the formulation of a *linear response* model for the stochastic phase dynamics of a free-running oscillator perturbed by white noise sources. The main interest in this regard centers around the effects of *phase diffusion*, which is measured in the time domain as *jitter* and in the frequency domain as *phase noise*.

Phase noise/jitter is a consequence of the inescapable shot and/or thermal noise sources [1], present in all dissipative circuit structures, modulating the oscillator phase. This phase modulation will result in a broadening of the frequency-domain spectrum, which without noise, would be a series of impulses at the harmonics of the carrier. In the time-domain, jitter manifests itself as an increased spread in the zero-crossings of the wave-forms over time. Figure 2.1 attempts to illustrate the above discussion, where the screens on the left-hand side considers a frequency/time-domain measurement without noise, which is then added on the right-hand side.

The noise driven oscillator phase will be identified as an *inhomogeneous diffusion process*, where by inhomogeneous we take to mean that the *diffusion constant* will depend both on time and the oscillator phase. Understanding the asymptotic properties of this process turns out to be a non-trivial task which will occupy the first part of this chapter. The goal of these introductory investigations will be to extract the *effective diffusion constant* D_{eff} which will allow us to identify the asymptotic statistics with a *Wiener process*, which is a trivial homogeneous diffusion process. In sections 2.2.1, 2.2.2 and 2.2.3 we give short introductions to three well-established methodologies for the analysis of single oscillators perturbed by noise. It is subsequently shown how D_{eff} is derived within each of these different frameworks.

2.1 A Linear Response Theory for Noise Forced Limit Cycle Solutions

A free-running oscillator, with n internal degrees of freedom, is described mathematically through the autonomous ordinary differential equation

$$\dot{x} = f(x) \tag{2.1}$$

where $x(t) : \mathbb{R} \to \mathbb{R}^n$ is a vector in n dimensional state space and $f(\cdot) : \mathbb{R}^n \to \mathbb{R}^n$ is the *vector field* of the autonomous system. Equation (2.1) has a periodic solution $x_{ss}(t+2\pi) = x_{ss}(t)$, where a period of 2π is the result a time normalization $t \to t\omega_0$, with $T_0 = 2\pi/\omega_0$ being the true period of the solution. Furthermore, since the oscillation is assumed asymptotically stable, any orbit corresponding to an arbitrary set of initial conditions will approach this solution asymptotically with time. Mathematically speaking, we say that there exist a *ω-limit set* $\gamma \equiv \{x_{ss}(\phi) | \phi \in [0, 2\pi]\}$ which in this case is also known as a *limit cycle*. From the above definition of γ we see that points in the limit cycle are indexed by a single periodic state variable ϕ which is referred to as the *phase* of the oscillator.

For all purposes, noise, as it exists in room temperature electrical circuits, can be modelled as a *small signal* when compared to the steady-state signal of any practically relevant oscillator. The complete response of (2.1), forced by noise, can therefore be written as the sum of a noiseless steady state and a small signal noise response

$$x(t) = x_{ss}(t) + y(t) \tag{2.2}$$

where $|y|/|x_{ss}| \ll 1$ for all time t. The branch of ODE perturbation analysis which considers solutions of the form (2.2) is known collectively as *linear response theory*. This name refers back to the condition of small perturbative noise signals which allows for the use of linearization techniques to approximate the solution.

[1] we will not consider colored noise as *e.g.* $1/f$-noise, although this would be possible within the framework presented here. See the paper [16] for a discussion of this issue.

We have split the text in this section up into two subsections. In 2.1.1 we consider the derivation of relevant *stochastic differential equation* (SDE) which is then used in 2.1.2 to produce the relevant *Fokker-Planck equation*; a parabolic partial differential equation which solves for the time dependent *probability density* of the stochastic oscillator phase.

2.1.1 Deriving the Oscillator Phase Stochastic Differential Equation

Using the notation in (2.2), we can write (2.1) as

$$\dot{x}_{ss} + \dot{y} = f(x_{ss} + y) \approx f(x_{ss}) + A(t)y \tag{2.3}$$

where the $\approx$ sign in the above equation refers to fact that we cut the Taylor expansion of f at the first term [2]. In (2.3), $A(t) : \mathbb{R} \to \mathbb{R}^{n\times n}$ is the 2π periodic *Jacobian* of the vector field, taken at every point of the limit cycle γ, indexed by time t

$$A(t) = \left.\frac{df}{dx}\right|_{x=x_{ss}(t)} \tag{2.4}$$

which is a 2π periodic $n \times n$ matrix. Inserting $\dot{x}_{ss} = f(x_{ss})$, which follows from (2.1), into (2.3), we get

$$\dot{y} = A(t)y \tag{2.5}$$

Inspecting (2.5), we see that the noise response, y, is solved for by the *first variational* of (2.1); this constitutes the essence of linear response theory.

We now consider the Jacobian at a fixed point on the limit cycle $A(t_0)$. As will be established, there exist an eigenvector of the Jacobian $A(t_0)$ in the direction tangent to the limit cycle, which is the direction of the oscillator phase increase. Furthermore, the eigenvalue corresponding to this eigenvector is zero, resulting in a *neutrally stable* phase variable. From (2.1), it is seen that the vector field in question is autonomous, which means that the solution will not depend on the *absolute time* but only on the *elapsed/relative time*, given the initial conditions. By perturbing tangentially to the limit cycle γ we stay on the same orbit, albeit with new initial conditions. The system in (2.5) does not counteract this change of initial conditions since this event simply resets the origin of *absolute time* which, as discussed above, is inconsequential when considering linear response of autonomous vector fields. From the above description, it should be clear that a tangential perturbation/shift implies a zero response from the variational equation in (2.5). Consider a state-space vector y_1, which represents the part of $y(t_0)$ in (2.5) which lies in a direction tangential to γ. Using (2.5), we find for a tangential perturbation at time $t = t_0$

$$\dot{x}_{ss}(t_0 + s) = f(x_{ss}(t_0 + s)) + A(t_0)y_1 \tag{2.6}$$

illustrating that the response to the perturbation still lies on the orbit x_{ss} but now with an added phase shift, s, representing the new initial conditions. However, since the system in (2.1) is *autonomous* we have that

$$\dot{x}_{ss}(t_0 + s) = f(x_{ss}(t_0 + s)) \tag{2.7}$$

which, when used in (2.6), must mean that

$$A(t_0)y_1 = 0 \tag{2.8}$$

[2] this means that the solution will be correct up to order $O(|y|^2)$.

We see that the tangent perturbation, y_1, lies in the *null space*, or *kernel*, of $A(t_0)$ which is another way of saying that y_1 is an eigenvector of $A(t_0)$ with eigenvalue 0.

State space volume/area outside the limit cycle will contract while volume/area inside γ will expand. This follows from the assumption of a stable limit cycle γ which implies that any perturbation of the steady state in a direction normal to γ will relax back to the limit cycle. Furthermore, since the response to small noise-like signals is modelled by the linear equation in (2.5), this relaxation will be exponential. From the above discussion we then conclude that $A(t_0)$ will have $n-1$ eigenvectors in directions normal to γ and the corresponding eigenvalues must all have real parts less than zero. Furthermore, $A(t_0)$ has one, *and only one*, eigenvector with eigenvalue zero corresponding to the eigenvector tangential to γ. Since the time index t_0 in the above derivations was arbitrarily chosen, we can generalize the results to hold for all times t. We summarize as follows

note 2.1 *the phase of a free-running oscillator is without reference since the solution corresponding to an autonomous vector field does not depend on the absolute time or, equivalently, since Barkhausen's criterion is upheld for any phase offset. The degree of freedom introduced by an arbitrary oscillator phase leaves the Jacobian matrix, $A(t)$, singular with rank $n-1$. The null space of this matrix is spanned by a vector tangential to the oscillator limit cycle γ at the phase ϕ; corresponding to the time t. The remaining eigenvalues of $A(t)$, corresponding to directions normal to γ, all have negative real parts.*

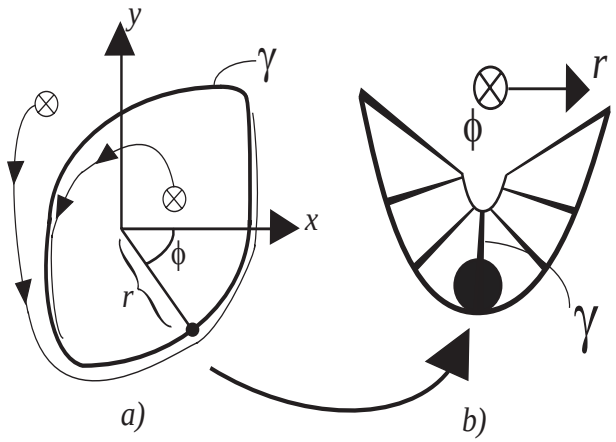

Figure 2.2: a) : an asymptotically stable oscillator represented by the limit cycle γ. State space volume inside the limit cycle expands while that outside contracts. This is illustrated by the two orbits with initial conditions, as represented by the symbol $\otimes$, inside and outside γ, respectively. The oscillator state is symbolized by a solid dot $\bullet$. b) : a view the parallel to the complex plane $\mathbb{C}$ with the origin being place at limit cycle γ. Here, a curve representing a Lyapunov function [21], is superimposed onto the plot. This function represents the potential responsible for the asymptotic stability of the oscillator.

In figure 2.2 we illustrate some of the points made above for a 2 dimensional oscillator [3]. In part *a)* of the figure, the limit cycle γ is plotted in the complex plane $\mathbb{C}$, where the oscillator steady-state, as represented by a solid dot $\bullet$, is referenced by an amplitude and a phase $z(t) = r(t)\exp(j\phi(t))$. In part *b)* we make a cut in the complex plane, letting the cut run through the limit cycle γ. From this cut we can then plot a view parallel to the plane $\mathbb{C}$, with the origin of the coordinate system being placed at γ. Onto this, we superimpose a curve representing the state-space potential which is responsible for the contraction/expansion of volume in the two regions of state space separated by γ. This function is sometimes called the *Lyaponov function* of the system [21]. The oscillator state is still represented by a solid dot $\bullet$.

The figure, together with the previous discussion, as summarized in note 2.1, paves the way for a particular simple *mechanical analogy* of the qualitative dynamics of an arbitrary free-running oscillator. Imagine a plane surface, wherein a furrow/channel has be carved. In figure 2.2 *a)* we see this furrow from above, and in *b)* we have changed the perspective so that we now view *along* the channel. The oscillator state is represented by a ball; initially at rest somewhere in this carved furrow/channel. If we give this ball a short push in a direction along the channel, it will move, and then come to rest at another point further down the channel. The ball has moved to a new equilibrium, illustrating the neutrally stable response of perturbations tangent to the limit cycle. However, if we give a short push in the direction normal to the channel then the ball will, pulled by the potential force (gravity), relax back to the point of origin; illustrating the asymptotic stability of perturbation normal to the limit cycle. The model sketched above, albeit too simple to pass for a realistic representation of a specific oscillator, does supply us with a good qualitative understanding of basic oscillator dynamics. More importantly, the mathematical rigorous results obtained using *equivalence theory*, as reviewed in section 1.1, ensures us, that if we understand this simple mechanical model we have understood the qualitative important dynamics of *all isochronous oscillators* [4].

As explained in [14], noise-forcing can be introduced into the formulation in (2.1) by adding to the right-hand side, a vector

$$B(x_{ss}(t))\chi(t) \tag{2.9}$$

where $\chi(\cdot) : \mathbb{R} \rightarrow \mathbb{R}^p$ is a $p \times 1$ column vector consisting of p uncorrelated, zero mean, unit variance, Gaussian white noise sources and $B(\cdot) : \mathbb{R}^n \rightarrow \mathbb{R}^{n\times p}$ is a $n \times p$ matrix accounting for the modulation of the noise sources by the steady-state solution. Furthermore, this matrix also contains information pertaining to the powers/variances of the individual noise sources in $\chi(t)$. From the above description, it is seen that (2.9) is a $n \times 1$ stochastic column vector.

The noise perturbations will continuously reset the initial condition of the orbit, which means that we now operate with a time-dependent oscillator phase $\phi(t)$. However, since we consider a time-normalized formulation we now introduce the oscillator time variable $\alpha(t)$, as

$$\phi(t) = \omega_0\alpha(t) \tag{2.10}$$

where ω_0 is steady-state frequency of the oscillator in radians. Although α have units of time, we choose to refer to it as the *oscillator phase*. The time-dependent phase

[3] referring to the *center-manifold theorem*, which was discussed in 1.1, we know that the 2 dimensional oscillator constitutes a *prototype system*. Any qualitative behavior, observed in higher order "real" oscillators, can thus also be modelled by the system in figure 2.2

[4] an isochronous oscillator describes a system where the frequency is independent of the amplitude. See also discussion in section 1.1.1, on page 21.

behavior witnessed from (2.10) means that we can no-longer talk about the *oscillator phase* as an absolute entity; but this means that we can no-longer refer to the time as an absolute entity. Instead we have to introduce the concept of *instantaneous time/phase* s

$$s = t + \alpha(t) \tag{2.11}$$

corresponding to the instantaneous frequency ω

$$\omega = \omega_0\left(1 + \frac{d\alpha}{dt}\right) \tag{2.12}$$

We can then write the left-hand side of (2.3) as

$$\dot{x}_{ss}(t + \alpha(t)) + \dot{y}(t) = \dot{x}_{ss}(s)\left(1 + \frac{d\alpha}{dt}\right) + \dot{y}(t) \tag{2.13}$$

Equating (2.13) to the right-hand side of (2.3), with the noise vector in (2.9) added, we get

$$\begin{gathered}\dot{x}_{ss}(s)\left(1 + \frac{d\alpha}{dt}\right) + \dot{y}(t) = f\big(x_{ss}(s)\big) + A(s)y(t) + B(x_{ss}(s))\chi(t) \Leftrightarrow \\ \dot{x}_{ss}(s)\frac{d\alpha}{dt} + \dot{z}(s) = A(s)z(s) + B(x_{ss}(s))\chi(t)\end{gathered} \tag{2.14}$$

where we in the last line have used $\dot{x}_{ss}(s) = f\big(x_{ss}(s)\big)$, which follows from (2.1) and we have introduced the new state vector z, as

$$z(s) = y(t) \tag{2.15}$$

Furthermore, since $d\alpha/dt$ is on the order $O(|y|)$, we find that

$$\frac{dz}{dt} = \left(1 + \frac{d\alpha}{dt}\right)\frac{dz}{ds} \approx \frac{dz}{ds} \tag{2.16}$$

since the second order term $dz/ds \times d\alpha/dt$ can be ignored [5].

Let us assume that we, by some means, have created an *orthogonal projection operator* [6] $P(\cdot)$, which projects onto the direction tangential to γ at the phase point indexed by its argument. The noise forcing function $B(x_{ss}(s))\chi(t)$ is a state vector that can be split up into normal and tangential components, with respect to the limit cycle γ. Using the operator P we can hence write (2.14) as [7]

$$\dot{x}_{ss}(s)\frac{d\alpha}{dt} + \dot{z}(s) = \underbrace{(1 - P(s))\big\{A(s)z(s) + B(x_{ss}(s))\chi(t)\big\}}_{\text{normal component}} + \underbrace{P(s)B(x_{ss}(s))\chi(t))}_{\text{tangential component}} \tag{2.17}$$

[5] in the original linear response formulation derived in (2.3) we also ignored terms on the order $O(|y|^2)$ implying that the approximation in (2.16) is legal within this framework.

[6] a projection operator P defines two subspaces U and V such, that if x is an arbitrary vector in the vector space X, then we have $Px \in U$ and $(1 - P)x \in V$. The projection is *orthogonal* if we can write the vector space as the direct sum of the two subspaces $X = U \oplus V$. This must then mean that $P(1 - P) = 0 \Rightarrow P^2 = P$. The noise response y in (2.5) *lives* on the so-called *tangent space* of the manifold γ referring to the fact that y models the linear response of the oscillator. On this tangent space P takes the form of an $n \times n$ matrix.

[7] referring to footnote 6, the operator P will divide a vector x into component normal to γ, as given by $(1 - P)x$, and a component tangential to γ, given by Px. These two components will be orthogonal.

In the above we have used the calculation [8]

$$P(s)A(s)z(s) = A(s)P(s)z(s) = 0 \tag{2.18}$$

which follows because $P(s)z(s)$ is a vector tangential to γ and this vector lies in the null space of $A(s)$, as explained in note 2.1 on page 39. This mean that we in (2.17) can write

$$A(s)z(s) = A(s)z(s) - 0 = A(s)z(s) - P(s)A(s)z(s) = [1 - P(s)]A(s)z(s) \tag{2.19}$$

Since the right-hand side of (2.17) splits up into these two orthogonal projections, the same must apply for the left-hand side. However, from (2.1) we have that $\dot{x}_{ss}(s) = f(x_{ss}(s))$ and since the state-space vector field f, by definition, lies tangential to the orbits and, furthermore, since the limit cycle γ is just another orbit, we have that the vector $\dot{x}_{ss}(s)$ must lie tangential to γ [9]. This implies that $\dot{z}(s)$ is a vector *normal* to γ (*i.e.* $P(s)\dot{z}(s) = 0$) and we can hence write (2.17) as

$$\begin{gathered} P(s)\dot{x}_{ss}(s)\frac{d\alpha}{dt} + (1 - P(s))\dot{z}(s) = \\ (1 - P(s))\big\{A(s)z(s) + B(x_{ss}(s))\chi(t)\big\} + P(s)B(x_{ss}(s))\chi(t) \end{gathered} \tag{2.20}$$

The $p \times 1$ noise vector $\chi(t)$ is written explicitly as $\chi(t) = [\chi_1(t)\ \chi_2(t)\ \cdots \chi_p(t)]^T$, where $\big\langle \chi_i(t)\chi_j(t) \big\rangle = \delta_{ij}$. From the above description, and footnote 7, $P(s)B(x_{ss}(s))\chi(t)$ must be a vector proportional to $\dot{x}_{ss}(s)$ and we can therefore write (see footnote 9)

$$P(s)B(x_{ss}(s))\chi(t) = P(s)\dot{x}_{ss}(s)\sum_i \rho_i(s)\chi_i(t) \tag{2.21}$$

where $\rho_i : \mathbb{R} \to \mathbb{R}$ are a set 2π periodic real functions. Since a sum of uncorrelated Gaussian noise source is statistically identical to a single Gaussian noise source, we can write the sum of modulated noise sources in (2.21) in terms of an equivalent single *macro* source [14] [10]

$$\sum_i \rho_i(s)\chi_i(t) \triangleq \sqrt{\sum_i (\rho_i(s))^2}\xi(t) = \rho(s)\xi(t) \tag{2.22}$$

where $\xi(\cdot) : \mathbb{R} \to \mathbb{R}$ is a zero mean, unit variance, scalar *macro* Gaussian white noise source and $\rho(\cdot) : \mathbb{R} \to \mathbb{R}$ is a 2π periodic modulation function. The identification in (2.22) follows from the fact that the two representations have the same power and hence the same statistics [11]

$$\left\langle \left(\sum_i \rho_i(s)\chi_i(t) \right)^2 \right\rangle = \sum_i \rho_i(s)\rho_j(s)\delta_{ij} = \sum_i \rho_i(s)^2 \tag{2.23}$$

where we used that the individual noise components, $\chi_i(t)$, are uncorrelated. Operating with P on both sides of (2.20), with the definitions in (2.21) and (2.22) inserted, we get [12]

[8] P will commute A *i.e.* $PA = AP$. This follows since P projects onto the null space of A.

[9] *i.e.* $P(s)\dot{x}_{ss}(s) = \dot{x}_{ss}(s)$.

[10] by the symbol $\triangleq$ we take to mean that while the expressions on either side are not equal they are "equal by definition".

[11] a Gaussian noise source is fully described by it's mean and variance/power.

[12] here it is used that if P is a orthogonal projection operator which implies $P(1-P)x = Px - P^2x = Px - Px = 0$ and $P^2x = Px$ for all vectors x. See footnote 6 on page 41. Furthermore, from the above discussion we have $P(s)\dot{x}_{ss}(s) = \dot{x}_{ss}(s)$.

$$\dot{x}_{ss}(s)\frac{d\alpha}{dt} = \dot{x}_{ss}(s)\rho(s)\xi(t) \tag{2.24}$$

In coordinate form, this vector equation leads to the following *stochastic differential equation* (SDE) for the oscillator phase $\alpha(t)$

$$\boxed{\frac{d\alpha}{dt} = \rho(t+\alpha)\xi(t)} \tag{2.25}$$

where we have used the definition of s in (2.11). The above equation illustrates that the phase of a free-running oscillator α is a *neutrally stable* variable since the righthand side only consist of a stochastic forcing function.

2.1.2 Deriving the Oscillator Phase Asymptotic Statistics - the Fokker-Planck Equation

As discussed in appendix A.3, according to the Stratonovich formulation, starting from the SDE in (2.25), we can write the following *Fokker-Planck equation* [39]

$$\frac{\partial p(x,t|x',t')}{\partial t} = \left[\frac{\partial}{\partial x}\rho(t+x)\frac{\partial \rho(t+x)}{\partial x} + \frac{1}{2}\frac{\partial^2}{\partial x^2}\rho^2(t+x)\right]p(x,t|x',t') \tag{2.26}$$

a partial differential equation which solves for the time-dependent probability density of stochastic oscillator phase variable $\alpha(t)$, condition on sharp (deterministic) initial values $\alpha(t') = x'$ at time $t = t'$

$$p(x,t|x',t') = \big\langle \delta(\alpha(t)-x)\big\rangle\Big|_{\alpha(t')=x'} \tag{2.27}$$

where $\big\langle\cdot\big\rangle$ denotes the *ensemble average*. Throughout this section we shall assume the problem is characterized in terms of *natural boundary conditions*

$$\lim_{x\to\pm\infty} p(x,t|x',t') = 0 \quad \text{for all } t \tag{2.28}$$

From (2.27) we get the following initial density

$$p(x,t'|x',t') = \delta(x-x') \tag{2.29}$$

implying that the phase of the oscillator is known at the start of the experiment.

Before we start to investigate possible solutions to (2.26), we shall digress and look at a simplified version of this equation. Often, one find examples in the literature [40],[41] where it is claimed that the phase dynamics of a noise perturbed oscillator is described by the *diffusion equation*

$$\frac{\partial p(x,t|x',t')}{\partial t} = D\frac{\partial^2 p(x,t|x',t')}{\partial x^2} \tag{2.30}$$

with the *diffusion constant* D being a positive real number. This equation is trivial and the solution is easily found as [39]

$$p(x,t|x',t') = \frac{1}{\sqrt{4\pi D(t-t')}}\exp\left(-\frac{(x-x')^2}{D(t-t')}\right) \tag{2.31}$$

Equation (2.31) describes a so-called Wiener Process which is characterized by a constant mean and a variance that increases linearly with time. In figure 2.3, we plot (2.31) for four different times. The plot illustrates how probability mass diffuses out to either side, with increasing time, causing the distribution to approach a uniform characteristic, asymptotically with time. We can interpret the curves in figure 2.3 by noting that the diffusion equation in (2.30) models the integration of white noise with power D [13]. This can be viewed as the limit process of a sum of zero mean, uncorrelated, Gaussian variables with power D. Since the terms are uncorrelated, the power of the sum will equal the sum of the powers of the individual terms resulting in an variance which increases linearly with time.

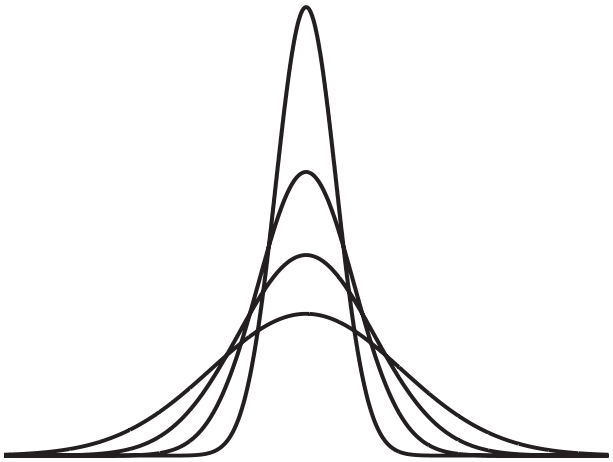

Figure 2.3: The Wiener Process for four different times. The plots illustrate how the variance of the Wiener process increases linearly with time [39], [42].

Unlike (2.30), equation (2.26) is non-trivial and an analytical solution is not easily achieved. From equation (2.26), and the discussion in appendix A.3, we see that we can define a *drift coefficient*

$$D_\alpha(t+x) \equiv \lim_{\tau\to 0}\frac{1}{\tau}\Big\langle\big(\alpha(t+\tau)-\alpha(t)\big)\Big\rangle\Big|_{\alpha(t)=x} = \rho(t+x)\frac{\partial\rho(t+x)}{\partial x} \tag{2.32}$$

and a diffusion coefficient

$$D_{\alpha\alpha}(t+x) \equiv \lim_{\tau\to 0}\frac{1}{\tau}\Big\langle\big(\alpha(t+\tau)-\alpha(t)\big)^2\Big\rangle\Big|_{\alpha(t)=x} = \rho^2(t+x) \tag{2.33}$$

which are both periodic with period 2π. Furthermore, any periodic function multiplied with its own derivative will have zero DC and we therefore have

$$\frac{1}{2\pi}\int_0^{2\pi} D_\alpha(\eta)d\eta = 0 \tag{2.34}$$

The diffusion coefficient in (2.33) will, however, have a nonzero mean [14], and we write

[13] see appendix A.2 on page 137 for a discussion of stochastic integration.

[14] this follows from the fact that ρ^2 is a positive function and a periodic function. Thus this function is either zero or there exist a DC level sufficient to keep it positive at all times.

$$\rho^2(t+x) = \rho_0 + \rho_1(t+x) \tag{2.35}$$

where ρ_1 is a 2π periodic function, implying that

$$\frac{1}{2\pi}\int_0^{2\pi} D_{\alpha\alpha}(\eta)d\eta = \rho_0 \tag{2.36}$$

From (2.32) and (2.33) it is seen that the drift coefficient controls the dynamics of the mean of the distribution while the diffusion coefficient controls the evolution of the variance. We can then make the following heuristic observation

note 2.2 *the distribution, solving the inhomogeneous diffusion equation in* (2.26)*, with boundary conditions in* (2.28) *and initial distribution* (2.29)*, will oscillate around the initial mean value $\alpha(t') = x'$, while a finite time average diffusion will cause the distribution to approach a uniform characteristic, asymptotically with time.*

From the above note we can write the asymptotic solution to the inhomogeneous solution as

$$\lim_{t\to\infty} p(x,t|x',t') = 0 \tag{2.37}$$

implying that after all the transients have died out the distribution is completely uniform on the real line.

In [14], Demir *et al.* derive the asymptotic statistics using some rather complicated calculations, involving a Fourier expansion of the *characteristic function* [15]. Equation (23) in [14, p. 663] gives the following result for the asymptotic value of the oscillator phase characteristic function

$$\lim_{t\to\infty} C(\omega,t) = \exp\left(j\omega m - \frac{1}{2}\rho_0 t\right) \tag{2.38}$$

where m is a real constant [16] and we have used the notation from (2.36). Since a characteristic function of the form

$$C(\omega) = \exp\left(j\omega\mu - \frac{1}{2}\sigma\right) \tag{2.39}$$

implies a Gaussian distribution with mean μ and variance σ, the authors of [14] use the result in (2.38) to state the following result

Theorem 2.1 (Theorem 7.7 in [14], p. 663) *the solution of the inhomogeneous diffusion equation in* (2.26) *becomes Gaussian, asymptotically with time; with a constant mean and a variance that increases linearly with time according to $\sigma(t) = \rho_0 t$.*

[15] the characteristic function $C(\omega,t)$ of a stochastic process $\xi(t)$ with probability density $p(x,t)$ is defined as $C(\omega,t) = \langle \exp(j\omega\xi(t))\rangle = \int_{-\infty}^{\infty} \exp(j\omega x)p(x,t)dx$. [39]

[16] although it is not discussed in [14], it seems reasonable to assume that $m = x'$, where x' is the initial value of the phase α, as seen from (2.29).

where ρ_0 is defined in (2.36). Comparing the above statement with our discussion on the homogeneous diffusion equation, theorem 2.1 expresses that the solution to (2.26) approaches the Wiener process asymptotically with time.

Theorem 2.1 and the expression in (2.38) can be very confusing. Basically, (2.38) is saying the same as (2.37); that is, that the distribution becomes completely uniform, asymptotically with time. The expression in (2.38) only makes sense with the introduction of an *effective diffusion constant*, something which was not properly explained by the authors of [14]. The asymptotic statistics of the process $\alpha(t)$ are hence described in terms of an effective diffusion constant D_{eff} and using the result from theorem 2.1 we can then write

$$D_{eff} = \lim_{t\to\infty} \frac{\left\langle (\alpha(t) - \alpha(0))^2 \right\rangle}{2t} = \rho_0 \tag{2.40}$$

Re-normalizing time $t \to t/2\pi \times T_0$, where T_0 is the oscillator period, and using the notation from (2.36), we get the final result

$$\boxed{D_{eff} = \bar{D}_{\alpha\alpha} = \frac{1}{T_0}\int_0^{T_0} D_{\alpha\alpha}(\eta)d\eta} \tag{2.41}$$

The oscillator phase $\phi(t)$ was related to the time variable $\alpha(t)$ in (2.10), on page 40. We can also define the effective diffusion constant in terms of this variable

$$D_{eff} = \bar{D}_{\phi\phi} = \omega_0^2 \bar{D}_{\alpha\alpha} \tag{2.42}$$

We note that the results in (2.41) and (2.42) characterize the asymptotic statistics of the phase variables $\alpha(t)$ and $\phi(t)$ using the trivial Wiener process with a constant unspecified mean and with a diffusion constant which is calculated from the DC value of the original time periodic diffusion constant.

2.1.3 Calculating the Oscillator Spectrum

Having identified the asymptotic statistics of the oscillator phase $\alpha(t)$ with the trivial Wiener process, with power $D_{eff} = \bar{D}_{\alpha\alpha}$ and mean m, we can write [17]

$$E\big[\alpha(t+\tau)\alpha(t)\big] = m^2 + \bar{D}_{\alpha\alpha}\min(t, t+\tau) \tag{2.43}$$

which follows from the fact that disjoint intervals of the Wiener process are uncorrelated as discussed in appendix A.2. We then define the new phase variable β_{ik} through

$$\beta_{ik}(t,\tau) = i\alpha(t) - k\alpha(t+\tau) \tag{2.44}$$

where i and k represent integers. Using the result from theorem 2.1 and equation (2.43) we can then find the asymptotic statistics of the Gaussian variable β_{ik}. First we find the mean [18]

[17] see appendix A.2 for a more in-depth discussion of the Wiener process and for an explanation of the calculations included in this section.

[18] in the following $E[X]$ refers to the ensemble mean of X and $V[X] = E[X^2] - (E[X])^2$ refers to the ensemble variance.

$$\lim_{t\to\infty} E\big[\beta_{ik}(t,\tau)\big] = (i-k)m \tag{2.45}$$

and then the variance

$$\begin{gathered}\lim_{t\to\infty} V\big[\beta_{ik}(t,\tau)^2\big] = E\big[\beta_{ik}(t,\tau)^2\big] - \big(E\big[\beta_{ik}(t,\tau)\big]\big)^2 = \\ i^2 E\big[\alpha(t)^2\big] + k^2 E\big[\alpha(t+\tau)^2\big] - 2ikE\big[\alpha(t+\tau)\alpha(t)\big] - (i-k)^2 m^2 = \\ i^2(m^2 + \bar{D}_{\alpha\alpha}(t)) + k^2(m^2 + \bar{D}_{\alpha\alpha}(t+\tau)) - 2ik(m^2 + \bar{D}_{\alpha\alpha}\min(t, t+\tau)) - (i-k)^2 m^2 = \\ i^2\bar{D}_{\alpha\alpha}t + k^2\bar{D}_{\alpha\alpha}(t+\tau) - 2ik\bar{D}_{\alpha\alpha}\min(t,t+\tau) = (i-k)^2\bar{D}_{\alpha\alpha}t + k^2\bar{D}_{\alpha\alpha}\tau - 2ik\bar{D}_{\alpha\alpha}\min(0,\tau)\end{gathered} \tag{2.46}$$

where we have used that $\min(t, t+\tau) = t + \min(0,\tau)$. The spectrum is calculated as the Fourier transform of the autocorrelation function $R(t,\tau)$, which is defined as

$$\begin{gathered}R(t,\tau) = E[x_{ss}(t+\alpha(t))x_{ss}^*(t+\tau+\alpha(t+\tau))] = \\ \sum_{i=-\infty}^{\infty}\sum_{k=-\infty}^{\infty} X_i X_k^* \exp(j\omega_0(i-k)t)\exp(-j\omega_0 k\tau)E[\exp(j\omega_0\beta_{ik}(t,\tau))]\end{gathered} \tag{2.47}$$

where we have written the Fourier decomposition of the steady-state oscillator solution $x_{ss}(t)$, as

$$x_{ss}(t) = \sum_{n=-\infty}^{\infty} X_n \exp(jn\omega_0 t) \tag{2.48}$$

The term $E[\exp(j\omega_0\beta_{ik}(t,\tau))]$ in (2.47) is the characteristic function for the stochastic variable β_{ik} (see footnote 15, on page 45). According to (2.46) the variance of this variable will be infinite, asymptotically with time, for $i \neq k$ resulting in a zero characteristic function (see (2.39)). Therefore only the terms $i = k$ will survive asymptotically in (2.47) and we can write

$$\lim_{t\to\infty} R(t,\tau) = \sum_{i=-\infty}^{\infty} X_i X_i^* \exp(-j\omega_0 k\tau)\exp\left(-\frac{1}{2}i^2\omega_0^2\bar{D}_{\alpha\alpha}|\tau|\right) \tag{2.49}$$

where we have used the expression for the characteristic function of a Gaussian variable, given in (2.39), and we have written (2.46) for $i = k$ as

$$i^2\bar{D}_{\alpha\alpha}\tau - 2i^2\bar{D}_{\alpha\alpha}\min(0,\tau) = i^2\bar{D}_{\alpha\alpha}|\tau| \tag{2.50}$$

By Fourier transforming (2.49) we then finally find the oscillator power-density spectrum as

$$S(\omega) = \sum_{i=-\infty}^{\infty} X_i X_i^* \frac{\omega_0^2 i^2\bar{D}_{\alpha\alpha}}{(\frac{1}{2}\omega_0^2 i^2\bar{D}_{\alpha\alpha})^2 + (\omega + i\omega_0)^2} \tag{2.51}$$

showing the expected Lorentzian characteristic at each harmonic [14].

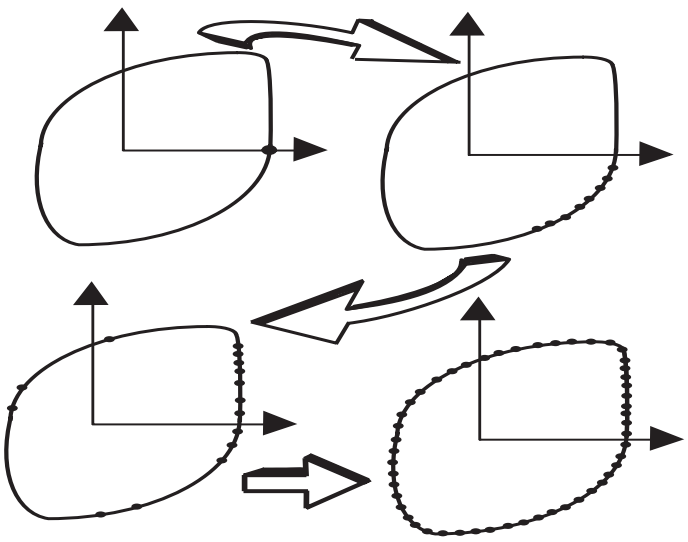

Figure 2.4: A qualitative illustrations of the ensemble oscillator phase evolution. The plots are based on the qualitative remarks in note 2.2, on page 45. The ensemble starts with a fixed phase as shown in the top left-hand part of the figure. Following the arrows it is then seen how the phase approaches an uniform distribution, asymptotically with time.

2.1.4 An Alternative Model of the Asymptotic Phase Statistics of a Free-Running Oscillator.

What follows here is an alternate derivation of the asymptotic oscillator statistics which avoids the complex and tedious calculations which led to theorem 7.7 in [14], as repeated in theorem 2.1, on page 45. In this report we choose to interpret the results in (2.38) (and (2.37)) very simply, as follows

note 2.3 *the oscillator phase becomes completely random, corresponding to a uniform distribution, asymptotically with time.*

In figure 2.4 we illustrate how the oscillator phase approaches a uniform distribution, asymptotically with time. Assume that we start with an ensemble of N oscillators all placed the phase $\alpha(0) = 0$, corresponding to the initial distribution in (2.29), for $x' = 0$. Because of the non-zero DC diffusion component ρ_0, the distribution for the N oscillator ensemble will start to distribute itself on the circle (see note 2.2 on page 45). Assume now that the distribution is completely diffused as described by (2.37). Then, if the limit cycle in figure 2.4 is divided into M "phase-points", there will be N/M oscillators at each point. This follows from the fact that at each phase-point ϕ there are oscillators which have phase $\phi + 2k\pi$ where $k \in \mathbb{Z}$. This means that there will be an ensemble of oscillators at each phase point of the limit cycle in figure 2.4.

We now consider the variable β_{ik} which was first defined in (2.44)

$$\beta_{ik} = i\alpha(t+\tau) - k\alpha(t) \tag{2.52}$$

For $i \neq k$ the above variable will be completely uniform on the circle since both terms will be uniform and since not all of this is removed by the "asymmetric" difference. This will then correspond to the asymptotic distribution in (2.37) which results in a zero characteristic function, as seen from the discussion in the previous section in connection with equation (2.39). The terms $i \neq k$ will then not contribute to the correlation function in (2.47) and hence neither to the spectrum. We therefore only need to consider (2.52) for $i = k$ and we define the *oscillator self-referenced phase* (SR-P) as

$$\Delta_\alpha(t,\tau) = \alpha(t+\tau) - \alpha(t) \tag{2.53}$$

This variable is <u>not</u> uniform since the randomness is removed by the "symmetric" difference. The oscillator phase drift and diffusion coefficients first written in (2.32) and (2.33), are repeated here

$$D_\alpha(t+x) \equiv \lim_{\tau\to 0}\frac{1}{\tau}\big\langle(\alpha(t+\tau)-\alpha(t))\big\rangle\Big|_{\alpha(t)=x} = \rho(t+x)\frac{\partial\rho(t+x)}{\partial x} \tag{2.54}$$

$$D_{\alpha\alpha}(t+x) \equiv \lim_{\tau\to 0}\frac{1}{\tau}\big\langle(\alpha(t+\tau)-\alpha(t))^2\big\rangle\Big|_{\alpha(t)=x} = \rho^2(t+x) \tag{2.55}$$

Assuming that we knew the value $\lim_{t\to\infty}\alpha(t)$, that is, if $\lim_{t\to\infty}\alpha(t)$ was *sharp*, then we could directly use (2.54)-(2.55) to describe the asymptotic evolution of the mean and variance of the SR-P. However, as witnessed from the above discussion and as summarized in note 2.3 and figure 2.4, the oscillator phase becomes completely random asymptotically with time. As explained above, if we divide the limit cycle γ into M points then there would be N/M oscillators at each point. In the following we assume that the M phase points are contained in the set Π and that these points are uniformly distributed. From (2.54) and (2.55) it is then seen that the oscillator <u>ensemble</u> mean and power would evolve as (see footnote 18, on page 46)

$$\lim_{t\to\infty}\frac{dE[\Delta_\alpha(t,\tau)]}{d\tau} = \lim_{M,N\to\infty}\frac{1}{N}\sum_{x\in\Pi}\frac{N}{M}D_\alpha(t+x) = \int_0^{2\pi} D_\alpha(t+x)dx = \bar{D}_\alpha = 0 \tag{2.56}$$

$$\lim_{t\to\infty}\frac{dV[\Delta_\alpha(t,\tau)]}{d\tau} = \lim_{M,N\to\infty}\frac{1}{N}\sum_{x\in\Pi}\frac{N}{M}D_{\alpha\alpha}(t+x) = \int_0^{2\pi} D_{\alpha\alpha}(t+x)dx = \bar{D}_{\alpha\alpha} = \rho_0 \tag{2.57}$$

where we can equate the integrals in the phase variable x with the time averages, as both D_α and $D_{\alpha\alpha}$ are symmetric in these variables (*i.e.* they are invariant with respect to $x \leftrightarrow t$). Also note that we can use (2.54)-(2.55) to describe the evolution of the statistics since there are an ensemble of oscillators, and not just one, at each of the M points in Π. This follows from the asymptotic distribution from (2.37) where the oscillator phase is completely flat on the real line implying that there is an ensemble at each phase ϕ, corresponding to the oscillators at $\cdots, \phi-4\pi, \phi-2\pi, \phi, \phi+2\pi, \phi+4\pi, \cdots$. The main points of the above discussion are illustrated in figure 2.5 where an arbitrarily derived $\rho(\cdot)$ function is considered.

We can now write the following asymptotic probability density for the single oscillator SR-P

$$\lim_{t\to\infty} p(\Delta_\alpha(t,\tau)) = \lim_{t\to\infty} \left\langle \delta(\Delta_\alpha(t,\tau) - x) \right\rangle = \frac{1}{\sqrt{4\pi\rho_0|\tau|}} \exp\left(-\frac{x^2}{\rho_0|\tau|}\right) \tag{2.58}$$

The above derivation hence find the result that, asymptotically with the time, the single oscillator SR-P becomes a Gaussian variable with zero mean and power $\sigma(t) = \rho_0 t$. This is essentially the same result as was predicted in theorem 2.1 (Theorem 7.7 in [14], p. 663), on page 45, however, **the above derivation avoids the lengthy and tedious calculations which were necessary to derive this result in [14] and, more importantly, it provides a clearer, more intuitive understanding of the situation**. A short paper or letter which considers the simplified formulation of the single oscillator noise problem derived in the above text, is currently being prepared [43].

2.2 Review of 3 Popular Oscillator Phase Noise Methodologies

The previous two sections showed how, starting from the general state space ODE's, a stochastic differential equation governing the dynamics of the noise perturbed free-running oscillator's phase was derived. This equation was then treated using the Fokker-Planck formalism and we showed how the asymptotic statistics of the original inhomogeneous diffusion equation was described by a simple Wiener process with the *effective diffusion constant* being equal to the *average diffusion constant*, as shown in (2.41).

In this section we shall investigate how these very general results translate into practical algorithms for the calculation of phase noise spectra of free-running oscillators. There exist numerous different models in the literature, and many variants within each model, however, three main categories are easily identified

- *Phase Macro Models*
- *Linear Time Varying Phase-Filters*
- *Averaging Methods*

The text in the two previous sections was heavily inspired by the work of Demir *et al.* who developed the so-called *phase macro model* in [14]. The paper [14], gives a practical algorithm for the numerical characterization of the phase noise spectrum of an oscillator perturbed by white noise. Starting from the circuit net-list, the formulation assumes only that an asymptotically stable limit cycle exist for the particular choice of circuit parameters. The formulation is hence very general, being independent of circuit topology, parameters and encompassing all types of oscillators (harmonic, ring, relaxation *etc.*). In this author's opinion, the work by Demir *et al.* represents the most complete oscillator phase-noise model, based on rigorous theory and formulated to allow for easy integration into commercial CAD systems, published to date[19]. In section 2.2.1 we shall give a short introduction to phase macro model.

[19] with regard to the theory outlined in [14], it is only fair to mention that not all of it is new. Both Edson [44] and, perhaps more importantly, Lax [45] had already developed much of the theory of phase diffusion in self-sustained oscillators. Furthermore, Kaertner [17] had formulated the problem using a projection formalism which has many similarities with the model in [14]. However, the authors of [14] were the first to use Floquet theory thus obtaining a formulation that could be integrated into CAD environments like SPICE™ and SPECTRE™.

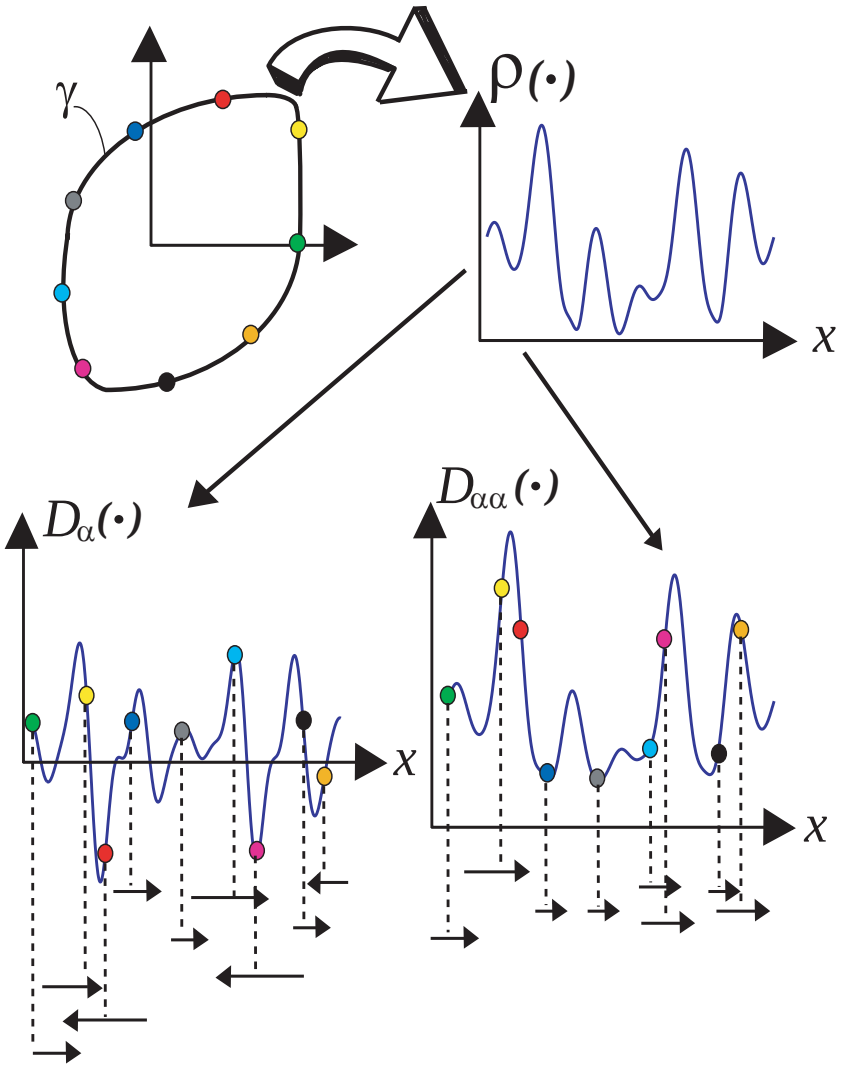

Figure 2.5: in the limit $t \to \infty$ the oscillator phase ensemble (N realizations) is completely diffused, corresponding to a uniform distribution on the limit cycle γ, as illustrated in the top left part of figure. Here the oscillator phase is represented by $M = 9$ *phase-points*, as illustrated using colored dots. Assuming $N = 900$, there will be $N/M = 100$ oscillators at each of the points ●, ●, ● *etc.* In the top right part of the figure, the $\rho(\cdot)$ function (see (2.25), on page 43), as a function of the limit cycle phase x, is shown. From this function one can derive the *drift* and *diffusion* coefficients, $D_\alpha(\cdot)$ and $D_{\alpha\alpha}(\cdot)$, respectively, as seen from (2.54)-(2.55). In the bottom left part of the figure $D_\alpha(\cdot)$ is plotted while the curve in the bottom right part of the figure illustrates $D_{\alpha\alpha}(\cdot)$. Each of the arrows beneath the plots represents the evolution of the mean and variance (see (2.54)-(2.55)) for the $M/N = 100$ oscillators initially placed at the phase-point corresponding to the colored dot. As is seen from the $D_\alpha(\cdot)$ plot, the ensemble at some phase-points experience an increase ($\rightarrow$) in the mean while others are decreased ($\leftarrow$); the sum result for all $N = 900$ realizations/oscillators being zero, since the mean of $D_\alpha(\cdot)$ is zero (see (2.56)). From the $D_{\alpha\alpha}(\cdot)$ plot, however, we see that at all the M phase-points the ensemble experience an increase ($\rightarrow$) in the spread/variance; the sum result being equal to the mean ρ_0 (see (2.57)).

Section 2.2.2 reviews an earlier model, developed by Hajimiri [46], which treats the oscillator as a *linear periodic time varying* (LPTV) filter. This model has proven extremely popular with circuit designers due to its rather heuristic, non-mathematical, formulation. Demir calls it a *phenomenological* model [47], thus hinting at the complete lack of any discussion regarding stochastic process theory. The model contains a parameter q_{max} which represents the maximum charge displacement across the capacitor on the node considered [46].

Finally, in section 2.2.3 we investigate averaging theory as applied to a noise forced free-running harmonic oscillators. This method was introduced by Kurokawa in [32]. Since the formulation only concerns harmonic/sinusoidal oscillators the Kurokawa method does not attain the high level of generality possessed by the two previously described models. Furthermore, the procedure can not easily be used for numerical characterization. We include the model here, since no review of phase noise methodologies would be complete without a mention of averaging procedures, but also because we shall use this formulation later in chapter 4, where we investigate a ring of coupled harmonic oscillators.

No matter how one choose to express the problem it is clear from the discussion in the previous sections, that the end-result must involve the derivation of the effective diffusion constant, as shown in (2.41). The following three sections will hence illustrate how this constant is found within each of the three different formulations.

2.2.1 Demir's Phase Macro Model

In [14] Demir introduced the concept of a *phase macro model*. The model extends earlier contributions by Kaertner and Lax [17] by applying Floquet theory [20] to the analysis hence obtaining a formulation that lends itself well to numerical characterization and which is easily integrated into standard CAD environments such as SPICE™ and SPECTRE™. The model is based on a numerically derived steady-state and its corresponding *mondromy matrix* (MM), which is a special *state transition matrix* (STM). If the *shooting method* [48] is used to derive the steady-state then the MM is automatically calculated as part of the procedure. This then means that the phase noise calculation is almost free once a steady-state solution has been found.

The phase macro model has its origin in a single ordinary differential equation (ODE) forced by white noise

$$\dot{x} = f(x) + B(x)\chi(t) \tag{2.59}$$

where $x(t) : \mathbb{R} \to \mathbb{R}^n$ is a vector in n dimensional state space, $f(\cdot) : \mathbb{R}^n \to \mathbb{R}^n$ is the vector field of the autonomous system containing an asymptotically stable limit cycle, $\chi(t) : \mathbb{R} \to \mathbb{R}^p$ is vector of p uncorrelated white noise sources and $B(\cdot) : \mathbb{R}^n \to \mathbb{R}^{n\times p}$ describes the modulation of the noise by the state variables. The small noise perturbations in (2.59) results in equally small variations around the limit cycle and this response is then solved, to a first order approximation, through the variational equation

$$\dot{w} = A(t)w + B(x_{ss})\chi(t) \tag{2.60}$$

with $x = x_{ss} + w$, where $x_{ss}(t + T_0) = x_{ss}(t)$ is the asymptotically stable solution of noise free equation (2.59), $w = x - x_{ss}$ is the response of the system to the perturbation caused by the noise sources and $A(t) : \mathbb{R} \to \mathbb{R}^{n\times n}$ is the Jacobian of the vector field f as defined in (2.4). Having derived the set of nonhomogeneous linear time varying ODEs

[20] see appendix D for an introduction to the Floquet theoretic concepts discussed here.

in (2.60) which solves for the linear noise response w, the authors use *Floquet Theory* to propose a solution for the homogenous part

$$w(t) = \Phi(t, t_0)w_0 \tag{2.61}$$

where the initial condition at $t = t_0$ is given by w_0 and $\Phi(\cdot,\cdot) : \mathbb{R} \times \mathbb{R} \to \mathbb{R}^{n\times n}$ is the *state transition matrix* (STM)

$$\Phi(t, t_0) = \exp\left\{\int_{t_0}^{t} A(\eta)d\eta\right\} \quad ; \quad \Phi(t_0, t_0) = I \tag{2.62}$$

where I is and $n \times n$ identity matrix. We hence see that the STM is simply a *Greens function* of the system in (2.60). Using Floquet theory, it is shown in [14] how the STM can be formulated in the form

$$\Phi(t, t_0) = \sum_{i}^{n} u_i(t) \exp(\mu_i(t - t_0))v_i^T(t_0) \tag{2.63}$$

where the vectors $u_i, v_i : \mathbb{R} \to \mathbb{C}^n$ are the *Floquet eigenvectors* and $\mu_i \in \mathbb{C}$ are the *Floquet exponents*. The Floquet eigenvectors constitute a *bi-orthogonal set*

$$v_i(t)^T u_j(t) = \delta_{ij} \quad \text{for all } t \tag{2.64}$$

Since we are dealing with a linear system in (2.60), it should be clear that we can find the particular solution corresponding to any initial condition using the Greens function in (2.63). With respect to phase-noise analysis, the key observation is that one of the Floquet exponents must be zero. This follows from the discussion in section 2.1.1 where we showed that oscillator phase was characterized as a neutrally stable state variable (see note 2.1 on page 39). If we denote $\mu_1 = 0$ we see that the projection operator in the direction of the phase is given by

$$P(s) = u_1(s)v_1^T(s) \tag{2.65}$$

where $s = t + \alpha(t)$ is the *instantaneous time* introduced in (2.11), on page 41. Note that (2.65) is the unspecified orthogonal projection operator discussed earlier in section 2.1.1. Using the notation $v^T = v_1^T B(x_{ss}) : \mathbb{R} \to \mathbb{R}^p$ we can derive the following stochastic differential equation

$$\frac{d\alpha}{dt} = v^T(t + \alpha(t))\chi(t) = v^T(s)\chi(t) \tag{2.66}$$

Using (2.33) and (2.41), with $v^T = \rho$, we can identify the effective/averaged diffusion coefficient as

$$\boxed{\bar{D}_{\alpha\alpha} = \frac{1}{T_0}\int_0^{T_0} v^T(\eta)v(\eta)d\eta = \frac{1}{T_0}\int_0^{T_0} v_1^T(\eta)B\big(x_{ss}(\eta)\big)v_1(\eta)B^T\big(x_{ss}(\eta)\big)d\eta} \tag{2.67}$$

An inherent problem with the phase macro model lies with the premise that the state transition matrix has a single unique eigenvalue equal to 1. Theoretically this of course has to hold for a stable oscillation, however, numerically speaking this could

represent a problem. In high Q oscillators, a large number of eigenvalues often cluster around the value $1 + j0$ in the complex plane, making the identification of the correct eigenvalue/eigenvector difficult. This problem and a possible solution was addressed in [16].

2.2.2 Hajimiri's Impulse Sensitivity Function

In [46], Hajimiri introduced the following vector impulse response function

$$h_\phi(t,\tau) = u(t-\tau)\frac{\Gamma(\omega_0\tau)}{q_{max}}\,, \tag{2.68}$$

where $h(\cdot,\cdot) : \mathbb{R}\times\mathbb{R} \to \mathbb{R}^p$, t is the absolute time, τ is arrival time of the noise impulse, $u(\cdot) : \mathbb{R} \to \mathbb{R}$ is a unit step function, $\Gamma(\cdot) : \mathbb{R} \to \mathbb{R}^p$ is the so-called *impulse sensitivity function* (ISF) [46], $\omega_0 = 2\pi/T_0$ is the steady-state frequency and q_{max} is a normalization constant. In (2.68), we have assumed that the state equations where perturbed by a vector of uncorrelated white noise sources $\chi(t) : \mathbb{R} \to \mathbb{R}^p$, as was the case in the last section (see (2.59)).

The representation in (2.68) can be derived from the SDE in (2.25) since the neutral stability of the phase variable is included in the unit step function u and the periodic weight function ρ is now given by $\Gamma(\omega_0(t + 2\pi)) = \Gamma(t)$. However, this way of treating an SDE using linear filter theory is a very heuristic approach which completely ignores stochastic process theory (see discussion in appendix A.2).

The response function in (2.68) describes a LPTV filter, were the input signals are the white noise sources χ and the output is the oscillator phase

$$\phi(t) = \frac{1}{q_{max}}\int_{-\infty}^{t}\big[\Gamma(\omega_0\tau)\big]^T\chi(\tau)d\tau\,, \tag{2.69}$$

Equation (2.69) can of also be written as a first order differential equation with periodic coefficients

$$\frac{d\phi(t)}{dt} = \frac{1}{q_{max}}\big[\Gamma(\omega_0 t)\big]^T\chi(t)\,. \tag{2.70}$$

which is seen to be identical, in form, with our SDE in (2.25). Using the results in (2.70) and (2.41) we can derive the averaged diffusion coefficient for the ISF theory as

$$\boxed{\bar{D}_{\phi\phi} = \frac{1}{T_0}\frac{1}{q_{max}^2}\int_0^{T_0}\big[\Gamma(\omega_0\eta)\big]^T\Gamma(\omega_0\eta)d\eta} \tag{2.71}$$

2.2.3 Kurokawa's Model - Harmonic Oscillators

In this section we shall discuss averaging theory of noise forced harmonic oscillators. The term *harmonic oscillator* can either refer to a loss-free (Hamiltonian), linear oscillator or to a situation where the higher harmonics are so well suppressed that the solution, to a

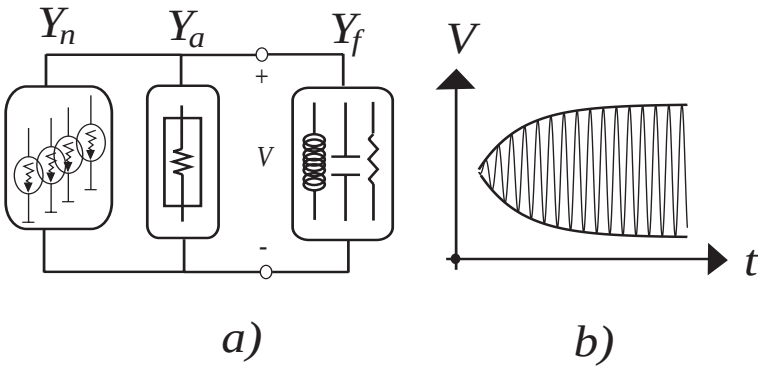

Figure 2.6: a) Splitting the feedback oscillator up into two parts. b) the solution is *quasi sinusoidal* which implies a harmonic carrier with slowly moving amplitude and phase transients.

good approximation, can be called harmonic/sinusoidal. Considering the last alternative, we can write the solution using a *quasi-sinusoidal* [21] function

$$v(t) = A(t)\cos(\omega_0 t + \phi(t)) = \Re\{A(t)\exp(j[\omega_0 t + \phi(t)])\} \tag{2.72}$$

where both the envelope A and phase ϕ are *slowly moving* functions of time. These two functions represent the response of the system to small noise perturbations. The *slowness* of these response-functions is a direct result of a narrowband/high Q circuit in the feedback path, which is implied by the assumption of higher harmonic cancellation.

The premise of slow amplitude and phase transients means that we can set

$$\frac{d^n\phi}{dt^n} = \frac{d^n A}{dt^n} \approx 0 \quad \text{for } n > 1 \tag{2.73}$$

and using this together with the definition in (2.72) we find

$$\frac{d^n v}{dt^n} = \Re\left\{\left[j\left(\omega_0 + \frac{d\phi}{dt}\right) + \frac{1}{A}\frac{dA}{dt}\right]^n A e^{j\omega t+\phi}\right\} \tag{2.74}$$

Comparing the result in (2.74) with the effect of carrying out the same operation on an arbitrary harmonic solution $z = \Re\{r\exp(j\omega t)\}$ we see that we can define the effective frequency of the *quasi-sinusoidal* solution through

$$\omega \to \left(\omega_0 + \frac{d\phi}{dt}\right) - j\frac{1}{A}\frac{dA}{dt} \tag{2.75}$$

which is also known as *Kurokawa's substitution* [32], [33]. We now divide the oscillator circuit up into a passive resonance circuit admittance Y_f and a nonlinear admittance Y_a which represents the action of energy restoring circuit element as illustrated in figure 2.6. Barkhausen's criterion is then written as

$$[Y_f(\omega, A) - Y_a(A)]v = 0 \tag{2.76}$$

In appendix B we show how to derive the *averaged amplitude/phase state equations* starting from an equation like (2.76). Linearizing the amplitude/phase equations around the steady-state solution we find the following two coupled first order ODE's

[21] we refer to the text in section 1.2 for a more detailed discussion of averaging theory and the quasi-sinusoidal approximation

$$\frac{d\delta A}{d\tau} = sG_L\delta A + G_n, \tag{2.77}$$

$$\frac{d\delta\phi}{d\tau} = rG_L\delta A + B_n \tag{2.78}$$

where it is assumed that the state variables can be written as $\phi = \hat{\phi}+\delta\phi$, $A = \hat{A}+\delta A$, with the constants $(\hat{\phi}, \hat{A})$ describing the steady-state limit cycle and $(\delta\phi, \delta A)$ modelling the linear noise response. The noise admittance $Y_n = G_n + jB_n$ is a complex stochastic variable which models the white noise sources in the circuit. The statistics of these variables are thoroughly described in appendix A.1. In (2.77)-(2.78) we have furthermore introduced the time normalization $\tau = \omega_0/(2Q) \times t$.

As discussed in appendix B, in order to arrive at the system (2.77)-(2.78) we have already applied an averaging procedure and we therefore note that the averaged phase diffusion coefficient $\bar{D}_{\phi\phi}$ from (2.42) can be derived directly from the ODE in (2.77)-(2.78). All we have to do is identify the *neutrally stable* state variable. From (2.78), we see that the phase ϕ is not neutrally stable since the righthand side of (2.78) depends on δA. This coupling from the amplitude to the phase is the result of a nonlinear reactive impedance which results in *AM to PM* conversion. Instead, we now introduce the new phase variable $\delta\psi$ through

$$\delta\psi = \delta\phi - \left(\frac{r}{s}\right)\delta A \tag{2.79}$$

Using (2.77)-(2.78), the dynamic equation for this variable can be written

$$\frac{d\delta\psi}{d\tau} = B_n - \left(\frac{r}{s}\right)G_n \tag{2.80}$$

This equation, with only uncorrelated noise functions on the righthand side, is on the form an averaged (2.25) and we can write the averaged phase diffusion coefficient directly from this equation

$$\boxed{\bar{D}_{\phi\phi} = \left(\frac{\omega_0}{2Q}\right)^2\left\{1 + \left(\frac{r}{s}\right)^2\right\}\frac{N_0}{P_0}} \tag{2.81}$$

where we have re-normalized time $t = 2Q/\omega_0\tau$ and N_0/P_0 is the *noise to signal ratio* (see appendix A.1). Inspecting (2.81), we see that it differs from the two earlier definitions of the effective diffusion constant in (2.67) and (2.71) by not including an averaging operation. As explained above, equation (2.80) is already averaged and so this procedure is implicitly included in the definition (2.81). Furthermore, we note that (2.81) includes a finite AM-PM noise component and that this part is proportional to the factor $(r/s)^2$. This is a quite general result which we shall discuss further in chapter 4 where we investigate ring coupled oscillators, perturbed by white noise.

Chapter 3

A Phase Macro Model for Coupled Oscillator Systems

The single oscillator *phase macro model*, which was introduced by Demir *et al.* in [14] [1], prescribes an algorithm for the numerical derivation of the phase-noise characteristics of an asymptotically stable limit cycle solution perturbed by white noise sources. The formulation is *unified*; it only assumes an asymptotically stable limit cycle and can therefore be applied to all kinds of oscillators. Furthermore, since the noise characterization is derived numerically, the model is independent of circuit topology and parameters. The algorithm proceeds by calculating the eigenvalues and eigenvectors of the *monodromy matrix*, which represents a *return map* for the limit cycle, and is a special *state transition matrix* (STM) [2]. This map is derived as a part of the steady-state calculation [14], [48]. The vector corresponding to the eigenvalue $\lambda = 1$ is then identified with the direction in state space tangential to the limit cycle. By integrating the Jacobian of the vector field for one period, with this tangential vector as initial condition, one obtains a set of vectors all pointing in directions tangential to the limit cycle. These vectors are in turn used to create an *orthogonal projection operator* which will collect the component of the system noise, at the various phase points, pointing in a direction *along* the limit cycle. Using this formulation, one can set up a stochastic differential equation (SDE) for the oscillator phase which can then be solved through stochastic integration techniques [3].

A projection formalism, for the single oscillator phase noise characterization, was formulated 11 years prior to [14], in the paper [17] by Kaertner. Still, the formulation in [14] has become much more widespread [4]. This is most likely due to a more user-friendly notation and, perhaps more importantly, the fact that the Demir formulation can be easily integrated into standard CAD environments such *e.g.* SPICE™ and SPECTRE™. Finally, we should mention the early work of Lax [45] on noise in oscillators, which served as inspiration for the authors of both [14] and [17].

The purpose of this chapter is to introduce an extension of the single oscillator projection formalism [14], [17], which intends to enlarge the scope of the model to incorporate coupled oscillators. Since coupled oscillators, assuming synchronization has taken place,

[1] the phase macro model was reviewed in section 2.2.1 on page 52.

[2] we refer to appendix D for a discussion of STM's and the Monodromy Matrix.

[3] see the discussion in chapter 2 and appendix A.2, on page 137, for further information on the single oscillator phase macro model and stochastic integration.

[4] a quick check in Google Scholar™ reveals that the Demir formulation has been cited by 208 papers, the Kaertner paper has 33 citations and the Kurokawa method, described in section 2.2.3, has around 200 citations ([32]+[33]). None of these can however match the Hajimiri phase noise paper [46] (see section 2.2.2 on page 54) which has been cited 471 times.

also represent an asymptotically stable periodic solution, one could be led to the conclusion that a limit cycle representation would suffice as a model for the system dynamics. We would then not need new theory to handle these elaborate systems; instead, we could use the formulation in [14] directly. However, as will now be shown, with regard to the system noise response, this assumption would lead to loss of information. We start with a formal definition of the concept of *phase-noise*

Definition 3.1 *The concept of phase-noise pertains to the contribution of the total noise envelope which cannot be removed by an ideal limiter circuit.*

which then leads to the theorem

Theorem 3.1 *All noise tangential to the invariant manifold constitutes phase-noise.*

The theorem is proven by noting that an ideal limiter responds to amplitude/energy of the input signal while the invariant manifold is a topological construction related to the phase/timing characteristic of the waveform. The theorem says directly that in order to calculate the phase-noise of a noise perturbed steady-state, one has to take into account the manifold on which this solution resides. From the discussion in section 1.1.2, on page 23, we know that the orbits of the symmetric n-coupled oscillator solution approach the n-torus $\mathbb{T}^n = \underbrace{\mathbb{S}^1 \times \mathbb{S}^1 \cdots \times \mathbb{S}^1}_{n \text{ times}}$, asymptotically with time.

Previous Work

The phase noise macro model has been applied to the modelling of locked systems in the following previous publications

- *[49] A. Mehrotra 2002* : The full PLL noise problem is analyzed using elements from the original phase macro-model. The paper proceeds by setting up a linear first-order stochastic differential equation for the system; the so-called *Ornstein-Uhlenbeck* equation, which is then solved for the spectrum of the noise perturbed PLL. We note the following differences between that paper and our contribution

  1 The theory is not general to locked systems, but relies on a very specific PLL-model containing a certain set of components (*i.e.* filters, phase comparators *etc.*)

  2 Since the model is not a state-space form, the theory outlined in that paper cannot be directly integrated into a CAD environment such as SPICE. The model relies on the user dividing the different circuit components into categories. This is very different from the original phase macro model in [14] where the process of calculating the spectrum was only based on the CAD program supplying a steady-state solution.

- *[50] X. Lai & J. Roychowdhury 2004* : In this paper the phase macro model is used to study the nonlinear behavior of injection locked systems. The model does not include noise but instead the locking signal takes the place of a perturbing signal.

- *[47] A. Demir 2006* : Here the author discusses how to include $1/f$-noise sources into the phase macro model formulation. The paper also discuses the PLL noise problem, but as with [49], it relies on a specific PLL model and not on a state space formulation.

3.1 The General Model Formulation

We consider the m dimensional, noise forced, autonomous system, representing n coupled oscillators perturbed by white noise sources

$$\dot{x} = f(x) + B(x(t))\chi(t) \tag{3.1}$$

where $x(t) : \mathbb{R} \to \mathbb{R}^m$ is the state vector, $f(\cdot) : \mathbb{R}^m \to \mathbb{R}^m$ is the vector field, $B(\cdot) : \mathbb{R}^m \to \mathbb{R}^{m\times p}$ represents the modulation of the noise sources by the signal and $\chi(\cdot) : \mathbb{R} \to \mathbb{R}^p$ is a column vector containing p zero mean, unit variance, uncorrelated Gaussian white noise sources (see discussion in connection with (2.9), on page 40). Since we consider the coupling of n separate parts we can write the state vector $x(t)$ as

$$x(t) = \begin{bmatrix} x_1(t) \\ x_2(t) \\ \vdots \\ x_n(t) \end{bmatrix} \tag{3.2}$$

where $x_i(t) : \mathbb{R} \to \mathbb{R}^{n_i}$ is the state sub-vector belonging to the i'th oscillator and we have

$$n_1 + n_2 + \cdots n_n = m \tag{3.3}$$

The vector field can also be divide into smaller parts

$$f(x) = \begin{bmatrix} f_1(x_1;\kappa x) \\ f_2(x_2;\kappa x) \\ \vdots \\ f_n(x_n;\kappa x) \end{bmatrix} \approx \begin{bmatrix} f_1(x_1) \\ f_2(x_2) \\ \vdots \\ f_n(x_n) \end{bmatrix} + \kappa \begin{bmatrix} h_{11}(x_1) & h_{12}(x_1) & \cdots & h_{1n}(x_1) \\ h_{21}(x_2) & h_{22}(x_2) & \cdots & h_{2n}(x_2) \\ \vdots & \vdots & \ddots & \vdots \\ h_{n1}(x_n) & h_{n2}(x_n) & \cdots & h_{nn}(x_n) \end{bmatrix} \begin{bmatrix} x_1 \\ x_2 \\ \vdots \\ x_n \end{bmatrix} \tag{3.4}$$

where $f_i(\cdot) : \mathbb{R}^n \to \mathbb{R}^{n_i}$ represents the vector field of the i'th oscillator, $\kappa \in \mathbb{R}$ is a small parameter ($|\kappa| \ll 1$) representing the weakness of the coupling and $h_{ij}(\cdot) : \mathbb{R}^{n_j} \to \mathbb{R}^{n_i}$ denotes the first order Taylor approximation of the coupling from the j'th to the i'th oscillator, where

$$h_{ij} = \left.\frac{\partial f_i}{\partial x_j}\right|_{\kappa=0} \tag{3.5}$$

The noise vector in (3.1) is written as

$$\chi(t) = \begin{bmatrix} \chi_1(t) \\ \chi_2(t) \\ \vdots \\ \chi_n(t) \end{bmatrix} \tag{3.6}$$

where $\chi_i(\cdot) : \mathbb{R} \to \mathbb{R}^{p_i}$ is the system noise of the i'th oscillator and

$$p_1 + p_2 + \cdots + p_n = p \tag{3.7}$$

This notation means that we can write the modulation matrix, B, as [5]

[5] the vector in (3.6) and the matrix in (3.8) does not include the possibility of noise in the coupling circuitry. This will suffice for modelling unilaterally coupled oscillators like the injection locked oscillator architecture that we shall investigate in the following section. For bilaterally coupled oscillators the formulations in (3.6) and (3.8) will probably have to be updated.

$$B = \begin{bmatrix} B_{11}(x_1;\kappa x) & 0 & \cdots & 0 \\ 0 & B_{22}(x_1;\kappa x) & \cdots & 0 \\ \vdots & \vdots & \ddots & \vdots \\ 0 & 0 & \cdots & B_{nn}(x_n;\kappa x) \end{bmatrix} \tag{3.8}$$

where $B_{ij}(\cdot) : \mathbb{R}^{n_i} \to \mathbb{R}^{n_i \times p_j}$ models the noise-coupling of j'th oscillator to it's i'th counterpart. The system in (3.1), without the noise forcing function, will contain a periodic solution $x_{ss}(t+T) = x_{ss}(t)$, where $T = 2\pi/\omega$ is the period of the solution

$$x_{ss}(t) = \begin{bmatrix} x_{ss,1}(t) \\ x_{ss,2}(t) \\ \vdots \\ x_{ss,n}(t) \end{bmatrix} \tag{3.9}$$

where $x_{ss,i}(t) : \mathbb{R} \to \mathbb{R}^{n_i}$ is the component of the T periodic steady-state solution belong to the i'th oscillator domain. Due to the noise perturbation in (3.1) the phase of the oscillator will represent an unspecified, although monotonic [14], function of time. If we write the phase of the i'th oscillator as

$$\phi_i(t) = \omega\alpha_i(t) \tag{3.10}$$

then steady-state solution, after time normalization [6], can be written

$$x_{ss}(t + \alpha_d(t)) = x_{ss}(t + \alpha_1(t) + \alpha_2(t) + \cdots + \alpha_n(t)) \tag{3.11}$$

where

$$\phi_d = \omega\alpha_d = \sum_{i=1}^{n} \phi_i \tag{3.12}$$

is the so-called *diagonal phase* [7]. We now introduce the *instantaneous time*, s, as

$$s = t + \alpha_d(t) \tag{3.13}$$

Using the same derivations which led to (2.14) on page 41 we derive the following *linear response system*

$$\dot{x}_{ss}(s)\frac{d\alpha_d}{dt} + \dot{y}(t) = A(s)y(t) + B(x_{ss}(s))\chi(t) \tag{3.14}$$

where $y(t) : \mathbb{R} \to \mathbb{R}^m$ is the *linear response vector*, which is formally defined as the difference between the state space solution and the steady-state solution

$$y(t) = x(s) - x_{ss}(s) \tag{3.15}$$

and $A(t) : \mathbb{R} \to \mathbb{R}^{m \times m}$ is the system Jacobian which is calculated as the first derivative of the vector field f. Comparing the above equation with (2.14) in section 2.1.1 we see that they are identical if we substitute α_d for α. Following the derivations in section 2.1.1 we then find that $\dot{x}_{ss}(s)$ lies in the null space of the Jacobian, $A(s)$, which means that we can write the following SDE for the neutrally stable α_d

[6] by normalizing the time we now have a 2π periodic solution vector $x_{ss}(t + 2\pi) = x_{ss}(t)$.

[7] see section 4.5.1, on page 105, where the concept of *diagonal phase* is applied to the linear response analysis of unidirectional ring of n oscillators perturbed by noise.

$$\frac{d\alpha_d}{dt} = \rho(t + \alpha_d)\xi(t) \tag{3.16}$$

where $\rho(\cdot) : \mathbb{R} \to \mathbb{R}$ is a 2π periodic function and $\xi(\cdot) : \mathbb{R} \to \mathbb{R}$ is a zero mean, unit variance Gaussian *macro noise source*. The equation in (3.16) is similar to (2.25), derived in section 2.1.1 and is hence solved in a similar way, using stochastic integration, as illustrated in section 2.1.2 and 2.1.4. So far, nothing new, compared to the single oscillator formulation, has been introduced. This just illustrates the fact that

note 3.1 *in the direction of the diagonal phase $\phi_d = \omega\alpha_d$, as defined in* (3.12)*, the coupled system acts like a single oscillator.*

According to theorem 3.1, we need to find the projection operators which will project the linear response system

$$\dot{y}(t) = A(s)y(t) + B(x_{ss}(s))\chi(t) \tag{3.17}$$

onto the manifold $\mathbb{T}^n$. Following the formulation in [14] we now define

$$z(s) = y(t) \tag{3.18}$$

as well as the approximation

$$\frac{dz(s)}{dt} = \frac{dz(s)}{ds}\left(1 + \frac{d\alpha_d}{dt}\right) = \frac{dz(s)}{ds} + O(|y|^2) \tag{3.19}$$

since $d\alpha_d/dt = O(|y|)$. Linear response theory is a first order approximation which means that second, and higher, order terms are neglected. Using (3.19) we can then write (3.17) as

$$\dot{z}(s) = A(s)z(s) + B(x_{ss}(s))\Psi(s) \tag{3.20}$$

where we have define $\Psi(s) = \chi(t)$. As explained in appendix D, the solution of (3.20), with initial condition $z(s_0)$, can be specified by the so-called *state-transition matrix* (STM) $\Phi(s, s_0)$

$$z(s) = \Phi(s, s_0)z(s_0) + \int_{s_0}^{s} \Phi(s, \eta)B(x_{ss}(\eta))\Psi(\eta)d\eta \tag{3.21}$$

which is a map that brings the initial condition $z(s_0)$ forward in time to $z(s)$. A steady-state algorithm, like the *shooting method* [48], will return the special STM $\Phi(2\pi, 0)$, known as the *monodromy matrix* (MM) [8], and this map hence constitutes all the information available to the CAD program about the properties of the solution and the manifold on which it lies. As was shown in appendix D, the *monodromy matrix* represents a *return map* which brings the linear response solution $z(s)$ one period forward in time. Since $z(s)$ represents the linearization around a asymptotically stable solution, $x_{ss}(t)$, one of the eigenvalues of this map will be zero, corresponding to the phase shift invariance of

[8] in the paper [14] it is also explained how to derive $\Phi(2\pi, 0)$ when the steady-state is found using Harmonic Balance (HB) techniques.

the diagonal phase ϕ_d. As explained on page 162 in appendix D the monodromy matrix can be written as

$$\Phi(2\pi, 0) = \sum_{i=1}^{m} \lambda_i P_i \tag{3.22}$$

where $P_i = u_i(0)v_i^T(0) = u_i(2\pi)v_i^T(2\pi) \equiv u_i v_i^T$ are a set of orthogonal projection operators, $u_i(t)$, $v_i(t) : \mathbb{R} \to \mathbb{R}^m$ are the 2π periodic Floquet eigenvectors and dual eigenvectors, respectively, and $\lambda_i = \exp(\mu_i 2\pi)$ is the Floquet multipliers with μ_i being the Floquet characteristic components [9]. Referring to theorem 3.1, on page 58, in order to characterize phase noise of the n coupled oscillator case we then need n orthogonal projection operators P_i which will project onto the manifold $\mathbb{T}^n$.

We start by stating the following theorem

Theorem 3.2 (Existence) *the monodromy matrix representing the linearized dynamics of n weakly coupled oscillators will have n eigenvectors u_i spanning the tangent space of the invariant manifold.*

proof : The invariant manifold $\mathbb{M} \approxeq \mathbb{T}^n$ of the uncoupled oscillators is normally hyperbolic (see discussion in section 1.1.2, on page 23). This follows from the fact that we consider coupling of asymptotically stable oscillators. Hence, assuming weak coupling, there will exist a slightly perturbed invariant manifold for the coupled oscillators $\mathbb{M}_\epsilon$, where $\mathbb{M}_\epsilon \approxeq \mathbb{T}^n + O(|\epsilon|)$. Here epsilon is a small number $|\epsilon| \ll 1$ representing the weak coupling. Since there exist an invariant manifold $\mathbb{M}_\epsilon$ for the coupled case there will exist an invariant tangent space $\mathbb{TM}_\epsilon$. The eigenvectors $\{u_i\}_{i=1}^m$ span the invariant tangent and normal spaces in $\mathbb{R}^m$ and there will hence exist n monodromy eigenvectors $u_k = \left\{k \in [1, 2, \cdots, m] \; | u_k \in \mathbb{TM}_\epsilon\right\}$, spanning the tangent space $\mathbb{TM}_\epsilon$.

Corollary 3.1 *There will exist n unique orthogonal projection operators operators P_i projecting onto the invariant manifold tangent space $\mathbb{TM}_\epsilon$. These orthogonal projection operators are chosen as $P_k = u_k v_k^T = \left\{k \in [1, 2, \cdots, m] \; | u_k \in \mathbb{TM}_\epsilon\right\}$*

One of the above described operators will correspond to the neurally stable variable ϕ_d. Letting $P_1 = u_1 v_1^T$ represent this case, we see that this operator is easily found since we will have $\lambda_1 = 1$ [10]. Furthermore, as explained in connection with (3.14), $\dot{x}_{ss}$ lies in the null-space of the Jacobian which mean that it is a Floquet vector with eigenvalue $\lambda = 1$. From the above discussion it is then seen that we can set

$$u_1(t) = \dot{x}_{ss}(t) \tag{3.23}$$

We then need the remaining $n-1$ vectors : $u_k = \left\{k \in \{2, \cdots, m\} | u_k \in \mathbb{TM}_\epsilon\right\}$. Two obvious questions now arise

1. how do we identify these remaining vectors?
2. how do we interpret the equations resulting from the projection onto $\mathbb{TM}_\epsilon$?

[9] for an explanation of these parameters we refer to appendix D.

[10] this identification is unique since only one eigenvalue can be equal to $1 + j0$ for an asymptotically stable periodic solution. The derivation of the projection operator P_1 essentially constitutes the single oscillator characterization. See the discussion in section 2.1.1 on page 38.

The answers to the above questions will depend on the specific coupling scenario (bilateral, unilateral, ring, all-to-all *etc.*) under consideration. We shall hence deal with these problems on a case-to-case basis.

Although the proposed algorithm includes all types of coupled oscillators we shall only investigate the special case of a *sub-harmonic injection locked oscillator* (S-ILO), as described in the paper [51]. A paper is being prepared that will describe the general case [52].

3.2 A Phase Macro Model for the Sub-Harmonic Injection Locked Oscillator (S-ILO)

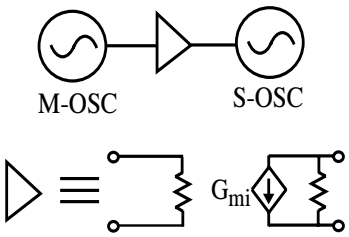

Figure 3.1: The Injection Locking Scenario : the coupling is one-way (unilateral) from the master oscillator (M-OSC) to the slave oscillator (S-OSC).

In this section we investigate the case of two unilaterally weakly coupled oscillators, where the coupling direction is from the *master oscillator (M-OSC)* to the *slave oscillator (S-OSC)*. This scenario is also known by the name *injection locked oscillator (ILO)* and we illustrate this setup in figure 3.1. Injection locking is used frequently in RF and optical design architectures as low-power frequency multipliers/dividers [12] or in the place of a full PLL structure [53] which is often a costly and power-expensive way to realize synthesizers at RF frequencies. Injection locking is also used in phase-noise measuring equipment [54]. As was mentioned in the introduction to this report, it has also long been known that the injection of a low-noise reference can be used as a method of *cleaning* the phase of a noisy carrier [32], [55], [56], [57]. This property is explained, briefly, by noting that the master imprints its *pattern* on the slave counterpart which then inherits all of its frequency related properties including jitter.

In this text the frequency of the M-OSC is denoted ω_1 and the frequency of the S-OSC is denoted ω_2. The sub-harmonic injection locked (S-ILO) scenario then stipulates

$$\omega_2 = N\omega_1 - \Delta\omega \tag{3.24}$$

where $\Delta\omega$ is a small frequency difference between fundamental harmonic of the S-OSC and the N'th harmonic of the M-OSC. The solution x_{ss} hence oscillates with period ω_1 and in the following we shall assume that time normalization, with respect to this frequency, has been carried out. The $\Gamma \times \mathbb{S}^1$ symmetric steady-state solution [11] lies on the invariant manifold $\mathbb{T}^2$, as illustrated in figure 3.2.

Referring to the block diagram in figure 3.1 and the discussion in the previous section, we can divide the state-space into two components : x_1 belonging to the M-OSC and x_2

[11] see the text in section 1.1.2 for a discussion on symmetrically coupled oscillators. Here Γ refers to the unidirectional coupling from the M-OSC to the S-OSC and $\mathbb{S}^1$ refers to the offset invariance of the solution along the diagonal phase α_d.

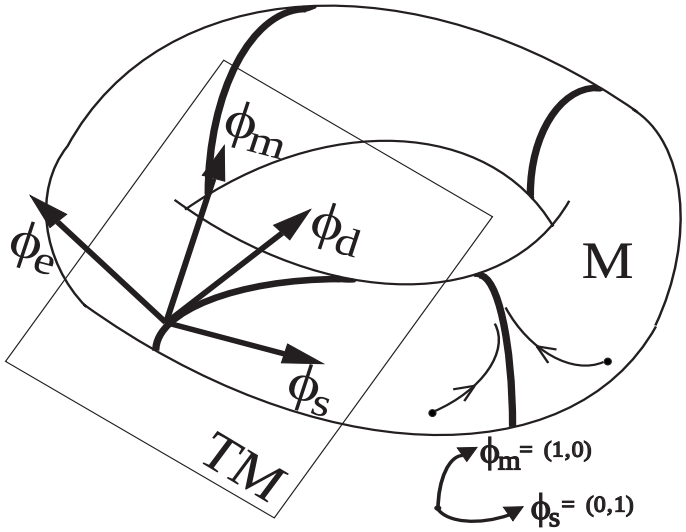

Figure 3.2: The two-torus $\mathbb{T}^1 = \mathbb{S}^1 \times \mathbb{S}^1$ is an invariant manifold $\mathbb{M}$ in the $\Gamma \times \mathbb{S}^1$ symmetric canonical domain (see discussion in section 1.1.2). Orbits on the torus will approach the ω-limit set which is shown as a heavily drawn line. Points on the torus use the *canonical basis* $\phi_m = (1, 0)$, $\phi_s = (0, 1)$ and these vectors span the tangent space $\mathbb{TM}$. The two other vectors shown is the *diagonal phase* $\phi_d = (1, 1)$ and the *error phase* $\phi_e = (1, -1)$.

belonging to the S-OSC. This means that we write $x(t) = [x_1(t)\ x_2(t)]^T$, where $x(t) : \mathbb{R} \to \mathbb{R}^n$, $x_1(t) : \mathbb{R} \to \mathbb{R}^{n_1}$, $x_2(t) : \mathbb{R} \to \mathbb{R}^{n_2}$ and $n_1 + n_2 = n$. Furthermore, we split the vector field and noise sources in (3.1) as $f = [f_1\ f_2]^T$, $f_1(\cdot) : \mathbb{R}^{n_1} \to \mathbb{R}^{n_1}$, $f_2(\cdot) : \mathbb{R}^n \to \mathbb{R}^{n_2}$, $\chi(t) = [\chi_1(t)\ \chi_2(t)]^T$, $\chi_1(t) : \mathbb{R} \to \mathbb{R}^{p_1}$, $\chi_2(t) : \mathbb{R} \to \mathbb{R}^{p_2}$, $p_1 + p_2 = p$. Since the coupling is assumed unilateral the noise modulation matrix B can be written as

$$B(x) = \begin{bmatrix} B_{11}(x_1) & \mathbf{0} \\ \mathbf{0} & B_{22}(x_1, x_2) \end{bmatrix} \tag{3.25}$$

where $B_{11}(\cdot) : \mathbb{R}^{n_1} \to \mathbb{R}^{n_1 \times p_1}$, $B_{22}(\cdot) : \mathbb{R}^n \to \mathbb{R}^{n_2 \times p_2}$. We can then write the general expression (3.1), for the S-ILO as

$$\dot{x}_1 = f_1(x_1) + B_{11}(x_1)\chi_1(t) \tag{3.26}$$
$$\dot{x}_2 = f_2(x_2; \kappa x_1) + B_{22}(x)\chi_2(t) \tag{3.27}$$

In (3.27) $|\kappa| \ll 1$ is a small parameter representing the weak coupling between the two sub-systems. We assume that the system of equations (3.26)-(3.27), without noise, supports a stable periodic steady-state solution which we denote $x_{ss}(t) = [x_m(t)\ x_s(t)]^T$, where $x_m(t) : \mathbb{R} \to \mathbb{R}^{n_1}$, $x_s(t) : \mathbb{R} \to \mathbb{R}^{n_2}$.

3.2.1 Deriving the Torus Projection Operators for the S-ILO

In order to gain a qualitative understanding of the situation we start by deriving an analytical representation of the *monodromy matrix* (MM), or *return-map*, $\Phi(2\pi, 0)$ from the simple $\Gamma \times \mathbb{S}^1$ symmetric normal-form/averaged equations (see discussion in section 1.1.2). As explained in appendix D.1, this map can be derived from the normal-form Jacobian matrix. We then move on to consider the asymmetric canonical equations.

Finally we discuss how the canonical projection operators can be interpreted in the "real" physical domain.

According to the discussion in section 1.1.2, on page 23, and section 1.2, on page 28, the normal form/averaged state equations will have the form

$$\frac{dA_i}{d\tau} = \mu_{o,i}\left[1-\left(\frac{A_i}{\alpha}\right)^2\right]A_i + \kappa\Lambda_i(A_m,A_s,\phi_m,\phi_s) \qquad i=m,s \tag{3.28}$$

$$\frac{d\phi_i}{d\tau} = \frac{2Q_i}{\omega_i}\Delta\omega_i + b_iA_i^2 + \kappa\Phi_i(A_m,A_s,\phi_m,\phi_s) \qquad i=m,s \tag{3.29}$$

where we refer to the discussion in the above mentioned sections for an explanation of the different parameters. In (3.28)-(3.29) we have labelled the M-OSC and S-OSC state variables by subscripts m and s, respectively. Since the M-OSC in figure 3.1 is not coupled to the S-OSC we find that $\Lambda_m = \Phi_m = 0$. Following the discussion in section 1.1.2, on page 23, and section 1.2, on page 28, it is seen, that using either normal-form or averaging methods, one obtains (for harmonic locking) $\Lambda_s(A_m,A_s,\phi_m,\phi_s) = A_m\cos(\phi_m-\phi_s)$ and $\Phi_s(A_m,A_s,\phi_m,\phi_s) = \frac{A_m}{A_s}\sin(\phi_m-\phi_s)$. Furthermore, we have $\Delta\omega_m = 0$ and $\Delta\omega_s = \Delta\omega$, as seen from (3.24). We can then write (3.28)-(3.29) as

$$\frac{dA_m}{d\tau} = \mu_{o,m}\left[1-\left(\frac{A_m}{\alpha}\right)^2\right]A_m \tag{3.30}$$

$$\frac{d\phi_m}{d\tau} = 2Q_m + b_mA_m^2 \tag{3.31}$$

$$\frac{dA_s}{d\tau} = \mu_{o,s}\left[1-\left(\frac{A_s}{\alpha}\right)^2\right]A_s + \kappa A_m\cos\big(N[\phi_m-\phi_s]\big) \tag{3.32}$$

$$\frac{d\phi_s}{d\tau} = \frac{2Q_s}{\omega_1}\frac{\Delta\omega}{N} + b_sA_s^2 + \kappa\frac{A_m}{A_s}\sin\big(N[\phi_m-\phi_s]\big) \tag{3.33}$$

where we consider the N'th subharmonic of the S-OSC phase $\phi_s \to N\phi_s$. We can now derive the linear response system by considering first order Taylor expansion of (3.30)-(3.33) around the steady-state $(\hat{A}_i,\hat{\phi}_i)$ $(i=m,s)$ [12]

$$\frac{1}{\hat{A}}\frac{d\delta A_m}{d\tau} = -2\mu_{o,m}\frac{\delta A_m}{\hat{A}} \tag{3.34}$$

$$\frac{d\delta\phi_m}{d\tau} = 2b_m\hat{A}^2\frac{\delta A_m}{\hat{A}} \tag{3.35}$$

$$\frac{1}{\hat{A}}\frac{d\delta A_s}{d\tau} = -2\mu_{o,s}\frac{\delta A_s}{\hat{A}} + N\kappa\cos\big(N\Delta\hat{\phi}\big)\frac{\delta A_m}{\hat{A}} - N\kappa\sin\big(N\Delta\hat{\phi}\big)(\delta\phi_m-\delta\phi_s) \tag{3.36}$$

$$\frac{d\delta\phi_s}{d\tau} = 2b_s\hat{A}^2\frac{\delta A_s}{\hat{A}} + N\kappa\sin\big(N\Delta\hat{\phi}\big)\left(\frac{\delta A_m}{\hat{A}}-\frac{\delta A_s}{\hat{A}}\right) + N\kappa\cos\big(N\Delta\hat{\phi}\big)(\delta\phi_m-\delta\phi_s) \tag{3.37}$$

where $\Delta\hat{\phi} = \hat{\phi}_m - \hat{\phi}_s$ and we have assumed $\hat{A}_m \approx \hat{A}_s \approx \alpha$ [13]. The system in (3.34)-(3.37) can be written on matrix form as

[12] we refer here to the discussion in section 4.5, on page 103, where we study the unidirectional ring, for an example of how these linear response equations are derived from the normal-form/averaged state equations.

[13] this approximation will serve to simplify the formulation without decreasing the range of this, already, very qualitative model.

$$\dot{z} = Jz \tag{3.38}$$

where $J \in \mathbb{R}^{4\times4}$ is the Jacobian of the averaged system and z is the linear response vector

$$z = \begin{bmatrix} \frac{\delta A_m}{\hat{A}} & \delta\phi_m & \frac{\delta A_s}{\hat{A}} & \delta\phi_s \end{bmatrix}^T \tag{3.39}$$

As explained in appendix D.1, on page 163, it is possible to derive an analytical expression for the monodromy matrix (MM) eigenvectors u_i and dual eigenvectors v_i, by calculating the eigenvector of the normal-form Jacobian J. The eigenvalues of J will then equal the characteristic multipliers μ_i of the MM. From (3.34)-(3.37), we write Jacobian matrix as

$$J = \begin{bmatrix} \alpha_1 & 0 & 0 & 0 \\ \rho_1 & 0 & 0 & 0 \\ \zeta & \gamma & \alpha_2 & -\gamma \\ -\gamma & \zeta & \gamma+\rho_2 & -\zeta \end{bmatrix} \tag{3.40}$$

where

$$\alpha_1 = -2\mu_{o,m} \tag{3.41}$$
$$\alpha_2 = -2\mu_{o,s} \tag{3.42}$$
$$\rho_1 = 2b_m\hat{A}^2 \tag{3.43}$$
$$\rho_2 = 2b_s\hat{A}^2 \tag{3.44}$$
$$\gamma = -N\kappa\sin(N\Delta\hat{\phi}) \tag{3.45}$$
$$\zeta = N\kappa\cos(N\Delta\hat{\phi}) \tag{3.46}$$

If we assume that the system is close to symmetry so that $\Delta\hat{\phi} \approx 0$, $\gamma \approx 0$ and that we have no AM-to-PM conversion (*i.e.* $\rho_1 = \rho_2 = 0$), then find the following eigenvector/eigenvalue pairs by inspection [14]

$$\mu = \begin{bmatrix} 0 \\ \alpha_1 \\ \alpha_2 \\ -\zeta \end{bmatrix} \quad ; \quad U = \begin{bmatrix} 0 & 1 & 0 & 0 \\ 1 & 0 & 0 & 0 \\ 0 & 0 & 1 & 0 \\ 1 & 0 & 0 & 1 \end{bmatrix} \tag{3.47}$$

where the eigenvalues are written in the column vector $\mu = [\mu_1\ \mu_2\ \mu_3\ \mu_4]^T$ and the eigenvector corresponding to the eigenvalue μ_i is written in the i'th column of the matrix U. The eigenvalue of the diagonal phase $\phi_d = [0\ 1\ 0\ 1]^T$ is seen to have the Flouquet characteristic component $\mu_1 = 0$ corresponding to the characteristic multiplier $\lambda_1 = 1$. It is seen that two of the eigenvectors lie in the two-torus tangent space $\mathbb{TM}$ (see figure 3.2); namely, $\phi_d = [0\ 1\ 0\ 1]^T$ and $\phi_s = [0\ 0\ 0\ 1]^T$ with corresponding eigenvalues 0 and $-\zeta$ respectively. We have therefore found the following $\mathbb{T}^2$ *Floquet eigenvectors* for the $\Gamma \times \mathbb{S}^1$ symmetric case

$$u_1(t) = \phi_d(t) \tag{3.48}$$
$$u_2(t) = \phi_s(t) \tag{3.49}$$

[14] the two eigenvectors corresponding to eigenvalues α_1, α_2 are only approximate. These vectors are not important at this point in the analysis.

We now consider the transpose matrix

$$J^T = \begin{bmatrix} \alpha_1 & \rho_1 & \zeta & -\gamma \\ 0 & 0 & \gamma & \zeta \\ 0 & 0 & \alpha_2 & \gamma + \rho_2 \\ 0 & 0 & -\gamma & -\zeta \end{bmatrix} \tag{3.50}$$

Using the same approximations as above, we then find the following eigenvector/eigenvalue pairs by inspection (see footnote 14)

$$\mu \begin{bmatrix} 0 \\ \alpha_1 \\ \alpha_2 \\ -\zeta \end{bmatrix} \quad ; \quad V = \begin{bmatrix} 0 & 1 & 0 & 0 \\ 1 & 0 & 0 & -1 \\ 0 & 0 & 1 & 0 \\ 0 & 0 & 0 & 1 \end{bmatrix} \tag{3.51}$$

We see that the two dual Floquet eigenvectors corresponding to the eigenvectors in (3.48)-(3.49) are the M-OSC phase $\phi_m = [0\ 1\ 0\ 0]^T$ and the *error phase* $\phi_e = [0\ -1\ 0\ 1]^T$. We have therefore found the following *Floquet dual eigenvectors* for the $\Gamma \times \mathbb{S}^1$ symmetric case

$$v_1(t) = \phi_m(t) \tag{3.52}$$
$$v_2(t) = \phi_e(t) \tag{3.53}$$

From the discussion in connection with (3.22) and in appendix D, we see that we can derive the following two-torus orthogonal projection operators

$$P_1 = u_1 v_1^T = \phi_d \phi_m^T \tag{3.54}$$
$$P_2 = u_2 v_2^T = \phi_s \phi_e^T \tag{3.55}$$

We summarize as follows

note 3.2 *The range of P_1 is the diagonal phase ϕ_d while the null-space of the operator is the S-OSC phase ϕ_s. This should interpreted as the M-OSC distributing its phase to the S-OSC. The range of P_2 is the S-OSC phase ϕ_s while the null-space is the diagonal phase ϕ_d. We see that perturbations tangent to $\mathbb{T}^2$ and diagonal to ϕ_d transfers to the S-OSC phase while the M-OSC is left unaffected due to the unilateral coupling.*

We now impose a structure on the canonical state-space manifolds and hence on the canonical solutions

Definition 3.2 *Let $\mu_{o,s}$ be a parameter that describes the strength of attraction of the S-OSC amplitude to it's limit cycle. Furthermore, let b_s represent curvature of the isochrones at the S-OSC limit cycle. Finally, let γ be parameter on the order of the coupling strength $O(N|\kappa|)$.*

We shall say that the canonical S-ILO lies on a normally hyperbolic manifold, iff the following condition

$$\epsilon = \frac{\sqrt{\gamma(2b_s + \gamma)}}{2\mu_{o,s}} \ll 1$$

is satisfied.

For $b_s = 0$ this condition reverts to the well-known form ($N = 1$)

$$\mu_{o,s} \gg \frac{1}{2} O(|\kappa|) \tag{3.56}$$

which was the original definition of a normally hyperbolic manifold, first stated (1.73), on page 27, in chapter 1. This normal hyperbolic attribute is derived from the assumption of *weak coupling*, as stated in note 1.6 on page 27. It is a necessary condition in order to ensure stability of the orbits and the manifold on which they lie.

Using the above definition we can state the theorem

Theorem 3.3 *There exist two unique Floquet eigenvectors $u_1(t) = \phi_d$ and $u_2(t) = \phi_s + O(|\epsilon|)$ to the asymmetric canonical normal-form equations in* (3.30)-(3.33) *and these vectors will span the tangent space of the perturbed canonical invariant manifold. The two corresponding dual Floquet vectors $v_1(t)$ and $v_2(t)$ will correctly represent the added AM-to-PM noise contribution introduced by asymmetry and non-isochronous operation. The two orthogonal normal form projection operators $P_1(t) = u_1(t)v_1^T(t) = \phi_d(t)v_1^T(t)$ and $P_2(t) = u_2(t)v_2^T(t) = \phi_s(t)v_2^T(t)$ will hence project onto the invariant manifold.*

proof : the proof follows from theorem 3.2 and corollary 3.1, on page 62, and the calculations in appendix C.4, on page 153.

We now move from the canonical, over into the physical domain where the solution orbits of (3.26)-(3.26) "live". The following definition states the condition for a normally hyperbolic manifold in the physical domain

Definition 3.3 *Let μ correspond to the Floquet characteristic exponent of the S-OSC which was original 0 in uncoupled scenario. Let μ_x be the Floquet characteristic exponent, different from μ, with the largest real part. Furthermore, let γ be a parameter on the order of the asymmetry between the M-OSC and S-OSC.*

We shall say that the S-ILO lies on a normally hyperbolic manifold, iff the following condition

$$\epsilon = \frac{\gamma}{|\mu_x|} \ll 1$$

is satisfied.

The following theorem, which is stated without a proof [15], was inspired by theorem 3.3 and the calculations in appendix C.5, on page 156

Theorem 3.4 *If the steady-state solution of the autonomous ODE in* (3.26)-(3.27) *represents an ILO solution, then there will exist two unique Floquet eigenvectors $u_1 = [u_{11}\ u_{12}]^T = [\dot{x}_m\ \dot{x}_s]^T = \dot{x}_{ss}$, $u_2 = [u_{21}\ u_{22}]^T = [\mathbf{0}\ \dot{x}_s]^T + O(|\epsilon|)[\mathbf{0}\ y]^T$, $y \in \mathbb{C}^{n_2}$, $||y||_2 \leq 1$, and these vectors will span the tangent space of the invariant manifold. The second Floquet exponent μ_2 represent the* effective coupling strength. *The corresponding dual*

[15] the author was not able to complete the proof within the deadline for this report. A proof is however being worked on.

Floquet eigenvectors can be written as $v_1 = [v_{11}\ \mathbf{0}]^T$ *and* $v_2 = [-v_{11}\ v_{22}]^T + O(|\epsilon|)[z_1\ z_2]^T$ *and* $z_1 \in \mathbb{C}^{n_1}$, $z_2 \in \mathbb{C}^{n_2}$ $||z_1||_2, ||z_2||_2 \leq 1$. *The two projection operators* $P_1 = \dot{x}_{ss}(t)v_1^T(t)$ *and* $P_2 = [\mathbf{0}\ \dot{x}_s(t)]^T v_2^T(t)$ *will correctly represent the ILO phase-noise scenario.*

3.2.2 The Stochastic Differential Equations

From the discussion in the previous section we consider two projection operators P_1 and P_2. P_1 projects onto the neutrally stable direction as represented by the Floquet exponent $\mu_1 = 0$ and P_2 maps onto the subspace represented by the Floquet exponent $\mu_2 < 0$. We now return to the noise-forced state equations set up in (3.26)-(3.27). The noise contribution which results when P_1 is applied to the right-hand side of (3.26) is denoted $w_1 : \mathbb{R} \to \mathbb{R}^{1\times p_1}$

$$w_1(t) = v_{11}^T(t)B_{11}(x_m(t)) \tag{3.57}$$

where we have used the expression from theorem 3.4. Likewise the noise that results when P_2 is applied to the right-hand side of (3.27) is denoted $w_2 : \mathbb{R} \to \mathbb{R}^{1\times p} = w_{22} - w_{21}$. Here $w_{21} : \mathbb{R} \to \mathbb{R}^{1\times p_1}$ and $w_{22} : \mathbb{R} \to \mathbb{R}^{1\times p_2}$ are defined as

$$w_{21}(t) = v_{21}^T(t)B_{11}(x_m(t)) \tag{3.58}$$
$$w_{22}(t) = v_{22}^T(t)B_{22}(x_{ss}(t)) \tag{3.59}$$

where we again have used the notation from theorem 3.4. The phase variables α_d was used in section 3.1 in connection with the definition of an *instantaneous time*. In the following we shall let α_d represent the state-space coordinate for the "physical" vector $u_1(t) = \dot{x}_{ss}(t)$ and α_s the coordinate for the vector $u_2(t) = \dot{x}_s(t)$. We can then write the state space stochastic differential equations governing the dynamics of the noise perturbed injection locked oscillator as

$$\dot{\alpha}_d = w_1(t + \alpha_d)^T \chi_1(t) \tag{3.60}$$
$$\dot{\alpha}_s = |\mu_2|\alpha_e - w_{21}(t + \alpha_d)^T b_1(t) + w_{22}(t + \alpha_d)^T \chi_2(t) \tag{3.61}$$

where $\alpha_e = \alpha_m - \alpha_s$. As discussed previously the M-OSC distributes its phase to the S-OSC which explains why α_d has a component in both the α_m and α_s direction. We can therefore also write (3.60) as

$$\dot{\alpha}_m = w_1(t + \alpha_m)^T \chi_1(t) \tag{3.62}$$

The interpretation of the different representations in (3.62) and (3.60) will be discussed further in this and the next section.

From (3.62) we see that the M-OSC phase is without reference and it is therefore neutrally stable. Because the S-OSC is frequency locked to the M-OSC it is forced to counteract any change in the injected phase to ensure Barkhausens criterion is upheld at all times. We can then understand (3.60) as the S-OSC being neutrally stable but only *in the direction of the M-OSC phase*. Due to the neutral stability, the noise perturbations in the direction of the M-OSC phase builds up unhindered. Through the operator P_1 these perturbations are then transferred directly to the S-OSC phase. In figure 3.3(a)-3.3(b) we illustrate some of these points. The figures show the S-OSC phase, as represented by a ball, in the potential-well that was created in the saddle-node bifurcation, which initiated the synchronized state. The potential in figures 3.3(a)-3.3(b) represent one of

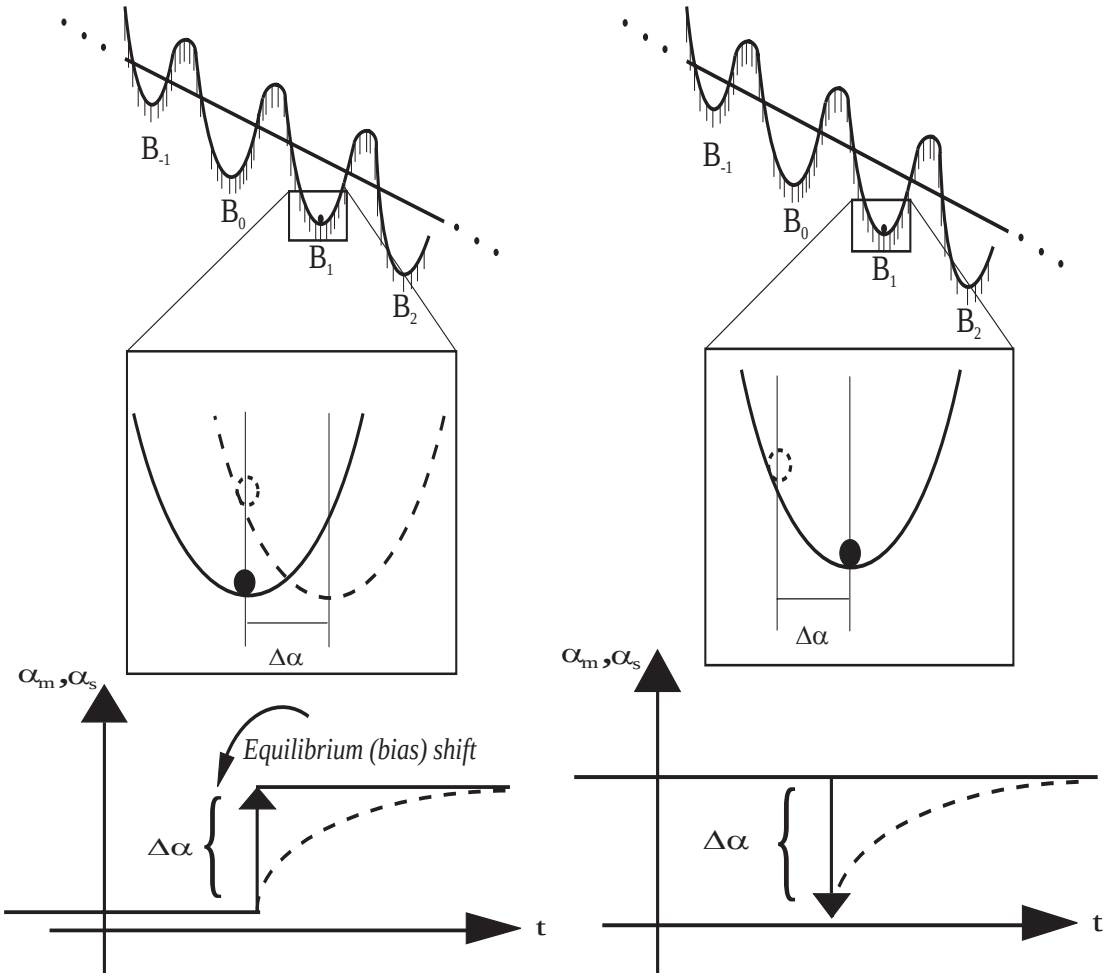

Figure 3.3: Illustrating the equivalence, in the S-OSC domain, of a α_m and a α_e directed perturbation. The phase of the S-OSC is depicted as a ball in a potential-well of the *inclined periodic potential*. Solid ball = phase before perturbation, dashed ball = phase after perturbation. a) The M-OSC phase is perturbed and the S-OSC phase will be removed from its equilibrium at the bottom of the well. The bottom part of the plot shows the transient of S-OSC phase in response to the perturbation. Note that the reference-perturbation shifts the equilibrium point of the well. b) In this figure the S-OSC phase is perturbed in the direction of α_e. The strength of the perturbation is equal to the reference perturbation in a) but the direction is now opposite. Apart from a constant reference the two situations are identical.

the wells in the *inclined periodic potential* as illustrated in the top part of the figures. The S-OSC phase is assumed in equilibrium at the bottom of the well. As will be further illustrated later, the M-OSC sets the equilibrium point of the potential-well and so at the time of perturbation this origin is shifted. The S-OSC phase, however, stays at the position where it was before the perturbation, now illustrated by a dashed dot in figure 3.3(a). The system, which represents a stable phase locked solution, will then initiate a transient to regain equilibrium which is shown in the lower part of the figure. After this has happened, both the M-OSC and the S-OSC have moved a step $\Delta\alpha$ which once again illustrates that both oscillators are neutrally stable in the direction of the M-OSC phase. Another way of saying this is that the M-OSC sets a phase reference that the S-OSC must follow. In figure 3.3(b) we see the response of the S-OSC to a $-\Delta\alpha$ perturbation generated by the operator P_2. Comparing the transients in figure 3.3(a) and 3.3(b) we see that they are identical except for the bias shift in figure 3.3(a).

3.2.3 Characterizing the Self-Referenced S-OSC Phase

Equation (3.62) describes the dynamics of the noise perturbed M-OSC phase. From the discussion in [14], section 2.1.2, section 2.2.1 and appendix A.2 we know that, asymptotically with time, this stochastic process is defined by

$$E[\alpha_m^2(t)] = D_{11}t \tag{3.63}$$
$$E[\alpha_m(t_1)\alpha_m(t_2)] = D_{11}\min(t_1, t_2) \tag{3.64}$$

where $D_{11} = \frac{1}{T_1}\int_0^{T_1} w_1^T(\eta)w_1(\eta)d\eta$ is the M-OSC *diffusion constant* and $T_1 = 2\pi/\omega_1$. For the S-OSC we define $D_{21} = \frac{1}{T_1}\int_0^{T_1} w_{21}^T(\eta)w_{21}(\eta)d\eta$. Using the same arguments as the author in [49] we define the S-OSC diffusion constant $D_{22} = \frac{1}{T_1}\int_0^{T_1} \exp(2|\mu_2|\eta)w_{22}^T(\eta)w_{22}(\eta)d\eta$. We can now write the system (3.60)-(3.62) on the simplified form

$$\dot{\alpha}_m = \sqrt{D_{11}}b_1(t) \tag{3.65}$$
$$\dot{\alpha}_s = |\mu_2|(\alpha_m - \alpha_s) + \sqrt{D_{21}}b_1(t) - \sqrt{D_{22}}b_2(t) \tag{3.66}$$
$$\dot{\alpha}_e = -|\mu_2|\alpha_e - \sqrt{D_{22}}b_2(t) \tag{3.67}$$

where $b_1 : \mathbb{R} \to \mathbb{R}$ and $b_2 : \mathbb{R} \to \mathbb{R}$ are Gaussian unit variance delta-correlated noise processes $\langle b_i(t_1)b_j(t_2)\rangle = \delta_{ij}\delta(t_1 - t_2)$. The system (3.65)-(3.67) illustrates the meaning behind the term *macro model* coined by the authors of [14]. We see that the model contains all the different stochastic perturbing signals in two uncorrelated noise contributions b_1 and b_2. In (3.65) we have chosen the representation where α_m model the neutrally stable variable. As discussed in the previous section, the actual neutral variable is the diagonal phase, α_d. We shall return to this point later. Furthermore, since D_{21} may be different from D_{11} the *error phase* is no longer defined as $\alpha_e = \alpha_m - \alpha_s$. Instead it simply represent the dynamics in the case where the M-OSC is silent ($b_1 = 0$).

Our aim is to derive steady state probability density of the S-OSC self-referenced phase (SR-P) $\Delta_s = \alpha_{s\tau} - \alpha_s$ ($\alpha_i \equiv \alpha_i(t)$, $\alpha_{i\tau} \equiv \alpha_i(t+\tau)$) which will be shown to be stationary. One way of doing this would be to write the Fokker-Planck equation for the system (3.65)-(3.67) and then solve this partial differential equation for the joint probability density conditioned on *sharp* initial conditions [39]. However, we shall follow a different and more intuitive approach here. Inspecting (3.66) and figures 3.3(a)-3.3(b) we see that the S-OSC phase α_s is perturbed in two distinct ways. Figure 3.3(b) represents an *internal*

perturbation caused by the S-OSC noise sources, as represented by b_2 in (3.66)-(3.67). In a fixed reference frame $b_1 = 0$, the dynamics due to this perturbation is captured by the *error phase* α_e in (3.67). This equation represents the S-OSC dynamics in the potential well under the assumption of a fixed reference frame. The perturbation theory discussed in this paper is linear in the sense that we do not consider *cycle slipping* [42] between the potential wells in figure 3.3(a)-3.3(b). This means that $\alpha_e \in [n/T_1; (n+1)/T_1]$ where and n is an arbitrary integer. Assuming a low noise-to-signal ratio, D_{22}, it can be shown that the steady-state solution to (3.67) is well approximated by a Gaussian distribution with mean zero and power $\sigma_e^2 = D_{22}/(2|\mu_2|)$ [42]. We shall subsequently assume that all transients have died out and that this stationary distribution has been reached. Using standard probability theory [39], [42] one then finds that $\Delta_e = \alpha_{e\tau} - \alpha_e$ is a Gaussian stochastic variable with mean zero and power

$$\sigma^2 = 2\sigma_e^2(1-\rho_\tau) = (D_{22}/|\mu_2|)(1-\rho_\tau) \tag{3.68}$$

where we have defined $\rho_\tau = \exp(\mu_2|\tau|)$.

Figure 3.3(a) shows the response of the S-OSC phase to an *external perturbation* as represented by the macro noise source b_1 in (3.65)-(3.66). From inspecting (3.66) and the transient in the lower part of figure 3.3(a) we see that the neutral stability of the M-OSC results in a shifted bias of the potential well (relocation of equilibrium). The *only* model capable of capturing this kind of neutrally stable behavior is on the form

$$\alpha_s = \int \eta(s)ds \tag{3.69}$$

where η is an unspecified, zero mean, noise source. This once again underlines that α_d, and not α_m, is the neutral variable. If we were dealing with a free-running oscillator, η would be δ-correlated and α_s would be represented by a Wiener process [14]. However, from figure 3.3(a) it is clear that η must be a colored noise source. Since the *relaxation time constant* of the potential in figure 3.3(a) is $|\mu_2|^{-1}$ and since the M-OSC perturbations are zero mean Gaussian with power D_{21}, it should be clear that η is zero mean Gaussian with an autocorrelation function which is given as [39]

$$\big\langle \eta(t)\eta(t+\tau)\big\rangle = (D_{21}/2|\mu_2|)\exp(\mu_2|\tau|) \tag{3.70}$$

The process defined as the integration of the variable described through (3.70) is non-stationary; however, its increment is a stationary Gaussian variable [47] with mean zero and power

$$\sigma^2 = D_{21}|\tau| - (D_{21}/|\mu_2|)(1-\rho_\tau) \tag{3.71}$$

Using (3.68) and (3.71) we can write the distribution function for the S-OSC SR-P, Δ_s, as

$$p(\Delta_s) = \frac{\exp\left[-\frac{\Delta_s^2}{2(2\sigma_s^2(1-\rho_\tau)+D_{21}|\tau|)}\right]}{\sqrt{2\pi(2\sigma_s^2(1-\rho_\tau)+D_{21}|\tau|)}} \tag{3.72}$$

So Δ_s is a stationary Gaussian distributed variable with mean zero and power

$$\sigma^2 = 2\sigma_s^2(1-\rho_\tau) + D_{21}|\tau| \tag{3.73}$$

where

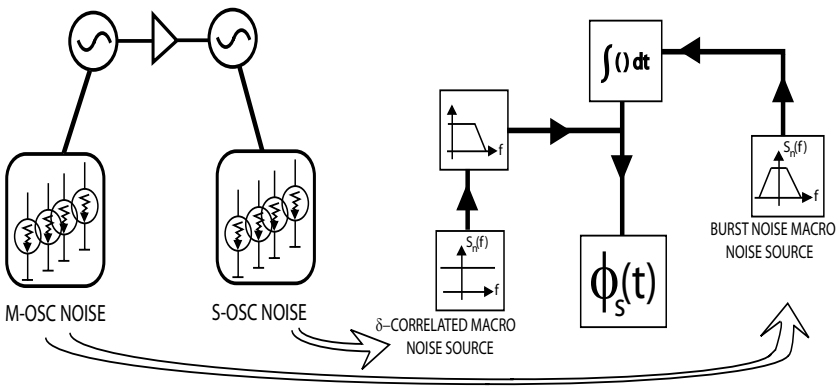

Figure 3.4: The ILO phase noise macro model. All M-OSC δ-correlated noise sources in are represented by a single burst noise source which is integrated directly into the S-OSC phase ϕ_s. All S-OSC delta correlated noise sources are represented by a single δ-correlated macro noise source.

$$\sigma_s^2 = (D_{22} - D_{21})/(2|\mu_2|) \tag{3.74}$$
$$\rho_\tau = \exp(\mu_2|\tau|) \tag{3.75}$$

From the above discussion it is seen that the total effect of the δ-correlated noise sources in the S-OSC domain are combined in a δ-correlated macro noise source with power D_{22}. Furthermore, the M-OSC noise sources are combined in a separate macro source. However, from (3.70) this source is not a δ-correlated but a burst (popcorn) macro noise source. In figure 3.4 we illustrate the phase macro model of the noise perturbed ILO.

3.2.4 The Spectrum of a Noise Perturbed Injection locked oscillator

We write the steady-state S-OSC solution using the Fourier expansion

$$x_s(t) = \sum_{i=-\infty}^{\infty} X_i e^{jiN\omega_1 t} \tag{3.76}$$

where it is used that the oscillation frequency of the S-OSC is $N\omega_1$. We then define the autocorrelation function of the noise perturbed ILO as

$$\Gamma_s(t, t+\tau) = E\big\{x_s(t+\alpha_s(t))x_s^*(t+\tau+\alpha_s(t+\tau))\big\} \quad . \tag{3.77}$$

Each term in the resulting sum will contain a factor

$$\exp(-jkN\omega_1\tau)E[\exp(jN\omega_1\beta_{ik}(t,\tau))] \tag{3.78}$$

where i, k are summing integers and we have defined the new variable

$$\beta_{ik}(t,\tau) = i\alpha_s - k\alpha_{s\tau} \tag{3.79}$$

We see that we have to specify the *characteristic function* for this stochastic variable. Let us first note that for $i = k$ we have $\beta_{ik}(t,\tau) = k\Delta_s$ which was proven in the last section to be a zero mean stationary stochastic variable. Using the fact that $\alpha_s = \alpha_e + \alpha_m$

we can write $E[\beta_{ik}(t,\tau)] = (i-k)m$ and $E[\beta_{ik}(t,\tau)^2] \propto (i-k)^2 t$ (see [14], [49]). Since the characteristic function of a Gaussian stochastic variable with mean m and power σ^2 is equal to $\exp(jm - 0.5 * \sigma^2)$ we see that all components of the characteristic function for $i \neq k$ vanish asymptotically with time. Using the results of the above discussion together with (3.73) we find the following asymptotically stationary autocorrelation function for the S-OSC

$$\lim_{t\to\infty} \Gamma(t, t+\tau) = \Gamma(\tau) = \sum_{i=-\infty}^{\infty} |X_i|^2 e^{-jiN\omega_1\tau} \exp\left(-\frac{1}{2} iN\omega_1 [2\sigma_s^2(1-\rho_\tau) + D_{21}|\tau|]\right) \tag{3.80}$$

In appendix C.6 we use the result in (3.80) to find the spectral density of the S-OSC. Using the definition of single sideband (SSB) phase noise spectrum [14]

$$\mathfrak{L}(\omega_m) = 10 \log\left\{ S(\omega_1 + \omega_m)/(2|X_1|^2) \right\} \tag{3.81}$$

together with the identity

$$D_{21} + 2\sigma_s^2 |\mu_2| = D_{22} \tag{3.82}$$

which can be derived from (3.74), we can write the SSB phase-noise of the S-OSC at frequency offset ω_m as

$$\mathfrak{L}_s(\omega_m) = 10 \log\left[\frac{(N\omega_1)^2 D_{22} [\omega_m^2 + \frac{D_{21}}{D_{22}} \mu_2^2]}{[(\frac{1}{2} N^2 \omega_1^2 D_{21})^2 + \omega_m^2][\mu_2^2 + \omega_m^2]} \right] \tag{3.83}$$

Letting the coupling go to zero as represented by $\mu_2 \to 0$ and using (3.82) the above expression reduces to

$$\mathfrak{L}_s(\omega_m) \underset{|\mu_2|\to 0}{=} 10 \log\left[\frac{(N\omega_1)^2 D_{22}}{(\frac{1}{2} N^2 \omega_1^2 D_{22})^2 + \omega_m^2} \right] \tag{3.84}$$

which is identical to the spectrum of a free-running oscillator [14]. Furthermore, if we let $D_{21} = D_{22}$ while keeping a finite coupling strength $|\mu_2|$ we again recover (3.84) from (3.83). This means that the boundary $D_{21} = D_{22}$ represents a qualitative change in the spectral density of the ILO. Here we shall use the term *locked* to describe the scenario $D_{21} < D_{22}$ and the term *tracking* [56] to describe $D_{21} > D_{22}$. The difference between the two situations is illustrated in figure 3.5.

We can now propose the following algorithm to derive the spectrum of a noise perturbed ILO using the phase macro model :

1. calculate the periodic steady state and the associated monodromy matrix.
2. find the Floquet eigenvector v_1 belonging to the neutral direction μ_1 and check if it has the form described in theorem 3.4, on page 69, *i.e.* search for an n_1 such that for all $i > n_1$ we have $v_1(i)/v_1(n_1) < \epsilon_1$[16] and $v_1(i)$ is the i'th component of v_1.

[16] ϵ_1 is a small number that must reflect the fact that the coupling is never 100% unilateral. We can choose ϵ_1 on the order 10^{-10}.

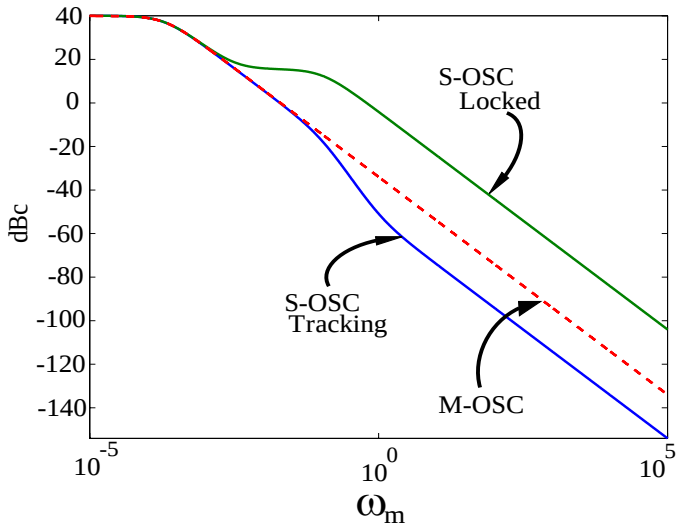

Figure 3.5: Figure illustrating the qualitative transition in the spectrum appearance as the boundary $D_{21} = D_{22}$ is crossed. The plot uses the parameters $N = 1$, $\omega_1 = 2\pi\ rad/s$, $D_{21} = 1 \times 10^{-5}$, $D_{22} = 1 \times 10^{-7}$ (tracking) and $D_{22} = 1 \times 10^{-2}$ (locked). Furthermore the locking bandwidth is chosen through the μ_2 parameter as $|\mu_2| = -\log_2(0.9)(2\pi/\omega_1)$.

3. Set $u_{12}(1 : n_2) = u_1(n_1 + 1 : n)$ and normalize this vector. Search all Floquet vectors u_i $(i \neq 1)$ for which $u_i(k)/u_i(n_1 + 1) < \epsilon_1$ for all $k \leq n_1$. Having found such a vector for $i = j$, set $u_{22}(1 : n_2) = u_j(n_1 + 1 : n)$ and normalize this vector. If $|u_{22}^T u_{12}| = 1 \pm \epsilon_2$ [17] then vectors are parallel and there is a possibility for an ILO solution.

4. set $u_1 = \dot{x}_{ss}(0)$ and $u_2 = \dot{x}_s(0)$ and normalize the projection vectors $u_i^T v_i = 1$.

5. Integrate the linearized dynamics for one period with the normalized v_1 and v_2 as initial conditions. Multiply by the noise modulation matrix B to create w_1, w_{21} and w_{22} (see (3.57)-(3.59)). The two diffusion constant D_{21} and D_{22} are then given as the mean of $w_{21}(t)^T w_{21}(t)$ and $\exp(2|\mu_2|t) \times (w_{22}(t)^T w_{22}(t))$, respectively.

6. Calculate the SSB spectrum according to (3.83).

Finally we would like to compare (3.83) with the noise-model for the S-ILO proposed in [55]. Using Harmonic Balance (HB) techniques the authors of of this paper derived the following expression for the S-OSC spectrum

$$\mathfrak{L}_s(\omega_m) = \frac{\{\cos(N\Delta\hat{\phi})\Delta\omega_L\}^2 N^2 \mathfrak{L}_m(\omega_m) + \Delta\Omega^2}{\omega_m^2 + \{\cos(N\Delta\hat{\phi})\Delta\omega_L\}^2} \tag{3.85}$$

where $\mathfrak{L}_s(\omega_m)$ and $\mathfrak{L}_m(\omega_m)$ is the phase noise of the S-OSC and the M-OSC, respectively, at offset frequency ω_m, $\Delta\omega_L$ is the locking range, $\Delta\hat{\phi}$ is a constant phase offset between the injected tone and the S-OSC phase, and $\Delta\Omega$ is related to the jitter of the S-OSC. This expression reveals two important traits. Firstly, since $\mathfrak{L}_m(\omega_m) \propto \omega_m^{-2}$ [58],

[17] ϵ_2 is a small number that must reflect the fact that $u_2 = \dot{x}_s + O(\epsilon)$ with ϵ being a small bound (see discussion in section 3.2.1 an theorem 3.2). Furthermore, we are dealing with finite precision steady-state and eigenvalue/vector calculations. The bound ϵ_2 will hence also depend on the truncation error of the integration routine as well as other parameters. We set ϵ_2 on the order 10^{-2}.

it is seen that the noise of the master dominates close to carrier. This represents the phase-cleaning property of the S-ILO which was briefly discussed in the introduction to this report. Secondly, inspecting (3.85) it is observed that the penalty for subharmonic locking is a factor N^2. The characteristics contained in the model in (3.85) have all been experimentally verified [54],[55] and should be inherent in any model trying to capture the main qualitative dynamics of a subharmonic ILO perturbed by noise. One flaw of the analysis in [55] is that the model is based on linear perturbation techniques. It was shown in [14] that these methods are incapable of capturing the correct asymptotic phase dynamics of free-running oscillators. This statement holds for all autonomous systems which converge to an asymptotically stable periodic solution and therefore also injection locked oscillators.

In order to compare our result with (3.85) we have work with a definition of phase noise in natural numbers. We can then write the phase noise of the M-OSC as

$$\mathfrak{L}_m(\omega_m) = \frac{\omega_1^2 D_{11}}{(\frac{1}{2}\omega_1^2 D_{11})^2 + \omega_m^2} \approx \frac{\omega_1^2 D_{11}}{\omega_m^2} \tag{3.86}$$

where the last approximation holds for $\omega_m \gg 0.5\omega_1 D_{21}$. Using this approximation we see that we can write (3.83) as (in natural numbers)

$$\mathfrak{L}_s(\omega_m) = \frac{(D_{21}/D_{11})N^2\mathfrak{L}_m(\omega_m)\mu_2^2 + (N\omega_1)^2 D_{22}}{\mu_2^2+\omega_m^2} \tag{3.87}$$

At this point it would be useful understand the physical significance of the second Floquet exponent μ_2. In the special case where M-OSC and S-OSC in figure 3.1 represent harmonic oscillators it is possible to derive an analytical expression of the dynamics on the torus $\mathbb{T}^1$ in figure 3.2. This can be done through center manifold reductions followed by normal form transformation and the use of averaging procedures [18]. In section 3.2.1 we carried out these calculations, and by inspecting (3.46) and (3.47), on page 66, we find that one can identify $|\mu_2|$ with the *effective locking bandwidth*

$$|\mu_2| = |\zeta| = N\kappa\cos(N\hat{\theta}_e) = \Delta\omega_L\cos(N\hat{\theta}_e) \tag{3.88}$$

where $\Delta\omega_L$ is the *locking bandwidth*. The fact that the effective locking bandwidth can be identified as the eigenvalue pertaining to the second Floquet eigenvector u_2 is another plus of the algorithm described above. Using the result in (3.88) together with the identification

$$\Delta\Omega = N\omega_1\sqrt{D_{22}} \tag{3.89}$$

we arrive at the expression (3.85) for the case $D_{21} = D_{11}$. Since (3.83) contains the result from [55] as an approximation we conclude that (3.83) captures all the important relevant qualitative properties of the noise perturbed S-ILO such as the $20\log(N)$ penalty for subharmonic locking, the fact that the M-OSC dominates close to the carrier *etc.* The situation where $D_{21} \neq D_{11}$ is however not contained in the model described in [55].

3.2.5 Verification of the Developed Model

In [59] Demir *et al.* demonstrate how to calculate the autocorrelation matrix of a noise perturbed circuit using a time domain formulation. Starting from the variational equation

[18] The literature pertaining to this type of analysis of coupled harmonic oscillators is vast, and we shall not attempt to review even a small portion of it here. Representative examples can be found in [32], [6],[38], [19]

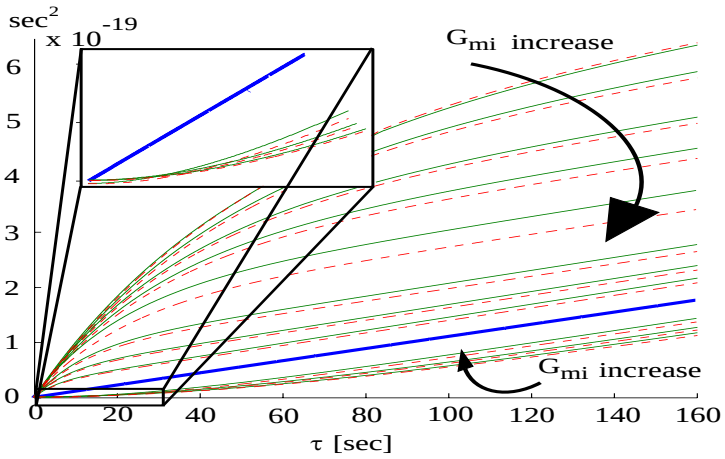

Figure 3.6: ILO#1 : The oscillator energy restoring circuit is modelled as a tanh nonlinearity : solid line = direct integration, dashed line = equation (3.73). The curves above the bold straight line represent the locked case ($T_{N2} = 290K$) and the curves below represents the tracking scenario $T_{N2} = 0.001K$.

and using results from the field of stochastic integration the authors derive an algorithm for the numerical calculation of the autocorrelation matrix. Later this theory in was extended in [60] so that it could be applied to phase noise in oscillators. We have implemented a small C-program [61] that implements the algorithm described in section 3.2.4 as well as the algorithm outlined in [60]. We shall use [60] as a method for verifying the result for the S-OSC SR-P in (3.73). Throughout this section we will assume linear coupling G_{mi} (see figure 3.1). Furthermore, the noise contribution from the circuit resistances R is assumed to be pure thermal noise with power density $i_n = \sqrt{4kT/R}$, where k is Boltzmann's constant and T is the absolute temperature, where we assume $T = 290K$ unless stated otherwise [19].

ILO#1 : Harmonic Oscillators

A simple LC tank oscillator is governed by the state equation

$$L\dot{i}_L = v_C \tag{3.90}$$
$$C\dot{v}_C = -i_L - v_C/R + G_M(v_C) \tag{3.91}$$

where v_C and i_L constitute the state variables in form of a capacitor voltage and a inductor current, respectively, and C, L, R are the passive components of a parallel LCR resonator tank circuit. Depending on the form of the energy restoring circuit component, as represented by the transconductance G_M, this system can model both harmonic as well as relaxation oscillators [20]. A common choice for G_M is the tanh nonlinearity which models the differential mode of a cross-coupled oscillator

$$G_M(v_C) = S \tanh\left(\left\{\frac{G_n}{S}\right\} v_C\right) \tag{3.92}$$

[19] we refer to the text in appendix A for a discussion on noise modelling.

[20] by the term *relaxation oscillators* we refer to periodic solution with multiple time constants and not *singular oscillators*.

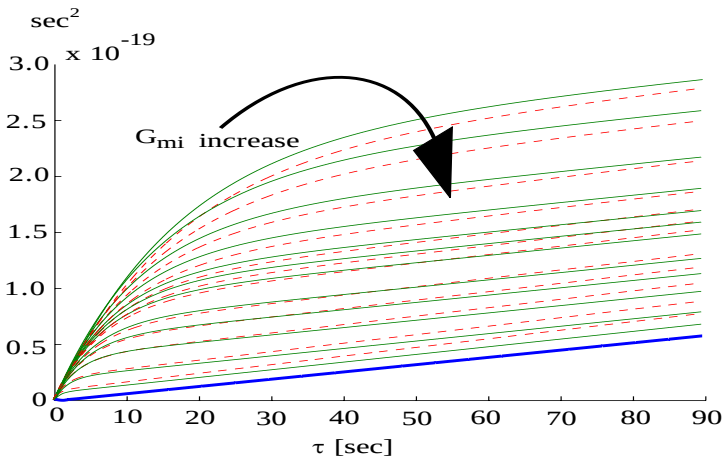

Figure 3.7: ILO#2 The oscillator energy restoring circuit is modelled as a third-order polynomial and the parameters are set to ensure a relaxation-type solution : solid line = direct integration, dashed line = equation (3.73).

which we shall now investigate. In the following, circuit components pertaining to the M-OSC will have subscripts 1 and S-OSC components will have subscripts 2. We choose $S_i = 1/R_i$, $G_{ni} = -2.5/R_i$, $R_1 = 500\Omega$, $R_2 = 50\Omega$, $L_i = 1.59H$, $C_i = L_i/100F$. The resonator components are chosen so that $\omega_1 = 2\pi$. In figure 3.6 we plot the power of the S-OSC SR-P Δ_s as a function of the observation time τ. The results of the direct integration of the SDE formulation in [60] is shown as solid lines and the curves based on the result in (3.73) is plotted as a dashed line. Also shown is the power of the M-OSC SR-P which plotted as straight bold line. Since $\sigma_s^2 > 0$ in this case we see that the curves initial slope is greater than the M-OSC SR-P slope and the asymptotic slope is equal to the M-OSC SR-P. The last point is a consequence of the fact that $D_{21} \approx D_{11}$ (see discussion in 3.2.3). Referring to the discussion in section 3.2.4 we know that the model described in this paper is capable of capturing the effect of *tracking*. This term pertains to a situation where the M-OSC is more noisy than the S-OSC and it is modelled here by a very low S-OSC noise temperature T_{N2}. In the lower part of figure 3.6 we show the curves corresponding to the oscillator ILO#1 in tracking mode with $T_{N2} = 0.001K$. Since $\sigma_s^2 < 0$ in this case we see that the curves initial slope is smaller than the M-OSC SR-P slope.

ILO#2 : Relaxation Oscillators

Considering the system of equations (3.90)-(3.91) with

$$G_M(v_C) = \left(a_i + m_i v_C + b_i v_C^2\right) v_C \tag{3.93}$$

Unlike the *differential mode oscillator* in (3.92), the above function is able to model the effects of a dynamic DC point. The parameters are given as : $a_i = 25.0/R_i$, $b_i = (2/3)a_i$, $m_i = 0.25a_i$, $R_i = 500\Omega$, $L_i = 1.59H$, $C_i = L_i/100F$. This will ensure that the solutions of the individual oscillators will converge onto a relaxation-type orbit with the second Floquet character being equal to $\lambda_2 \approx 0.04$ (almost singular solution). In figure 3.7 we compare the theoretic results in (3.73) with the direct SDE integration for this type of oscillator. To model a situation where the S-OSC is more noisy than the M-OSC (locked

solution) we raise the noise floor of the S-OSC by setting $T_{N2} = 5000K$. Since $\sigma_s^2 > 0$ in this case we see that the curves initial slope is greater than the M-OSC SR-P slope.

ILO#3 : Third Order Ring Oscillators

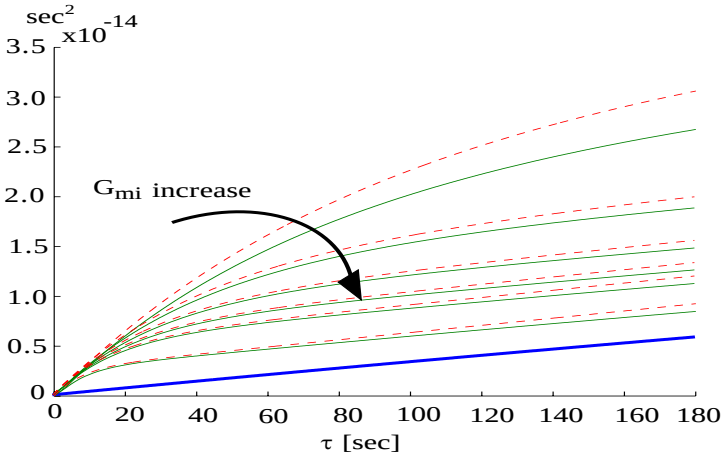

Figure 3.8: ILO#3. The oscillator energy restoring circuit is modelled as a tanh nonlinearity : solid line = direct integration, dashed line = equation (3.73).

In this case we have the state equations

$$C\dot{v}_{Ci} = -v_{Ci}/R + \tanh\big(G_m v_{Cj}\big)/R \quad i \in \{0,1,2\} \tag{3.94}$$

where $j = i - 1 \mod 3$. We choose $R_1 = 1k\Omega$, $R_2 = 10k\Omega$, $C_1 = 1mF$, $C_2 = 0.1mF$ resulting in an oscillation frequency of $\omega_1 \approx 2\pi$. In figure 3.8 we compare the theoretic results in (3.73) with the direct SDE integration for this type of oscillator.

Chapter 4

n Unilaterally Ring-Coupled Harmonic Oscillators Perturbed by White Noise

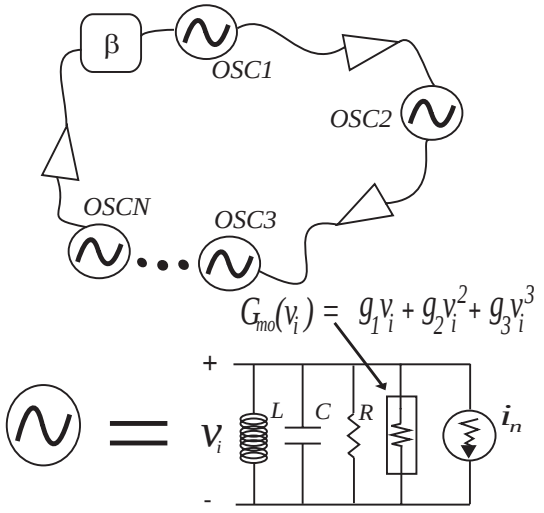

Figure 4.1: n unilaterally ring coupled van der Pol oscillators

Figure 4.1 shows n LC oscillators coupled unilaterally in a ring configuration with an explicit phase shift of β radians inserted between oscillator $\#n$ and oscillator #1. In the following we shall also refer to this structure as the *unilateral ring*, the *unidirectional ring* or simply the *ring*. The structure in figure 4.1 is a multi-mode system[1], implying that the circuit can oscillate in n different frequency locked states, also called a *modes*. The analysis in this chapter will concentrate on investigating the characteristics of the circuit in figure 4.1 in the so-called *dominant mode* where each oscillator trails its immediate neighbor by a fixed phase shift of $-\beta/n$ radians. We shall argue, that starting from "normal" initial conditions, the unilateral ring will always start up in this mode. Although we shall cover many different areas with regards to the analysis of the unidirectional ring,

[1]note that in this report, the term "multi-mode system" does not imply a multi-mode oscillation although this is a real possible [62],[63]. We simply mean that the circuit contains the possibility of different modes.

the main emphasis will be put on explaining the newly discovered *coupling induced AM-PM noise conversion* phenomena [6],[19],[20].

The text can be divided into two parts, with sections 4.1-4.4 involving the various steady-state issues while sections 4.5-4.7 discuss the linear response of the system to white noise perturbations. We start in section 4.1 by investigating which modes are possible with the coupling structure in figure 4.1. The natural way to approach this issue is to take advantage of the inherent symmetry of the network and examine the configuration using *group theoretic* methods, as was introduced in section 1.3. As will be shown in section 4.1.1, using this methodology it is possible to derive a complete list of all the modes which are *flow invariant* with regard to the actions contained in the symmetry group of the circuit in figure 4.1. However, the symmetry approach is not the only option and in section 4.1.2 we shall present an alternative steady-state procedure. Section 4.2 gives a short overview of the main areas of application for the unilateral ring, which has been extensively studied in connection with low-power/noise RF/microwave *multi-phase signal generation*.

The canonical amplitude/phase equations of the n oscillator unilateral ring are derived in section 4.3 using an averaging approach [2]. In the model described in this chapter we assume that each oscillator cell in the coupling network can be described as a van der Pol unit [38] [42], which is represented by the state equations

$$L\frac{\partial i_L}{\partial t} = -v_C \tag{4.1}$$

$$C\frac{\partial v_C}{\partial t} = i_L - \frac{v_C}{R} + G_{mo}(v_C) \tag{4.2}$$

These equations model a dampened parallel LC circuit shunted by a third order *nonlinear negative resistance* $G_{mo}(v_C) = g_1 v_C + g_2 v_C^2 + g_3 v_C^3$, as illustrated in figure 4.1, where v_C is the capacitor voltage and i_L is the inductor current. At this point a relevant question would be :

will fixing the type of oscillator this early in the process yield a less general model?

The answer to this question is, fortunately, *no!* We refer here to the discussion in section 1.1 where it was shown that the van der Pol oscillator is the simplest model that is still be able to faithfully capture all of the qualitative dynamics of an arbitrarily higher order isochronous harmonic oscillator. Briefly, this follows from the *center-manifold theorem*, which reduces the state space of an arbitrary higher dimensional system to the complex plane, and from the *normal form method*, which equates all qualitative equivalent nonlinear terms. Furthermore, as was explained in section 1.1, the averaging procedure is nothing but an analytical shortcut to produce these normal form equations. The averaged van der Pol equations are therefore the natural choice used by most authors to model the qualitative dynamics of coupled oscillators without inherent frequency control (varactors).

The usual approach towards a qualitative analysis of coupled oscillators is to consider the *phase-only model* [3] [27],[64], [65] where the amplitude equations are neglected. However, as will be illustrated in the last three sections, in some situations, the phase-only

[2] averaging theory, as it is applied to harmonic oscillators, is thoroughly explained, by example, in appendix B where a general non-isochronous second order oscillator is studied. We refer readers not familiar with this subject to this text as an user-friendly introduction to the theory.

[3] the Andronov-Hopf normal form, which is the relevant normal form for harmonic oscillators, preserves the symmetry of the circle $\mathbb{S}^1$. Considering only asymptotic dynamics or assuming a very tight coupling

approach fails to produce a reliable [4] model. This will become apparent in section 4.4 where we investigate the linear stability of the dominant mode. Among other things, it will be shown that the amplitude equations are necessary to predict the stability of the configuration $(n, \beta) = (2, \pi)$, known as the *cross-coupled quadrature oscillator* (CCQO), where the phase shift equals $-\pi/2$. Then in section 4.5 we shall begin to look at the main subject of this chapter, namely the above mentioned *coupling induced AM to PM noise conversion*. The phenomena is investigated for the general n oscillator ring structure using three different analytical methods which all lead to the same result. We end this chapter in section 4.7 with a detailed study of the CCQO. The stochastic normal form differential equations of this specific circuit were studied, by the author, in a series of papers [6],[19],[20] with emphasis on characterizing the noise properties through linear response theory. The text contains an extensive review of the model, including all those calculations which were too bulky to be included in the papers.

4.1 Modes of n Unidirectional Ring Coupled Identical Harmonic Oscillators

In this section we shall investigate the steady-state properties of the unidirectional ring in figure 4.1. The steady-states are represented by frequency-locked solutions, or *modes*, where the n oscillators are synchronized and there exist fixed phase shift (possible zero) between each of the cells. We shall approach the problem from two different directions. Section 4.1.1 investigates the method described in [29], where the system is characterized through the isotropy subgroups corresponding to the *spatio-temporal symmetries* of the different modes while section 4.1.2 describes a simpler, although less general, algorithm. The two proposals produce different results, and this is briefly discussed in section 4.1.3.

Referring to the discussion in section 1.1, the $\mathbb{Z}_n \times \mathbb{S}^1$ *phase-only* representation of the system in figure 4.1 is written as

$$\frac{d\phi_i}{dt} = 1 + \kappa\Phi_i(\phi_1, \cdots, \phi_n) \quad i = 1, 2, \cdots n \tag{4.3}$$

where ϕ_i is the phase of the i'th oscillator, κ is a positive parameter representing the *coupling strength* and $\Phi = [\Phi_1\ \Phi_2\ \cdots\ \Phi_n]$ is the $\mathbb{Z}_n$ equivariant vector field. The derivation of the system in (4.3), from the original state equations describing the physical dynamics, was explained in detail in section 1.1 [5].

4.1.1 Ashwins's Symmetry Approach

Steady-state analysis of (4.3), based on the symmetry of the coupled oscillator network, was pioneered by Ashwin in [29] [6]. This work, in turn, was inspired by Golubitsky *et*

to the limit cycles it is seen that the amplitude can be *adiabatically* removed. In this case the orbit state is referenced by a single variable indexing the angle on the circle $\mathbb{S}^1$. This index is the so-called *phase* of the oscillator.

[4] by *reliable*, we take to mean a model which faithfully captures *all* qualitative effects, including linear stability and response, of the original oscillator system.

[5] briefly, (4.3) follows by employing the center manifold theorem and the normal form method while insisting on a *normal hyperbolic invariant manifold* - the so-called n-torus $\mathbb{T}^n$. A normally hyperbolic torus implies that the coupling strength κ is around one order of magnitude smaller than the dissipation in the individual oscillators. The discussion in this text is hence limited to the *weak coupling scenario* [66],[29].

[6] a review of basic group theory concepts was given in section 1.3 and we refer the readers, unfamiliar with the subject, to this text.

al. [25], [37]. Here we review the methods and results derived in [29] for the purpose of identifying the *spatio-temporal* symmetric modes of the circuit in figure 4.1. Following this review we attempt to extend the original formulation in [29], which only discusses the case $\beta = 0$, to included a finite explicit phase shift ($\beta \neq 0$).

Zero Explicit Phase Shift : $\beta = 0$

In section 1.3 we introduced the analytical framework of *group theory*, as applied to the steady-state analysis of n identical coupled oscillators. It was shown that the modes of a coupled cell structure, where the coupling network exhibited the symmetry Γ, was found from the *isotropy subgroups* Σ of the group $\Gamma \times \mathbb{S}^1$. The *coupling symmetry* of figure 4.1, for $\beta = 0$, is represented by the *cyclic group* $\mathbb{Z}_n$ which signifies that we can rotate the structure in one direction only (clockwise). We are therefore interested in finding the isotropy subgroups of $\mathbb{Z}_n \times \mathbb{S}^1$. The isotropy subgroups Σ, which represent the *spatial-temporal symmetry* of the solutions, can be split up into a spatial $\pi_s(\Sigma)$ and a temporal $\pi_t(\Sigma)$ projection, respectively. We can therefore explicitly divide any action in Σ as follows

$$\gamma \in \Sigma \Rightarrow \gamma = (\sigma, w) \quad ; \quad \sigma \in \pi_s(\Sigma) \quad ; \quad w \in \pi_t(\Sigma) \tag{4.4}$$

In this chapter we consider $\Gamma = \mathbb{Z}_n$. The spatial projection of Σ must hence be a subgroup of $\mathbb{Z}_n$. This means that it is equal to $\mathbb{Z}_m$ for some m dividing n [21], [25], [29] [7]. We therefore assume that we can write

$$\underbrace{n}_{n \text{ oscillators}} = \underbrace{m}_{m \text{ oscillators}} \times \underbrace{k}_{\text{in } k \text{ groups}} \tag{4.5}$$

As seen from the above equation, for $m \neq n$ we consider several *groups*, each containing a set of identical oscillators. This loss of coherence must be the result of a *symmetry-breaking bifurcation* [37]. As explained in section 1.3 the group $\mathbb{Z}_m$ is generated by m *cycle*. However, using (4.5), this generator can also be written as σ^k where σ is now the *n-cycle* defined in (1.96)-(1.97) on page 33. The main points of the above discussion are explained pictorially in figure 4.2, where we consider the example $n = 12$. From this figure we see that, *considering only spatial symmetry*, we can write the oscillators in the ring as [8]

$$z_i = a_i \quad , \quad a_i = a_j \text{ for } i = j \mod k \tag{4.6}$$

where a_i is an arbitrary unit length phasor, as represented by a colored dot in the figure. Using (4.4), the generators of the isotropy subgroups Σ, are then written as (σ^k, w). Taking the m'th power of this action, we get

$$(\sigma^k, w)^m = (\sigma^{km}, w^m) = (1, w^m) \tag{4.7}$$

Hence, we must have that $w^m = 1$, which means that

$$w = \omega^{kp} \quad p \in \{0, 1, 2, \cdots, m-1\} \tag{4.8}$$

where we have introduced the notation

[7] see figure 1.2 on page 34

[8] as explained in section 1.3, through normalization, the state of the individual oscillators can be described by a unit length phasor $z_i = \exp(j\phi_i)$.

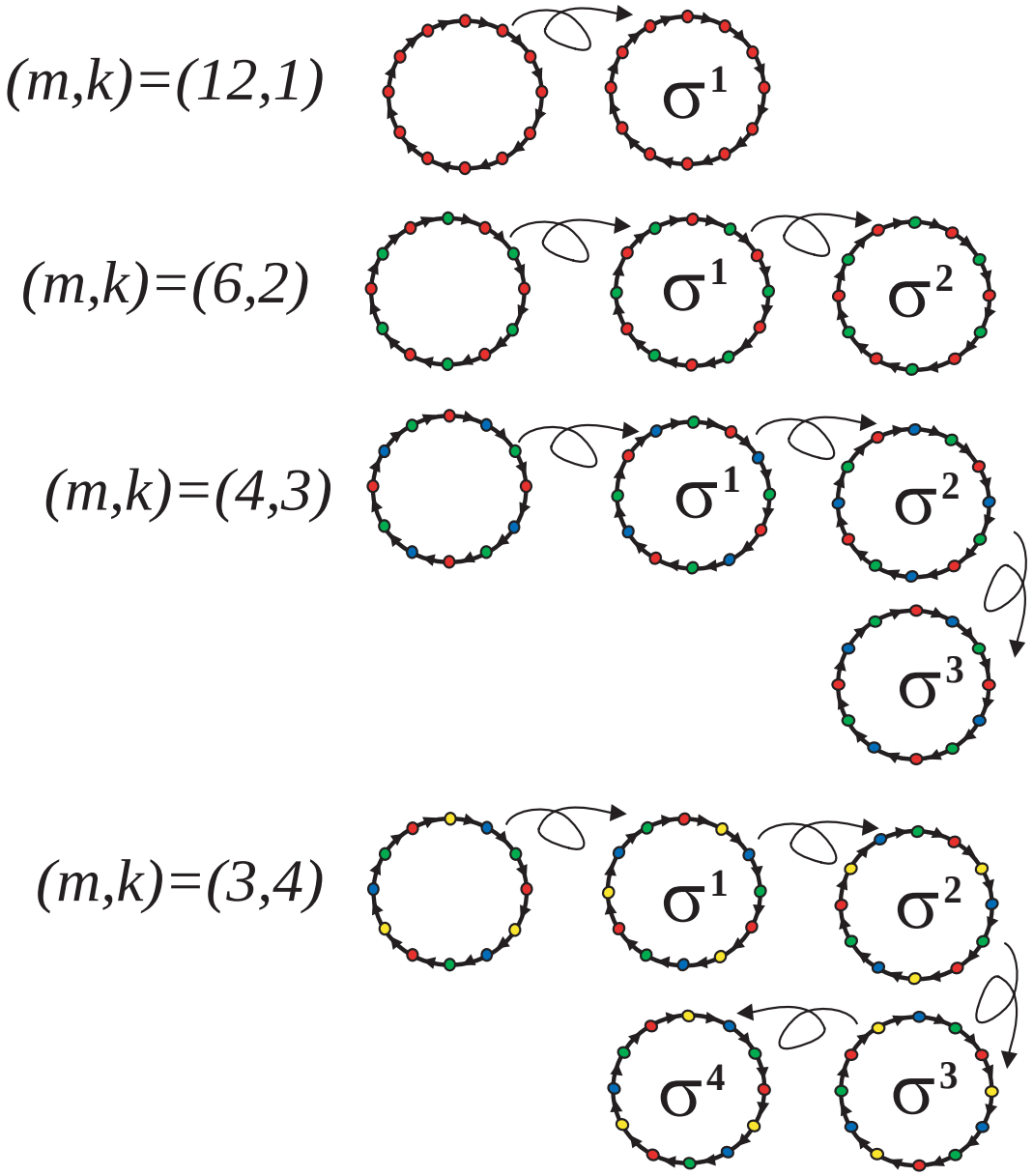

Figure 4.2: The spatial symmetry of n coupled oscillators, with $\Gamma = \mathbb{Z}_n$, will be $\pi_s(\Sigma) = \mathbb{Z}_m$ where m divides n, which means that $n = m \times k$. In the above figure this is illustrated for $n = 12$ oscillators. This division splits the 12 oscillators up into k groups of m oscillators each. The oscillators belonging to the same group are here represented by colored dots : group #1 = •, group #2 = •, group #3 = • *etc.* The figure shows the effect of operating on the constellation with the *n-cycle* $\sigma = (1, 2, \cdots, n)$ as symbolized by the *looped arrow* $\looparrowright$. As is seen, the operator σ^k brings the constellation back to its original form. Note that the subgroup $(m, k) = (2, 6)$ is not included due to lack of space in the figure.

$$\omega = e^{j\frac{2\pi}{n}} \tag{4.9}$$

From (4.8) we see that the temporal projection of Σ is a subgroup of $\mathbb{Z}_n$, as predicted in section 1.3 (see note 1.3 on page 35). The isotropy subgroups hence get the form [29]

$$\mathbb{Z}_m(p) = (\sigma^k, \omega^{kp}) \quad p \in \{0, 1, 2, \cdots, m-1\} \tag{4.10}$$

If we first consider the case $p = 0$, then the fixed space of $(\sigma^k, 1)$ is simply k groups of m in-phase oscillators, where the absolute phase of the group members is arbitrary (depending on initial conditions). Moving on to $p = 1$, the fixed space of (σ^k, ω^k) still divides the n oscillators into k groups of m oscillators, but now the phase-shift between two adjacent oscillators within the group must be ω^k. From this description follows that the fixed space of (4.10) consists of k groups of m oscillators where the phase shift between the constituents of the same groups are $\omega^{kp} = \exp(j2\pi p/m)$. Using (4.6), we write this as

$$\boxed{\text{fix}(\mathbb{Z}_m(p)) = \{z \in \mathbb{T}^n | z_i = a_i \omega^{ip} \ ; \ a_i = a_j \text{ for } i = j \mod k\}} \tag{4.11}$$

In figure 4.8 we illustrate the modes in (4.11) for the $n = 12$ oscillators, where $(m, k) = (4, 3)$. As is seen from the figure, the p parameter controls the the relative phase shift of the oscillators within each group.

Finite Implicit Phase Shift $\beta \neq 0$

We are looking for isotropy subgroups of the symmetry $\mathbb{Z}_n^\beta \times \mathbb{S}^1$, where $\mathbb{Z}_n^\beta$ represents the symmetry of a ring with an explicit phase shift β. This is equivalent to considering the original symmetry $\mathbb{Z}_n \times \mathbb{S}^1$ operating on the *broken ring* $\phi \in [0; 2\pi - \beta]$. Using this formulation, the spatial subgroup has not changed from the above example and we therefore have $\pi_s(\Sigma) = \mathbb{Z}_m$. An action of $\pi_s(\Sigma)$ can then be written as σ^k, where σ is the *n-cycle* and $n = m \times k$ as explained in connection with (4.5). However, because of the added explicit phase shift we must write (4.7) as

$$(\sigma^k, w)^m = (\sigma^{km}, w^m) = (1, w^m) = (1, e^{-j\beta}) \tag{4.12}$$

since the temporal part of the action must offset the explicit phase shift added to each oscillator, as it is rotated around the ring. This means that we have

$$w = \gamma^k \omega^{kp} \quad p \in \{0, 1, 2, \cdots, m-1\} \tag{4.13}$$

where ω is still given by (4.9) and

$$\gamma = e^{-j\frac{\beta}{n}} \tag{4.14}$$

Following the same procedure which led to the derivation of (4.11), with (4.13) substituted for (4.8), we find the following fixed point space for the isotropy subgroups $\mathbb{Z}_m^\beta(p)$

$$\boxed{\text{fix}(\mathbb{Z}_m^\beta(p)) = \{z \in \mathbb{T}^n | z_i = a_i \gamma^i \omega^{ip} \ ; \ a_i = a_j \text{ for } i = j \mod k\}} \tag{4.15}$$

4.1.2 Rogge's Method

We now turn to the analysis described in [64],[65] where an alternative approach is employed to find the different modes of the ring.

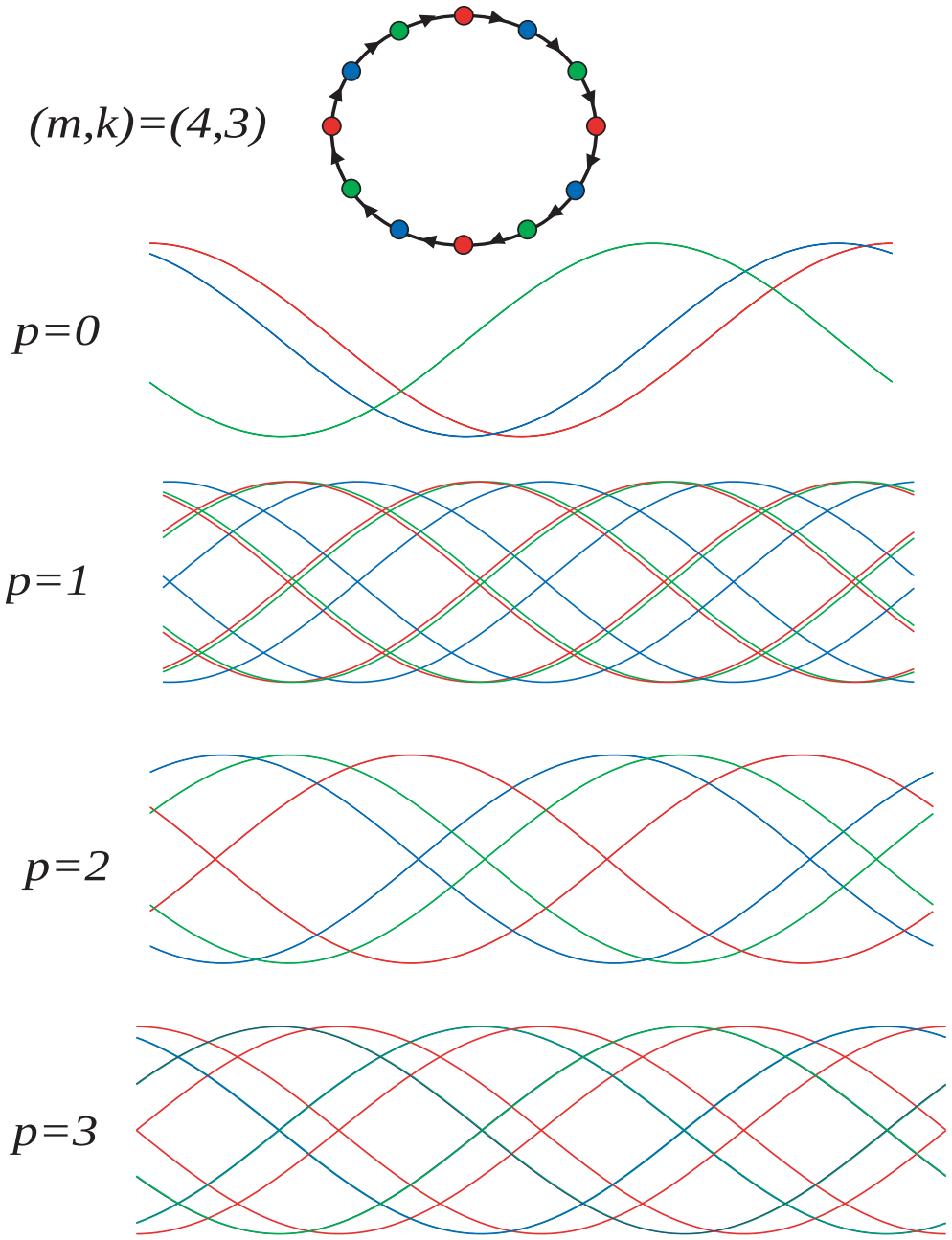

Figure 4.3: Illustrating the fixed space in (4.11) for $n = 12$ and $(m, k) = (4, 3)$. The oscillators belonging to the same group are here represented by colored dots : group #1 = •, group #2 = •, group #3 = •. The relative phase shift of oscillators belonging to the same group depends on the parameter p as $\phi = 2\pi/n \cdot k \cdot p = 2\pi/m \cdot p$ where $p = \{0, 1, \cdots, m-1\}$ (see (4.11)). Hence, for $p = 0$ the oscillators belonging to the same group are phase shifted $\phi = 0$, for $p = 1$ the shift is $\phi = \pi/2$, $p = 2$ gives $\phi = \pi$ and $p = 3$ gives $\phi = 3\pi/2$. The solution is invariant to a constant phase shift within one group, since the phasors a_i in (4.11) are not specified (the group phase shift has no significance in the above plots).

Zero Implicit Phase Shift $\beta = 0$

We can write the canonical normal form in (4.3) explicitly as

$$\frac{d\phi_i}{dt} = 1 + \kappa \sin(\psi_i) \quad i = 1, 2, \cdots n \tag{4.16}$$

where we have defined the *phase differences*

$$\psi_i = \phi_i - \phi_{i-1} \quad i = 1, 2, \cdots n-1 \tag{4.17}$$

Using the definition in (4.17), we can write (4.16) as

$$\dot{\psi}_i = \kappa\big(\sin(\psi_{i+1}) - \sin(\psi_i)\big) \quad i = 1, 2, \cdots n-1 \tag{4.18}$$

A fixed point of (4.18) must then imply that $\psi_i = \psi_{i+1}$ or $\psi_i = \pi - \psi_{i+1}$ which can be written

$$(\psi_i - \psi_{i+1})(\psi_i + \psi_{i+1} - \pi) = 0 \tag{4.19}$$

Adding all $n-1$ phase differences gives the result

$$\sum_{i=1}^{n-1} \psi_i = (\phi_1 - \phi_n) + (\phi_2 - \phi_1) + \cdots + (\phi_n - \phi_{n-1}) = 0 \tag{4.20}$$

The above sum, is defined modulus 2π. It is possible to *lift* [22] the coordinates in the above sum off the manifold $\mathbb{T}^{n-1}$ and onto $\mathbb{R}^{n-1}$. Carrying out this procedure means that we can write (4.19) as

$$\sum_{i=1}^{n-1} \psi_i = 2\pi p \quad p \in \{0, 1, \cdots, n-1\} \tag{4.21}$$

where $\psi_i \in \mathbb{S}^1$. The next step of the analysis then follows from assuming that ψ_i is equal to $\alpha \in \mathbb{S}^1$ or $\pi - \alpha$, where α is undetermined at this point. This choice, which follows from (4.19), is then inserted into (4.21), giving us the result

$$\boxed{m\alpha + (n-m)(\pi - \alpha) = 2\pi p \quad \alpha \in \mathbb{S}^1 \ , \ p \in \{0, 1, \cdots, n-1\}} \tag{4.22}$$

Finite Implicit Phase Shift $\beta \neq 0$

In this case the sum of the phase differences ψ_i *plus the implicit phase shift* β must equal zero modulus 2π. This means that we can write (4.21) as

$$\sum_{i=1}^{n-1} \psi_i + \beta = 2\pi p \quad p \in \{0, 1, \cdots, n-1\} \tag{4.23}$$

Following the procedure which led to equation (4.22), with (4.23) substituted for (4.21), gives the following result

$$\boxed{m\alpha + (n-m)(\pi - \alpha) + \beta = 2\pi p \quad \alpha \in \mathbb{S}^1 \ , \ p \in \{0, 1, \cdots, n-1\}} \tag{4.24}$$

4.1.3 Discussion

The modes found using Ashwin's symmetry method are summarized in equations (4.11) and (4.15), which lists the fixed point spaces, corresponding to the flow invariant orbits of the structure in figure 4.1, for $\beta = 0$ and $\beta \neq 0$, respectively. Likewise, equations (4.22) and (4.24) in the previous section list the possible modes as predicted by Rogge in his PhD thesis [65]. Unfortunately, the two methods do not produce the same results. First of all the two methods do not even produce the same number of modes! This is perhaps most easily seen for $n = 3$ where (4.11) predicts 3 possible modes while (4.22) includes $3 \times 3 = 9$ modes. More specifically, the method described in [65] predicts the existence of the so called *elementary solutions* [65, p. 91] which refers to $\alpha = 0$ and $m \neq n$ in (4.22) and (4.24). These modes are not found when using the formulation in [29]. Considering the ring, with the parameters $(n, \beta) = (3, 0)$, we get following 3 modes from (4.11) : 1 in-phase and 2 rotating wave $\pm\pi/3$. These modes are also found in (4.15) (in multiple copies), however, here we furthermore get modes with one group of 2 in-phase oscillators plus one oscillator which is phase-shifted π radians respective to this group. These are the elementary solutions for $(n, \beta) = (3, 0)$. In [8], which considers the circuit in figure 4.1 with $\beta = \pi$, the mode analysis is similar to what is found in [64],[65]. Here the authors find the circuit modes, specified by n identical phase shifts α, according to the formulation

$$n\alpha + \beta = 2\pi p \quad p \in \{0, 1, \cdots n-1\} \tag{4.25}$$

which is identical to (4.24) with $n = m$. We then see that the formulation in [8] simply ignores the elementary solutions. It seems that the methods in [29], for $m = n$ *i.e.* no symmetry breaking, and equation (4.25) leads to the same results.

It is important to note that the different modes in (4.11) and (4.15) are not the result of a bifurcation. We assume that the Jacobian, with respect to the explicit phase shift β, is non-singular and therefore, according to the *implicit function theorem* [9], the different orbits simply represents a continuous re-mapping of the fixed points [10], as a function of the parameter β. From this description we see that *mode numbers* in (4.11) and (4.15) must correspond to the same orbit, with new fixed points. In section 4.4, where we consider stability and start-up issues, the following points will be of significant importance

note 4.1 *the mode numbers* (m, p)*, in* (4.11) *and* (4.15)*, represent the same two orbits, where* (4.15) *simply models the re-mapping of the fixed points by the parameter* β*. Most importantly the mode* $\mathbb{Z}_n(0)$*, corresponding to the in-phase mode in* (4.11)*, is paired with the rotating wave mode* $\mathbb{Z}_n^{\beta}(0)$ *in* (4.15) *where the constant phase shift around the ring is equal to* $-\beta/n$*.*

By using the symmetry considerations in (4.11) and (4.15) we were able to make the above observation, something which could not be done with the less sophisticated methods described in [8] and [65].

[9] see footnote 34 on page 31.

[10] since we here consider periodic solutions, the introduction of the term "fixed points", which is normally connected with transient systems, could, potentially, be confusing to some. However, by looking at the problem through the formulation of a *Poincaré map* [21] this notation is perfectly reasonable/legal.

4.2 Practical Applications of the Unidirectional Ring

Below we will include a list of some of the known areas of application for the unidirectional ring in figure 4.1. This configuration has found uses, both as an electrical device, as well as a mathematical model for the description of complex spatio-temporal symmetries. Compared to other forms of coupling, such as *all-to-all* [27] and the *bilateral ring* [63], the unilateral coupled ring structure is only very rarely used as a model to describe frequency locked behavior in physical/biological systems. This, obviously, is connected with the abundance of bilateral coupling, and the nearly non-existence of unilateral coupling, in nature.

Many of the references collected by the author during his thesis, mostly dealing with the analysis and design of *quadrature oscillators*, are included in this text. The idea is that the interested reader could use this reference list as a starting point towards a self-study of the subject. For a longer list of applications and references we refer to the PhD thesis [65].

1. *Multi-phase Oscillators* : In modern transceiver designs, multi-phase, and more specifically quadrature, signals are an essential part of an efficient modulation/de-modulation scheme. This is the case with the so-called I/Q de-modulation methods found in zero-IF and low IF receivers as well as in the various image-reject architectures. Multi-phase sources are also used in data recovery circuits (DRC) and in fractional N dividers [11] to mention but a few areas. With so many potential applications the research into an efficient electronic derivation of these signals has been intense.

   In 1996 Rofougaran *et al.* [5] proposed a novel CMOS oscillator producing quadrature outputs. This circuit consisted of two *differential* LC oscillators coupled unilaterally in a ring structure, where one of the couplings was a *cross-connection*, thus introducing an explicit 180^o phase shift [11]. This configuration, which is known as the *cross-coupled quadrature oscillator* (CCQO), has since become one of the most popular methods of producing quadrature signals and it has been implemented in all kinds of variations and using many different technologies. The success lies primarily with a low power consumption and good phase noise performance. The main emphasis of research, with regards to this circuit, has centered on creating design rules which would help limit phase noise and quadrature error. It is now well established that there exist a tradeoff between these two design goals [6], [7], [8], [19], [20], [67], [68]. We have collected quite a few papers on this circuit and we shall categorize them according to whether the main emphasis is on analysis or circuit implementation.

   analysis : [6], [7], [8], [19], [20], [67], [68], [69], [70], [71], [72], [73].

   circuit : [5], [74], [75], [76], [77], [78], [79], [80],[81], [82], [83], [84].

   There exist several alternatives to the ring coupled architecture for the derivation of multi-phase signals. Some of these are listed below

   - *Polyphase filters* : Polyphase filters are Hilbert-type filters which are build using passive $R-C$ components [85]. With a single source on the input, the two outputs of this all-pass filter supply the quadrature signals. The main problems

[11] note that the oscillators have to be differential for this to work. We see that this circuit corresponds to figure 4.1 with the parameters $(n, \beta) = (2, \pi)$.

encountered in integrated designs are related to chip size, power consumption and to a lesser extent matching and bandwidth. In order to achieve a reasonable bandwidth, several stagger-tuned sections have to be cascaded. This in turn requires the filters to be preceded by noisy, power-hungry buffers [86],[87].

- *Frequency dividers* : By dividing the frequency of a signal, operating at 2ω, by 2, quadrature signals at frequency ω will result. This architecture can be very power hungry especially in its simplest form consisting of two D flip-flops in a negative feedback loop. However, variants which consider injection locked LC or ring oscillators will perform better [88],[89].
- *Ring Oscillators* : By construction, ring oscillators produce multi-phase signals. Due to the low Q and relative high power consumption, this option has a very poor power/noise product [89], [90].
- *Super-Harmonic Coupling* : This is a rather new proposal works by coupling two differential oscillators in a *common-mode* node [91], [92]. This means that the second harmonic of the oscillators synchronize leading to the desired phase relationship. Of the above options, super-harmonic coupling seems, by far, to be the superior alternative. It might even outperform the CCQO. However, because this configuration is still very new, this issue deserves further investigations.

2. *Antenna arrays* : The two papers [9], [93] by Dussopt *et al.* document the work on creating a circular polarized patch antenna by feeding each patch by the output of a four stage unidirectional ring. As discussed in the papers, this construction gives a wide bandwidth.

3. *n-legged Animal Locomotion* : In the book [37], Golubitsky *et al.* give a rare example illustrating the unidirectional ring model applied to explain a biological phenomena. They consider the neural network responsible for locomotion of an n-legged animal. In this model a single neuron, as modelled by a harmonic oscillator, is responsible for the movement of each leg.

4.3 A Quasi-Sinusoidal Model of the Unilateral Ring

In this section we shall derive the state equations which model the dynamics of the circuit in figure 4.1 as well as the linear response equations which will be used in stability and noise calculations. The oscillator cells are modelled as simple damped parallel resonators shunted by a third order negative resistance and the coupling is assumed nonlinear. Referring to the discussion in the introduction to this chapter and in section 1.1, we know that this particular model will faithfully capture the qualitative dynamics of any ring coupled system of *isochronous* harmonic oscillators of arbitrary complexity. Several different modes are possible with the ring configuration in figure 4.1, as was discussed in section 4.1. However, in this chapter we shall limit our analysis to the *dominant mode* (see discussion in section 4.4) which is characterized by a fixed phase shift $-\beta/n$ between neighboring cells. Assuming identical oscillators we can set up the following KCL at cell $\#i$ in figure 4.1 [12]

[12] since we in (4.26) only consider capacitor voltages we will not use the notation v_C, i_L from figure 4.1 and equations (4.1)-(4.1) to indicate capacitor voltages and inductor currents. Instead we use the lighter notation v_i, where it should be clear that $v_i \equiv v_{C,i}$.

$$C\dot{v}_i + \left(\frac{1}{R} - G_{mo}(v_i)\right)v_i + \frac{1}{L}\int v_i dt = G_{mc}(v_{i-1})v_{i-1} \quad i \in \{2, 3 \cdots n\} \tag{4.26}$$

where v_i is the capacitor voltages, C, R, L are the capacitive, resistive and inductive parts, respectively, of a parallel LRC resonator, G_{mo} models the oscillator energy restoring circuit element and G_{mc} is the nonlinear coupling transconductance. Here, we shall model both nonlinear components through a second order polynomial

$$G_{mx}(v) = g_{x0} + g_{x1}v + g_{x2}v^2 \quad x \in \{o, c\} \tag{4.27}$$

We have left out oscillator #1 in (4.26), which, as is seen from figure 4.1, constitutes a special case since the injected current is shifted by a constant phase β. We will start by deriving the averaged equations from (4.26), ignoring oscillator #1, which will then be included at a later point.

In this chapter we consider *harmonic oscillators* or *nearly harmonic oscillators* where the solution is dominated by the contribution from the first harmonic. The analysis in these chapter is hence *quasi-sinusoidal/harmonic* [13] by which we mean that the solution can be modelled as a harmonic carrier modulated by *slow wave* amplitude and phase signals. For this to be a valid assumption with the oscillators in (4.26) we must require that [6], [42]

$$\frac{g_{o0} - G_L}{G_L}\frac{1}{Q} = \frac{\mu_0}{Q} \lessapprox 0.1 \tag{4.28}$$

where $G_L = 1/R$ [14] and

$$Q = \omega_0 RC = R\sqrt{\frac{C}{L}} \tag{4.29}$$

is the *oscillator quality factor* and

$$\omega_0 = \frac{1}{\sqrt{LC}} \tag{4.30}$$

is the *natural frequency* of the LC bandpass filter.

Considering the travelling wave mode ($\beta \neq 0$), we see that each oscillator cell in figure 4.1 will be injected with an external current which is out of phase with the internal oscillator current. The result is that each oscillator is forced to operate at a frequency ω_1 which is different from the natural frequency ω_0 of the resonator. Equivalently, the resonator will be operated at a finite phase shift ψ. An expression for ω_1 as a function of ψ follows directly from standard textbook formulas [94] for the parallel RCL circuits [15]

$$\frac{\omega_1}{\omega_0} = \pm\frac{\tan(\psi)}{2Q} + \frac{1}{2Q}\sqrt{4Q^2 + \tan^2(\psi)} \tag{4.31}$$

For a large Q-factor the above equation reduces to

[13] we refer the reader to section 1.2 and appendix B for a discussion of averaging techniques and quasi-sinusoidal analysis.

[14] here we use the notation $1/R = G_L$ where the subscript L refers to the "load". We do not not use the standard notation $1/R = G$ due to the similar symbols for the oscillator and coupling transconductances G_{mo} and G_{mc}, respectively.

[15] see also the master thesis [38].

$$\Delta\omega = (\omega_1 - \omega_0) = \pm\omega_0 \frac{\tan(\psi)}{2Q} \tag{4.32}$$

We now write a phasor expression for the assumed quasi-sinusoidal capacitor voltage signals

$$v_i(t) = A_i(t)\cos\big(\omega_1 t + \phi_i(t)\big) = \Re\{A_i(t)\exp(j\Phi_i(t))\} \quad i \in \{1, 2\cdots n\} \tag{4.33}$$

where

$$\Phi_i(t) = \omega_1 t + \phi_i(t) \tag{4.34}$$

In (4.33), $A(t)$ and $\phi(t)$ are the *slow moving*, also termed *quasi-static*, amplitude and phase signals, respectively. Following the framework laid out in appendix B.1.1 we now proceed to find the single pole, or first order Taylor, approximation for the parallel resonator

$$\begin{gathered} Y(\omega) = G_L\left[1 + jQ\left(\frac{\omega}{\omega_0} - \frac{\omega_0}{\omega}\right)\right] \approx G_L\left[1 + jQ\left(\frac{\omega_1}{\omega_0} - \frac{\omega_0}{\omega_1}\right)\right] + \\ jG_LQ\left(\frac{1}{\omega_0} + \frac{\omega_0}{\omega_1^2}\right)(\omega - \omega_1) = G_L\big[1 + j\tan(\psi)\big] + jG_LQ\left(\frac{\omega_1}{\omega_0} + \frac{\omega_0}{\omega_1}\right)\frac{(\omega - \omega_1)}{\omega_1} \end{gathered} \tag{4.35}$$

where we have used [94]

$$\tan(\psi) = Q\left(\frac{\omega_1}{\omega_0} - \frac{\omega_0}{\omega_1}\right) \tag{4.36}$$

Using (4.31) we further find

$$\begin{gathered} \frac{\omega_1}{\omega_0} + \frac{\omega_0}{\omega_1} = \frac{\omega_1^2 + \omega_0^2}{\omega_1\omega_0} = \frac{\left(\pm\frac{\omega_0\tan(\psi)}{2Q} + \frac{\omega_0}{2Q}\sqrt{4Q^2 + \tan^2(\psi)}\right)^2 + \omega_0^2}{\omega_1\omega_0} = \\ \frac{\frac{\omega_0}{2Q^2}\left(\tan^2(\psi) + 4Q^2 \pm \tan(\psi)\sqrt{4Q^2 + \tan^2(\psi)}\right)}{\pm\frac{\omega_0\tan(\psi)}{2Q} + \frac{\omega_0}{2Q}\sqrt{4Q^2 + \tan^2(\psi)}} = \frac{1}{Q}\sqrt{4Q^2 + \tan^2(\psi)} \end{gathered} \tag{4.37}$$

The last equal sign in (4.37) follows from the identity

$$\begin{gathered} \tan^2(\psi) + 4Q^2 \pm \tan(\psi)\sqrt{4Q^2 + \tan^2(\psi)} = \\ \left(\pm\tan(\psi) + \sqrt{4Q^2 + \tan^2(\psi)}\right)\sqrt{4Q^2 + \tan^2(\psi)} \end{gathered} \tag{4.38}$$

Inserting (4.37) in (4.35) we get the following approximation for the narrow-band RCL filter

$$Y(\omega) \approx G_L\big[1 + j\tan(\psi)\big] + jG_L\sqrt{4Q^2 + \tan^2(\psi)}\frac{(\omega - \omega_1)}{\omega_1} \tag{4.39}$$

Introducing the Kurokawa substitution [32], [33], [38] which was discussed in section 2.2.3 and appendix B

$$\omega \to \omega_1 - j\frac{1}{\hat{A}}\frac{dA}{d\tau} + \frac{d\phi}{d\tau} \tag{4.40}$$

while using (4.33) and (4.39), equation (4.26) is written as

$$\begin{gathered} Y_i(\omega)v_i - G_{mo}(v_i)v_i = G_{mc}(v_{i-1})v_{i-1} \Leftrightarrow \\ \left\{G_L\left(1 + j\frac{2Q}{\omega_0}\Delta\omega\right) + jG_L\frac{2Q}{\omega_1}\left[j\frac{1}{A}\frac{dA_i}{dt} - \frac{d\phi_i}{dt}\right]\right\}A_i\exp(j\Phi_i) + G_{mo}(v_i)A_i\exp(j\Phi_i) = \\ G_{mc}(v_{i-1})A_{i-1}\exp(j\Phi_{i-1}) \end{gathered} \tag{4.41}$$

where we have used (4.32) as well as the approximation

$$\sqrt{4Q^2 + \tan^2(\psi)} \approx 2Q \tag{4.42}$$

which is valid for moderate Q and ψ values. As explained and demonstrated in appendix B.1.1 we can then find the amplitude and phase equations by :

1. taking the real part on both sides of (4.41).
2. multiplying with $\cos(\Phi_i(t))$ and $\sin(\Phi_i(t))$, respectively.
3. averaging the resulting equations over one period $T_1 = 2\pi/\omega_1$ of the carrier.

At this point we return to the above mentioned special case of oscillator #1 in figure 4.1. Following the above derivations, we see that this case can be taken into account by simply exchanging $\exp(j\Phi_{i-1})$ with $\exp(j\Phi_{i-1} + j\beta)$ in (4.41). There is therefore no need for any further derivations to include this case into the formulation. We find the following $2n$ coupled first order ODE's describing the *quasi-sinusoidal* dynamics of the circuit in figure 4.1 [6], [19], [20]

$$\begin{aligned} \frac{1}{\hat{A}_i}\frac{dA_i}{d\tau_i} &= \mu_{o,i}\left[1 - \left(\frac{A_i}{\alpha_i}\right)^2\right]\frac{A_i}{\hat{A}_i} + \frac{G_{mc,i}(A_{i-1})}{G_{Li}}\cos\big(\phi_{i-1} - \phi_i + \beta\delta_{1i}\big)\frac{A_{i-1}}{\hat{A}_i} && (4.43) \\ \frac{d\phi_i}{d\tau_i} &= \frac{2Q_i}{\omega_{0i}}\Delta\omega_i + \frac{G_{mc,i}(A_{i-1})}{G_{Li}}\sin\big(\phi_{i-1} - \phi_i + \beta\delta_{1i}\big)\frac{A_{i-1}}{A_i} && (4.44) \\ i &\in \{1, 2, \cdots, n | i = 1 \Rightarrow i - 1 = n\} \end{aligned}$$

where all parameters have received a subscript i in order to allow for a possible introduction of asymmetry at a later stage in the analysis. The parameter μ_o was defined in connection with equation (4.28), δ_{ij} is the *Kroenecker delta function*. We have defined the *slow time* τ and the *free running amplitude* α as

$$\tau_i = \frac{\omega_{0i}}{2Q_i}t \tag{4.45}$$

$$\alpha_i = \sqrt{\frac{4}{3}\frac{(g_{o0,i} - G_{Li})}{g_{o2,i}}} \tag{4.46}$$

Furthermore, the transconductances G_{mo} and G_{mc} now refer to the *first harmonic describing functions*

$$G_{mx,i} = g_{x0,i} - \frac{3}{4}g_{x2,i}A_i^2 \quad x \in \{o, c\} \tag{4.47}$$

For the purpose of stability and noise calculations we shall now proceed to derive the *linear response equations* from the nonlinear system in (4.43)-(4.44). We start by defining the amplitude and phase difference of the i'th oscillator through

$$A_i = \hat{A}_i + \delta A_i \tag{4.48}$$

$$\phi_{i-1} - \phi_i = \Delta\hat{\phi}_i + \delta\phi_{i-1} - \delta\phi_i \tag{4.49}$$

where $\delta A_i, \delta\phi_i$ describe small perturbations off the steady state, $(\hat{A}_i,\ \hat{\phi}_i)$, of the i'th oscillator and

$$\Delta\hat{\phi}_i = \hat{\phi}_{i-1} - \hat{\phi}_i \tag{4.50}$$

Although our analysis in this chapter is restricted to the dominant mode $\Delta\hat{\phi}_i = -\beta/n$, where the phase shift is independent of the oscillator index i, we keep the expressions general by using the notation $\Delta\hat{\phi}_i$. The steady-state amplitude is given by $\hat{A}_i$ and this parameter can be found by setting (4.43) equal to zero

$$\begin{aligned}
&\mu_{o,i}\left[1 - \left(\frac{\hat{A}_i}{\alpha_i}\right)^2\right] + \frac{\widehat{G}_{mc,i}(\hat{A}_{i-1})}{G_{Li}}\cos\big(\Delta\hat{\phi}_i + \beta\delta_{1i}\big)\frac{\hat{A}_{i-1}}{\hat{A}_i} = 0 \Leftrightarrow \\
&\left(\frac{\hat{A}_i}{\alpha_i}\right)^2 = 1 + \frac{1}{\mu_{o,i}}\frac{\widehat{G}_{mc,i}(\hat{A}_{i-1})}{G_{Li}}\cos\big(\Delta\hat{\phi}_i + \beta\delta_{1i}\big)\frac{\hat{A}_{i-1}}{\hat{A}_i} \Leftrightarrow \\
&\hat{A}_i = \alpha_i\sqrt{1 + \frac{1}{\mu_{o,i}}\zeta_i\cos\big(\Delta\hat{\phi}_i + \beta\delta_{1i}\big)}
\end{aligned} \tag{4.51}$$

where we have assumed that $\hat{A}_{i-1}/\hat{A}_i \approx 1$ which is true for all practical cases and we have introduced the *coupling strength* ζ_i as

$$\zeta_i = \frac{\widehat{G}_{mc,i}(\hat{A}_{i-1})}{G_{Li}} \tag{4.52}$$

where from (4.47) we have

$$\widehat{G}_{mc,i}(\hat{A}_i) = g_{c0,i} - \frac{3}{4}g_{c2,i}\hat{A}_i^2 \tag{4.53}$$

The dynamics of the perturbations $\delta A_i, \delta\phi_i$ are solved, to a first order approximation, by the *first variational* of (4.43)-(4.44), which we write as

$$\frac{1}{\hat{A}_i}\frac{d\delta A_i}{d\tau_i} = \delta_{A1,i}\frac{\delta A_i}{\hat{A}_i} + \delta_{A2,i}\frac{\delta A_{i-1}}{\hat{A}_i} + \delta_{A3,i}(\delta\phi_{i-1} - \delta\phi_i) \tag{4.54}$$

$$\frac{d\delta\phi_i}{d\tau_i} = \delta_{\phi1,i}\frac{\delta A_i}{\hat{A}_i} + \delta_{\phi2,i}\frac{\delta A_{i-1}}{\hat{A}_i} + \delta_{\phi3,i}(\delta\phi_{i-1} - \delta\phi_i) \tag{4.55}$$

where we have defined the different parts of the Jacobian as

$$\delta_{A1} = \mu_{o,i}\left[1 - 3\left(\frac{\hat{A}_i}{\alpha_i}\right)^2\right] = -2\mu_{o,i} - 3\zeta_i \cos\left(\Delta\hat{\phi}_i + \beta\delta_{1i}\right) = -\mu_{a,i} \tag{4.56}$$

$$\delta_{A2,i} = \zeta_i(1 - 2\mu_{c,i})\cos(\Delta\hat{\phi}_i + \beta\delta_{1i}) \tag{4.57}$$

$$\delta_{A3,i} = -\zeta_i \sin(\Delta\hat{\phi}_i + \beta\delta_{1i}) \tag{4.58}$$

$$\delta_{\phi 1,i} = -\zeta \sin(\Delta\hat{\phi}_i + \beta\delta_{1i}) \tag{4.59}$$

$$\delta_{\phi 2,i} = \zeta_i(1 - 2\mu_{c,i})\sin(\Delta\hat{\phi}_i + \beta\delta_{1i}) \tag{4.60}$$

$$\delta_{\phi 3,i} = \zeta_i \cos(\Delta\hat{\phi}_i + \beta\delta_{1i}) \tag{4.61}$$

where we in (4.56) have used the definition in (4.51) and μ_c is a parameter which indicates the nonlinearity of the coupling function

$$\mu_{c,i} = \frac{g_{c0,i} - \widehat{G}_{mc,i}}{\widehat{G}_{mc,i}} \tag{4.62}$$

The factor $\zeta_i(1 - 2\mu_{c,i})$ in (4.57) and (4.60) originates from the first derivative of the term $G_{mc,i}(A_{i-1})A_{i-1}/G_{Li}$ in (4.43)-(4.44) with respect to A_{i-1}. Using (4.47) and (4.52), we can write this derivative as

$$\begin{aligned} &\frac{g_{c0,i} - 3 \times \frac{3}{4}g_{c2,i}\hat{A}_{i-1}^2}{G_{Li}} = \frac{\widehat{G}_{mc,i} - \frac{2}{3}g_{c2,i}\hat{A}_{i-1}^2}{G_{Li}} = \zeta_i - \frac{\frac{2}{3}g_{c2,i}\hat{A}_{i-1}^2}{G_{Li}} = \\ &\zeta_i - \frac{2(g_{c0,i} - \widehat{G}_{mc,i})}{G_{Li}} = \zeta_i\left(1 - 2\frac{g_{c0,i} - \widehat{G}_{mc,i}}{\widehat{G}_{mc,i}}\right) = \zeta_i(1 - 2\mu_{c,i}) \end{aligned} \tag{4.63}$$

4.4 Linear Start-Up and Stability Analysis

In this section we shall utilize the linear response equations derived in the previous section to investigate the stability of the ring in figure 4.1. As discussed previously in section 4.1, the ring coupled system is a *multi-mode* circuit, potentially being capable of oscillating in n different phase configurations. A complete analysis would then have to consider the stability of each of these modes; an undertaking that would inevitably lead to tedious and complex calculations. In this report we are not interested in modes which only occur for *special* initial conditions; instead, we consider a practical electric circuit where the capacitor voltages and inductor currents are initially assumed zero. As the power is turned on, the oscillator starts up with oscillation being induced either by inherent noise, a DC turn-on transient spike or a small injected pulse. We therefore consider the initial condition $(v_{Ci}, i_{Li}) = (0, 0)$ and we are interested in identifying the possible modes that could occur in a small region around this point in state-space. It can be shown that the *symmetric* ring [16] will always start up in the same mode, which we refer to here as the *dominant mode*. For zero phase shift ($\beta = 0$), this mode is the *in-phase* mode $\mathbb{Z}_n(0)$ in (4.11). We can easily construct a heuristic "proof" for this statement as follows

in the in-phase mode the current injected into each oscillator is, as the name suggests, in-phase with the internal oscillator current. This means that the all the injected current goes toward increasing the amplitude/power of the oscillators. From this description it

[16] although we consider the analysis of the completely symmetric circuit here, the results obviously also hold, in a slightly altered form, for the nearly symmetric circuit. As explained in note 1.9 on page 32, this follows from the *implicit function theorem*.

is obvious that the in-phase open-loop gain, of the structure in figure 4.1 linearized fixed point $(v_{ci}, i_{Li}) = (0, 0)$*, is larger than what can be occur for any other mode in the system. Barring some-kind of* multi-mode *solution, which is not considered in this text, only the mode with the highest open-loop gain survives [8].*

In section 4.1.3 it was explained how the in-phase mode $\mathbb{Z}_n(0)$ in (4.11), was really the same orbit as the travelling wave mode $\mathbb{Z}_n^\beta(0)$ in (4.15), where (4.15) simply modelled a re-mapping of the fixed points. This was summarized in note 4.1 on page 88. From this important identification we argue, although we shall not prove it, that the start-up mode selection of in-phase oscillations in the unilateral ring, with $\beta = 0$, is inherited by the travelling wave mode $\mathbb{Z}_n^\beta(0)$ in (4.15), for $\beta \neq 0$. The mapping of system properties, including open-loop gain, as a function of an introduced explicit phase shift, must be continuous. Hence, the argument is most certainly true for *small* β. That it remains true for an arbitrary β cannot be proved here. However, we refer numerical experiments done by the author and the linear open-loop calculations made in [8] for the special case $(n, \beta) = (3, \pi)$, which all point in this direction.

From the above arguments and definitions, we state the following

note 4.2 *The in-phase mode,* $\mathbb{Z}_n(0)$ *in* (4.11)*, is dominant for the symmetric ring with* $\beta = 0$*. By the term dominant we imply that the symmetric ring in figure 4.1, after noise/small pulse-induced start-up, from the initial conditions* $(v_{Ci}, i_{Li}) = (0, 0)$*, always oscillates in this mode. For* $\beta \neq 0$ *the mode selection property is inherited by the travelling wave mode* $\mathbb{Z}_n^\beta(0)$ *in* (4.15)*, where each oscillator is phase shifted* $-\frac{\beta}{n}$ *.*

From the description in the above note, we can write the dominant solution as

$$\Delta\hat{\phi}_i = \begin{cases} \Delta\hat{\phi} = -\frac{\beta}{n} & i = 2, 3 \cdots n \\ \Delta\hat{\phi} - \beta & i = 1 \end{cases} \tag{4.64}$$

and we see that the phase-shift of the dominant mode $\Delta\hat{\phi}$ becomes independent of i. As can be gathered from note 4.2, we shall in the following limit the scope to n identical oscillators (see footnote 16), which means that parameter subscripts in (4.54)-(4.55) and (4.56)-(4.61) can be ignored.

We start this section by deriving the Jacobian of the system in (4.43)-(4.44) for the dominant mode in (4.64). We then proceed to consider the cases $\beta = 0$ and $\beta \neq 0$ separately. In section 4.4.1, we consider the in-phase mode for $\beta = 0$, while the travelling wave mode, for $\beta \neq 0$, is considered in 4.4.2. In order for a mode to be stable *all* eigenvalues of the Jacobian must have negative real parts. In [65], an investigation of the linear stability of n unidirectional ring coupled *phase only* oscillators was undertaken. The strategy here was to use Gershgorin's theorem [17] which allowed for the stability calculations to be made for an arbitrary n. In section 4.4.1 we shall explicitly calculate all the eigenvalues of the in-phase mode with $\beta = 0$. Although much of the information

[17] Gershgorin's theorem states that the eigenvalues of a matrix can be found inside circles in the complex plan, with centers being given by the diagonal elements and radii calculated as the sum of the absolute row members, corresponding to the diagonal being considered [95].

gained in this process is a repetition of what was said in [65], we also find some new results. More specifically, the *phase-only* model used in [65] predicts that the in-phase mode will be stable for all coupling strengths while we show that instability can occur if the nonlinearity of the coupling transconductance is sufficiently strong.

Unfortunately, neither Gershgorin's theorem nor explicit calculation of the eigenvalues is possible for the travelling mode with $\beta \neq 0$. For small β, or large n [18], the stability is inherited from the in-phase mode but for larger β and moderate n nothing specific can be said from the results in 4.4.1. We are interested in the specific case $\beta = \pi$ and the dominant mode $-\pi/n$. This circuit finds practical use as a multi-phase RF and microwave source [19]. Because of the analytic difficulties we are forced to consider special cases. In 4.4.2 we shall therefore investigate the configuration $(n, \beta) = (2, \pi)$, which is known as the *cross-coupled quadrature oscillator* (CCQO). The asymmetry and noise properties of the CCQO was investigated by the author in the papers [6], [19], [20] and in section 4.7 we shall review this theory in detail.

In both 4.4.1 and 4.4.2 the analytical results are verified by numerical integration results from the C-program [61] constructed by the author. One of the procedures of this program plots the eigenvalues of the *Monodromy Matrix* (MM) [20], which is a *state transition matrix* (STM), as a function of some circuit parameter. Briefly, if J is the state space Jacobian, the MM is defined as

$$\Phi(T_1, 0) = \exp(JT_1) \tag{4.65}$$

where T_1 is the oscillator period. The eigenvalues of this matrix λ_M, which are called the *characteristic multipliers*, are related to the Jacobian eigenvalues λ through

$$\lambda_M = \exp(\lambda T_1) \tag{4.66}$$

which, for a stable solution, lies inside the unit circle $|z| \leq 1$ in the complex plane $z \in \mathbb{C}$.

Since we consider a stable oscillator, the Jacobian will contain a zero eigenvalue [21]. As this eigenvalue is implied, we do not need to include it in the calculations. By introducing the *phase difference* perturbation variables $\delta\theta$, from the phase perturbation variables $\delta\phi$ in (4.49), as

$$\delta\theta_i = \delta\phi_{i-1} - \delta\phi_i \quad i = 1, 3, \cdots, n-1 \tag{4.67}$$

we cut the dimension of the state-space system by 1. This decrease accounts for the zero eigenvalue which is removed by this change of notation. We hence consider the $2n-1 \times 1$ perturbation vector

$$\delta v = \begin{bmatrix} \delta A_1 \\ \vdots \\ \delta A_n \\ \delta\theta_1 \\ \vdots \\ \delta\theta_{n-1} \end{bmatrix} \tag{4.68}$$

[18] for small β or large n we have that the rotating wave mode phase shift $-\beta/n$ is close to zero. This mode hence has the same properties as the in-phase solution.

[19] see discussion in section 4.2.

[20] we refer to appendix D for a complete tutorial on Floquet theory, STM's and MM's.

[21] see note 2.1 in section 2.1.1 on page 39.

The linear response of the system (4.43)-(4.44) is then written as

$$\delta\dot{v} = J\delta v \tag{4.69}$$

where J is the $2n-1 \times 2n-1$ *Jacobian* of the system. We shall write this matrix on the block form

$$J = \begin{bmatrix} J_{11} & J_{12} \\ J_{21} & J_{22} \end{bmatrix} \tag{4.70}$$

where the division into sub-matrices follows directly from the state vector in (4.68), which is seen to be split into a δA and a $\delta\theta$ part. Using (4.54)-(4.55) and (4.56)-(4.61) we see that these matrices can be written for the symmetric circuit (indices i are ignored)

$$J_{11} = \begin{bmatrix} -\mu_a & 0 & 0 & 0 & \cdots & \zeta(1-2\mu_c)\cos(\Delta\hat{\phi}) \\ \zeta(1-2\mu_c)\cos(\Delta\hat{\phi}) & -\mu_a & 0 & 0 & \cdots & 0 \\ 0 & \zeta(1-2\mu_c)\cos(\Delta\hat{\phi}) & -\mu_a & 0 & \cdots & 0 \\ 0 & 0 & \ddots & \ddots & \cdots & 0 \\ \vdots & \vdots & 0 & \ddots & \ddots & \vdots \\ \vdots & \vdots & \vdots & \vdots & \ddots & \vdots \\ 0 & 0 & 0 & \cdots & \zeta(1-2\mu_c)\cos(\Delta\hat{\phi}) & -\mu_a \end{bmatrix} \tag{4.71}$$

where the positive parameter μ_a was defined in (4.56)

$$J_{12} = \begin{bmatrix} -\zeta\sin(\Delta\hat{\phi}) & 0 & 0 & 0 & \cdots & 0 \\ 0 & -\zeta\sin(\Delta\hat{\phi}) & 0 & 0 & \cdots & 0 \\ 0 & 0 & -\zeta\sin(\Delta\hat{\phi}) & 0 & \cdots & 0 \\ 0 & 0 & 0 & 0 & \cdots & 0 \\ \vdots & \vdots & 0 & \ddots & \cdots & \vdots \\ \vdots & \vdots & \vdots & \vdots & \ddots & \vdots \\ \zeta\sin(\Delta\hat{\phi}) & \zeta\sin(\Delta\hat{\phi}) & \zeta\sin(\Delta\hat{\phi}) & \zeta\sin(\Delta\hat{\phi}) & \cdots & \zeta\sin(\Delta\hat{\phi}) \end{bmatrix} \tag{4.72}$$

$$J_{21} = \begin{bmatrix} \gamma & 0 & 0 & 0 & \cdots & \beta & \alpha \\ \alpha & \gamma & 0 & 0 & \cdots & 0 & \beta \\ \beta & \alpha & \gamma & 0 & \cdots & 0 & 0 \\ 0 & \beta & \alpha & \gamma & \cdots & 0 & 0 \\ \vdots & \vdots & \ddots & \ddots & \ddots & \vdots & \vdots \\ 0 & 0 & \cdots & \beta & \alpha & \gamma & 0 \end{bmatrix} \tag{4.73}$$

$$\alpha = -\zeta\sin(\Delta\hat{\phi}) - \zeta(1-2\mu_c)\sin(\Delta\hat{\phi}) = -2\zeta(1-\mu_c)\sin(\Delta\hat{\phi}) \tag{4.74}$$

$$\beta = \zeta(1-2\mu_c)\sin(\Delta\hat{\phi}) \tag{4.75}$$

$$\gamma = \zeta\sin(\Delta\hat{\phi}) \tag{4.76}$$

$$J_{22} = \begin{bmatrix} -2\rho & -\rho & -\rho & -\rho & \cdots & -\rho & -\rho \\ \rho & -\rho & 0 & 0 & \cdots & 0 & 0 \\ 0 & \rho & -\rho & 0 & \cdots & 0 & 0 \\ 0 & 0 & \rho & -\rho & \cdots & 0 & 0 \\ \vdots & \vdots & \vdots & \ddots & \ddots & \vdots & \vdots \\ \vdots & \vdots & \vdots & \vdots & \ddots & \ddots & \vdots \\ 0 & 0 & 0 & \cdots & 0 & \rho & -\rho \end{bmatrix} \tag{4.77}$$

where $\rho = \zeta \cos(\Delta\hat{\phi})$.

4.4.1 Linear Stability of In-Phase Mode for the Unidirectional Ring with $\beta = 0$

We state the following theorem

Theorem 4.1 *The in-phase mode $\mathbb{Z}_n(0)$ for the unilateral ring of n harmonic oscillators, with $\beta = 0$, is stable, iff the condition*

$$\mu_c < \begin{cases} \frac{1}{2}\left(1 + \frac{2\mu_o + 3\zeta}{\zeta}\right) & \text{for } n \text{ even} \\ \\ \frac{1}{2}\left(1 + \frac{2\mu_o + 3\zeta}{\zeta \cos\left(\frac{\pi}{n}\right)}\right) & \text{for } n \text{ uneven} \end{cases}$$

is fulfilled.

proof : considering the in-phase mode, we have $\Delta\hat{\phi} = 0$. Inspecting (4.72) and (4.73) it is seen that both J_{12} and J_{21}, for this mode, are equal to the zero matrix. The eigenvalues of the Jacobian are hence found as the eigenvalues of the two matrices J_{11} in (4.71) and J_{22} in (4.77). These eigenvalues are calculated in appendix C.2 and C.3, respectively, for an arbitrary $\Delta\hat{\phi}$. From equation (C.27) in appendix C.2 and (C.42) in C.3, we have the following $2n-1$ eigenvalues

$$\lambda_i = \begin{cases} -\mu_a - \zeta(1 - 2\mu_c)\left\{\cos\left(i\frac{2\pi}{n}\right) + j\sin\left(i\frac{2\pi}{n}\right)\right\} & i = \{1, 2, \cdots, n\} \quad \text{for } n \text{ even} \\ -\mu_a - \zeta(1 - 2\mu_c)\left\{\cos\left(i\frac{\pi}{n}\right) + j\sin\left(i\frac{\pi}{n}\right)\right\} & i = \{1, 2, \cdots, n\} \quad \text{for } n \text{ uneven} \end{cases} \tag{4.78}$$

$$\lambda_i = \begin{cases} \zeta\left\{\cos\left(\frac{i\pi}{n}\right) - 1 + j\sin\left(\frac{i\pi}{n}\right)\right\} & i = \{n+1, n+2, \cdots, 2n-1\} \quad \text{for n even} \\ \zeta\left\{\cos\left(\frac{2i\pi}{n}\right) - 1 + j\sin\left(\frac{2i\pi}{n}\right)\right\} & i = \{n+1, n+2, \cdots, 2n-1\} \quad \text{for n uneven} \end{cases} \tag{4.79}$$

The eigenvalues for λ_i for $i = \{n+1, n+2 \cdots 2n-1\}$, shown in (4.79), will have a real part smaller than zero for all coupling strengths ζ. We therefore concentrate on the eigenvalues of J_{11} in (4.78). Using (4.56) we can write the *amplitude relaxation* parameter μ_a, for the in-phase mode $\mathbb{Z}_n(0)$, as

$$\mu_a = 2\mu_o + 3\zeta \tag{4.80}$$

Because of the term 3ζ, the only way the real parts of λ_i in (4.78) can become positive is if the factor $\zeta(1 - 2\mu_c)$ is negative. The largest positive term occurs when $i = n$ (n even) and $i = 1$ (n uneven).

For n even the condition for instability becomes

$$-2\mu_o - 3\zeta - \zeta(1-2\mu_c) > 0 \Leftrightarrow \mu_c > \frac{1}{2}\left(1 + \frac{2\mu_o + 3\zeta}{\zeta}\right) \tag{4.81}$$

while for n uneven we have

$$-2\mu_o - 3\zeta - \zeta(1-2\mu_c)\cos\left(\frac{\pi}{n}\right) > 0 \Leftrightarrow \mu_c > \frac{1}{2}\left(1 + \frac{2\mu_o + 3\zeta}{\zeta\cos\left(\frac{\pi}{n}\right)}\right) \tag{4.82}$$

In figure 4.4 we plot the MM eigenvalues λ_M of the in-phase mode $\mathbb{Z}_n(0)$, as a function of the coupling strength, for $n = 3$ and $n = 4$. In these plots the nonlinearity of the coupling is chosen sufficiently weak so that the stability of the system is increased with coupling. The *diagonal phase* [22] is neutrally stable which accounts for the eigenvalue at $z = 1 + j0$ in figures 4.4(a)-4.4(b). Then in figure 4.5 we plot the MM eigenvalues λ_M of the in-phase mode $\mathbb{Z}_n(0)$, as a function of the coupling nonlinearity, for $n = 3$. As predicted by theorem 4.1 : **as the coupling nonlinearity is increased, the stability of the coupled system is decreased.**

4.4.2 n=2, $\beta = \pi$: The Cross Coupled Quadrature Oscillator

The circuit in figure 4.1, with the particular choice of parameters $(n, \beta) = (2, \pi)$ corresponding to the dominant mode $\mathbb{Z}_2^{\pi}(0)$ in (4.15), is known as the *cross coupled quadrature oscillator* (CCQO). This configuration is of special practical importance since it constitutes a popular method of synthesizing RF quadrature signals [5], [74], which are an essential part of modern transceiver architectures. Later in this chapter we shall investigate the noise and asymmetry properties of this circuit when we in section 4.7 conduct a detailed review of the three papers [6], [19], [20]. The stability issue was not considered in either of these three publications since it was clear from numerical simulations that the quadrature mode $\mathbb{Z}_2^{\pi}(0)$ was stable. This section corrects this deficiency by calculating all three eigenvalues of Jacobian, which will confirm our initial assumptions of stability.

We consider the state variable

$$\delta v = \begin{bmatrix} \delta A_1 \\ \delta A_2 \\ \delta\theta_1 \end{bmatrix} \tag{4.83}$$

with $\delta\theta_1 = \delta\phi_2 - \delta\phi_1$. From (4.71)-(4.77), we get

$$J_{11} = -2\mu_0 I_2 \tag{4.84}$$

where I_2 is the 2×2 identity matrix

$$J_{12} = \begin{bmatrix} -\zeta\sin(-\pi/2) \\ \zeta\sin(-\pi/2) \end{bmatrix} = \begin{bmatrix} \zeta \\ -\zeta \end{bmatrix} \tag{4.85}$$

$$J_{21} = \begin{bmatrix} \zeta\sin(-\pi/2) + \zeta(1-2\mu_c)\sin(-\pi/2) \\ -\zeta\sin(-\pi/2) - \zeta(1-2\mu_c)\sin(-\pi/2) \end{bmatrix}^T = \begin{bmatrix} -2\zeta(1-\mu_c) \\ 2\zeta(1-\mu_c) \end{bmatrix}^T \tag{4.86}$$

$$J_{22} = 0 \tag{4.87}$$

Collecting all the contributions in (4.70), we can write the Jacobian as

[22] the diagonal phase ϕ_d is defined as $\phi_d = \sum_i \phi_i$. See also discussion in section 4.5.1 and chapter 3.

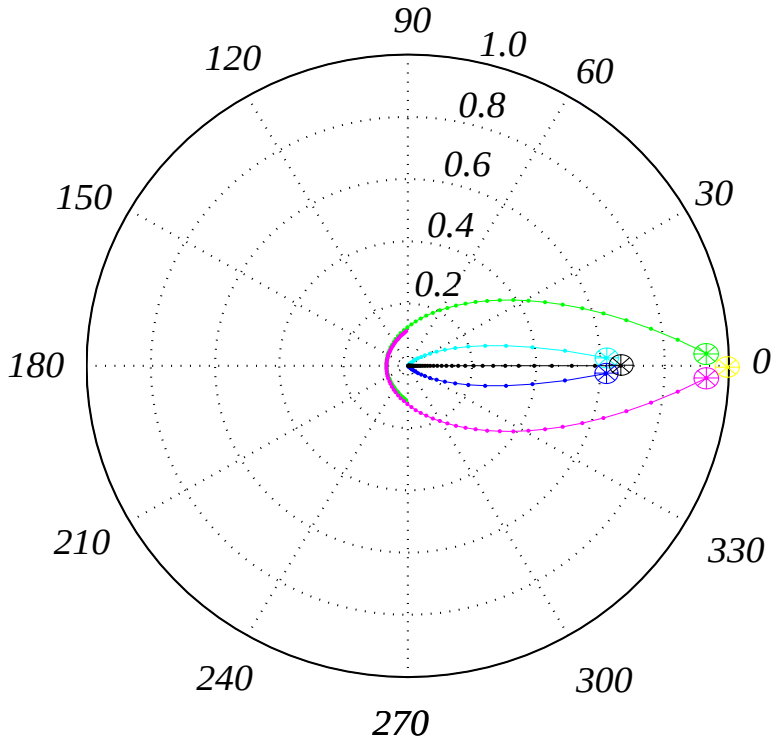

(a)

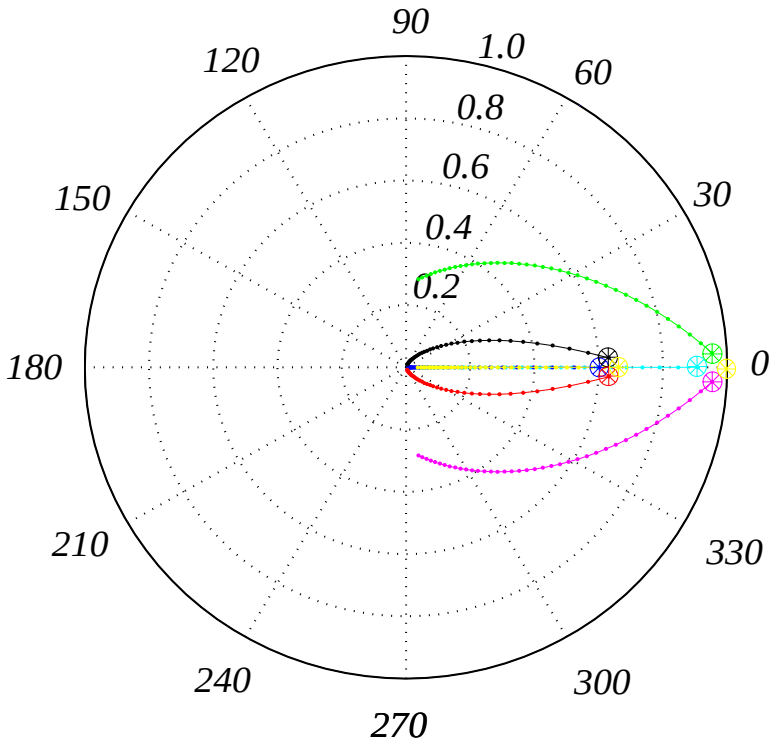

(b)

Figure 4.4: This plot concerns the *in-phase mode* $\mathbb{Z}_n(0)$ of the ring in figure 4.1, for $\beta = 0$. The figures show the MM eigenvalues λ_M (see (4.66)) for a) $n = 3$ and b) $n = 4$, as a function of the coupling strength ζ. In the plots the linear coupling transconductance g_{c0} is increased while the third order parameter g_{c2} is held constant (see (4.53)). The parameters for the symmetric ring is chosen as : $\mu_0 = 0.5$, $Q = 10.0$, $\alpha = 1.0$, $T_0 = 2\pi$. The starting point of the eigenvalue loci are indicated by the symbol $\otimes$.

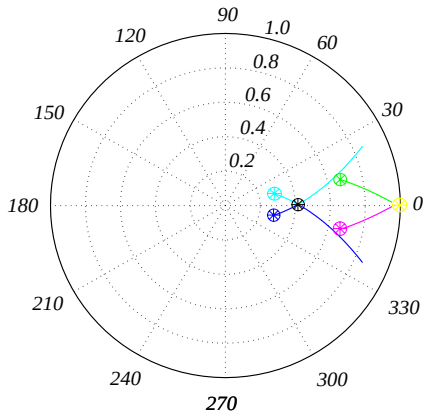

Figure 4.5: Investigating the *in-phase mode* $\mathbb{Z}_n(0)$ stability of the ring in figure 4.1 for $\beta = 0$, as function of increased coupling nonlinearity. The plot shows MM eigenvalues λ_M (see (4.66)), for $n = 3$, as a function of the third order coupling transconductance parameter g_{c2} (see (4.53)). The linear (first order) transconductance parameter g_{c0} is held constant. The plot illustrates how the ring could potentially loose stability through the increase of coupling nonlinearity, as predicted in theorem 4.1. The parameters for the symmetric ring is chosen as : $\mu_0 = 0.5$, $Q = 10.0$, $\alpha = 1.0$, $T_0 = 2\pi$. The starting point of the eigenvalue loci are indicated by the symbol $\otimes$.

$$J = \begin{bmatrix} -2\mu_0 & 0 & \zeta \\ 0 & -2\mu_0 & -\zeta \\ -2\zeta(1-\mu_c) & 2\zeta(1-\mu_c) & 0 \end{bmatrix} \tag{4.88}$$

From this expression the eigenvalues are easily found

$$\begin{gathered} (-2\mu_0 - \lambda)\big[(-2\mu_0 - \lambda)(-\lambda) - 2\zeta(1-\mu_c)\cdot -\zeta\big] - 2\zeta(1-\mu_c)\big(-(-2\mu_0-\lambda)\cdot\zeta\big) = \\ (-2\mu_0 - \lambda)\big[(2\mu_0+\lambda)\lambda + 2\zeta^2(1-\mu_c)\big] + 2\zeta^2(1-\mu_c)(-2\mu_0-\lambda) = \\ (-2\mu_0 - \lambda)\big[\lambda^2 + 2\mu_0\lambda + 4\zeta^2(1-\mu_c)\big] \Rightarrow \\ \lambda = \begin{cases} -2\mu_0 \\ -\mu_0 + \frac{1}{2}\sqrt{4\mu_0^2 - 8\zeta^2(1-\mu_c)} \\ -\mu_0 - \frac{1}{2}\sqrt{4\mu_0^2 - 8\zeta^2(1-\mu_c)} \end{cases} \end{gathered} \tag{4.89}$$

From the above derivation it is easily seen that all eigenvalues have real parts less than zero, as long as $\mu_c < 1$. In figure 4.6 we plot the MM eigenvalues λ_M, as a function of the coupling strength, for $n = 2$ and $n = 3$. In these plots the nonlinearity of the coupling is again chosen weak enough so that the stability of the system is increased with coupling. In figure 4.6(a), the eigenvalues of the CCQO dominant mode, $\mathbb{Z}_2^{\pi}(0)$, are shown. We see 4 loci, corresponding to the amplitude and phase of each of the two oscillators. The *diagonal phase* [23] is neutrally stable which accounts for the eigenvalue at $z = 1 + j0$. This corresponds to the zero eigenvalue of the Jacobian which was removed by the change of notation in (4.67). The stationary MM eigenvalue, which is easily spotted in figure 4.6(a), corresponds to the Jacobian eigenvalue $\lambda = -2\mu_0$ in (4.89) and the two remaining loci are calculated from (4.66) using the two remain complex conjugate eigenvalues in (4.89).

[23] the diagonal phase ϕ_d is defined as $\phi_d = \phi_1 + \phi_2$. See also discussion in section 4.5.1 and chapter 3.

Figure 4.6(b) shows the eigenvalue loci for the oscillator $(n, \beta) = (3, \pi)$ corresponding to the dominant mode $\mathbb{Z}_3^{\pi}(0)$.

4.5 Linear Response Noise Analysis - Coupling Induced AM to PM Noise Conversion

In chapter 2, where we summarized the linear response theory for single oscillators, it was shown how the asymptotic statistics were defined by a *diffusion process*, characterized by an *effective diffusion constant* [24]

$$D_{eff} = \bar{D}_{\phi\phi} \tag{4.90}$$

illustrating that, in this case, the *effective* and the *average* diffusion constants are identical. Then in section 2.2.3, we illustrated how the parameter in (4.90) could be extracted directly from the averaged state equations of the single oscillator.

The averaged equations for the ring in figure 4.1 were written in (4.43)-(4.44) in section 4.3. The linear response equations were then derived from this system as shown in (4.54)-(4.55). In this section we consider the linear response of the ring of n *identical oscillators* in the *dominant mode* $\Delta\hat{\phi} = -\beta/n$. The stability of this mode was discussed in the previous section and we shall here assume linear stability for all n and β. In figure 4.1, the oscillator cells are drawn with a white noise current source i_n in parallel with the resonator. This stochastic signal will in the following represent all the different noise perturbations present in the circuit. The process of lumping noise sources together in a single source involves the introduction of a circuit *noise factor* F [38], [96]. Here, the calculations are carried out for $F = 1$ and the results, so obtained, can then be re-normalized with the actual noise factor afterwards. We write the *available power* of a single thermal source as N_0, where

$$N_0 = 4kT \tag{4.91}$$

with k being Boltzman's constant [25] and T the absolute temperature in Kelvins. From the above discussion we can write

$$\left\langle i_{n,i}(t_1) i_{n,j}(t_2) \right\rangle = N_0 \delta_{ij} \delta(t_1 - t_2) \quad i, j \in \{1, 2, \cdots, n\} \tag{4.92}$$

where it is used that the noise sources belonging to the different cells are uncorrelated. If we introduce these noise sources on the righthand side of (4.41), then carry out the averaging procedure which led to (4.43)-(4.44) and finally derive the linear response equations in the same way we derived (4.54)-(4.55), we get the following set of equations

$$\frac{1}{\hat{A}} \frac{d\delta A_i}{d\tau} = \delta_{A1} \frac{\delta A_i}{\hat{A}} + \delta_{A2} \frac{\delta A_{i-1}}{\hat{A}} + \delta_{A3}(\delta\phi_{i-1} - \delta\phi_i) + G_{n,i} \qquad i = 1, 2, \cdots, n \tag{4.93}$$

$$\frac{d\delta\phi_i}{d\tau} = \delta_{\phi 1} \frac{\delta A_i}{\hat{A}} + \delta_{\phi 2} \frac{\delta A_{i-1}}{\hat{A}} + \delta_{\phi 3}(\delta\phi_{i-1} - \delta\phi_i) + B_{n,i} \qquad i = 1, 2, \cdots, n \tag{4.94}$$

where

[24] here the "overline" symbol refers to an averaging operation $\overline{f} = \frac{1}{T} \int_0^T f(\eta) d\eta$.
[25] $k = 1.38 \times 10^{-23} J/K$

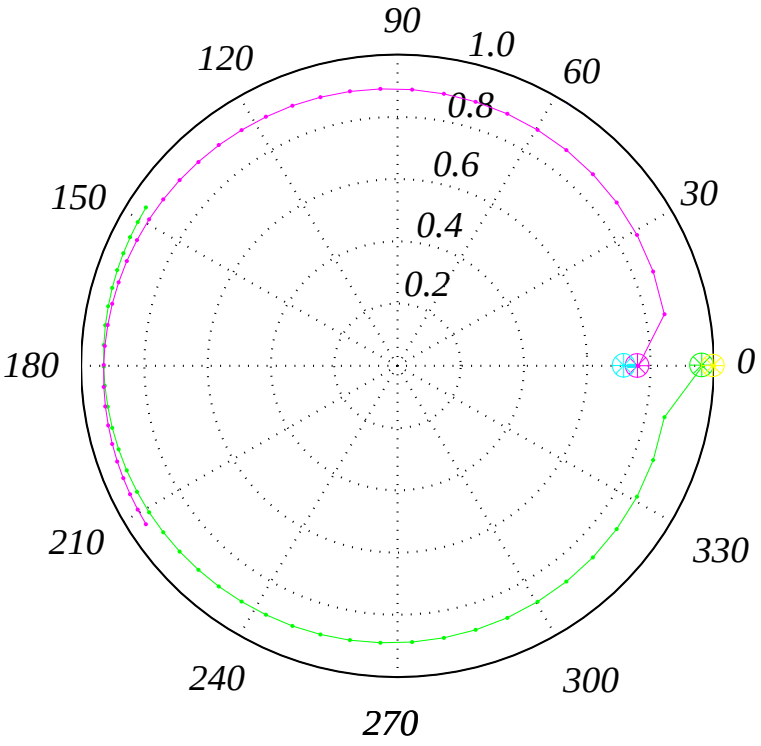

(a)

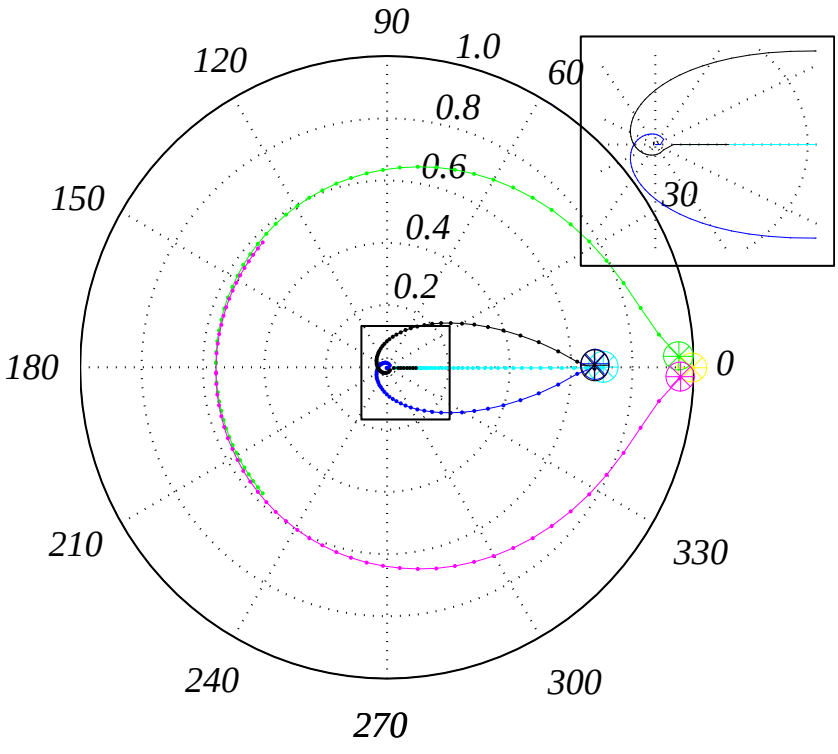

(b)

Figure 4.6: This plot concerns the *travelling wave mode* $\mathbb{Z}_n^\pi(0)$ of the ring in figure 4.1, for $\beta = \pi$. The figures show the MM eigenvalues λ_M (see (4.66)) for a) $n = 2$ and b) $n = 3$, as a function of the coupling strength ζ. In the plots the linear coupling transconductance g_{c0} is increased while the third order parameter g_{c2} is held constant (see (4.53)). The parameters for the symmetric ring is chosen as : $\mu_0 = 0.5$, $Q = 10.0$, $\alpha = 1.0$, $T_0 = 2\pi$. The starting point of the eigenvalue loci are indicated by the symbol $\otimes$.

$$\delta_{A1} = -\mu_a = -2\mu_o - 3\zeta\cos\big(\Delta\hat{\phi}\big) \tag{4.95}$$
$$\delta_{A2} = \zeta(1-2\mu_c)\cos(\Delta\hat{\phi}) \tag{4.96}$$
$$\delta_{A3} = -\zeta\sin(\Delta\hat{\phi}) \tag{4.97}$$
$$\delta_{\phi 1} = -\zeta\sin(\Delta\hat{\phi}) \tag{4.98}$$
$$\delta_{\phi 2} = \zeta(1-2\mu_c)\sin(\Delta\hat{\phi}) \tag{4.99}$$
$$\delta_{\phi 3} = \zeta\cos(\Delta\hat{\phi}) \tag{4.100}$$

has been derived from (4.56)-(4.61) under the assumption of identical oscillators. In (4.93)-(4.94) $G_{n,i}$ and $B_{n,i}$ are narrow-band noise parameters, known as noise conductances and susceptances, respectively, which result when the noise currents in (4.92) are averaged. These narrow-band stochastic signals are thoroughly discussed in appendix A.1 and as shown in (A.27)-(A.28) we have the following statistics

$$\big\langle G_{n,i}(t_1)G_{n,j}(t_2)\big\rangle = \frac{N_0}{P_0}\delta_{ij}\delta(t_1-t_2) \tag{4.101}$$
$$\big\langle B_{n,i}(t_1)B_{n,j}(t_2)\big\rangle = \frac{N_0}{P_0}\delta_{ij}\delta(t_1-t_2) \tag{4.102}$$
$$\big\langle G_{n,i}(t_1)B_{n,j}(t_2)\big\rangle = 0 \quad \text{for all } i,j \text{ and } t_1,t_2 \tag{4.103}$$

where N_0 is given by (4.91) and P_0 is the *available power* of the oscillator signal

$$P_0 = \frac{\hat{A}^2}{2R} \tag{4.104}$$

As explained in section 2.2.3, the effective diffusion constant can be found directly once the *neutrally stable phase variable* has been identified from the averaged state equations. As we shall now proceed to show, this variable follows from the introduction of the *diagonal flow* state equations.

4.5.1 Deriving the Dynamics of the Diagonal Flow

The term *diagonal flow* refers to the neutrally stable flow of n coupled oscillators on the invariant torus $\mathbb{T}^n$ [29]. Here, the state variables consist of n phases which can be written on vector form $\phi_d = [\phi_1\ \phi_2\ \cdots\ \phi_n]$. The neutrally stable direction then corresponds to the synchronized solution which must be a vector that points along the *diagonal* $[1\ 1\ \cdots\ 1]$. This direction is neutrally stable, for the *phase-only* model, because it points along an orbit which is only determined up to a constant phase shift (see also discussion in chapter 2). If we consider ϕ_j as a component along the vector $[0\ \cdots\ 0\ 1\ 0\ \cdots\ 0]$, where the non-zero component is at index j, we can also write

$$\phi_d = \phi_1 + \phi_2 + \cdots + \phi_n = \sum_{i=1}^{n}\phi_i \tag{4.105}$$

For the ring in figure 4.1, in the travelling wave mode $\mathbb{Z}_n^\beta$ ($\beta \neq 0$), the phase only model is not sufficient to explain all qualitative behavior. The travelling wave mode is an *out of phase* mode which means that the amplitude and phase equations are coupled and we can therefore not simply ignore the amplitude equations. We must therefore insists on an amplitude/phase formulation, as was derived in (4.43)-(4.44). The neutrally stable

dynamics will still be given by the diagonal flow equations, but now these equations will involve amplitudes as well as phases.

We start by defining the phase of the *diagonal flow*

$$\phi_d = \frac{1}{n}\sum_{i=1}^{n}\phi_i \tag{4.106}$$

corresponding to the linear response

$$\delta\phi_d = \frac{1}{n}\sum_{i=1}^{n}\delta\phi_i \tag{4.107}$$

Using the identities

$$\sum_{i=1}^{n}(\delta\phi_{i-1}-\delta\phi_i) = (\delta\phi_n-\delta\phi_1)+(\delta\phi_1-\delta\phi_2)+\cdots+(\delta\phi_{n-1}-\delta\phi_n) = 0 \tag{4.108}$$

$$\sum_{i=1}^{n}(\delta A_i-\delta A_{i-1}) = (\delta A_1-\delta A_n)+(\delta A_2-\delta A_1)+\cdots+(\delta A_n-\delta A_{n-1}) = 0 \tag{4.109}$$

together with phase equation in (4.94), we can write the linear response for the diagonal phase in (4.106), as

$$\frac{d\delta\phi_d}{d\tau} = \frac{1}{n}\sum_i\big(\delta_{\phi 1}\frac{\delta A_i}{\hat{A}}+\delta_{\phi 2}\frac{\delta A_{i-1}}{\hat{A}}\big)+B_n =$$

$$\zeta\sin(\Delta\hat{\phi})\frac{1}{n\hat{A}}\sum_i\big(\delta A_i-(1-2\mu_c)\delta A_{i-1}\big)+B_n = 2\mu_c\zeta\sin(\Delta\hat{\phi})\frac{1}{n\hat{A}}\sum_i\delta A_i+B_n =$$

$$2\mu_c\zeta\sin(\Delta\hat{\phi})\delta A_d+B_n \tag{4.110}$$

where we have used the parameters in (4.98)-(4.99) and defined the *diagonal amplitude*

$$\delta A_d = \frac{1}{n\hat{A}}\sum_{i=1}^{n}\delta A_i \tag{4.111}$$

as well as the *total noise susceptance*

$$B_n = \frac{1}{n}\sum_{i=1}^{n}B_{n,i} \tag{4.112}$$

All n noise admittances are uncorrelated and they hence add in power. We can therefore write the statistics of total noise susceptance in (4.112), using (4.102), as

$$\big\langle B_n(t_1)B_n(t_2)\big\rangle = \frac{1}{n}\frac{N_0}{P_0}\delta(t_1-t_2) \tag{4.113}$$

The linear response amplitude equation is given by (4.93). Using this equation, as well as the definitions (4.95)-(4.96) and (4.108), we can write the following evolution equation for the diagonal amplitude linear response in (4.111)

$$\frac{d\delta A_d}{d\tau} = (\delta_{A1}+\delta_{A2})\delta A_d+G_n = -\mu_1\delta A_d+G_n \tag{4.114}$$

where we have defined the new *diagonal amplitude relaxation* parameter

$$\mu_1 = \mu_a - \zeta(1-2\mu_c)\cos(\Delta\hat{\phi}) \tag{4.115}$$

as well as the total *noise conductance*

$$G_n = \frac{1}{n}\sum_{i=1}^{n} G_{n,i} \tag{4.116}$$

Since all n noise admittances are uncorrelated they add in power and we can therefore write the statistics of total noise conductance in (4.116), using (4.101), as

$$\big\langle G_n(t_1)G_n(t_2)\big\rangle = \frac{1}{n}\frac{N_0}{P_0}\delta(t_1-t_2) \tag{4.117}$$

We can now summarize the results obtained so far by writing the *diagonal flow linear response equations*

$$\boxed{\begin{aligned} \frac{d\delta A_d}{d\tau} &= -\mu_1\delta A_d + G_n && (4.118)\\ \frac{d\delta\phi_d}{d\tau} &= 2\mu_c\zeta\sin(\Delta\hat{\phi})\delta A_d + B_n && (4.119)\end{aligned}}$$

where the *total noise admittance* $Y_n + jB_n$ is defined through (4.113) and (4.117) as well as

$$\big\langle G_n(t_1)B_n(t_2)\big\rangle = 0 \quad \text{for all } t_1, t_2 \tag{4.120}$$

which follows from using (4.103) on each product $B_{n,i}G_{n,j}$ of (4.120).

In the following three sections we shall use the diagonal flow state equations (4.118)-(4.119) to derive the effective diffusion constant $\bar{D}_{\phi\phi}$ of the structure in figure 4.1 by applying three different analytic techniques. In (4.5.2) we shall use the strategy first explained in section 2.2.3 for the single oscillator problem whereas section 4.5.3 will detail an approach entailing the derivation of a PLTV [26] impulse response function for the coupled oscillator system. Finally, in section 4.5.4 we shall investigate the issue using stochastic calculus. All three methods give the same result; namely, that nonlinear coupling will lead to *coupling induced AM-to-PM* noise conversion [27].

4.5.2 Calculating $\bar{D}_{\phi\phi}$ (Method #1) : Rotating the Averaged Phase Equation

Comparing the diagonal flow system (4.118)-(4.119) for the ring coupled system with the equivalent state equations for the single oscillator which were derived in (2.77)-(2.78) in section 2.2.3, we see that they seem very alike. The reason for this similarity lies with the fact that the coupled structure in figure 4.1 *acts* like a single oscillator in the diagonal direction.

Following the derivations made in section 2.2.3, with (4.118)-(4.119) substituted for (2.77)-(2.78), we see that the r and s parameters can be defined as

[26] *Periodic Linear Time Varying.*

[27] this should be seen as an independent verification, and a generalization, of the work documented in the three papers [6], [19], [20], which concerned the *cross-coupled quadrature oscillator* $(n,\beta) = (2,\pi)$. This work will be reviewed in section 4.7.

$$s = \mu_1 \tag{4.121}$$

$$r = 2\mu_c\zeta\sin(\Delta\hat{\phi}) \tag{4.122}$$

We then define $\delta\psi_d$ as the *diagonal flow neutrally stable state variable*

$$\delta\psi_d = \delta\phi_d - \left(\frac{r}{s}\right)\delta A_d = \delta\phi_d - \frac{2\mu_c\zeta\sin(\Delta\hat{\phi})}{\mu_1}\delta A_d \tag{4.123}$$

Differentiating with respect to time on both sides of the above equation while using (4.118)-(4.119), we find

$$\frac{d\delta\psi_d}{d\tau} = B_n - \frac{2\mu_c\zeta\sin(\Delta\hat{\phi})}{\mu_1}G_n \tag{4.124}$$

From the above equation it is clearly seen that $\delta\psi_d$ is a neutrally stable variable. This should evident since the righthand side contains a sum of uncorrelated white noise sources. Using (4.113), (4.117), (4.120), (4.45) and following the procedure laid out in section 2.2.3, we can then directly write the effective diffusion constant for the structure in figure 4.1 as

$$\begin{aligned}\bar{D}_{\phi\phi} &= \left(\frac{\omega_0}{2Q}\right)^2\left\{1+\left(\frac{2\mu_c}{\mu_1}\right)^2\zeta^2\sin^2(\Delta\hat{\phi})\right\}\frac{N_0}{nP_0} = \\ &\left(\frac{\omega_0}{2Q}\right)^2\left\{1+\left[\frac{2\mu_c}{2\mu_o+3\zeta\cos(\Delta\hat{\phi})-\zeta(1-2\mu_c)\cos(\Delta\hat{\phi})}\right]^2\zeta^2\sin^2(\Delta\hat{\phi})\right\}\frac{N_0}{nP_0} = \\ &\underline{\underline{\left(\frac{\omega_0}{2Q}\right)^2\left\{1+\left[\frac{\mu_c}{\mu_o+\zeta(1+\mu_c)\cos\left(\frac{\beta}{n}\right)}\right]^2\zeta^2\sin^2\left(\frac{\beta}{n}\right)\right\}\frac{N_0}{nP_0}}}\end{aligned} \tag{4.125}$$

where we have used that $\Delta\hat{\phi} = -\beta/n$ for the dominant mode $\mathbb{Z}_n^{\beta}(0)$ (see discussion in sections 4.1.1 and 4.4).

4.5.3 Calculating $\bar{D}_{\phi\phi}$ (Method #2) : A PLTV Impulse Response Characterization

As explained in appendix A.1 both the noise susceptance and the noise conductance of the i'th oscillator can be described as train of noise pulses. Since the total noise admittance $Y_n = G_n + jB_n$ as defined in (4.113), (4.117) and (4.120) consists of a sum uncorrelated noise sources we can also express them in this way

$$G_n(\tau) = \sum_i \xi_c(\tau_i)\delta(\tau-\tau_i) \tag{4.126}$$

$$B_n(t) = \sum_i \xi_s(\tau_i)\delta(\tau-\tau_i) \tag{4.127}$$

where

$$\left\langle \xi_c(\tau_i)\xi_c(\tau_j)\right\rangle = \left\langle \xi_s(\tau_i)\xi_s(\tau_j)\right\rangle = \delta_{ij}\frac{N_0}{P_0} \tag{4.128}$$

$$\left\langle \xi_s(\tau_i)\xi_c(\tau_j)\right\rangle = 0 \quad \text{for all } i,j \tag{4.129}$$

Since the pulse amplitude and arrival times are independent from one pulse to the next and, further, since the susceptance and conductance contributions are uncorrelated, we can formulate the following strategy towards the derivation of a PLTV response function

- find the linear response of the system to one noise susceptance/conductance pulse.
- calculate the *time-average* over all the pulses in the series (4.126)-(4.127).
- use the fact that stationary Gaussian processes are *ergodic* [97], [39] to substitute the ensemble-averages in (4.128)-(4.129) for the time-averages.
- add the contributions from the orthogonal sources B_n and G_n.

In the following we shall neglect writing the time index of the noise pulses in (4.126)-(4.127) as this is not important (since the process is *stationary*). This means that we simply write ξ_c or ξ_s.

Section 4.5 detailed the derivation of a system of equations for the diagonal flow as written in (4.118)-(4.119). We now imagine the following situation : at time $\tau = 0$ a noise conductance pulse ξ_c, as defined in (4.126), is exciting the system. Considering a system initially at rest, it is seen from (4.118)-(4.119) that this pulse must force the initial conditions

$$\delta A_d(0) = \xi_c \tag{4.130}$$

$$\delta\phi_d(0) = 0 \tag{4.131}$$

With the above initial conditions, equation (4.118) is easily integrated to produce the linear response of the diagonal amplitude to the noise conductance perturbation

$$\delta A_d(\tau) = \xi_c \exp(-2\mu_1\tau) \tag{4.132}$$

Inserting this result into (4.119) we get the following equation for the diagonal phase $\delta\phi_d$

$$\frac{d\delta\phi_d}{d\tau} = 2\mu_c\zeta\sin(\Delta\hat{\phi})\xi_c\exp(-\mu_1 t) \tag{4.133}$$

Integrating this equation, with the initial condition (4.131), we find the following impulse response of the diagonal phase to a noise conductance perturbation

$$\delta\phi_d(\tau) = \frac{2\mu_c}{\mu_1}\zeta\sin(\Delta\hat{\phi})\xi_c\big\{1-\exp(-2\mu_1\tau)\big\} \tag{4.134}$$

Letting τ tend towards infinity and taking the ensemble average on both sides of this equation we get

$$\lim_{\tau\to\infty}\left\langle\phi_d^2(\tau)\right\rangle = \frac{N_0}{nP_0}\left(\frac{2\mu_c}{\mu_1}\right)^2\zeta^2\sin^2(\Delta\hat{\phi}) \tag{4.135}$$

where we have used (4.128). The above equation describes the asymptotic mean square response of the diagonal phase to an amplitude perturbation.

We now move on to consider the introduction of a noise susceptance pulse ξ_s as defined in (4.127). From (4.118)-(4.119), this results in the following initial conditions

$$\delta A_d(0) = 0 \tag{4.136}$$
$$\delta \phi_d(0) = \xi_s \tag{4.137}$$

We then have to solve (4.119) with these new initial conditions. The solution is seen to be given by

$$\delta \phi_d(\tau) = \xi_s \quad \text{for } \tau > 0 \tag{4.138}$$

Taking the ensemble average we find

$$\left\langle \phi_d^2(\tau) \right\rangle = \frac{N_0}{nP_0} \quad \text{for } \tau > 0 \tag{4.139}$$

From (4.135) and (4.139) we see that asymptotically with time the total *root mean square* response of the diagonal phase to the noise forcing in (4.126)-(4.127) is a step with amplitude Δ, where

$$\Delta = \sqrt{\frac{N_0}{nP_0}\left\{1 + \left(\frac{2\mu_c}{\mu_1}\right)^2 \zeta^2 \sin^2(\Delta\hat{\phi})\right\}} \tag{4.140}$$

Such a step response is characterized stochastically as a Wiener process with diffusion constant Δ^2. Re-normalizing time according to (4.45) we find the following expression

$$\bar{D}_{\phi\phi} = \left(\frac{\omega_0}{2Q}\right)^2 \left\{1 + \left(\frac{2\mu_c}{\mu_1}\right)^2 \zeta^2 \sin^2(\Delta\hat{\phi})\right\} \frac{N_0}{nP_0} \tag{4.141}$$

which is identically to (4.125).

4.5.4 Calculating $\bar{D}_{\phi\phi}$ (Method #3) : the Stochastic Integration Approach

In this section we will investigate the *diagonal flow* dynamics using stochastic integration techniques. This procedure constitutes the correct way to treat any kind of *stochastic differential equation* (SDE). Hence, unlike the two previous attempts and especially the one in section 4.5.3, the results derived in this section are based on a rigorous and well-established theoretic foundation. The theory of stochastic integration, as it is applied to differential equations perturbed by white noise, was reviewed in appendix A.2.

The diagonal SDE, which was derived in equations (4.118)-(4.119) of section 4.5.1, is repeated here

$$\frac{d\delta A_d}{d\tau} = \mu_1 \delta A_d + G_n \tag{4.142}$$
$$\frac{d\delta \phi_d}{d\tau} = 2\mu_c \zeta \sin(\Delta\hat{\phi}) \delta A_d + B_n \tag{4.143}$$

As explained in appendix A.2 the above system of equations can also be written on the form [28]

$$d\delta A_d = \mu_1 \delta A_d d\tau + dW_1(\tau) \tag{4.144}$$

$$d\delta\phi_d = 2\mu_c\zeta \sin(\Delta\hat{\phi})\delta A_d d\tau + dW_2(\tau) \tag{4.145}$$

where W_1, W_2 are uncorrelated *Wiener processes* which are defined through

$$\big\langle W_1(\tau_1)W_1(\tau_2)\big\rangle = \big\langle W_2(\tau_1)W_2(\tau_2)\big\rangle = \frac{N_0}{nP_0}\min(\tau_1,\tau_2) \tag{4.146}$$

$$\big\langle W_1(\tau_1)W_2(\tau_2)\big\rangle = 0 \quad \text{for all } \tau_1,\tau_2 \tag{4.147}$$

Since equations (4.144)-(4.145) are linear we can solve them using a Greens function approach, on the condition of *sharp initial values* $(\delta A_d(0), \delta\phi_d(0))$ at time $t = 0$. Equation (4.144) is then solved as

$$\delta A_d(\tau) = \delta A_d(0)\exp(-\mu_1\tau) + \int_0^\tau \exp(-\mu_1(\tau - s))dW_1(s) \tag{4.148}$$

where the last integral involving dW_1 should be seen as a Riemann-Stieltjes type integral [39]. Since this integral is stochastic we can only characterize it through its moments. Furthermore, it should be noted that the Ito and Stratonovich interpretations gives the same result in this simple example [39]. The ensemble average is found as

$$\big\langle \delta A_d(\tau)\big\rangle = \delta A_d(0)\exp(-\mu_1 t) + \int_0^\tau \exp(-\mu_1(\tau - s))\big\langle dW_1(s)\big\rangle = \delta A_d(0)\exp(-\mu_1\tau) \tag{4.149}$$

where $\delta A_d(0)$ is the initial value of diagonal amplitude. We then find the auto-correlation function as

$$\begin{aligned}\big\langle \delta A_d(\tau_1)\delta A_d(\tau_2)\big\rangle &= \delta A_d^2(0)\exp(-\mu_1(\tau_1+\tau_2))+ \\ \int_0^{\tau_1}\int_0^{\tau_2} \exp(-\mu_1(\tau_1+\tau_2-s_1-s_2))\big\langle dW_1(s_1)dW_1(s_2)\big\rangle &= \\ \delta A_d^2(0)\exp(-\mu_1(\tau_1+\tau_2)) + \frac{N_0}{nP_0}\int_0^{\min(\tau_1,\tau_2)} \exp(-\mu_1(\tau_1+\tau_2-2s))ds &= \\ \delta A_d^2(0)\exp(-\mu_1(\tau_1+\tau_2)) + \frac{N_0}{nP_0 2\mu_1}\big(\exp(-\mu_1|\tau_1-\tau_2|) - \exp(-\mu_1(\tau_1+\tau_2))\big)\end{aligned} \tag{4.150}$$

where we have used the result ($f(x, y)$ is random function)

[28] Infact, (4.144)-(4.145) is the correct interpretation of the ambiguous definition in (4.142)-(4.143). Taken at face value these equations lead to *jump process* as was clearly seen in the last section. The Wiener process is continuous at all times and hence not a jump process. This subject is discussed in appendix A.2.

$$\int_0^x \int_0^y f(x',y')\big\langle dW_1(x')dW_1(y')\big\rangle dx'dy' = \frac{N_0}{P_0}\int_0^{\min(x,y)} f(\eta,\eta)d\eta \tag{4.151}$$

as explained in appendix A.2. We now turn to the solution of (4.145) which is written as

$$\delta\phi_d(\tau) - \delta\phi_d(0) = \alpha\int_0^\tau \delta A_d(s)ds + \int_0^\tau dW_2(s) \tag{4.152}$$

where we have introduced the notation

$$\alpha = 2\mu_c\zeta\sin(\Delta\hat{\phi}) \tag{4.153}$$

The variable $\phi_d(\tau)-\phi_d(0)$ is referred to as the *self-referenced phase* (SR-P) [16], [47]. The ensemble mean is found to be

$$\begin{aligned}\big\langle \delta\phi_d(\tau) - \delta\phi_d(0)\big\rangle = \alpha\int_0^\tau \big\langle\delta A_d(s)\big\rangle ds = \alpha\int_0^\tau A_d(0)\exp(-\mu_1 s)ds = \\ -A_d(0)\frac{2\mu_c\zeta\sin(\Delta\hat{\phi})}{\mu_1}\big\{1-\exp(-\mu_1\tau)\big\}\end{aligned} \tag{4.154}$$

where we have used the result from (4.149). Similarly we define the power of the SR-P to be

$$\big\langle(\delta\phi_d(\tau)-\delta\phi_d(0))^2\big\rangle = \alpha^2\int_0^\tau\int_0^\tau\big\langle\delta A_d(s_1)\delta A_d(s_2)\big\rangle ds_1ds_2 + \int_0^\tau\int_0^\tau\big\langle dW_1(s_1)dW_1(s_2)\big\rangle ds_1ds_2 \tag{4.155}$$

From (4.150) we see that we have to calculate two types of integrals. These are evaluated as

$$\int_0^\tau\int_0^\tau \exp(-\mu_1(s_1+s_2))ds_1ds_2 = \left(1-\frac{\exp(-\mu_1\tau)}{\mu_1}\right)^2 \tag{4.156}$$

and

$$\int_0^\tau\int_0^\tau \exp(-\mu_1|s_1-s_2|)ds_1ds_2 = 2\int_0^\tau ds_1\int_0^{s_1}\exp(-\mu_1(s_1-s_2))ds_2 = \frac{2}{\mu_1}\tau - \frac{1}{\mu_1^2}(1-\exp(-\mu_1\tau)) \tag{4.157}$$

Also, from the above discussion and the results in appendix A.2 we can find

$$\int_0^\tau\int_0^\tau\big\langle dW_1(s_1)dW_1(s_2)\big\rangle ds_1ds_2 = \frac{N_0}{nP_0}\min(\tau,\tau) = \frac{N_0}{nP_0}\tau \tag{4.158}$$

Inserting (4.150) into (4.155) and using (4.153), (4.156), (4.157), (4.158), we find

$$\left\langle (\delta\phi_d(\tau) - \delta\phi_d(0))^2 \right\rangle = \left(2\mu_c \zeta \sin(\Delta\hat{\phi}) \right)^2 \times$$
$$\left(\left[\delta A_d(0)^2 - \frac{N_0}{nP_0 2\mu_1} \right] \left\{ 1 - \frac{\exp(-\mu_1\tau)}{\mu_1} \right\}^2 + \frac{N_0}{nP_0} \left\{ \frac{1}{\mu_1^2}\tau - \frac{1}{2\mu_1^3}[1 - \exp(-\mu_1\tau)] \right\} \right) + \frac{N_0}{nP_0}\tau \tag{4.159}$$

The limit as τ goes to infinity is found to be

$$\lim_{\tau\to\infty} \left\langle (\delta\phi_d(\tau) - \delta\phi_d(0))^2 \right\rangle = \frac{N_0}{nP_0} \left\{ 1 + \left(\frac{2\mu_c \zeta \sin(\Delta\hat{\phi})}{\mu_1} \right)^2 \right\} \tau \tag{4.160}$$

For a diffusion process x, the *effective diffusion constant* [29] is defined through

$$D_{eff} \equiv \lim_{\tau\to\infty} \frac{\left\langle (\delta\phi_d(\tau) - \delta\phi_d(0))^2 \right\rangle}{\tau} \tag{4.161}$$

Using the change of notation $D_{eff} \to \bar{D}_{\phi\phi}$, together with the result in (4.160) and the time re-normalization $t = \omega_0/2Q$, we get the final result

$$\bar{D}_{\phi\phi} = \left(\frac{\omega_0}{2Q} \right)^2 \frac{N_0}{nP_0} \left\{ 1 + \left(\frac{2\mu_c}{\mu_1} \right)^2 \zeta^2 \sin^2(\Delta\hat{\phi}) \right\} \tag{4.162}$$

which is the same result found earlier in (4.125) and (4.141).

4.6 A new Definition of Oscillator Q

From the discussion in section 2.2.3 on page 54 and the results derived in the above section, we introduce the novel single/coupled oscillator Q-factor definition

$$Q = \frac{Q_0}{\sqrt{1 + \left(\frac{r}{s} \right)^2}} \tag{4.163}$$

where Q_0 is the DC resonator Q-factor, r is a parameter which describes the curvature of the isochrones and s describes the amplitude relaxation time of oscillator. The new definition in (4.163) has many advantages over previous definitions (see *e.g.* [41]) and these will be discussed in the paper [98], which is currently being written.

4.7 The Cross-Coupled Harmonic Quadrature Oscillator

This section will discuss the analysis of the *cross-coupled quadrature harmonic oscillator* (CCQ0) which is built from two harmonic sources coupled unilaterally in a ring with a 180^o phase shift between source #2 and source #1. A practical transistor implementation of such a structure is depicted in figure 4.7 where the individual oscillators are standard differential pair LC units and the coupling amplifier are common emitter differential pairs. The 180^o phase-shift is derived by cross-coupling one of the connections from the CE amplifiers to the oscillator blocks. In the above figure the oscillators and amplifiers are built using bipolar transistors, however, the quadrature oscillator is also often implemented

[29] see also the discussion in section 2.1.2, on page 43, for further discussion on the concept of effective diffusion constants.

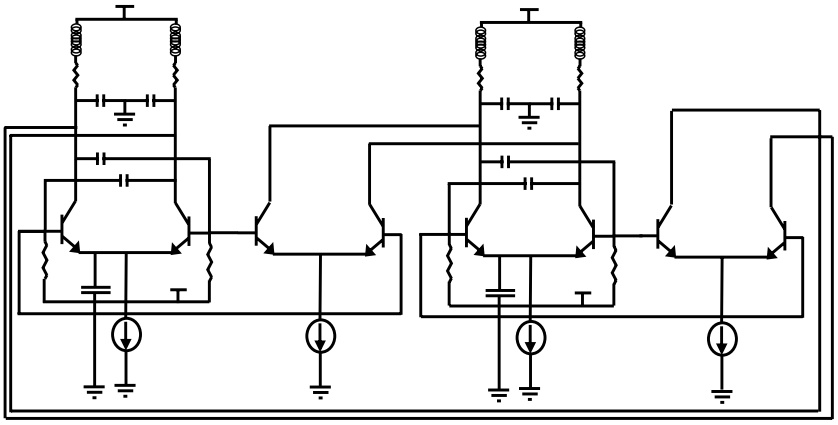

Figure 4.7: A popular circuit implementation of the *Cross-Coupled Quadrature Oscillator* (CCQO) using standard differential pair LC oscillators [74], [77]. The cross-coupling is easily spotted by following the connection from the CE amplifiers to the oscillator blocks. The CE oscillator capacitor is included improve the phase noise performance of the individual oscillators [46].

using CMOS transistors as was the case with the original circuit proposed by Rofougraan *et al.* in [5]. Understanding the noise properties of this circuit has turned out to be a non-trivial task which has occupied the author both in his master thesis [38], as well as in the initial part of the this thesis. This work resulted in three papers [6], [19], [20] which all centered around the new discovery of *coupling induced AM to PM noise conversion* which was discussed in the previous section for the general case of n oscillators. As explained in section 1.1, as well as in the introduction to this chapter, the van der Pol oscillator model is sufficiently complex to model all higher order isochronous harmonic oscillators. We shall therefore not investigate the complex circuit in figure 4.7, but instead we consider the equivalent canonical circuit in figure 4.8 where all transconductance blocks represent second order non-linear functions as described in equation (4.27) of section (4.3). We can relate the structure in figure 4.8 to the general ring of oscillators in figure 4.1 by choosing the parameters (n, β) as $n = 2$ and $\beta = \pi$. Hence, we shall be able to re-use the normal-form/averaged ODE equations derived earlier for the general structure.

In section 4.7.1 we set up the 4 nonlinear coupled ODE's which describe the dynamics of the oscillator in figure 4.8. The next two sub-sections then review the main parts of the analysis described in [6], [19], [20]. This includes an investigation of how parameter asymmetry will impact on the quadrature precision of the solution and a linear response noise analysis.

4.7.1 Deriving the CCQO Amplitude/Phase Equations

Using the equations derived for the general n oscillator case in (4.43)-(4.44) of section 4.3, we can directly write cross-coupled quadrature oscillator averaged state equations as

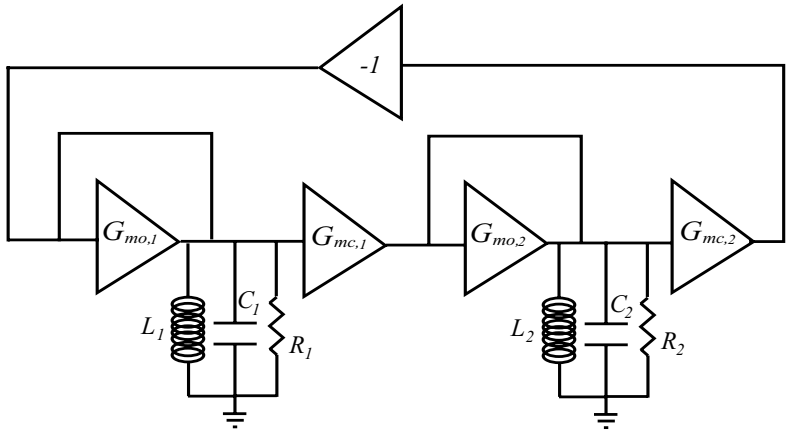

Figure 4.8: the cross-coupled quadrature harmonic oscillator (CCQO) block diagram. All amplifier blocks represent second order nonlinear functions as given in (4.27) on page 91. The oscillators are then standard *van der Pol units* [6], [42]. The above circuit is related to the general n oscillator ring in figure 4.1 through the choice of parameters $(n, \beta) = (2, \pi)$.

$$\frac{1}{\hat{A}}\frac{dA_1}{d\tau} = \mu_{o,1}\left[1 - \left(\frac{A_1}{\alpha_1}\right)^2\right]\frac{A_1}{\hat{A}} + \frac{G_{mc,2}(A_2)}{G_{L1}}\cos\big(\phi_2 - \phi_1 + \pi\big)\frac{A_2}{\hat{A}} \tag{4.164}$$

$$\frac{1}{\hat{A}}\frac{dA_2}{d\tau} = \mu_{o,2}\left[1 - \left(\frac{A_2}{\alpha_2}\right)^2\right]\frac{A_2}{\hat{A}} + \frac{G_{mc,1}(A_1)}{G_{L2}}\cos\big(\phi_1 - \phi_2\big)\frac{A_1}{\hat{A}} \tag{4.165}$$

$$\frac{d\phi_1}{d\tau} = \frac{2Q_1}{\omega_{0,1}}\Delta\omega_1 + \frac{G_{mc,2}(A_2)}{G_{L1}}\sin\big(\phi_2 - \phi_1 + \pi\big)\frac{A_2}{A_1} \tag{4.166}$$

$$\frac{d\phi_2}{d\tau} = \frac{2Q_2}{\omega_{0,2}}\Delta\omega_2 + \frac{G_{mc,1}(A_1)}{G_{L2}}\sin\big(\phi_1 - \phi_2\big)\frac{A_1}{A_2} \tag{4.167}$$

where ω_1 is the new oscillation frequency defined in (4.31) of section 4.3. Furthermore, using (4.32) of the same section we can write

$$\pm\Delta\omega_i = \pm(\omega_0 - \omega_i) = \frac{\tan(\psi_i)\omega_0}{2Q} \quad i = 1, 2 \tag{4.168}$$

All other parameters in (4.164)-(4.167) have already been discussed in connection with the derivations in section 4.3. If we now let the phases ϕ represent deviations around the stable quadrature mode (see discussion in section 4.4.2) we can write (4.164)-(4.167) on the form

$$\begin{aligned}
\frac{1}{\hat{A}}\frac{dA_i}{d\tau} &= \mu_{o,i}\left[1 - \left(\frac{A_i}{\alpha_i}\right)^2\right]\frac{A_i}{\hat{A}} - \frac{G_{mc,j}(A_j)}{G_{Li}}\sin\big(\phi_j - \phi_i\big)\frac{A_j}{\hat{A}} && (4.169)\\
\frac{d\phi_i}{d\tau} &= \frac{2Q_i}{\omega_0}\Delta\omega_i + \frac{G_{mc,j}(A_j)}{G_{Li}}\cos\big(\phi_j - \phi_i\big)\frac{A_j}{A_i} && (4.170)\\
i, j &\in \{1, 2\}\ i \neq j
\end{aligned}$$

In the following derivations we shall need to define the new parameters

$$K_{x,i} = \frac{g_{x2,i}}{g_{x0,i}} \quad x \in \{o, c\} \quad i \in \{1, 2\} \tag{4.171}$$

The K parameters represent the level of nonlinearity in the oscillator and coupling transconductances [6].

4.7.2 Asymmetry Considerations

The subject of asymmetry was briefly discussed in section 1.3 where we investigated the modes of a ring of n oscillators. It was noted that the *implicit function theorem* [25] ensures that there will be a continues path between the perfectly symmetric and the (slightly) asymmetric system. Basically, this means that for small deviations we should not expect any *symmetry breaking bifurcations* [37].

Since the phase variables now describe the dynamics around the quadrature mode, we can write the steady-state solutions in figure 4.8, as

$$v_{C1} = \hat{A}_1 \cos(\omega_1 t + \hat{\phi}_1) \tag{4.172}$$

$$v_{C2} = \hat{A}_2 \sin(\omega_1 t + \hat{\phi}_2) \tag{4.173}$$

where *hats*, as usual, represents steady-state (constant) variables. Setting the left-hand side in (4.169)-(4.170) equal to zero, and using (4.168), we can write

$$\mu_{o,i}\left[1 - \left(\frac{\hat{A}_i}{\alpha_i}\right)^2\right]\hat{A}_i = \mp\frac{\widehat{G}_{mc,j}}{G_{Li}} \sin(\Delta\hat{\phi})\hat{A}_j \tag{4.174}$$

$$\tan(\psi_i) = \frac{\widehat{G}_{mc,j}}{G_{Li}} \cos(\Delta\hat{\phi})\frac{\hat{A}_j}{\hat{A}_i} \tag{4.175}$$

$$(i, j) \in \{1, 2\}, \quad i \neq j$$

where $\Delta\hat{\phi} = \hat{\phi}_1 - \hat{\phi}_2$ and $\widehat{G}_{mc,j} = g_{c0,j} - 3/4 g_{c2,j}\hat{A}_j^2$ as shown in (4.53) on page 94. It should be noted that we now have that $\Delta\hat{\phi} = 0$ for the symmetric circuit. Dividing the two equations represented by (4.175) above, we get

$$\frac{\hat{A}_2}{\hat{A}_1} = \sqrt{\frac{\tan(\psi_1)}{\tan(\psi_2)}\frac{G_{L1}}{G_{L2}}\frac{\widehat{G}_{mc,1}}{\widehat{G}_{mc,2}}} \tag{4.176}$$

From (4.174) we can write

$$\left(\frac{\hat{A}_1}{\alpha_1}\right)^2 = 1 + \frac{\zeta_2}{\mu_{o,1}} \sin(\Delta\hat{\phi})\frac{\hat{A}_2}{\hat{A}_1} \tag{4.177}$$

$$\left(\frac{\hat{A}_2}{\alpha_2}\right)^2 = 1 - \frac{\zeta_1}{\mu_{o,2}} \sin(\Delta\hat{\phi})\frac{\hat{A}_1}{\hat{A}_2} \tag{4.178}$$

where $\zeta_i = \widehat{G}_{mc,i}/G_{Li}$ as seen from (4.52) on page 94. Dividing (4.177)-(4.178) we get

$$\left(\frac{\hat{A}_1}{\hat{A}_2}\right)^2\left(\frac{\alpha_2}{\alpha_1}\right)^2 = \frac{1+\frac{\zeta_2}{\mu_{o,1}}\sin(\Delta\hat{\phi})\frac{\hat{A}_2}{\hat{A}_1}}{1-\frac{\zeta_1}{\mu_{o,2}}\sin(\Delta\hat{\phi})\frac{\hat{A}_1}{\hat{A}_2}} \Leftrightarrow$$
$$-\sin(\Delta\hat{\phi})\left\{\left(\frac{\hat{A}_1}{\hat{A}_2}\right)^2\left(\frac{\alpha_2}{\alpha_1}\right)^2\frac{\zeta_2}{\mu_{o,1}}\frac{\hat{A}_1}{\hat{A}_2}+\frac{\zeta_1}{\mu_{o,2}}\frac{\hat{A}_2}{\hat{A}_1}\right\}=1-\left(\frac{\hat{A}_1}{\hat{A}_2}\right)^2\left(\frac{\alpha_2}{\alpha_1}\right)^2 \Leftrightarrow \quad (4.179)$$
$$\sin(\Delta\hat{\phi}) = \frac{\frac{\hat{A}_1}{\hat{A}_2}\frac{\alpha_2}{\alpha_1}-\frac{\hat{A}_2}{\hat{A}_1}\frac{\alpha_1}{\alpha_2}}{\frac{\zeta_1}{\mu_{o,2}}\left(\frac{\hat{A}_1}{\hat{A}_2}\right)^2\frac{\alpha_2}{\alpha_1}+\frac{\zeta_2}{\mu_{o,1}}\left(\frac{\hat{A}_1}{\hat{A}_2}\right)^2\frac{\alpha_1}{\alpha_2}}$$

Both (4.176) and (4.179) are too complex in their current form to be of any use. However, if we assume only small parameter asymmetry a significantly simplified form will result. In the following we therefore assume that we can write

$$\begin{aligned}\frac{\hat{A}_2}{\hat{A}_1}&=1+\varepsilon \quad \frac{g_{0c,1}}{g_{0c,2}}=1+\eta \quad \frac{\alpha_1}{\alpha_2}=1+\nu\\ \frac{L_1}{L_2}&=1+\epsilon_l \quad \frac{C_1}{C_2}=1+\epsilon_c \quad \frac{G_{L1}}{G_{L2}}=1+\epsilon_g\end{aligned} \quad (4.180)$$

where $|\varepsilon|, |\eta|, |\nu|, |\epsilon_l|, |\epsilon_c|, |\epsilon_g| \ll 1$ are small perturbations of the symmetric parameter set. Furthermore, the scope is limited to the case where nonlinearities of the active blocks are equal from one section to the next *i.e.* $K_{c,1} = K_{c,2} = K_c$ and $K_{o,1} = K_{o,2} = K_o$ (see (4.171)). Using the above definitions we can write

$$\frac{\widehat{G}_{mc,1}}{\widehat{G}_{mc,2}} = \frac{g_{0c,1}}{g_{0c,2}}\frac{1-\frac{3}{4}K_c\hat{A}_1^2}{1-\frac{3}{4}K_c\hat{A}_2^2} \approx (1+\eta)\frac{1-\frac{3}{4}K_c\hat{A}_1^2}{1-\frac{3}{4}K_c(1+2\varepsilon)\hat{A}_1^2} \approx$$
$$(1+\eta)\left(1+\frac{\frac{3}{2}K_c\hat{A}_1^2}{1-\frac{3}{4}K_c\hat{A}_1^2}\varepsilon\right) \approx (1+\eta)(1+2\lambda\varepsilon) \quad (4.181)$$

where we have introduced a new variable λ through

$$\lambda = \frac{\frac{K_c}{K_o}\mu_o}{1+(1-\frac{K_c}{K_o})\mu_o} \quad (4.182)$$

The derivation of equation (4.181) depends on the "smallness" of the parameter ε which furthermore means that we do not need subscripts in (4.182), since this term is multiplied by a factor $|\varepsilon| \ll 1$. The first step is to write

$$\left(\frac{\hat{A}_2}{\hat{A}_1}\right)^2 = (1+\varepsilon)^2 \approx 1+2\varepsilon \quad (4.183)$$

where we have set $\varepsilon^2 \approx 0$. Then we use the first order Taylor expansion

$$\frac{1}{1+x} \approx 1-x \quad \text{for } |x| \ll 1 \quad (4.184)$$

to write

$$\frac{1-\frac{3}{4}K_c\hat{A}_1^2}{1-\frac{3}{4}K_c(1+2\varepsilon)\hat{A}_1^2} \approx 1-\frac{1}{1-\frac{3}{4}K_c\hat{A}_1^2}\times -\frac{3}{4}K_c2\varepsilon\hat{A}_1^2 = 1+\frac{\frac{3}{2}K_c\hat{A}_1^2}{1-\frac{3}{4}K_c\hat{A}_1^2}\varepsilon \quad (4.185)$$

Using $\alpha = \sqrt{4(g_{o0} - G_L)/3g_{o2}}$, $\hat{A}_1 \approx \alpha$ and $\mu_o = (g_{o0} - G_L)/G_L$ and the definition in (4.171), we get

$$\frac{\frac{3}{2}K_c\hat{A}_1^2}{1 - \frac{3}{4}K_c\hat{A}_1^2} = \frac{2K_c\frac{g_{o0}-G_L}{g_{o2}}}{1 - K_c\frac{g_{o0}-G_L}{g_{o2}}} = \frac{2\frac{K_c}{K_o}\mu_o\frac{G_L}{g_{o0}}}{1 - \frac{K_c}{K_o}\mu_o\frac{G_L}{g_{o0}}} = \frac{2\frac{K_c}{K_o}\mu_o}{\frac{g_{o0}}{G_L} - \frac{K_c}{K_o}\mu_o} \tag{4.186}$$

The identity

$$1 + \mu_o = 1 + \frac{g_{o0} - G_L}{G_L} = \frac{G_L + g_{o0} - G_L}{G_L} = \frac{g_{o0}}{G_L} \tag{4.187}$$

means that equation (4.186) can be written

$$\frac{2\frac{K_c}{K_o}\mu_o}{\frac{g_{o0}}{G_L} - \frac{K_c}{K_o}\mu_o} = \frac{2\frac{K_c}{K_o}\mu_o}{1 + \mu_o - \frac{K_c}{K_o}\mu_o} = \frac{2\frac{K_c}{K_o}\mu_o}{1 + \big(1 - \frac{K_c}{K_o}\big)\mu_o} \tag{4.188}$$

Inserting (4.188) into (4.186), (4.186) into (4.185) and finally (4.185) into (4.181), we recover the last expression in (4.181).

Since we are investigating a frequency locked solution the frequency of the two oscillators must be identical. Considering first only inductor asymmetry and using the approximation

$$L_1 = L_2(1 + \epsilon_l) \Leftrightarrow \frac{\omega_{02}}{\omega_{01}} \approx 1 + \frac{1}{2}\epsilon_l\,, \quad |\epsilon_l| \ll 1 \tag{4.189}$$

$$\frac{\tan(\psi_2)}{\tan(\psi_1)} = 1 + \kappa\,, \quad |\kappa| \ll 1\,. \tag{4.190}$$

we can equate the oscillator frequencies as

$$\begin{aligned} \frac{\tan(\psi_2)}{2RC} + \omega_{02} &= \frac{\tan(\psi_1)}{2RC} + \omega_{01} \Leftrightarrow \\ \left(\frac{\tan(\psi_2)}{\tan(\psi_1)} - 1\right) &= \frac{2RC\big(\omega_{01} - \omega_{02}\big)}{\tan(\psi_1)} \Leftrightarrow \\ \kappa = \frac{2Q_2\big(\omega_{01} - \omega_{02}\big)}{\tan(\psi_1)\omega_{02}} &\approx -\frac{Q\epsilon_l}{\tan(\psi)} \end{aligned} \tag{4.191}$$

where, in the last line, subscripts become superfluous as $|\epsilon_l| \ll 1$. In the above equation we used the definition in (4.168) to write

$$\omega_1 = \frac{\tan(\psi_1)\omega_{0,1}}{2Q_1} + \omega_{0,1} = \frac{\tan(\psi_2)\omega_{0,2}}{2Q_2} + \omega_{0,2} \tag{4.192}$$

The above procedure can be repeated for asymmetries in the resonator capacitors and conductors giving us the final result

$$\kappa \approx -\frac{Q\big(\epsilon_l + \epsilon_c\big)}{\tan(\psi)} + \epsilon_g\,, \quad |\epsilon_l|, |\epsilon_c|, |\epsilon_g| \ll 1 \tag{4.193}$$

Using the results in (4.181) and (4.193) and the definitions in (4.180), we can write (4.176) and (4.179) on their final form

$$\frac{\hat{A}_2}{\hat{A}_1} = 1+\varepsilon = \sqrt{\frac{\tan(\psi_1)}{\tan(\psi_2)}\frac{G_{L1}}{G_{L2}}\frac{\widehat{G}_{mc1}}{\widehat{G}_{mc2}}} =$$
$$\sqrt{(1-\kappa)(1+\epsilon_g)(1+\eta)(1+2\lambda\varepsilon)} \approx 1+\frac{1}{2}(-\kappa+\epsilon_g+\eta+2\lambda\varepsilon)$$
$$1+\frac{Q(\epsilon_l+\epsilon_c)}{2\zeta}+\frac{1}{2}\eta+\lambda\varepsilon \Leftrightarrow$$

$$\boxed{\varepsilon \approx \frac{Q(\epsilon_l+\epsilon_c)}{2(1-\lambda)\zeta}+\frac{\eta}{2(1-\lambda)}} \qquad (4.194)$$

$$\sin(\Delta\hat{\phi}) = \frac{\frac{\hat{A}_1}{\hat{A}_2}\frac{\alpha_2}{\alpha_1}-\frac{\hat{A}_2}{\hat{A}_1}\frac{\alpha_1}{\alpha_2}}{\frac{\zeta_1}{\mu_{o,2}}\left(\frac{\hat{A}_1}{\hat{A}_2}\right)^2\frac{\alpha_2}{\alpha_1}+\frac{\zeta_2}{\mu_{o,1}}\left(\frac{\hat{A}_2}{\hat{A}_1}\right)^2\frac{\alpha_1}{\alpha_2}} =$$
$$\frac{(1-\varepsilon)(1-\nu)-(1+\varepsilon)(1+\nu)}{\frac{\zeta_1}{\mu_{o,2}}(1-\varepsilon)^2(1-\nu)+\frac{\zeta_2}{\mu_{o,1}}(1+\varepsilon)^2(1+\nu)} \approx \qquad (4.195)$$
$$-\frac{2\varepsilon+2\nu}{\frac{\zeta_1}{\mu_{o,2}}(1-2\varepsilon)(1-\nu)+\frac{\zeta_2}{\mu_{o,1}}(1+2\varepsilon)(1+\nu)} \approx -\frac{2\varepsilon+2\nu}{2\frac{\zeta}{\mu_o}}$$

Inserting (4.194) into (4.195) we get the final result

$$\boxed{\sin(\Delta\hat{\phi}) \approx -\frac{\mu_o}{1-\lambda}\frac{(\epsilon_l+\epsilon_c)Q}{2\zeta^2}-\frac{\mu_o}{1-\lambda}\frac{\eta}{2\zeta}-\mu_o\frac{\nu}{\zeta}} \qquad (4.196)$$

The inverse quadratic dependence on the coupling strength in the first term of (4.196) was first derived in [68] using graphical phasor analysis. Note, that the effect of conductor asymmetry is contained implicitly through ν.

Equations (4.194) and (4.196) were compared with SPECTRE Periodic Steady State (PSS) simulations in figure 2 of the paper [6] which is repeated here in figure 4.9. Here we have chosen an inductor asymmetry $\epsilon_l = 0.05\%$, a conductor asymmetry $\epsilon_g = 1\%$ and for the transconductance we use $\eta = 0.275\%$. It is important to note that simulations are performed on van der Pol oscillators with ideal third order coupling sections.

From figure 4.9 and (4.194), (4.196) it follows that the phase error dominates for lower couplings. For $\zeta > \mu_o$ [30] the amplitude error is more significant. This is an important result as amplitude and phase error degrade the image rejection equally when the oscillator is integrated in a receiver structure. The amplitude imbalance can however easily be removed by following the oscillator by a limiting buffer. Another interesting point, which can be extracted from (4.194) and (4.196), is that asymmetry in the passive parts of the resonator is the main source of amplitude and phase error. This is because they enter the equations multiplied by a factor Q.

[30] here $\mu_o = 0.5$ is used. In [6] it is shown that this value of μ_o corresponds to a cross-coupled pair working as an ideal limiter.

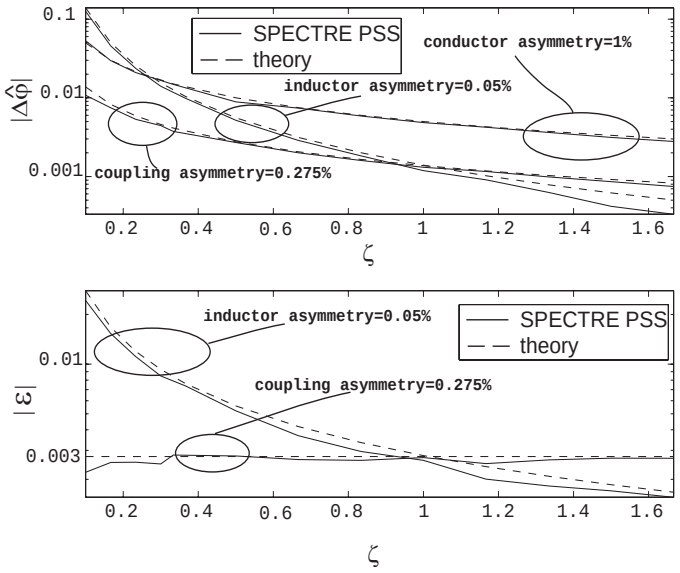

Figure 4.9: Figure taken from the paper [6]. Phase and amplitude error ($\varepsilon = \hat{A}_2/\hat{A}_1 - 1$) as a result small mismatches ($\epsilon_l = 0.05\%$, $\epsilon_g = 1\%$, $\eta = 0.275\%$) in the two resonators and coupling sections. Simulations are for van der Pol oscillators coupled through third order nonlinearities. Top figure - phase error (in radians): (4.196) = broken line, SPECTRE PSS simulation = solid line. Lower figure - amplitude error: (4.194) = broken line, SPECTRE PSS simulation = solid line.

4.7.3 Linear Response Noise Analysis

The linear response equations are derived from the nonlinear state equations in (4.169)-(4.170), in the same way as was shown for the general system in section 4.3 [31]. Referring to the discussion in that section we find the following 4 amplitude and phase equations for the symmetric circuit

$$\frac{1}{\hat{A}}\frac{d\delta A_i}{d\tau} = \mu_o\left[1-3\left(\frac{\hat{A}}{\alpha}\right)^2\right]\frac{\delta A_i}{\hat{A}} - \zeta\big(\delta\phi_j - \delta\phi_i\big) - G_{n,i} \tag{4.197}$$

$$\frac{d\delta\phi_i}{d\tau} = \zeta\big(1-2\mu_c\big)\frac{\delta A_j}{\hat{A}} - \zeta\frac{\delta A_i}{\hat{A}} - B_{n,i} \tag{4.198}$$

$$(i,j) \in \{1,2\}\,, \quad i \neq j$$

where the noise admittance $Y_n = G_n + jB_n$ noise was discussed in section 4.5. Noise sources stemming from the active parts of the oscillators are not modelled here where we assume that the noise is modelled as a single noise current in parallel with the resonator as seen from figure 4.8. However, this does not mean that the model is limited to fictive circuits with noiseless amplifiers. The oscillator *noise factor* F, which was also discussed in section 4.5, is defined as

$$F = \frac{\text{total available noise power}}{4kT} \tag{4.199}$$

where $N_0 = 4kT$ is the available noise power of a thermal resistor noise source. Hence by exchanging the current sources in figure 4.8 from sources with power $4kT$ to sources

[31] see equation (4.54)-(4.55) and (4.56)-(4.61) on page 94.

with power $4FkT$ we have included the effect of all the noise in the circuit. One can calculate this noise factor using *large-signal small-signal* analysis as shown in [96] and [38].

Fourier transforming the system of equations (4.197)-(4.198) one obtains

$$jx\frac{\widetilde{\delta A_i}}{\hat{A}} = \mu_o\left[1-3\left(\frac{\hat{A}}{\alpha}\right)^2\right]\frac{\widetilde{\delta A_i}}{\hat{A}} - \frac{\widehat{G}_{mc}}{G_L}\left(\widetilde{\delta\phi_j}-\widetilde{\delta\phi_i}\right) - \widetilde{G_{ni}} \tag{4.200}$$

$$jx\widetilde{\delta\phi_i} = \frac{\widehat{G}_{mc}}{G_L}(1-2\mu_c)\frac{\widetilde{\delta A_j}}{\hat{A}} - \frac{\widehat{G}_{mc}}{G_L}\frac{\widetilde{\delta A_i}}{\hat{A}} - \widetilde{B_{ni}} \tag{4.201}$$
$$(i,j)\in\{1,2\}\,,\quad i\neq j\,.$$

The tilde $\widetilde{\ }$ denotes a Fourier transformed variable and

$$x = \frac{\omega_m}{\omega_{3dB}} \tag{4.202}$$

with ω_m being the frequency offset from the carrier. The single sided power/cross-power spectral densities of the normalized noise conductances and susceptances are evaluated to be

$$\left\langle\widetilde{G_{n,i}}\widetilde{G_{n,j}}^*\right\rangle = \left\langle\widetilde{B_{n,i}}\widetilde{B_{n,j}}^*\right\rangle = \begin{cases}\frac{8kT}{\hat{A}^2G_L} = \frac{N_0}{P_0}\,, & i=j\\ 0\,, & i\neq j\end{cases} \tag{4.203}$$

$$\left\langle\widetilde{G_{n,i}}\widetilde{B_{n,i}}^*\right\rangle = \left\langle\widetilde{G_{n,i}}^*\widetilde{B_{n,i}}\right\rangle = 0\,,\quad i\in\{1,2\} \tag{4.204}$$

where $\langle\cdot\rangle$ denotes ensemble average, k is Boltzman's constant and T is the absolute temperature. N_0 is the available noise power, assuming 1Hz bandwidth, and P_0 is the signal power delivered to the load

$$N_0 = 4kT \tag{4.205}$$

$$P_0 = \frac{\hat{A}^2G}{2}\,. \tag{4.206}$$

Equations (4.200)-(4.201) can be written on matrix form as

$$\begin{bmatrix}\widetilde{G_{n1}}\\ \widetilde{G_{n2}}\\ \widetilde{B_{n1}}\\ \widetilde{B_{n2}}\end{bmatrix} = \begin{bmatrix}-2\mu_o-jx & 0 & \frac{\widehat{G}_{mc}}{G_L} & -\frac{\widehat{G}_{mc}}{G_L}\\ 0 & -2\mu_o-jx & -\frac{\widehat{G}_{mc}}{G_L} & \frac{\widehat{G}_{mc}}{G_L}\\ -\frac{\widehat{G}_{mc}}{G_L} & \frac{\widehat{G}_{mc}}{G_L}(1-2\mu_c) & -jx & 0\\ \frac{\widehat{G}_{mc}}{G_L}(1-2\mu_c) & -\frac{\widehat{G}_{mc}}{G_L} & 0 & -jx\end{bmatrix}\begin{bmatrix}\frac{\widetilde{\delta A_1}}{\hat{A}}\\ \frac{\widetilde{\delta A_2}}{\hat{A}}\\ \widetilde{\delta\phi_1}\\ \widetilde{\delta\phi_2}\end{bmatrix} \tag{4.207}$$

where

$$\mu_o\left[1-3\left(\frac{\hat{A}}{\alpha}\right)^2\right] = -2\mu_o \tag{4.208}$$

is valid for a symmetric circuit. Inverting the 2×2 matrix in (4.207) yields

$$\begin{bmatrix} \widetilde{\frac{\delta A_1}{\hat{A}}} \\ \widetilde{\frac{\delta A_2}{\hat{A}}} \\ \widetilde{\delta\phi_1} \\ \widetilde{\delta\phi_2} \end{bmatrix} = \frac{1}{2j\mu_o x + 4\left(\frac{\widehat{G}_{mc}}{G_L}\right)^2(1-\mu_c)} \begin{bmatrix} \underline{\underline{N}}_{11} & \underline{\underline{N}}_{12} \\ \underline{\underline{N}}_{21} & \underline{\underline{N}}_{22} \end{bmatrix} \begin{bmatrix} \widetilde{G_{n1}} \\ \widetilde{G_{n2}} \\ \widetilde{B_{n1}} \\ \widetilde{B_{n2}} \end{bmatrix} \tag{4.209}$$

$$\underline{\underline{N}}_{11} = \begin{bmatrix} -\frac{2jx\mu_o + 2\left(\frac{\widehat{G}_{mc}}{G_L}\right)^2(1-\mu_c)}{2\mu_o} & -\frac{2\left(\frac{\widehat{G}_{mc}}{G_L}\right)^2(1-\mu_c)}{2\mu_o} \\ -\frac{2\left(\frac{\widehat{G}_{mc}}{G_L}\right)^2(1-\mu_c)}{2\mu_o} & -\frac{2jx\mu_o + 2\left(\frac{\widehat{G}_{mc}}{G_L}\right)^2(1-\mu_c)}{2\mu_o} \end{bmatrix} \tag{4.210}$$

$$\underline{\underline{N}}_{12} = \begin{bmatrix} -\frac{\widehat{G}_{mc}}{G_L} & \frac{\widehat{G}_{mc}}{G_L} \\ \frac{\widehat{G}_{mc}}{G_L} & -\frac{\widehat{G}_{mc}}{G_L} \end{bmatrix} \tag{4.211}$$

$$\underline{\underline{N}}_{21} = \frac{\widehat{G}_{mc}}{G_L} \begin{bmatrix} a_1 & a_2 \\ a_2 & a_1 \end{bmatrix} \tag{4.212}$$

$$a_1 = \frac{\left(2jx\mu_o + 4\mu_c\left(\frac{\widehat{G}_{mc}}{G_L}\right)^2(1-\mu_c)\right)}{2jx\mu_o} \tag{4.213}$$

$$a_2 = \frac{\left(2jx\mu_o(2\mu_c - 1) + 4\mu_c\left(\frac{\widehat{G}_{mc}}{G_L}\right)^2(1-\mu_c)\right)}{2jx\mu_o} \tag{4.214}$$

$$\underline{\underline{N}}_{22} = \begin{bmatrix} -\frac{2jx\mu_o + 2\left(\frac{\widehat{G}_{mc}}{G_L}\right)^2(1-\mu_c)}{jx} & -\frac{2\left(\frac{\widehat{G}_{mc}}{G_L}\right)^2(1-\mu_c)}{jx} \\ -\frac{2\left(\frac{\widehat{G}_{mc}}{G_L}\right)^2(1-\mu_c)}{jx} & -\frac{2jx\mu_o + 2\left(\frac{\widehat{G}_{mc}}{G_L}\right)^2(1-\mu_c)}{jx} \end{bmatrix} \tag{4.215}$$

Equations (4.209)-(4.215) specify four transfer functions for each of the stochastic variables δA_1, δA_2, $\delta\phi_1$ and $\delta\phi_2$. $\underline{\underline{N}}_{11}$, $\underline{\underline{N}}_{12}$ $\underline{\underline{N}}_{21}$ and $\underline{\underline{N}}_{22}$ contain the AM to AM, PM to AM, AM to PM and PM to PM transfer functions, respectively. Circuit symmetry is assumed, and we can discard the subscripts as the response will be identical at each node. The input variables are random, so only the magnitude of the transfer functions need be considered. From (4.203)-(4.204) it is seen that all four random variables are uncorrelated. The amplitude and phase power spectra, assuming 1Hz bandwidth, are then derived by summing the contribution from each of the four noise admittances. Using (4.203)-(4.204), one obtains the following result

$$\left\langle \widetilde{\delta A^2} \right\rangle = \frac{\frac{N_0}{P_0}}{4(\mu_o x)^2 + 16\left(\frac{\widehat{G}_{mc}}{G_L}\right)^4(1-\mu_c)^2} \left\{ \frac{4x^2\mu_o^2 + 8\left(\frac{\widehat{G}_{mc}}{G_L}\right)^4}{4\mu_o^2} + 2\left(\frac{\widehat{G}_{mc}}{G_L}\right)^2 \right\} \tag{4.216}$$

$$\left\langle \widetilde{\delta\phi^2} \right\rangle = \frac{\frac{N_0}{P_0}}{4(\mu_o x)^2 + 16\left(\frac{\widehat{G}_{mc}}{G_L}\right)^4(1-\mu_c)^2} \times$$
$$\left\{ \frac{8(x\mu_o)^2\left(\frac{\widehat{G}_{mc}}{G_L}\right)^2\left(1 + (2\mu_c - 1)^2\right) + 32\left(\frac{\widehat{G}_{mc}}{G_L}\right)^6\mu_c^2(1-\mu_c)^2}{4(\mu_o x)^2} + \frac{4(\mu_o x)^2 + 8\left(\frac{\widehat{G}_{mc}}{G_L}\right)^4(1-\mu_c)^2}{x^2} \right\} \tag{4.217}$$

Close to the carrier these expressions simplify to

$$\lim_{\omega_m \to 0} \widetilde{\langle \delta A^2 \rangle} = \frac{\frac{N_0}{P_0}}{2\left(\frac{\widehat{G}_{mc}}{G_L}\right)^2 \left(1-\mu_c\right)^2} \left\{ \frac{\left(\frac{\widehat{G}_{mc}}{G_L}\right)^2 + \mu_o^2}{4\mu_o^2} \right\} \tag{4.218}$$

$$\lim_{\omega_m \to 0} \widetilde{\langle \delta \phi^2 \rangle} = \mathfrak{L}_C(\omega_m) = \left[\frac{\omega_1}{\sqrt{2}\sqrt{4Q^2 + \tan^2(\psi)}} \right]^2 \left[1 + \left(\frac{\mu_c}{\mu_o} \right)^2 \tan^2(\psi) \right] \frac{N_0}{P_0 \omega_m^2} \tag{4.219}$$

where $\mathfrak{L}_C(\omega_m)$ denotes phase noise of the coupled oscillator at offset ω_m and N_0/P_0 is the noise to signal power ratio. The $(\mu_c/\mu_o \tan(\psi))^2$ term in (4.219) originates from the $\underline{\underline{N}}_{21}$ transfer matrix, defined in (4.212), and therefore represents AM to PM noise conversion.

Equations (4.218) and (4.219) should return to the equivalent equations for the free-running case when the coupling tends towards zero

$$\lim_{\widehat{G}_{mc},\, \omega_m \to 0} \widetilde{\langle \delta A^2 \rangle} = \frac{N_0}{4\mu_o^2 P_0} \tag{4.220}$$

$$\lim_{\widehat{G}_{mc},\, \omega_m \to 0} \widetilde{\langle \delta \phi^2 \rangle} = \mathfrak{L}(\omega_m) = \left(\frac{\omega_0}{2Q} \right)^2 \frac{N_0}{P_0 \omega_m^2} \tag{4.221}$$

where it is used that

$$\lim_{\widehat{G}_{mc} \to 0} \omega_1 = \omega_0 \tag{4.222}$$

$$\lim_{\widehat{G}_{mc} \to 0} \omega_{3dB} = \frac{\omega_0}{2Q} \tag{4.223}$$

The results in (4.220)-(4.221) agree with those found in the literature [13], [33].

A figure comparing the theoretical results obtained here, with SPECTRE PNOISE simulations was given in figure 3 of the paper [6]. These curves are repeated here in figure 4.10. The figure shows plots of equation (4.219), relative to equation (4.221), together with a series of SPECTRE PNOISE simulations for six different μ_c/μ_o ratios as a function of the coupling strength ζ. The SPECTRE simulations are done on van der Pol oscillators coupled through third order voltage controlled current sources. In figure 4.10 we consider phase noise at a fixed offset for a cross-coupled quadrature oscillator, and an equivalent single oscillator unit. Figure 4.10 results when these two values, in dB, are subtracted and further normalized for the different operating frequencies [32]. The different curves in figure 4.10 are created by fixing K_c and then varying g_{c0}. The parameters μ_o and K_o are held constant throughout. The nonlinearity of the coupling sections is determined by K_c (see (4.171)). From figure 4.10 it is seen, that as the coupling strength increases, AM-PM conversion deteriorates the overall noise performance of the oscillator. However, from (4.194) and (4.196) we see that effects of circuit asymmetries are reduced through stronger coupling. It then follows that there exists a *trade-off* between phase noise and

[32] from (4.221) it is seen that the frequency changes with the coupling strength. As phase noise is proportional to the operating frequency squared (see (4.221)) normalization is achieved by including the factor $20\log(\omega_1/\omega_0)$.

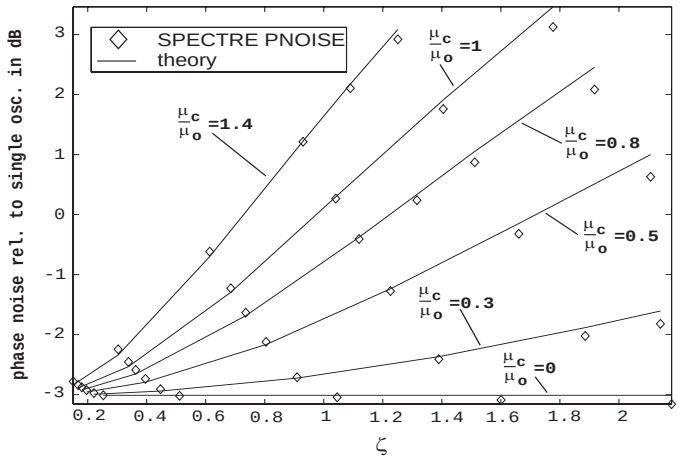

Figure 4.10: Figure taken from the paper [6]. The plots show (4.219) relative to (4.221) in dB as a function of the coupling strength ζ for six different μ_c/μ_o ratios. The simulations are of van der Pol oscillators coupled through a third order nonlinearity. SPECTRE PNOISE phase noise simulations = $\diamond$, theory = solid line. The different curves are created by fixing K_c (see (4.171)) and hence the nonlinearity of the coupling and varying g_{c0}. $\mu_o = 0.5$ throughout.

quadrature precision in a cross-coupled quadrature harmonic oscillator [6], [8], [19], [20], [68], [78]. Another interesting fact, which can be extracted from figure 4.10 and equation (4.219), is that the coupling transconductance nonlinearity impacts on the level of AM to PM conversion. By decreasing the nonlinearity of these blocks, equation (4.219) predicts that the close to carrier AM-PM conversion can be completely cancelled. This is the result of *coupling induced AM-to-PM* noise conversion that we also discussed earlier in section 4.5. It should however be noted that at the time when [6] was published this was a new result not found other places in the literature. Furthermore, this result could only be found through nonlinear analysis and is hence not be found when using linear models [7], [8], [67], [68]. Finally, it is noted from equation (4.219) that the AM-PM noise conversion is proportional to the square of the oscillator amplitude relaxation time [99], [100], as represented by the parameter $1/\mu_o^2$. This intuitively pleasing result is a characteristic of most LC oscillators. The above results illustrate that a highly tunable quadrature oscillator could be created, with low phase noise over the entire tuning range, if one could find a way to minimize the product of the coupling nonlinearity and the oscillator amplitude relaxation time.

Finally we want discuss the issue of a *quadrature oscillator Q factor* which was calculated using linear analysis in [7], [67]. In the case where the nonlinearity of coupling and oscillator transconductance are identical, it follows that

$$\frac{\mu_c}{\mu_o} = \frac{\frac{g_{c0}-\widehat{G}_{mc}}{\widehat{G}_{mc}}}{\frac{g_{o0}-\widehat{G}_{mo}}{\widehat{G}_{mo}}} = \frac{\widehat{G}_{mo}}{\widehat{G}_{mc}}\frac{g_{c2}}{g_{o2}} =$$
$$\frac{g_{o0}}{g_{c0}}\frac{1-\frac{3}{4}K_o\hat{A}^2}{1-\frac{3}{4}K_c\hat{A}^2}\frac{g_{c2}}{g_{o2}} = \frac{g_{o0}}{g_{o2}}\frac{g_{c2}}{g_{c0}} = \frac{K_c}{K_o} = 1 \tag{4.224}$$

where the relation $G = \widehat{G}_{mo}$ has been used. We now consider the case $\mu_c/\mu_o = 1$.

Comparing (4.219) with Leeson's model for phase noise in single oscillators [58], we can define a new Q-factor Q_C for the cross-coupled quadrature oscillator as

$$Q_C = \frac{1}{\sqrt{2}}\cos(\psi)\sqrt{4Q^2+\tan^2(\psi)} \approx \underbrace{\sqrt{2}}_{\substack{Mutual\\ Phase\\ Locking}} Q \underbrace{\cos(\psi)}_{\substack{AM-PM\\ Noise\\ Conversion}} \tag{4.225}$$

It lumps together the effects of mutual phase locking and AM-PM noise conversion. The result in (4.225) was first found in [7] [33] where a phase transfer function was derived through linear analysis. Later, the authors of [68] also derived it using graphical phasor analysis. In [7], it was found that phase-shifters inserted in-between the oscillator sections were needed in-order to make noise and quadrature orthogonal entities. This statement still holds. However, the nonlinear analysis detailed in this paper reveals a completely new aspect. Inspecting (4.219), we see that introducing linear coupling presents yet another way of eliminating the noise/quadrature trade-off.

[33] in [7] the noise-to-signal ratio is not normalized to the noise of a single oscillator. This is why the equivalent Q_2 factor in this paper includes a factor of 2 instead of a factor $\sqrt{2}$. Normalized to the same noise-to-signal ratio the two results are identical.

Conclusion

Besides the obvious need for a platform to present and explain the new findings and models investigated during the course of this project, the intention behind this report was to provide a complete, self-contained and easy-to-read introduction to the field of linear response analysis of coupled oscillating systems. In order to accomplish this goal chapter 1 included a detailed review of the main methods and techniques used in the qualitative analysis of coupled oscillators. This involved equivalence theory (pp. 13-28), averaging methods (pp. 28-31) and an introduction to symmetry calculations using *group theory* (pp. 31-35). Furthermore, an introduction to oscillator noise modelling, Kurokawa theory and Floquet theory was given in appendices A, B and D, respectively.

One of the main themes of the text in chapter 1 concerned the apparent similarity of noise-forced oscillator models derived using either the normal-form method or averaging techniques. It follows from this discussion that we can switch between these two formulations and expect similar results, thus allowing for the methods to complement each other, so to speak; something which could prove important for the construction of future coupled oscillator models. The averaging method is very easily applied to a given problem without involving too much algebra. It is the preferred method for developing qualitative models of coupled electrical oscillators perturbed by noise, implying that almost all electronic engineering literature on the subject will consider averaging. Alone for this reason it is important to familiarize oneself with the methodology. The normal-form method, however, is based on a rigorous analytical foundation where the transformation between "raw" and "normal" coordinate frames are described as the removal of *non-resonant* terms from the state equations. Using this procedure we are allowed a deep intuitive understanding of why some terms are "essential", and hence must remain in the final expression, while others are deemed redundant and, consequently, unimportant for the qualitative understanding of the asymptotic state dynamics. Although the work in this report on the relationship between normal-form and averaged equations was developed independently of any references, it is most certainly formally proven somewhere in the mathematical literature [34].

The report has contributed to new understanding in the following areas

- *A simplified model of the single oscillator noise problem and a new formulation for the derivation of the asymptotic phase statistics [43], (section 2.1.1, on page 38 and section 2.1.4, on page 48) :* the original work in the paper [14] was very complex and did not lead to a deeper understanding of the problem and it's solution. Through a simplified approach using figures and a less mathematical notation we derived a model which explained the statistics of the asymptotic free-running oscillator phase process, as prescribed by an inhomogeneous diffusion equation.

[34] apart from standard curriculum textbooks, the author of this report does not read mathematical literature (for obvious reasons) and hence has not been able to find a reference in this case.

- *A new definition of oscillator Q based on the normal-form equations of single and coupled oscillator structures [98], (section 4.6 on page 113):* this new definition should be seen as a redefinition of the oscillator Q originally proposed by Razavi in [41]. Using a linear feed-back model, Razavi derived the following oscillator Q-factor

$$Q = \frac{\omega_0}{2}\sqrt{\left(\frac{dA}{d\omega}\right)^2 + \left(\frac{d\Phi}{d\omega}\right)^2}$$

where $H(\omega) = A(\omega)\exp(j\Phi(\omega))$ is the linear open-loop transfer function and ω_0 is the steady-state frequency. Unlike the normal-form Q derived in this report, the above definition does not take nonlinear effects into account. It is furthermore the authors experience that it proves extremely difficult to use when dealing with complex coupled oscillator systems. The novel single/coupled oscillator Q proposed in this report is written as

$$Q = \frac{Q_0}{\sqrt{1 + \left(\frac{r}{s}\right)^2}}$$

where Q_0 is resonator Q-factor, r is a parameter which describes the isochrone curvature at the limit cycle and s represents the *amplitude relaxation time of oscillator* corresponding to a negative Floquet characteristic exponent. As witnessed from the discussions in section 2.2.3, on page 54, and section 4.5.1, on page 105, this formulation is extremely easy to use once the normal-form state equations have been derived.

- *A novel model of unilateral ring-coupled oscillators explaining the phenomena of coupling-induced added phase-noise and including the effects of nonlinear coupling transconductors [6], [19], [20], (section 4.7.3 on page 120, equation* (4.125) *on page 108 and equation* (4.219) *on page 123):* this case very clearly illustrates the points made above, concerning nonlinear effects. The previous models [7], [68] of this circuit structure had missed the implications of nonlinear coupling because they were based on linear formulations. Unlike these linear schemes, the normal-form approach guarantees that all essential dynamic behavior will be included in the final model. It is therefore the correct foundation for the qualitative study of oscillators, both coupled and free-running. Using the model derived here, the coupling induced noise was identified as an AM-PM contribution originating from the de-tuning of the resonator, a nonlinear coupling transconductor and a finite amplitude relaxation time constant. The phase-noise of the ring-coupled structure is expressed in terms of an *effective diffusion constant*

$$\bar{D}_{\phi\phi} = \left(\frac{\omega_0}{2Q}\right)^2 \left\{1 + \underbrace{\left(\frac{2\mu_c}{\mu_1}\right)^2 \zeta^2 \sin^2(\Delta\hat{\phi})}_{\text{added coupling noise}}\right\} \frac{N_0}{nP_0}$$

where $\omega_0/(2Q)$ is the resonator 3dB bandwidth (Q and ω_0 are the resonator quality factor and natural frequency, respectively), μ_c is related to the coupling linearity (linear coupling $\Rightarrow \mu_c = 0$), μ_1 is the effective amplitude relaxation time constant, ζ is the coupling strength, $\Delta\hat{\phi}$ is the steady-state phase shift of two neighboring oscillators (cells) in the ring, n is the number of cells in the ring and N_0/P_0 is the

noise-to-power ratio. The above expression gives a clear indication of the "cost" of coupling oscillators in a unilateral ring structure.

- *A new algorithm for the unified phase-noise characterization of coupled oscillating systems [51],[52], (chapter 3 on page 57) :* in chapter 3, a generalized, automated, topology and parameter independent phase-noise characterization of coupled oscillators, perturbed by white noise sources, was proposed. In principle, this model could be applied to any kind of coupled system, however, due to time-constraints it was only possible to include a discussion considering a single example in this report; namely the *subharmonic injection locked oscillator* (S-ILO). It was shown how one could identify the two orthogonal projection operators which would project onto the invariant manifold. Using the obtained projection operators we derived two coupled stochastic differential equations (SDE) which were solved for the asymptotic probability density of the S-OSC phase. Two diffusion constants, D_{21} and D_{22}, where D_{21} represents the noise injected by the master oscillator (M-OSC) and D_{22} the S-OSC noise, completely characterize the asymptotic stochastic S-OSC phase properties. This should be compared with the single oscillator case where only one constant was necessary to model the system. Generally, n diffusion constants are then necessary to describe the n oscillator coupled system, corresponding to a n dimensional invariant manifold. Using the asymptotic probability density for the self-referenced (SR-P) S-OSC oscillator phase, derived from the SDE system described above, we were able to calculate the single sideband (SSB) phase-noise spectrum of the S-ILO, as

$$\mathfrak{L}_s(\omega_m) = 10\log\left[\frac{(N\omega_1)^2 D_{22}[\omega_m^2+\frac{D_{21}}{D_{22}}\mu_2^2]}{[(\frac{1}{2}N^2\omega_1^2 D_{21})^2+\omega_m^2][\mu_2^2+\omega_m^2]}\right]$$

where ω_m is the offset from the S-OSC carrier frequency ω_1, in radians, N is the harmonic of the M-OSC which locks to the S-OSC fundamental, μ_2 is the second Floquet characteristic exponent which was seen to be equal to the *effective locking bandwidth* (see (3.88), on page 76).

The theoretic expressions were verified against raw integration of the stochastic differential equations and with earlier (linear) models found in the literature.

It should be stressed that the coupled oscillator phase macro-model proposed in this report is a work-in-progress, and that the formulation presented here hence might not constitute the "final say" in this matter, so to speak. Future work in this respect will concentrate on solidifying the model formulation by introducing a more rigorous mathematical treatment. Work also needs to be done in order to improve the efficiency and robustness of the numerical algorithm implemented in the program [61]. Finally, it is the authors intention to extend the S-ILO model, described here, to include other coupled oscillating systems [52]. It could also be interesting develop a formulation which included colored noise sources like $1/f$ noise. In [15], Demir showed how this could be done for the single oscillator phase macro-model.

List of Publications

The following publications are part of this thesis

- *published :* [6], [19], [20], [101]

- *submitted :* [51]
- *to be submitted :* [52], [43], [98]

Appendix A

The Noise Appendix : Narrow-band Noise / Stochastic Integration / The Fokker-Planck Equation

In section 2.2.3, chapter 4 and appendix B we consider a prototype harmonic oscillator consisting of a dampened parallel RCL resonator, shunted by a negative resistance non-linear energy restoring circuit component (see *e.g.* figure 4.1, on page 80). The active circuits and the resonator loss resistance will introduce thermal/shot noise sources into the problem formulation. As explained several places in this report, these noise sources can be collected in a single white-noise current source, in parallel with the resonator, by the introduction of a so-called *noise factor* F [38], [96]. Since we consider *linear* response noise analysis, we can without consequence re-normalize the noise power and set $F = 1$. In conclusion, given that an oscillator noise factor has somehow been derived, the statistics of the noise forcing function is fully characterized through a single stationary [1] white-noise current source i_n, with correlation function

$$\Gamma(t_1, t_2) = \left\langle i_n(t_1) i_n(t_2) \right\rangle = \Gamma(\tau) = \frac{4kT}{R}\delta(\tau) \tag{A.1}$$

where R is the loss resistance of the resonator, k is Boltzmanns constant [2], T is the absolute temperature and we have defined $\tau = t_1 - t_2$. The double-sided spectral density S_n is found by Fourier transforming the correlation function in (A.1)

$$S_n(f) = \frac{2kT}{R} \tag{A.2}$$

which, according to the definition of *ideal white noise*, is independent of frequency [3]. We can then find the power at any frequency f_0, per Hz bandwidth, as

$$\sigma_n^2 = \frac{\left\langle i_n(t)^2 \right\rangle}{\Delta f} = \frac{2}{\Delta f} \times \int_{f_0 - \frac{1}{2}\Delta f}^{f_0 + \frac{1}{2}\Delta f} S_n(f) df = \frac{4kT}{R} \quad [A^2 \cdot s] \tag{A.3}$$

[1] a process is stationary if the statistics are independent of the absolute measurement time and hence only depends on the time intervals between measurements. For the correlation Γ, between the two variables $i_n(t_1)$ and $i_n(t_2)$, this means that $\Gamma(t_1, t_2) = \Gamma(t_1 - t_2)$ [39].

[2] $k = 1.38 \times 10^{-23} J/K$.

[3] this is of course only an approximation since this would require an infinite energy signal [102].

A.1 Narowband Noise

In section 1.2, chapter 4 and appendix B, we discuss *averaging theory*, as it is applied to noise forced harmonic oscillators. In the averaged oscillator state equations, we no longer consider the white-noise current source i_n discussed above, but instead, the two new narrowband noise processes i_{nc} and i_{ns}

$$i_{nc}(t) = \frac{2}{T_0} \int_{t-T_0}^{t} i_n(\eta) \cos(\omega_0 \eta) d\eta \tag{A.4}$$

$$i_{ns}(t) = \frac{2}{T_0} \int_{t-T_0}^{t} i_n(\eta) \sin(\omega_0 \eta) d\eta \tag{A.5}$$

with $T_0 = 2\pi/\omega_0$ being the steady-state oscillator period. It is the purpose of this appendix to characterize the statistics of these two noise currents.

The first step in the analysis considers the creation of an *periodic ensemble*

1. We assume that we have measured, and stored, an infinite long time series of the noise current i_n.
2. This time series is then split-up into pieces of length T.
3. Each piece is copied an infinite number of times and then glued together to form a infinite length *periodic* noise signal.
4. Continuing this process for each piece, we now have an infinite number of periodic noise signals, which consequently form a *periodic ensemble*
5. In the limit $T \to \infty$ this ensemble has the same statistics as i_n, defined through (A.1)-(A.3).

From the above description we can write the noise current as

$$i_n(t) = \lim_{f \to 0} \sum_{n=1}^{\infty} \left[a_n \cos(2\pi n f t) + b_k \sin(2\pi n f t) \right] \tag{A.6}$$

where $f = 1/T$ is the fundamental harmonic and the stochastic variables, a_n and b_n, must account for the statistics of the ensemble. Since we are considering a stationary process we can calculate the power at any time. Choosing the time t so that $2nft = i$, with i being an arbitrary, even or uneven, integer, we can derive

$$\left\langle a_{n_1} a_{n_2} \right\rangle = \left\langle b_{n_1} b_{n_2} \right\rangle = \delta_{n_1,n_2} \sigma_n^2 \tag{A.7}$$

$$\left\langle a_{n_1} b_{n_2} \right\rangle = 0 \quad \text{for all } n_1, n_2 \tag{A.8}$$

where we used the notation from (A.3) and δ_{ij} is the Kroenecker delta-function.

We now choose f such that it is a submultiple of the oscillation frequency $f_0 = Nf$. We can then write (A.6) as

$$i_n(t) = i_x(t) \cos(2\pi f_0 t) - i_y(t) \sin(2\pi f_0 t) \tag{A.9}$$

where

$$i_x(t) = \lim_{f\to 0} \sum_{n=1}^{\infty} \left[a_n \cos(2\pi(n-N)ft) + b_n \sin(2\pi(n-N)ft)\right] \tag{A.10}$$

$$i_y(t) = \lim_{f\to 0} \sum_{n=1}^{\infty} \left[a_n \sin(2\pi(n-N)ft) - b_n \cos(2\pi(n-N)ft)\right] \tag{A.11}$$

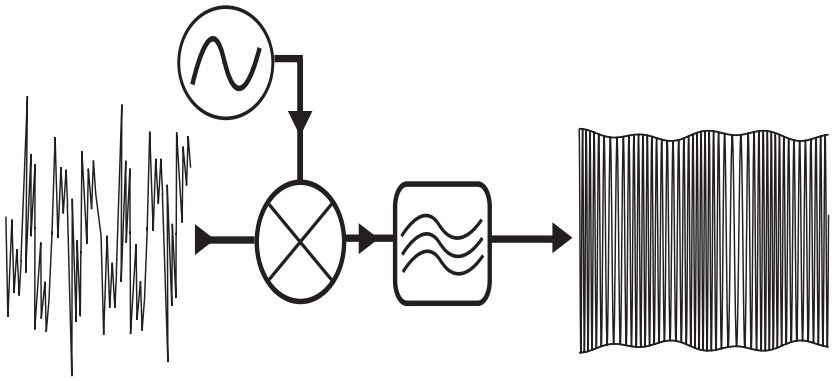

Figure A.1: The averaging operation. The averaged wide-band thermal noise source is represented by a carrier modulated by slow amplitude/phase signals.

The actions of averaging operator in (A.4)-(A.5) is illustrated in figure A.1. It consist of an ideal mixer followed by a filter with transfer function

$$h(t) = \begin{cases} \frac{1}{T_0} & t \in [-T_0/2; T_0/2] \\ 0 & \text{otherwise} \end{cases} \tag{A.12}$$

corresponding to the filter response

$$H(f) = \frac{\sin(\pi f T_0)}{\pi f T_0} \tag{A.13}$$

which is a low-pass filter with a finite $3db$ bandwidth B. We therefore approximate (A.13) as

$$H(f) \approx \begin{cases} 1 & f \in [-B; B] \\ 0 & \text{otherwise} \end{cases} \tag{A.14}$$

We now define i_{nc} and i_{ns} from the currents i_x and i_y in (A.10)-(A.11), including only that part of the spectrum which lies inside a bandwidth $[f_0 - B; f_0 + B]$

$$i_{nc}(t) = \lim_{f\to 0} \sum_{n=-k}^{k} \left[a_{n+N} \cos(2\pi nft) + b_{n+N} \sin(2\pi nft)\right] \tag{A.15}$$

$$i_{ns}(t) = \lim_{f\to 0} \sum_{n=-k}^{k} \left[a_{n+N} \sin(2\pi nft) - b_{n+N} \cos(2\pi nft)\right] \tag{A.16}$$

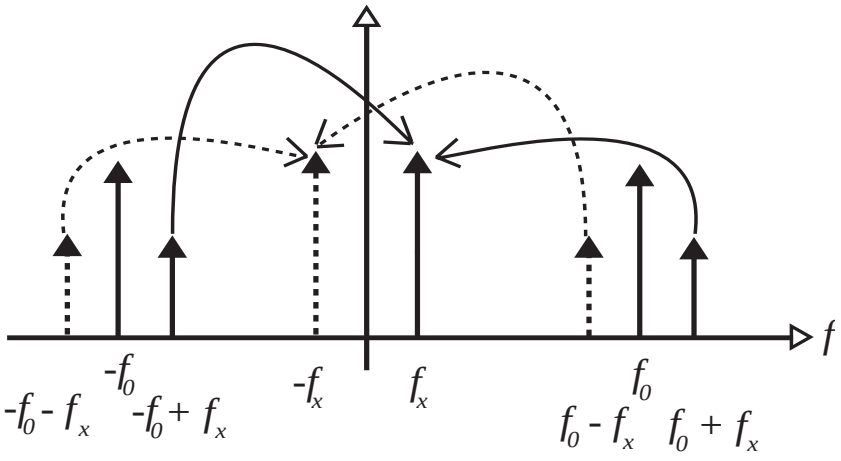

Figure A.2: The effect of the averaging procedure in (A.4)-(A.5), illustrated in the frequency domain.

where k is an integer chosen so that $kf \leq B$. Hence i_{nc} and i_{ns} are narrow-band, or *slow*, signals by which we mean that they will not vary significantly over one period of the carrier, as is also illustrated in figure A.1.

We now consider an arbitrary integer $n = Q$ in (A.15). The spectral components of the narrow-band current source i_{nc}, at the frequency Qf, are

$$a_{N-Q}\cos(2\pi Qft) - b_{N-Q}\sin(2\pi Qft) + a_{N+Q}\cos(2\pi Qft) + b_{N+Q}\sin(2\pi Qft) \quad \text{(A.17)}$$

We see that it consist of 4 components, corresponding to the two sidebands $\pm f_0 \pm Qf$, as illustrated in figure A.2. The process in (A.15) is stationary and we can therefore choose calculate the power at any time t. By choosing the time such that $Qft = i$, with i being and arbitrary integer, we find the power, per Hz, at Qf is equal to

$$P_Q = \left\langle a_{N-Q}^2 \right\rangle + \left\langle a_{N+Q}^2 \right\rangle = 2\sigma_n^2 \quad \text{(A.18)}$$

where we have used (A.7)-(A.8). We see that the power, per Hz, of i_{nc} is twice that of i_n. This is explained from figure A.2, where it is seen that both the sideband at $f_0 + f_x$ and that at $-f_0 + f_x$ are down-converted by the averaging procedure to the sideband at f_x, resulting in twice the power. The frequency used above was chosen arbitrarily and the result will hence apply for all the frequencies inside the bandwidth B. Furthermore, the discussion above, pertaining to i_{nc} in (A.15), also holds for i_{ns} in (A.16) and we can therefore write the double-sided spectral densities of the two narrow-band currents, using (A.2), as

$$G_{ns}(f) = G_{nc}(f) = S_n(f - f_0) + S_n(f + f_0) = \frac{4kT}{R} \quad |f| \leq B \quad \text{(A.19)}$$

Using (A.3), with (A.19) substituted for $S_n(f)$, we can then find the power, per Hz, of these two process as

$$\sigma_{ns}^2 = \sigma_{nc}^2 = 2 \times \sigma_n^2 = \frac{8kT}{R} \quad \text{(A.20)}$$

We also find that

$$\left\langle i_{ns}(t)i_{nc}(t)\right\rangle = 0 \tag{A.21}$$

where we have used that a_n and b_n are uncorrelated, as is seen from (A.8). Since all contributions in (A.9), outside the filter bandwidth B, are eventually removed by the averaging procedures (A.4)-(A.5), we would get the same end-results if we started with a definition of the noise current, i_n, where all these redundant components were simply neglected. This leads to the definition of the *narrow-band noise current*

$$\boxed{i_n(t) = i_{nc}(t)\cos(\omega_0 t) - i_{ns}(t)\sin(\omega_0 t)} \tag{A.22}$$

Using (A.19) and (A.21) we summarize the above results as

$$\left\langle i_{nc}(t_1)i_{nc}(t_2)\right\rangle = \left\langle i_{ns}(t_1)i_{ns}(t_2)\right\rangle = \frac{8kT}{R}\delta(t_1 - t_2) \tag{A.23}$$

$$\left\langle i_{ns}(t_1)i_{nc}(t_2)\right\rangle = 0 \quad \text{for all } t_1, t_2 \tag{A.24}$$

A.1.1 The Noise Admittance $Y_n = G_n + jB_n$

Often, the narrow-noise current sources i_{nc} and i_{ns}, defined in the previous section, are represented in the noise forced averaged equations through the *noise admittance* $Y_n = G_n + jB_n$ [13]. In appendix B we derive the averaged equations of a general noise forced 2-dimensional oscillator. As is seen from these calculations, we normalize the noise-forced amplitude/phase equations by dividing with factor AG (see (B.33)-(B.34) on page 145) and we therefore consider the new noise forcing functions $i_{nc}/(AG)$ and $i_{ns}/(AG)$, respectively. Here, A is the signal amplitude and G is the resonator loss conductance. We can write the noise perturbed oscillator amplitude as $A = \hat{A} + \delta A$, where $\hat{A}$ is the *steady-state* amplitude of the noiseless oscillator and δA is a small *noise transient*. Since both i_{ns}, i_{nc} and δA are small signals of same order, we can ignore the cross products and hence define the new noise forcing functions

$$\boxed{\begin{aligned} G_n(t) &= \frac{i_{nc}(t)}{\hat{A}G} \quad (A.25)\\ B_n(t) &= \frac{i_{ns}(t)}{\hat{A}G} \quad (A.26)\end{aligned}}$$

where G_n and B_n are the narrow-band *noise conductance* and *noise susceptance*, respectively. Using (A.23)-(A.24) we can then characterize these two noise processes through

$$\left\langle G_n(t_1)G_n(t_2)\right\rangle = \left\langle B_n(t_1)B_n(t_2)\right\rangle = \frac{8kT}{\hat{A}^2 G}\delta(t_1 - t_2) = \frac{N_0}{P_0}\delta(t_1 - t_2) \tag{A.27}$$

$$\left\langle G_n(t_1)B_n(t_2)\right\rangle = 0 \quad \text{for all } t_1, t_2 \tag{A.28}$$

where

$$N_0 = 4kT \quad [A \cdot V \cdot s] \tag{A.29}$$

$$P_0 = \frac{\hat{A}^2 G}{2} \quad [A \cdot V] \tag{A.30}$$

Here N_0 is the *available noise power*, in a 1 Hz bandwidth, and P_0 is the *signal power* dissipated in the loss conductance.

A.1.2 A Pulse Train Noise Model

Since i_n is a thermal/white noise source we can write it as train of ideal delta pulses [32], [97]

$$i_n(t) = \sum_i \xi_i \delta(t - t_i) \tag{A.31}$$

where the pulse amplitudes ξ_i and pulse arrival times t_i are independent from one pulse to the next. The arrival times of the pulses are specified as a *Poison process* [4], which depends on a single parameter λ, known as the *rate* of the process. Briefly, besides the independence of arrival times, this implies that the chance of observing a pulse only depends on the length of the observation interval and not on the specific measurement time. If $N(\tau)$ specifies the number of pulses in the interval τ, we have

$$\left\langle N(\tau) = 1 \right\rangle = \lambda\tau \tag{A.32}$$

So, in the mean, one pulse arrives in each interval of length $1/\lambda$. Stationary Gaussian processes are *ergodic* [97], implying that the time average of (A.31) equals the ensemble average in (A.3)

$$\begin{aligned} \overline{i_n^2} = \lim_{T_x \to \infty} \frac{1}{T_x} \int_{t-T_x}^{t} i_n^2(\eta) d\eta = \lim_{T_x \to \infty} \frac{1}{T_x} \int_{t-T_x}^{t} \sum_i \sum_j \xi_i \delta(\eta - t_i) \times \xi_j \delta(\eta - t_j) d\eta = \\ \lim_{T_x \to \infty} \frac{1}{T_x} \sum_{i=i_1}^{i_2} \xi_i^2 \end{aligned} \tag{A.33}$$

where i_1 and i_2 are chosen so that all pulses in the interval $[t - T_x; t]$ are included in the sum. In the following we specify the pulse powers through their ensemble values $\left\langle \xi_i^2 \right\rangle$. From (A.32), we should expect to observe λT pulses in the interval $[t - T; t]$, and so using (A.3), the ergodic property yields

$$\frac{4kT}{R} = \lim_{T_x \to \infty} \frac{T_0 \lambda}{T_0} \left\langle \xi_i^2 \right\rangle \Leftrightarrow \left\langle \xi_i^2 \right\rangle = \frac{4kT}{R\lambda} \quad [C^2] \tag{A.34}$$

Using (A.4) and (A.31), we can find an expression for the narrow-band noise source i_{nc}

[4] the stochastic variable $N(\tau)$, which accounts for the number of *events* inside the interval $[t - \tau, t]$, is specified through a Poison process if $P(N(\tau) = k) = \frac{(\lambda\tau)^k \exp(-\lambda\tau)}{k!}$.

$$\begin{aligned} i_{nc}(t) = \frac{2}{T_0}\int_{t-T_0}^{t} i_n(\eta)\cos(\omega_0\eta)d\eta = \frac{2}{T_0}\int_{t-T_0}^{t}\sum_i \xi_i\delta(\eta-t_i)\cos(\omega_0\eta)d\eta \\ = \sum_i \frac{2}{T_0}\int_{t-T_0}^{t}\xi_i\delta(\eta-t_i)\cos(\omega_0\eta)d\eta \end{aligned} \tag{A.35}$$

in the time $t \in [t_i, t_i + T_0]$ the integral in the above equation is equal to

$$\frac{2}{T_0}\int_{t-T_0}^{t}\xi_i\delta(\eta-t_i)\cos(\omega_0\eta)d\eta = \frac{2\xi_i}{T_0}\cos(\omega_0 t_i) \tag{A.36}$$

As explained in [32], the averaging procedure has turned the delta pulse into a pulse of length T_0. If we define a new averaged delta function $\tilde{\delta}$ as

$$\tilde{\delta}(t) = \begin{cases} \frac{1}{T_0} & t \in [0; T_0] \\ 0 & \text{otherwise} \end{cases} \tag{A.37}$$

then we can write (A.35) as

$$i_{nc}(t) = \sum_i 2\xi_i\cos(\omega_0 t)\tilde{\delta}(t-t_i) \tag{A.38}$$

Likewise, we can write the narrow-band source i_{ns} as

$$i_{ns}(t) = \sum_i 2\xi_i\sin(\omega_0 t)\tilde{\delta}(t-t_i) \tag{A.39}$$

As explained in section A.1.1, we can then define the noise admittance $Y_n = G_n + jB_n$ through

$$G_n(t) = \sum_i \xi_{c,i}\tilde{\delta}(t-t_i) \tag{A.40}$$

$$B_n(t) = \sum_i \xi_{s,i}\tilde{\delta}(t-t_i) \tag{A.41}$$

where

$$\xi_{c,i} = \frac{2\xi_i}{\hat{A}G}\cos(\omega_0 t) \tag{A.42}$$

$$\xi_{s,i} = \frac{2\xi_i}{\hat{A}G}\sin(\omega_0 t) \tag{A.43}$$

Taking the time average of $G_n(t_1)G_n(t_2)$, $B_n(t_1)B_n(t_2)$ and $G_n(t_1)B_n(t_2)$, using (A.40)-(A.41), (A.42)-(A.43) and (A.34), as well as the ergodicity property, we reclaim the statistics in (A.27)-(A.28).

A.2 Stochastic Integration

We consider the scalar [5] stochastic differential equation (SDE)

$$\frac{dx}{dt} = h(x,t) + g(x,t)i_n(t) \tag{A.44}$$

where $i_n(t)$ is a zero mean, delta-correlated, unit power Gaussian noise current source, which was characterized in the beginning of this appendix [6]. This kind of equation occurs naturally in the modelling of any finite dimensional system forced by noise. As is seen from (A.44), the formulation includes the possibility of both additive and multiplicative noise [7]. Equation (A.44) is known as a *Langevin equation* [8] and the noise source ξ is often referred to as a Langevin force.

Although it correctly states the dynamics being considered, the formulation in (A.44) can lead to erroneous interpretations. Stated briefly, the problem is that the left-hand side contains a derivative while the right-hand side contains a delta-correlated, *i.e.* infinitely fast moving, forcing function. From this description, one could be led to the conclusion that the resulting waveform $x(t)$ is *discontinuous*. The fact that realizations of (A.44) are actually *continuous* [39] illustrates quite clearly that we should be careful when using (A.44).

We can get around this ambiguity by choosing to interpret (A.44) in terms of the Riemann-Stejltes integral

$$\int_{t_0}^{t} dx = \underbrace{\int_{t_0}^{t} h(x,s)ds}_{\text{standard integral}} + \underbrace{\int_{t_0}^{t} g(x,s)dW(s)}_{\text{stochastic integral}} \tag{A.45}$$

where W is a standard zero mean, unit power *Wiener process* [39]. This process is defined as the integration of the white noise process i_n

$$W(t) - W(t_0) = \int_{t_0}^{t} i_n(s)ds \tag{A.46}$$

In figure A.3 we illustrate this, where we have modelled the white noise source i_n as a train of pulses [9]

$$i_n(t) = \sum_i \xi_i \delta(t - t_i) \tag{A.47}$$

with ξ being defined in (A.34). With the aim of deriving the statistics of the process in (A.45), we now consider the increment process

[5] although a treatment of vector SDE's would produce more general results, we only consider the scalar case here. For a more complete treatment of the subject the reader is referred to [39].

[6] see (A.1) and (A.3) on page 130.

[7] if the function g in (A.44) depends on the state variable x, then i_n is known as multiplicative noise.

[8] named after Paul Langevin who was the first person introduce this notation around 1908. In the original work, which was the result of efforts to attempt a simplification of Einsteins famous 1905 paper on *Brownian motion*, Langevin did not use the concept of white noise, but instead the similar assumption that the state variable and the forcing function were uncorrelated at all times $\langle x(t)i_n(t)\rangle = 0$.

[9] see discussion in appendix A.1.2.

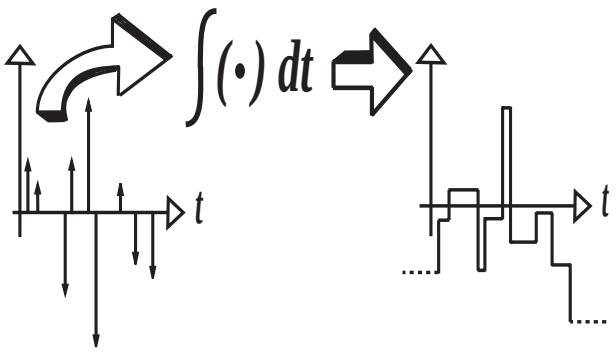

Figure A.3: The Wiener Process (right curve), is defined as the integration of white noise as represented by an pulse train (↑) [32] (left curve), where the arrival time and size of the pulses are completely independent from one occurrence to the next.

$$\Delta W(t_1, t_0) = W(t_1) - W(t_0) = \int_{t_0}^{t_1} i_n(s)ds = \sum_{i=i_0}^{i_1} \xi_i \tag{A.48}$$

where i_1 and i_2 are chosen so that all pulses in the interval $[t_0; t_1]$ are counted. Assuming we have two disjoint intervals $R_1 = [t_0; t_1]$ and $R_2 = [t_2; t_3]$, *i.e.* $t_1 < t_2$ or $t_3 < t_0$, we easily find

$$\big\langle \Delta W(t_1, t_0)\Delta W(t_3, t_2)\big\rangle = \left\langle \sum_{i=i_0}^{i_1} \xi_i \times \sum_{j=i_2}^{i_3} \xi_j \right\rangle = 0 \tag{A.49}$$

since

$$\big\langle \xi_i \xi_j \big\rangle = \delta_{ij} \frac{4kT}{R\lambda} \tag{A.50}$$

as discussed in section A.1.2. From (A.49) we get the important results that two non-overlapping Wiener increments are uncorrelated. Moving on to the case where the two intervals *overlap*, we can split correlation integral up into two contributions

$$\big\langle \Delta W(t_1, t_0)\Delta W(t_3, t_2)\big\rangle = \left\{ \sum_{i=i_0}^{i_1} \big\langle \xi_i^2 \big\rangle + \sum_j \sum_i \big\langle \xi_i \xi_j \big\rangle \right\} \tag{A.51}$$

where i_0 and i_1 are chosen so as to collect the pulses in the interval $t \in R_1 \cap R_2$ and the last term concerns pulses in the interval $t \in R_1 \cup R_2$, but for different indices $i \neq j$. From (A.50) we see that the last term in (A.51) can be set to zero. The length of the interval $t \in R_1 \cap R_2$ is equal to $\min(t_1, t_3) - \max(t_0, t_2)$. From the discussion in appendix A.1.2, we know that we should expect $\lambda[\min(t_1, t_3) - \max(t_0, t_2)]$ pulses in this interval. We can therefore write (A.51) as

$$\begin{aligned}\big\langle [W(t_1)-W(t_0)][W(t_3)-W(t_2)]\big\rangle &= \Big\langle \int_{t_0}^{t_1} i_n(s_1)ds_1 \int_{t_2}^{t_3} i_n(s_2)ds_2 \Big\rangle = \\ \int_{t_0}^{t_1}\int_{t_2}^{t_3} \big\langle i_n(s_1)i_n(s_2)\big\rangle ds_1 ds_2 &= \lambda\big\langle \xi_i^2\big\rangle \big(\min(t_1,t_3)-\max(t_0,t_2)\big) = \\ \sigma_n^2\big(\min(t_1,t_3)-\max(t_0,t_2)\big) &= \min(t_1,t_3)-\max(t_0,t_2)\end{aligned} \tag{A.52}$$

since i_n is assumed to be a unit power process. We now consider the process in (A.46) with $t_0 = 0$ and the initial condition $W(0) = 0$. We then see that we should set $t_0 = t_2 = 0$ in (A.52) and hence that $\max(t_0, t_2) = 0$. Furthermore, the initial condition specifies $W(t_0) = W(t_2) = 0$ and we can then write (A.52) as

$$\boxed{\begin{aligned}\big\langle W(t_1)W(t_2)\big\rangle &= \min(t_1,t_2) && \text{(A.53)}\\ \big\langle W(t)^2\big\rangle &= t && \text{(A.54)}\end{aligned}}$$

where (A.54) follows directly from (A.53) and we have changed the notation $t_3 \to t_2$.

We now return to the original integral in (A.45). Here the first term should be calculated using standard calculus, while the second integral is a so-called *stochastic integral* which requires a special calculus (*i.e.* a stochastic calculus). There exist two interpretations this type of integral, referred to as the *Ito* and the *Stratonovich* integral, respectively [39]. The difference between these two interpretations has implications for the process statistics, only if one considers *multiplicative* noise. If g in (A.45) does not depend on x, as is the case for additive noise, then the two integrals produce the same result. In this section we limit the scope to additive noise sources and we can therefore write the second integral in (A.45) as

$$I_s(t,t_0) = \int_{t_0}^{t} g(s)dW(s) \tag{A.55}$$

Since this is stochastic integral we can only solve it in the *mean limit*. Using the initial condition $W(t_0) = 0$ it follows from the above discussion that W is a *zero mean* variable, which means that

$$\boxed{\big\langle I_s(t,t_0)\big\rangle = \Big\langle \int_{t_0}^{t} g(s)dW(s)\Big\rangle = \int_{t_0}^{t} g(s)\big\langle dW(s)\big\rangle = 0} \tag{A.56}$$

From the definitions in (A.53)-(A.54) we then find

$$\big\langle I_s(t_1,t_0)I_s(t_2,t_0)\big\rangle = \Big\langle \int_{t_0}^{t_1} g(s_1)dW(s_1) \int_{t_0}^{t_2} g(s_2)dW(s_2) \Big\rangle =$$

$$\int_{t_0}^{t_1}\int_{t_0}^{t_2} g(s_1)g(s_2)\big\langle dW(s_1)dW(s_2)\big\rangle = \int_{t_0}^{t_1}\int_{t_0}^{t_2} g(s_1)g(s_2)\delta(s_1-s_2)ds_1ds_2 =$$

$$\int_{t_0}^{\min(t_1,t_2)} g^2(s)ds$$

Using $\min(t_1,t_2) = (t_1+t_2-|t_1-t_2|)/2$, we can therefore write

$$\boxed{\big\langle I_s(t_1,t_0)I_s(t_2,t_0)\big\rangle = \int_{t_0}^{(t_1+t_2-|t_1-t_2|)/2} g^2(s)ds} \qquad (A.57)$$

Furthermore, letting $t_1 = t_2 = t$, we get

$$\boxed{\big\langle I_s(t,t_0)^2\big\rangle = \int_{t_0}^{t} g^2(s)dt} \qquad (A.58)$$

A.3 The Fokker-Planck Equation

In the previous section we saw how it was possible, using stochastic integration, to derive the time-varying mean and power of the process $x(t)$ defined through the SDE

$$\frac{dx}{dt} = h(x,t) + g(x,t)i_n(t) \qquad (A.59)$$

The stochastic variable $x(t)$ is described through the time varying probability density $p(y,t) = \big\langle \delta(x(t)-y)\big\rangle$. Using that $x(t)$ is a Markov process we can define the conditional probability density $P(y,t+\tau|y',t)$ through

$$p(y,t+\tau) = \int P(y,t+\tau|y',t)p(y',t)dy' \qquad (A.60)$$

By writing the function $P(y,t+\tau|y',t)$ in terms of its characteristic function [10] and using the identity

$$\frac{1}{2\pi}\int_{-\infty}^{\infty} (ju)^n \exp(-ju(y-y'))du = \left(-\frac{\partial}{\partial y}\right)^n \delta(y-y') \qquad (A.61)$$

[10] the characteristic function $C_\xi(u)$ of a stochastic variable ξ is defined as the Fourier transform of the probability function $p(x,t) = \delta(\xi(t)-x) : C_\xi(u) = \int_{-\infty}^{\infty} p(x,t)\exp(jxu)dx = \big\langle \exp(j\xi u)\big\rangle$. This function can also be written as [39] $C_\xi(u) = 1 + \sum_{n=1}^{\infty}(iu)^n M_n/n!$, where $M_n = \big\langle \xi^n \big\rangle$.

one can easily derive [39]

$$P(y,t+\tau|y',t) = \left[1 + \sum_{n=1}^{\infty} \frac{1}{!n}\left(-\frac{\partial}{\partial y}\right)^n M_n(y,t,\tau)\right]\delta(y-y') \tag{A.62}$$

where M_n the n'th moment of the conditional density

$$M_n(y,t,\tau) = \left\langle (y(t+\tau) - y(t))^n \right\rangle\Big|_{y(t)=y'} \tag{A.63}$$

Inserting (A.62) into (A.60), using the definition

$$p(y,t+\tau) - p(y,t) = \frac{\partial p}{\partial t}\tau + O(\tau^2) \tag{A.64}$$

and taking the limit $\tau \to 0$ we derive the *Fokker-Planck equation*

$$\frac{\partial p}{\partial t} = \left[\frac{\partial}{\partial y}D^{(1)}(y,t) + \frac{1}{2}\frac{\partial^2}{\partial y^2}D^{(2)}(y,t)\right]p(y,t) \tag{A.65}$$

where we have defined

$$D^{(n)}(y,t) = \lim_{\tau\to 0}\frac{1}{\tau}\left\langle (y(t+\tau) - y(t))^n \right\rangle\Big|_{y(t)=y'} \tag{A.66}$$

which are zero for $n > 2$ with the noise source in (A.59) [39].

Using the Stratonovich interpretation [39] of the stochastic integral in (A.45), we can derive the following drift and diffusion coefficients

$$\boxed{\begin{aligned} D^{(1)}(y,t) &= h(y,t) + g(y,t)\frac{\partial}{\partial y}g(y,t) \quad \text{(A.67)} \\ D^{(2)}(y,t) &= g^2(y,t) \quad \text{(A.68)} \end{aligned}}$$

The second term in (A.67) represents *noise induced drift*, which is an effect connected with multiplicative noise sources that is not seen with pure additive noise. This is easily seen, since for pure additive noise g, in (A.67)-(A.68), would be independent of y.

Appendix B

Deriving the Averaged Stochastic Differential Equations for a General Class of Second Order Oscillators

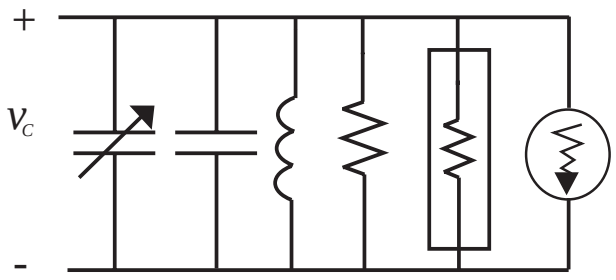

Figure B.1: LC oscillator with nonlinear varactor.

Figure B.1 shows a prototype LC oscillator including a nonlinear tuning varactor. A KCL at the only node of the circuit gives the following equation

$$C(v)\dot{v} + \left(\frac{1}{R} - G(v)\right)v + \frac{1}{L}\int v dt = i_n \tag{B.1}$$

where the meaning of the different symbols should be evident from inspecting the figure. Both the nonlinear reactance and conductance are modelled using a third order characteristic

$$G(v_C) = g_0 + g_1 v_C + g_2 v_C^2 \tag{B.2}$$

$$C(v_C) = c_0 + c_1 v_C + c_2 v_C^2 \tag{B.3}$$

If the quality factor of the resonator in figure B.1 is sufficiently high we can assume that the steady-state solution is almost sinusoidal or *quasi sinusoidal*. Such circuits are amenable to the procedure of averaging as explained in note 1.2 on page 30. In this appendix we shall derive the averaged stochastic differential equations governing the dynamics of the noise forced circuit in figure B.1. Averaging methods applied to noise forced electrical oscillators was pioneered by Kurokawa [32], and we shall therefore often refer to it as *Kurokawa's theory* or simply *Kurokawa theory*.

B.1 A van der Pol Oscillator with a Varactor

The capacitor voltage in figure B.1 can be written as a Fourier series

$$v_C = A(t)\cos(\omega_1 t + \phi(t)) + hh. \tag{B.4}$$

where *hh.* refers to higher harmonics, which must be negligible, referring to the original quasi-sinusoidal assumption. In (B.4), ω_1 is the steady-state fundamental frequency which may be different from the DC resonator *natural frequency* ω_0

$$\omega_0 = \frac{1}{\sqrt{c_0 L}} \tag{B.5}$$

with c_0 being the DC capacitance from (B.3). The derivative of the expression in (B.4) is easily found to be

$$\dot{v}_C = \dot{A}\cos(\omega_1 t + \phi) - A(\omega_1 + \dot{\phi}_1)\sin(\omega_1 t + \phi) + hh. \tag{B.6}$$

Comparing this expression with the result of differentiating a sinusoid with constant amplitude and phase, we see that we have defined the new frequency

$$\boxed{\omega_1 \to \omega_1 - j\frac{\dot{A}}{A} + \dot{\phi}_1} \tag{B.7}$$

which is known as *Kurokawa's substitution*. Using integration by parts on (B.4), we find

$$\begin{aligned}\int v_C(t')dt' = \frac{A}{\omega_1 + \dot{\phi}_1}\sin(\omega_1 t + \phi) - \int \dot{A}_1 \sin(\omega_1 t + \phi)dt + hh. = \\ \frac{A}{\omega_1 + \dot{\phi}_1} + \frac{\dot{A}_1}{\omega_1^2}\cos(\omega_1 t + \phi) - \int \ddot{A}_1 \cos(\omega_1 t + \phi)dt + hh.\end{aligned} \tag{B.8}$$

where the last integral can be set to zero since $\ddot{A}_1 \ll 1$. Furthermore, since $|\dot{\phi}_1| \ll 1$ we have

$$\frac{A}{\omega_1 + \dot{\phi}_1} \approx \frac{A}{\omega_1} - \frac{A}{\omega_1^2}\dot{\phi}_1 \tag{B.9}$$

Using the above derivations we can write (B.8) as

$$\int v_C(t')dt' = \left(\frac{A}{\omega_1} - \frac{A}{\omega_1^2}\dot{\phi}_1\right)\sin(\omega_1 t + \phi) + \frac{\dot{A}_1}{\omega_1^2}\cos(\omega_1 t + \phi) \tag{B.10}$$

Inserting the two expressions (B.6) and (B.10) into (B.1), multiplying with $\sin(\omega_1 + \phi)$, and averaging over one cycle, we get

$$\begin{aligned}-\overline{C}_s(\omega_1 + \dot{\phi}_1 A) - \overline{G}_s + \left(\frac{1}{L\omega_1} - \frac{1}{L\omega_1^2}\dot{\phi}_1 A\right) = i_{ns}(t) \Leftrightarrow \\ \left(\frac{1}{L\omega_1} - \overline{C}_s\omega_1 - \overline{G}_s\right) - \left(\overline{C}_s + \frac{1}{L\omega_1^2}\right)\dot{\phi}_1 A = i_{ns}(t)\end{aligned} \tag{B.11}$$

Similarly, multiplying the same expression with $\cos(\omega_1 + \phi)$ and averaging over one cycle, we get

$$\begin{aligned}\overline{C}_c\dot{A}_1 + \left(\frac{1}{R} - \overline{G}_c\right)A + \frac{1}{L}\frac{\dot{A}_1}{\omega_1^2} = i_{nc}(t) \Leftrightarrow \\ \left(\overline{C}_c + \frac{1}{L\omega_1^2}\right)\dot{A}_1 + \left(\frac{1}{R} - \overline{G}_c\right)A = i_{nc}(t)\end{aligned} \tag{B.12}$$

where ($T_1 = 2\pi/\omega_1$)

$$i_{nc}(t) = \frac{2}{T_1}\int_{t-T_1}^{t} i_n(t')\cos(\omega_1 t + \phi)dt' \tag{B.13}$$

$$i_{ns}(t) = \frac{2}{T_1}\int_{t-T_1}^{t} i_n(t')\sin(\omega_1 t + \phi)dt' \tag{B.14}$$

represent slow moving orthogonal envelopes of the averaged white-noise current source i_n. The statistics of these two processes are discussed in detail in appendix A.1. In (B.11) and (B.12) we have further defined the averaged capacitance and conductance parameters

$$\overline{C}_s = \frac{2}{T_1}\int_{t-T_1}^{t} C(v_C)\sin^2(\omega_1 t + \phi)dt' \tag{B.15}$$

$$\overline{C}_c = \frac{2}{T_1}\int_{t-T_1}^{t} C(v_C)\cos^2(\omega_1 t + \phi)dt' \tag{B.16}$$

$$\overline{G}_c = \frac{2}{T_1}\int_{t-T_1}^{t} G(v_C)\cos^2(\omega_1 t + \phi)dt' \tag{B.17}$$

$$\overline{G}_s = \frac{2}{T_1}\int_{t-T_1}^{t} G(v_C)\cos(\omega_1 t + \phi)\sin(\omega_1 t + \phi)dt' \tag{B.18}$$

Inserting (B.4) into (B.2)-(B.3), using standard trigonometric calculations, we find

$$G(v)\cos(\omega_1 t + \phi) = dc. + g_0\cos(\omega_1 t + \phi) + \frac{3}{4}g_2 A^2\cos(\omega_1 t + \phi) + hh. \tag{B.19}$$

$$C(v)\cos(\omega_1 t + \phi) = dc. + c_0\cos(\omega_1 t + \phi) + \frac{3}{4}c_2 A^2\cos(\omega_1 t + \phi) + hh. \tag{B.20}$$

$$C(v)\sin(\omega_1 t + \phi) = dc. + c_0\sin(\omega_1 t + \phi) + \frac{1}{4}c_2 A^2\sin(\omega_1 t + \phi) + hh. \tag{B.21}$$

where *dc.* refers to constant/time-independent terms. Inserting (B.19)-(B.21) into (B.15)-(B.18) gives the result

$$\overline{C}_s = c_0 + \frac{1}{4}c_2 A^2 \tag{B.22}$$

$$\overline{C}_c = c_0 + \frac{3}{4}c_2 A^2 \tag{B.23}$$

$$\overline{G}_c = g_0 + \frac{3}{4}g_2 A^2 \tag{B.24}$$

$$\overline{G}_s = 0 \tag{B.25}$$

Using these expressions we can write (B.11) and (B.12) as

$$\left(\frac{1}{L\omega_1} - c_0\omega_1 - \frac{\omega_1}{4}c_2A^2\right) - \left\{c_0 + \frac{1}{4}c_2A^2 + \frac{1}{L\omega_1^2}\right\}\dot{\phi} = \frac{1}{A}i_{ns}(t) \tag{B.26}$$

$$\left\{c_0 + \frac{3}{4}c_2A^2 + \frac{1}{L\omega_1^2}\right\}\dot{A} + \left(G - g_0 - \frac{3}{4}g_2A^2\right)A = i_{nc}(t) \tag{B.27}$$

In the above expressions curly brackets (*i.e.* {}) signify that the expression inside these brackets are multiplied by an amplitude/phase derivative. This derivative is small, $|\dot{\phi}|, |\dot{A}| \ll 1$, which follows from the assumption of quasi-sinusoidal operation. We can write the amplitude as a steady-state $\hat{A}$ plus a small noise/signal transient δA. The nonlinear terms inside these brackets, which stem from the capacitance expression in (B.22)-(B.23), can then also be written as such a sum (*i.e.* $C = \widehat{C} + \delta C$). However, terms of order $(\delta A, \delta\phi) \times \delta C$ are very small and will therefore be ignored. We can therefore substitute $\hat{A}$ for A inside the curly brackets in (B.26)-(B.27). From (B.3), and using (B.4), we now write the *steady-state* average resonator capacitance $\overline{C}$, as

$$\overline{C} = \int_{t-T_1}^{t} C(v_C(t'))dt' = c_0 + \frac{1}{2}c_2\hat{A}^2 \tag{B.28}$$

where we have used $\hat{A}$ since we consider the transient-free steady-state. In the steady-state, the inductive and capacitive energy must balance, which translates into the expression

$$\omega_1\overline{C} = \frac{1}{L\omega_1} \tag{B.29}$$

Using (B.28) and (B.29), and referring to the above discussion, we can write curly brackets in (B.26)-(B.27), as

$$c_0 + \frac{1}{4}c_2\hat{A}^2 + \frac{1}{L\omega_1^2} = \overline{C} - \frac{1}{4}c_2\hat{A}^2 + \overline{C} = 2\overline{C} - \frac{1}{2}(\overline{C} - c_0) = \frac{3}{2}\overline{C} - \frac{1}{2}c_0 = c_+ \tag{B.30}$$

$$c_0 + \frac{3}{4}c_2\hat{A}^2 + \frac{1}{L\omega_1^2} = \overline{C} + \frac{1}{4}c_2\hat{A}^2 + \overline{C} = 2\overline{C} + \frac{1}{2}(\overline{C} - c_0) = \frac{5}{2}\overline{C} - \frac{1}{2}c_0 = c_- \tag{B.31}$$

Furthermore, using (B.29), we can rewrite the first bracket of (B.26) as

$$\frac{1}{L\omega_1} - c_0\omega_1 - \frac{\omega_1}{4}c_2A^2 = \frac{\omega_1}{4}c_2A^2 \tag{B.32}$$

Inserting (B.30)-(B.32) into (B.26)-(B.27), we get

$$\frac{\omega_1}{4}c_2A^2 - c_+\dot{\phi}_1 = \frac{1}{A}i_{ns}(t) \tag{B.33}$$

$$c_-\dot{A}_1 + \left(G - g_0 - \frac{3}{4}g_2A^2\right)A = i_{nc}(t) \tag{B.34}$$

Then using the following re-normalization of the time

$$\tau = \frac{\omega_0}{2Q} = \frac{1}{2R\overline{C}} \tag{B.35}$$

we reach the final form of the amplitude/phase equations

$$\boxed{\begin{aligned} \frac{1}{\hat{A}}\frac{dA}{d\tau} &= s\left[1-\left(\frac{A}{\alpha}\right)^2\right]\frac{A}{\hat{A}} + \Upsilon_1 G_n(t) \quad \text{(B.36)} \\ \frac{d\phi}{d\tau} &= rA^2 + \Upsilon_2 B_n(t) \quad \text{(B.37)} \end{aligned}}$$

where

$$s = \Upsilon_1 \mu_o \tag{B.38}$$

$$r = \Upsilon_2 \frac{\omega_1 c_2}{4G} \tag{B.39}$$

$$\Upsilon_1 = \frac{2\overline{C}}{c_-} \tag{B.40}$$

$$\Upsilon_2 = \frac{2\overline{C}}{c_+} \tag{B.41}$$

$$\mu_o = \frac{g_0 - G}{G} \tag{B.42}$$

$$\alpha = \sqrt{\frac{4}{3}\frac{(g_0 - G)}{g_2}} \tag{B.43}$$

We have also used the concept of a *noise admittance* $Y_n = G_n + jB_n$

$$G_n(t) = \frac{i_{nc}(t)}{\hat{A}G} \tag{B.44}$$

$$B_n(t) = \frac{i_{ns}(t)}{\hat{A}G} \tag{B.45}$$

which was discussed in appendix A.1.1.

B.1.1 A Phasor Approach

The aim of this section is to illustrate that there exist a shortcut to the derivation of the averaged amplitude/phase equations in (B.36)-(B.37). The method relies on the introduction of phasor notation and we hence write (B.4) as

$$v_C = \Re\{A\exp(j[\omega_1 t + \phi])\} = \Re\{A\exp(j\Phi)\} \tag{B.46}$$

where we from the start ignore the higher harmonics since they will not play a role in the final result. The next step consists of writing the resonator characteristic as a single pole approximation

$$Y(\omega) = G + j\omega C(v_C) - j\frac{L}{\omega} \approx G + j\omega_1 C(v_C) - j\frac{L}{\omega_1} + j\left(C(v_C) + \frac{L}{\omega_1^2}\right)(\omega - \omega_1) \tag{B.47}$$

Using Kurokawa's substitution in (B.7) we can write a KCL for the circuit in figure B.1 as

$$Y(\omega)v_C = G(v_C)v_C + i_n(t) \Leftrightarrow$$
$$\left\{G + j\omega_1 C(v_C) - j\frac{L}{\omega_1} + j\left(C(v_C) + \frac{L}{\omega_1^2}\right)\left[-j\frac{\dot{A}}{A} + \dot{\phi}\right]\right\}A\exp(j\Phi) = \tag{B.48}$$
$$G(v_C)A\exp(j\Phi) + i_n(t)$$

Taking the real part on both sides of this equation, multiplying the with $\cos(\Phi)$ and $\sin(\Phi)$, respectively, and averaging the result over one period $T_1 = \omega_1/2\pi$, we get

$$GA + \left(\overline{C}_c + \frac{L}{\omega_1^2}\right)\dot{A} = G_c A + i_{nc}(t) \tag{B.49}$$

$$-\omega_1\overline{C}_s + \frac{L}{\omega_1} - \left(\overline{C}_s + \frac{L}{\omega_1^2}\right)\dot{\phi} = i_{ns}(t) \tag{B.50}$$

Since (B.49) and (B.50) are identical to (B.12) and (B.11), respectively, we again reach the result in (B.36)-(B.37).

Although the phasor method and the *Kurokawa method* basically represent the same averaging procedure, it should be evident from the above derivations that the phasor method demands much less algebra to reach the same result. We shall therefore use it throughout this report. We conclude this section with a 7 step "recipe" for the derivation of the amplitude/phase equations of the noise perturbed LC oscillator shown in figure B.1

1. write the state equations for the oscillator using phasor notation.
2. derive the single pole approximation of the oscillator resonator characteristic.
3. insert Kurokawa's substitution (B.7).
4. take the real part on both sides of the equation.
5. separate orthogonal components by multiplying each side by $\cos(\omega_1 t + \phi)$ and $\sin(\omega_1 t + \phi)$, respectively.
6. remove all the higher harmonics in the resulting equations by averaging over one period.
7. include the narrow band noise processes i_{nc} and i_{ns}.

Appendix C

Various Derivations

This appendix contains the various calculations which were too long to be included in the main text.

C.1 Section 1.1.1 : Normal-Form Calculations

We consider the arbitrary nonlinear system

$$\dot{z} = Jz + F_2(z) + F_3(z) + \cdots F_{r-1}(z) + O(|z|^r) \tag{C.1}$$

The *close to unity* change of coordinates

$$z = w + h_k(w) \tag{C.2}$$

with $w \in \mathbb{C}$, $h_k : \mathbb{C} \to \mathbb{H}_k$ and $k < r$, is then introduced. The left-hand side of (C.1) transforms to

$$\dot{z} = \dot{w} + Dh_k(w)\dot{w} = \big(I + Dh_k(w)\big)\dot{w} \tag{C.3}$$

where $Dh_k(w)$ is the Jacobian of the map h_k. Since $Dh_k(w)$ is a matrix containing $k-1$ order monomials, we can write

$$\big(I + Dh_k(w)\big)^{-1} = I - Dh_k(w) + O(|w|^k) \tag{C.4}$$

Multiplying both sides of (C.1) with $\big(I + Dh_k(w)\big)^{-1}$, using (C.2), (C.3) and the above identity, we get

$$\dot{w} = \big(I - Dh_k(w) + O(|w|^k)\big)\big\{J(w+h_k(w)) + F_2(w+h_k(w)) + \cdots + F_{r-1}(w+h_k(w)) + O(|w|^r)\big\} \tag{C.5}$$

The nonlinear terms are transformed as

$$F_j(w + h_k(w)) = F_j(w) + O(|w|^{j+k}) \tag{C.6}$$

which means that we have

$$\big[I - Dh_k(w) + O(|w|^k)\big]F_j(w + h_k(w)) = F_j(w) + O(|w|^{j+k-1}) \tag{C.7}$$

with $j + k - 1 \geq k + 1$. We therefore have the following result of applying the transformation in (C.2) to the system in (C.1)

$$\dot{w} = Jw + F_2(w) + \cdots + \Big\{ F_k - Dh_k(w)Jw + Jh_k(w) \Big\} + \tilde{F}_{k+1}(w) + \cdots + \tilde{F}_{r-1}(w) + O(|w|^r) \tag{C.8}$$

In the above equation, $\tilde{F}$ signifies that terms of order larger than k are changed, in some unspecified way, by the transformation (C.2). The specifics are not important, unless one aims to carry-out the actual calculations; but what is very important is that the transformation preserves the lower order terms $F_i \quad i = 2, 3, \cdots, k-1$. In (C.8) we have collected terms of order k inside a *curly bracket*. From this, we see that if we could choose h_k in (C.2) so that

$$F_k(w) = Dh_k(w)Jw - Jh_k(w) \tag{C.9}$$

then we could completely remove F_k. Since the transformation leaves the lower order terms unchanged we can systematically treat each function F_k without destroying the earlier obtained results.

We now define the *Lie bracket*

$$L_J^{(k)}(h_k) = [h_k(z), Jz] = -\big(Dh_k(z)Jz - Jh_k(z)\big) \tag{C.10}$$

Using the operator in (C.10) we will be able to remove some of the nonlinear k'th order terms in (C.1) while we will be forced to leave others. The vector space $\mathbb{H}_k$ can be written

$$\mathbb{H}_k = \mathrm{Im}L_J^{(k)} \oplus \mathbb{M} \tag{C.11}$$

where $\mathrm{Im}L_J^{(k)}$ denotes the *range/image* of $L_J^{(k)}$ and $\mathbb{M}$ is it's *complement space*. The range contains the section of vector space that can be *reached* by the operator, which in our case means that monomials contained in $\mathrm{Im}L_J^{(k)}$ can be removed by the transformation (C.2). Those monomials which are not contained in $\mathrm{Im}L_J^{(k)}$ are by definition contained in $\mathbb{M}$ and these terms can <u>never</u> be removed by (C.2). In [21] it is shown that $\mathbb{M} \equiv \mathrm{Ker}L_{J^*}^{(k)}$, where Ker refers to the *kernel* of (C.10) and J^* is the *Hermitian* [1] of the Jacobian. We can then write (C.11) as

$$\mathbb{H}_k = \mathrm{Im}L_J^{(k)} \oplus \mathrm{Ker}L_{J^*}^{(k)} \tag{C.12}$$

From the above discussion it is seen that all k'th order nonlinear terms in the normal form are forced to lie in the vector space $\mathrm{Ker}L_{J^*}^{(k)}$. As shown in [21], we have

$$e^{L_{J^*}^{(k)} s} h_k(z) = e^{-J^* s} h_k\big(e^{J^* s} z\big) \tag{C.13}$$

where $s \in \mathbb{R}$ is introduced as a *parameter* of the group, generated by J^*. Now if $h_k(z) \in \mathrm{Ker}L_{J^*}^{(k)}$ then we must have

$$e^{L_{J^*}^{(k)} s} h_k(z) = \big\{ I + L_{J^*}^{(k)} s + \frac{1}{2}\big(L_{J^*}^{(k)} s\big)^2 + \cdots \big\} h_k(z) = h_k(z) \tag{C.14}$$

and so, using (C.13), we get the following definition of $\mathrm{Ker}L_{J^*}^{(k)}$

$$KerL_{J^*}^{(k)} = \{ h_k(z) \in \mathbb{H}_k | e^{-J^* s} h_k\big(e^{J^* s} z\big) = h_k(z) \} \tag{C.15}$$

Equation (C.15) says, that if $h_k \in \mathrm{Ker}L_{J^*}^{(k)}$, then h_k is *equivariant* with regard to the actions contained in the one-parameter group $e^{J^* s}$.

[1] the Hermitian of a matrix is derived by transposing the matrix followed by complex conjugation.

C.2 Calculating the Eigenvalues of the Matrix J_{11} on page 98

We need to find the eigenvalues of the matrix

$$J_{11} = \begin{bmatrix} -\mu_a & 0 & 0 & 0 & \cdots & \zeta(1-2\mu_c)\cos(\Delta\hat{\phi}) \\ \zeta(1-2\mu_c)\cos(\Delta\hat{\phi}) & -\mu_a & 0 & 0 & \cdots & 0 \\ 0 & \zeta(1-2\mu_c)\cos(\Delta\hat{\phi}) & -\mu_a & 0 & \cdots & 0 \\ 0 & 0 & \ddots & \ddots & \cdots & 0 \\ \vdots & \vdots & 0 & \ddots & \ddots & \vdots \\ \vdots & \vdots & \vdots & \vdots & \ddots & \vdots \\ 0 & 0 & 0 & \cdots & \zeta(1-2\mu_c)\cos(\Delta\hat{\phi}) & -\mu_a \end{bmatrix} \tag{C.16}$$

Using the substitutions

$$\alpha_1 = -\mu_a \tag{C.17}$$

$$\alpha_2 = \zeta(1-2\mu_c)\cos(\Delta\hat{\phi}) \tag{C.18}$$

we instead consider the general $n \times n$ matrix M

$$M = \begin{bmatrix} \alpha_1 & 0 & 0 & 0 & \cdots & \alpha_2 \\ \alpha_2 & \alpha_1 & 0 & 0 & \cdots & 0 \\ 0 & \alpha_2 & \alpha_1 & 0 & \cdots & 0 \\ 0 & 0 & \ddots & \ddots & \cdots & 0 \\ \vdots & \vdots & \vdots & \ddots & \ddots & \vdots \\ 0 & 0 & 0 & \cdots & \alpha_2 & \alpha_1 \end{bmatrix} \tag{C.19}$$

The characteristic polynomial $C_M(\lambda)$ can be written

$$C_M(\lambda) = (\alpha_1 - \lambda) \times \det(M_1) - \alpha_2 \times \det(M_2) \tag{C.20}$$

where the two $n-1 \times n-1$ matrices M_1 and M_2 are given as

$$M_1 = \begin{bmatrix} \alpha_1 - \lambda & 0 & 0 & \cdots & 0 \\ \alpha_2 & \alpha_1 - \lambda & 0 & \cdots & 0 \\ 0 & \ddots & \ddots & \cdots & 0 \\ \vdots & \vdots & \ddots & \ddots & \vdots \\ 0 & 0 & \cdots & \alpha_2 & \alpha_1 - \lambda \end{bmatrix} \tag{C.21}$$

and

$$M_2 = \begin{bmatrix} 0 & 0 & 0 & \cdots & \alpha_2 \\ \alpha_2 & \alpha_1 - \lambda & 0 & \cdots & 0 \\ 0 & \ddots & \ddots & \cdots & 0 \\ \vdots & \vdots & \ddots & \ddots & \vdots \\ 0 & 0 & \cdots & \alpha_2 & \alpha_1 - \lambda \end{bmatrix} \tag{C.22}$$

It is easily found that

$$\det(M_1) = (\alpha_1 - \lambda)^{n-1} \tag{C.23}$$

Furthermore, one can derive the result

$$\det(M_2) = \begin{cases} \alpha_2^{n-1} & \text{for } n \text{ even} \\ -\alpha_2^{n-1} & \text{for } n \text{ uneven} \end{cases} \tag{C.24}$$

We therefore get

$$C_M(\lambda) = \begin{cases} (\alpha_1 - \lambda)^n - \alpha_2^n & \text{for } n \text{ even} \\ (\alpha_1 - \lambda)^n + \alpha_2^n & \text{for } n \text{ uneven} \end{cases} \tag{C.25}$$

The eigenvalues are found by setting $C_M(\lambda) = 0$ and we find

$$\lambda_i = \begin{cases} \alpha_1 - \exp(ji2\pi/n)\alpha_2 & \text{for } n \text{ even} \\ \alpha_1 - \exp(ji\pi/n)\alpha_2 & \text{for } n \text{ uneven} \end{cases} \tag{C.26}$$

Using the substitutions in (C.17)-(C.18) we get the final result

$$\lambda_i = \begin{cases} -\mu_a - \zeta(1-2\mu_c)\cos(\Delta\hat{\phi})\big\{\cos(i2\pi/n) + j\sin(i2\pi/n)\big\} & \text{for } n \text{ even} \\ -\mu_a - \zeta(1-2\mu_c)\cos(\Delta\hat{\phi})\big\{\cos(i\pi/n) + j\sin(i\pi/n)\big\} & \text{for } n \text{ uneven} \end{cases} \tag{C.27}$$

C.3 Calculating the Eigenvalues of the Matrix J_{22} on page 99

We need to find the eigenvalues of the $n-1 \times n-1$ matrix

$$J_{22} = \begin{bmatrix} -\zeta\cos(\Delta\hat{\phi}) - \zeta\cos(\Delta\hat{\phi}) & -\zeta\cos(\Delta\hat{\phi}) & -\zeta\cos(\Delta\hat{\phi}) & -\zeta\cos(\Delta\hat{\phi}) & -\zeta\cos(\Delta\hat{\phi}) \\ \zeta\cos(\Delta\hat{\phi}) & -\zeta\cos(\Delta\hat{\phi}) & 0 & 0 & 0 \\ 0 & \zeta\cos(\Delta\hat{\phi}) & -\zeta\cos(\Delta\hat{\phi}) & 0 & 0 \\ 0 & 0 & \zeta\cos(\Delta\hat{\phi}) & -\zeta\cos(\Delta\hat{\phi}) & 0 \\ \vdots & \vdots & 0 & 0 & 0 \\ \vdots & \vdots & \vdots & \vdots & \vdots \\ 0 & 0 & \cdots & \zeta\cos(\Delta\hat{\phi}) & -\zeta\cos(\Delta\hat{\phi}) \end{bmatrix} \tag{C.28}$$

In the following we make the substitution $n-1 \to n$ in order to ease the notation. Taking the factor $\zeta\cos(\Delta\hat{\phi})$ outside, we instead consider the $n \times n$ matrix M

$$M = \begin{bmatrix} -2 & -1 & -1 & -1 & -1 \\ 1 & -1 & 0 & 0 & 0 \\ 0 & 1 & -1 & 0 & 0 \\ \vdots & \vdots & \ddots & \ddots & \vdots \\ 0 & 0 & \cdots & 1 & -1 \end{bmatrix} \tag{C.29}$$

where the eigenvalues of J_{22} is found as the eigenvalues of M times a factor $\zeta\cos(\Delta\hat{\phi})$. The $n-1 \times n-1$ matrix N is derived from M by removing the first row and column

$$N_{n-1} = \begin{bmatrix} -1 & 0 & 0 & 0 \\ 1 & -1 & 0 & 0 \\ \vdots & \ddots & \ddots & \vdots \\ 0 & 0 & 1 & -1 \end{bmatrix} \tag{C.30}$$

The characteristic polynomial $C^N_{n-1}(\lambda) = \det(N_{n-1} - I\lambda)$ is easily found to be

$$C^N_{n-1}(\lambda) = (-1-\lambda)^{n-1} \tag{C.31}$$

From (C.29) it is then seen that the characteristic polynomial $C^M(\lambda) = det(M - I\lambda)$ can be written as

$$C^M(\lambda) = (-2-\lambda) \times C^N_{n-1}(\lambda) - P_{n-1}(\lambda) \tag{C.32}$$

where the polynomial $P_{n-1}(\lambda)$ derived from the sub-determinant

$$P_{n-1}(\lambda) = \begin{vmatrix} -1 & -1 & -1 & -1 & -1 \\ 1 & -1-\lambda & 0 & 0 & 0 \\ 0 & 1 & -1-\lambda & 0 & 0 \\ 0 & \vdots & \ddots & \ddots & \vdots \\ 0 & 0 & \cdots & 1 & -1-\lambda \end{vmatrix} \tag{C.33}$$

From this definition we see that $P_{n-1}(\lambda) = -C^N_{n-2}(\lambda) - P_{n-2}(\lambda)$. This means that we can write

$$C^M(\lambda) = (-2-\lambda)(-1-\lambda)^{n-1} - \sum_{i=n-2}^{0} (-1)^{(n-2)-i+1}(-1-\lambda)^i \tag{C.34}$$

where we have used the definition

$$P_2(\lambda) = \begin{vmatrix} -1 & -1 \\ 1 & -1-\lambda \end{vmatrix} = -(-1-\lambda) + 1 = -P_1(\lambda) + P_0(\lambda) \tag{C.35}$$

We now define

$$\rho = \lambda + 1 \Leftrightarrow \lambda = \rho - 1 \tag{C.36}$$

which, when inserted into (C.34), gives

$$C^M(\rho) = (-1-\rho)(-\rho)^{n-1} - \sum_{i=n-2}^{0} (-1)^{(n-2)-i+1}(-\rho)^i = \\ (-1-\rho)(-\rho)^{n-1} - (-1)^1(-\rho)^{n-2} - (-1)^2(-\rho)^{n-3} - \cdots - (-1)^{n-2}(-\rho) - (-1)^{n-1} \tag{C.37}$$

If n is even we get

$$C^M(\rho) = -(-1-\rho)\rho^{n-1} + \rho^{n-2} + \rho^{n-3} + \cdots + \rho + 1 = \rho^n + \rho^{n-1} + \rho^{n-2} + \rho^{n-3} + \cdots + \rho + 1 \tag{C.38}$$

If n is uneven we get

$$C^M(\rho) = (-1-\rho)\rho^{n-1} - \rho^{n-2} - \rho^{n-3} - \cdots - \rho - 1 = -(\rho^n + \rho^{n-1} + \rho^{n-2} + \rho^{n-3} + \cdots + \rho + 1) \tag{C.39}$$

The eigenvalues of the matrix M in (C.29) are found as solutions to the equation $C^M(\rho) = 0$ and we therefore have to find the roots of the polynomial

$$\rho^n + \rho^{n-1} + \rho^{n-2} + \rho^{n-3} + \cdots + \rho + 1 = 0 \tag{C.40}$$

The roots of this polynomial are given as

$$\rho_i = \begin{cases} \cos\left(\frac{i\pi}{n+1}\right) + j\sin\left(\frac{i\pi}{n+1}\right) & i = \{1, 2 \cdots n\} \quad \text{for n even} \\ \cos\left(\frac{2i\pi}{n+1}\right) + j\sin\left(\frac{2i\pi}{n+1}\right) & i = \{1, 2 \cdots n\} \quad \text{for n uneven} \end{cases} \tag{C.41}$$

Using (C.36) and making the substitution $n \to n-1$, while remembering the factor $\zeta\cos(\Delta\hat{\phi})$, we get the following eigenvalues λ for the matrix J_{22} in (C.28)

$$\lambda_i = \begin{cases} \zeta\cos(\Delta\hat{\phi})\left\{\cos\left(\frac{i\pi}{n}\right) - 1 + j\sin\left(\frac{i\pi}{n}\right)\right\} & i = \{1, 2 \cdots n-1\} \quad \text{for n even} \\ \zeta\cos(\Delta\hat{\phi})\left\{\cos\left(\frac{2i\pi}{n}\right) - 1 + j\sin\left(\frac{2i\pi}{n}\right)\right\} & i = \{1, 2 \cdots n-1\} \quad \text{for n uneven} \end{cases} \tag{C.42}$$

These eigenvalues have real-parts less than zero as long as $|\Delta\hat{\phi}| < \pi/2$.

C.4 Calculations Used in the Proof of Theorem 3.3 on page 68

The Jacobian of the averaged system, which was derived in (3.40) in section 3.2.1, is repeated here

$$J = \begin{bmatrix} \alpha_1 & 0 & 0 & 0 \\ \rho_1 & 0 & 0 & 0 \\ \zeta & \gamma & \alpha_2 & -\gamma \\ -\gamma & \zeta & \gamma + \rho_2 & -\zeta \end{bmatrix} \tag{C.43}$$

where $\alpha_{(1,2)} = -2\mu_{o,(m,s)}$, $\rho_{1,2} = 2b_{m,s}\hat{A}^2$

$$\gamma = -N\kappa\sin(N\Delta\hat{\phi}) \tag{C.44}$$

$$\zeta = N\kappa\cos(N\Delta\hat{\phi}) \tag{C.45}$$

We refer to the discussion in section 3.2.1, on page 64, for an explanation of the different parameters in (C.43). Using MAPLE™ we find the following eigenvalues and eigenvectors of the matrix in (C.43)

$$\mu = \begin{bmatrix} 0 \\ \alpha_1 \\ \delta_+ \\ \delta_- \end{bmatrix} \quad ; \quad U = \begin{bmatrix} 0 & \pi_1 & 0 & 0 \\ 1 & \pi_2 & 0 & 0 \\ 0 & \pi_3 & \pi_4 & \pi_5 \\ 1 & 1 & 1 & 1 \end{bmatrix} \tag{C.46}$$

where

$$\delta_\pm = -\frac{1}{2}\zeta + \frac{1}{2}\alpha_2 \pm \frac{1}{2}\sqrt{(\alpha_2 + \zeta)^2 - 4\gamma(\rho + \gamma)} \tag{C.47}$$

If we assume that we have weak coupling, then we must have

$$(\alpha_2+\zeta)^2 \gg 4\gamma(\rho_2+\gamma) \quad \text{for all } \Delta\hat{\phi} \tag{C.48}$$

The above expression refers to the condition of *normally hyperbolicity* as it was stated in definition 3.2 in section 3.2.1. Using (C.48), we can then approximate

$$\frac{1}{2}\sqrt{(\alpha_2+\zeta)^2-4\gamma\rho_2-4\gamma^2} \approx \frac{\alpha_2+\zeta}{2} - \frac{\gamma(\rho_2+\gamma)}{\alpha_2+\zeta} \tag{C.49}$$

which means that the expressions in (C.46), (C.47) can be simplified as follows

$$\delta_+ \approx -\frac{\zeta}{2}+\frac{\alpha_2}{2}+\frac{\alpha_2+\zeta}{2}-\frac{\gamma(\rho_2+\gamma)}{\alpha_2+\zeta} = \alpha_2 - \frac{\gamma(\rho_2+\gamma)}{\alpha_2+\zeta} \tag{C.50}$$

$$\delta_- \approx -\frac{\zeta}{2}+\frac{\alpha_2}{2}-\frac{\alpha_2+\zeta}{2}-\frac{\gamma(\rho_2+\gamma)}{\alpha_2+\zeta} = -\zeta - \frac{\gamma(\rho_2+\gamma)}{\alpha_2+\zeta} \tag{C.51}$$

$$\pi_4 = \frac{\gamma}{-\delta_+ + \alpha_2} \approx \frac{\gamma}{\frac{\gamma(\rho_2+\gamma)}{\alpha_2+\zeta}} = \frac{\alpha_2+\zeta}{\rho_2+\gamma} \tag{C.52}$$

$$\pi_5 = \frac{\gamma}{-\delta_- + \alpha_2} \approx \frac{\gamma}{\alpha_2+\zeta} \tag{C.53}$$

$$\pi_1 = -\frac{\alpha_1[\alpha_1(\alpha_1-\alpha_2)+\zeta(\alpha_1-\alpha_2)+\gamma(\gamma+\rho_2)]}{-\alpha_1[\gamma\zeta+\zeta(\rho_2+\rho_1)+\gamma(\alpha_2-\alpha_1)]-\gamma^2\rho_1-\gamma\rho_2\rho_1+\zeta\rho_1\alpha_2} \approx -\frac{\alpha_1}{\gamma} \tag{C.54}$$

$$\pi_2 = \frac{\rho_1}{\alpha_1}\pi_1 \approx -\frac{\rho_1}{\gamma} \tag{C.55}$$

$$\pi_3 = -\frac{\alpha_1[\gamma\rho_1+\zeta\alpha_1+\zeta^2\gamma^2]}{-\alpha_1[\gamma\zeta+\zeta(\rho_2+\rho_1)+\gamma(\alpha_2-\alpha_1)]-\gamma^2\rho_1-\gamma\rho_2\rho_1+\zeta\rho_1\alpha_2} \approx -\frac{\alpha_1}{\alpha_2}\frac{\zeta}{\gamma} \tag{C.56}$$

In the above expressions we have set second order terms like γ^2 equal to zero which is within the bounds of the theory. Furthermore, it is seen that $\pi_1 \gg \pi_2, \pi_3$ and that $\pi_1, \pi_2, \pi_3 \gg 1$. In the following we assume that $\alpha_2 \gg \alpha_1$ which is the case if $Q_m/Q_s \gg 1$, where Q_m and Q_s are the M-OSC and S-OSC Q-factors, respectively. Inserting the above expression in (C.46), and remembering that the eigenvectors must be normalized, we find

$$\mu \approx \begin{bmatrix} 0 \\ \alpha_1 \\ \alpha_2 \\ -\zeta \end{bmatrix} \quad ; \quad U \approx \begin{bmatrix} 0 & 1 & 0 & 0 \\ 1 & \frac{\rho_1}{\alpha_1} & 0 & 0 \\ 0 & \epsilon_1 & 1 & \epsilon_4 \\ 1 & \epsilon_2 & \epsilon_3 & 1 \end{bmatrix} \tag{C.57}$$

where $\epsilon_1 = -\frac{\zeta}{\alpha_1}$, $\epsilon_2 = \frac{\gamma}{\alpha_1}$, $\epsilon_3 = \frac{\rho_2+\gamma}{\alpha_2}$ and $\epsilon_4 = \frac{\gamma}{\alpha_2}$. By inspecting (C.44)-(C.45) it is seen that all the epsilon parameters are on the order of the coupling and hence are small (*i.e.* $|\epsilon_i| \ll 1$).

Inspecting (C.57) we can hence conclude that

note C.1 *there exist two Floquet eigenvectors $u_1(t) = \phi_d(t)$ and $u_2(t) = \phi_s(t) + O(|\epsilon|)$ ($\epsilon = \gamma/\alpha_2$) spanning the tangent space of the perturbed invariant manifold. The second Floquet characteristic multiplier is given as $\mu_2 = N\kappa\cos(N\Delta\hat{\phi})$ and represents effective coupling strength.*

We now consider the transposed matrix

$$J^T = \begin{bmatrix} \alpha_1 & \rho_1 & \zeta & -\gamma \\ 0 & 0 & \gamma & \zeta \\ 0 & 0 & \alpha_2 & \gamma+\rho_2 \\ 0 & 0 & -\gamma & -\zeta \end{bmatrix} \tag{C.58}$$

Using MAPLE™ we find the following eigenvalue and eigenvectors

$$\mu = \begin{bmatrix} 0 \\ \alpha_1 \\ \alpha_2 \\ -\zeta \end{bmatrix} \quad ; \quad V = \begin{bmatrix} -\frac{\rho_1}{\alpha_1} & 1 & \theta_{1+} & \theta_{1-} \\ 1 & 0 & \theta_{2+} & \theta_{2-} \\ 0 & 0 & \theta_{3+} & \theta_{3-} \\ 0 & 0 & 1 & 1 \end{bmatrix} \tag{C.59}$$

The different parameters are given as

$$\theta_{1\pm} = -\frac{-\rho_2\rho_1\gamma - \gamma^2\rho_1 - \rho_1\zeta\delta_\pm + \zeta\rho_1\alpha_2 - \zeta\delta_\pm\gamma - \zeta\delta_\pm\rho_2 + \gamma\delta_\pm^2 - \gamma\delta_\pm\alpha_2}{(-\delta_\pm+\alpha_2)\delta_\pm(-\delta_\pm+\alpha_1)} \approx$$
$$-\frac{-\rho_1\zeta\delta_\pm + \zeta\rho_1\alpha_2 - \zeta\delta_\pm\gamma - \zeta\delta_\pm\rho_2 + \gamma\delta_\pm^2 - \gamma\delta_\pm\alpha_2}{(-\delta_\pm+\alpha_2)\delta_\pm(-\delta_\pm+\alpha_1)} \Rightarrow \tag{C.60}$$
$$\theta_{1+} \approx \frac{\alpha_2\zeta(\rho_1+\gamma)}{\left(\frac{\gamma(\rho_2+\gamma)}{\alpha_2+\zeta}\right)\alpha_2(\alpha_1-\alpha_2)} \approx \frac{\alpha_2}{\alpha_1}\frac{\zeta}{\gamma} \quad ; \quad \theta_{1-} \approx \frac{\alpha_2\zeta(\rho_1+\gamma)}{\zeta(\zeta+\alpha_2)(\zeta+\alpha_1)} \approx \frac{\rho_1+\gamma}{\alpha_1} \tag{C.61}$$

$$\theta_{2\pm} = \frac{-\rho_2\gamma - \gamma^2 - \zeta\delta_\pm + \zeta\alpha_2}{(-\delta_\pm+\alpha_2)\delta_\pm} \approx \frac{\zeta}{\delta_\pm} \quad \Rightarrow \theta_{2+} \approx \frac{\zeta}{\alpha_2} \quad ; \quad \theta_{2-} \approx -1 \tag{C.62}$$

$$\theta_{3\pm} = -\frac{\gamma+\rho_2}{-\delta_\pm+\alpha_2} \quad \Rightarrow \theta_{3+} \approx -\frac{\alpha_2+\zeta}{\gamma} \quad ; \quad \theta_{3+} \approx -\frac{\gamma+\rho_2}{\zeta+\alpha_2} \tag{C.63}$$

where all higher order terms like γ^2 have been deleted and we have used (C.50)-(C.51). From the above results it should be clear that $\theta_{1+}, \theta_{3+} \gg \theta_{2+}$, $\theta_{1+}, \theta_{3+} \gg 1$ and $\theta_{3+} > \theta_{1+}$. We can therefore write the following eigenvalues and normalized vectors from (C.59)

$$\mu \approx \begin{bmatrix} 0 \\ \alpha_1 \\ \alpha_2 \\ -\zeta \end{bmatrix} \quad ; \quad V \approx \begin{bmatrix} -\boxed{\frac{\rho_1}{\alpha_1}} & 1 & 1 & \boxed{\frac{\rho_1+\gamma}{\alpha_1}} \\ 1 & 0 & \epsilon_6 & -1 \\ 0 & 0 & -1 & \boxed{-\frac{\gamma+\rho_2}{\alpha_2}} \\ 0 & 0 & -\epsilon_6 & 1 \end{bmatrix} \tag{C.64}$$

where ϵ_6 is an unspecified constant chosen to make the u and v vectors bi-orthogonal (see appendix D). In (C.64), the boxed contributions represent AM-to-PM. From the above expression we see that we no longer find the simple dual vectors $v_1(t) = \phi_m(t)$ and $v_2(t) = \phi_s(t)$ as was discussed in section 3.2.1 for the symmetric case. However, this is only correct because the dual Floquet eigenvectors are supposed to cover the complement of the *null-space* of the projection operators. When the oscillators are symmetric and *isotropic* the null-space includes the entire amplitude space; while with asymmetric oscillators and inherent frequency control there will be a cross-over part (AM-to-PM). We summarize as follows

note C.2 *the two Floquet dual eigenvectors $v_1(t)$ and $v_2(t)$, corresponding to the invariant manifold vectors $u_1(t)$ and $u_2(t)$, correctly predict the added AM-to-PM noise conversion introduced by asymmetry, inherent frequency control or non-harmonic limit cycle. This means, that under the condition of a normal hyperbolic manifold, the two normal form projection operators $P_1(t) = u_1(t)v_1^T(t) = \phi_d(t)v_1^T(t)$ and $P_2(t) = u_2(t)v_2^T(t) = \phi_s(t)v_2^T(t)$ will correctly represent the S-ILO phase noise scenario.*

C.5 The ILO Monodromy Matrix

Due to the unilateral coupling from the M-OSC to the S-OSC in the S-ILO scenario (see figure 3.1, on page 63) we can write the monodromy matrix (MM) as

$$\Phi \equiv \Phi(T,0) = \begin{bmatrix} \Phi_{11} & \mathbf{0} \\ \Phi_{21} & \Phi_{22} \end{bmatrix} \tag{C.65}$$

where $\Phi_{11} \in \mathbb{R}^{n_1 \times n_1}$, $\Phi_{21} \in \mathbb{R}^{n_2 \times n_1}$, $\Phi_{11} \in \mathbb{R}^{n_2 \times n_2}$. From the discussion in appendix D we know that we can write the following Floquet decomposition of the MM

$$\Phi = \sum_{i=1}^{n} \lambda_i u_i v_i^T = \sum_{i=1}^{n_1} \lambda_{1,i} u_{1,i} v_{1,i}^T + \sum_{i=1}^{n_2} \lambda_{2,i} u_{2,i} v_{2,i}^T \tag{C.66}$$

where the Floquet vectors have the following form

$$u_{1,i} = \begin{bmatrix} u_{1m,i} \\ u_{1s,i} \end{bmatrix} \tag{C.67}$$

$$v_{1,i} = \begin{bmatrix} v_{1m,i} \\ \mathbf{0} \end{bmatrix} \tag{C.68}$$

$$u_{2,i} = \begin{bmatrix} \mathbf{0} \\ u_{2s,i} \end{bmatrix} \tag{C.69}$$

$$v_{2,i} = \begin{bmatrix} v_{2m,i} \\ v_{2s,i} \end{bmatrix} \tag{C.70}$$

where $u_{1m,i}, v_{1m,i}, v_{2m,i} \in \mathbb{C}^{n_1}$ and $u_{1s,i}, u_{2s,i}, v_{2s,i} \in \mathbb{C}^{n_2}$. The vectors in (C.67)-(C.70) follow from inspection of (C.65) and its transposed [2].

Comparing (C.65) and (C.66) and using (C.67)-(C.70) we see that we can write the block matrices as

[2] the Floquet vectors u_i are eigenvectors of the MM while the dual Floquet vectors are eigenvectors of the transposed MM (see discussion in appendix D).

$$\Phi_{11} = \sum_{i=1}^{n_1} \lambda_{1,i} u_{1m,i} v_{1m,i}^T \tag{C.71}$$

$$\Phi_{22} = \sum_{i=1}^{n_2} \lambda_{2,i} u_{2s,i} v_{2s,i}^T \tag{C.72}$$

$$\Phi_{21} = \sum_{i=1}^{n_1} \lambda_{1,i} u_{1s,i} v_{1m,i}^T + \sum_{i=1}^{n_2} \lambda_{2,i} u_{2s,i} v_{2m,i}^T \tag{C.73}$$

One of the eigenvectors of the MM will have eigenvalue 1 and have a Floquet eigenvector which lies parallel to the periodic orbit. We can therefore write $\lambda_{1,1} = 1$ and

$$u_{1,1} = \begin{bmatrix} u_{1m,1} \\ u_{1s,1} \end{bmatrix} = \begin{bmatrix} \dot{x}_m \\ \dot{x}_s \end{bmatrix} \tag{C.74}$$

where the above vector by definition lies tangent to the periodic orbit $x_{ss}(t) = [x_m(t)\ x_s(t)]^T$. The Floquet eigenvectors and the dual Floquet eigenvectors form a *bi-orthogonal set* [3] which means that

$$u_{1,1}^T v_{1,1} = 1 \Leftrightarrow [\dot{x}_m^T\ \dot{x}_s^T][v_{1,m}\ \mathbf{0}]^T = \dot{x}_m^T v_{1,m} = 1 \tag{C.75}$$

where we have used the expressions in (C.67)-(C.68). Since (C.74) is an eigenvector of (C.65), with eigenvalue 1, we can write

$$\begin{bmatrix} \Phi_{11} & \mathbf{0} \\ \Phi_{21} & \Phi_{22} \end{bmatrix} \begin{bmatrix} \dot{x}_m \\ \dot{x}_s \end{bmatrix} = \begin{bmatrix} \dot{x}_m \\ \dot{x}_s \end{bmatrix} \tag{C.76}$$

The above equation can also be expressed through two block-equations

$$\Phi_{11} \dot{x}_m = \dot{x}_m \tag{C.77}$$

$$\Phi_{21} \dot{x}_m + \Phi_{22} \dot{x}_s = \dot{x}_s \tag{C.78}$$

Equation (C.77) merely states that the M-OSC is a free-running oscillator. Using the notation from (C.72)-(C.73) we can write (C.78) as

$$\begin{aligned} &\sum_{i=1}^{n_1} \lambda_{1,i} u_{1s,i} v_{1m,i}^T \dot{x}_m + \sum_{i=1}^{n_2} \lambda_{2,i} u_{2s,i} v_{2m,i}^T \dot{x}_m + \sum_{i=1}^{n_2} \lambda_{2,i} u_{2s,i} v_{2s,i}^T \dot{x}_s = \dot{x}_s \Leftrightarrow \\ &\lambda_{1,1} u_{1s,1} v_{1m,1}^T \dot{x}_m + \sum_{i=1}^{n_2} \lambda_{2,i} u_{2s,i} v_{2m,i}^T \dot{x}_m + \sum_{i=1}^{n_2} \lambda_{2,i} u_{2s,i} v_{2s,i}^T \dot{x}_s = \dot{x}_s \end{aligned} \tag{C.79}$$

where we have used that

$$\sum_{i=1}^{n_1} \lambda_{1,i} u_{1s,i} v_{1m,i}^T \dot{x}_m = \lambda_{1,1} u_{1s,1} v_{1m,1}^T \dot{x}_m \tag{C.80}$$

since we must have that

$$v_{1m,i}^T \dot{x}_m = \delta_{i1} \tag{C.81}$$

[3] the two sets of Floquet vectors form a bi-orthogonal set $u_i^T v_j = \delta_{ij}$ as discussed in appendix D.

This follows from (C.75) and the fact that the u_i and v_i vectors must form a bi-orthogonal set (see footnote 3). This means that all $v_{1m,i}$, except $v_{1m,1}$, must be orthogonal to $\dot{x}_m$. However, using (C.74), (C.75) and $\lambda_{1,1} = 1$, we can write

$$\lambda_{1,1} u_{1s,1} v_{1m,1}^T \dot{x}_m = \dot{x}_s \tag{C.82}$$

which, when inserted into (C.79), gives us the following *balance equation*

$$\boxed{\sum_{i=1}^{n_2} \lambda_{2,i} u_{2s,i} v_{2m,i}^T \dot{x}_m + \sum_{i=1}^{n_2} \lambda_{2,i} u_{2s,i} v_{2s,i}^T \dot{x}_s = 0} \tag{C.83}$$

From (C.83) we can derive the expression

$$v_{2m,i}^T \dot{x}_m = -v_{2s,i}^T \dot{x}_s \quad \text{for all } i \tag{C.84}$$

However, this also follows from the bi-orthogonality condition (see discussion in appendix D and footnote 3)

$$u_i^T v_j = \delta_{ij} \tag{C.85}$$

C.6 Computing the Spectrum of the Noise Perturbed ILO

In section 3.2.4 an expression for the asymptotically stationary autocorrelation function $\Gamma(\tau)$ was found in (3.80). The spectral density function is now found by Fourier transforming this expression. We shall use the approximation $\exp(-N\omega_1^2 k^2 \sigma_s^2 (1-\rho_t)) \approx 1 - N\omega_1^2 k^2 \sigma_s^2 (1-\rho_\tau)$ where k denotes the harmonic in question. This approximation is valid since $N\omega_1^2 k^2 \sigma_s^2 (1-\rho_\tau) \ll 1$ for all τ. Inserting this expression into equation (3.80), Fourier transforming and including a frequency displacement $N\omega_1$ due to the factor $\exp(jN\omega_1\tau)$, results in an expression for the S-OSC spectral density. Assuming $2\mu_2 \gg \omega_1^2 D_{21}$, we can simplify this expression, leaving us with the result

$$\begin{aligned} S_s(\omega) = \sum_{k=-\infty}^{\infty} |X_k|^2 \times \\ \frac{(kN\omega_1)^2 (D_{21} + 2\sigma_s^2 |\mu_2|)[(\omega + kN\omega_1)^2 + \frac{D_{21}\mu_2^2}{D_{21} + 2|\mu_2|\sigma_s^2}]}{[(\frac{1}{2}N^2\omega_1^2 k^2 D_{21})^2 + (\omega + kN\omega_1)^2][\mu_2^2 + (\omega + kN\omega_1)^2]} \end{aligned} \tag{C.86}$$

Appendix D

Floquet Theory

The text in this appendix is inspired by the derivations in [14]. We shall use the index s to symbolize time instead of the usual t and we write the dimension of the state vectors as m. These symbols are chosen to match the notation in chapter 3 [1]. The system is assumed time normalized so that we operate with a period $T = 2\pi$.

We consider the linear homogeneous ODE

$$\dot{z}(s) = A(s)z(s) \tag{D.1}$$

where $z(\cdot) : \mathbb{R} \to \mathbb{R}^m$ and $A(\cdot) : \mathbb{R} \to \mathbb{R}^{m\times m}$. The solution to (D.1), with initial condition $z(s_0)$, is then written

$$z(s) = \Phi(s, s_0)z(s_0) = \sum_{i=1}^{m} \exp\big(\mu_i(s - s_0)\big)u_i(s)v_i^T(s_0)z(s_0) \tag{D.2}$$

where $\Phi(s, s_0)$ is the *state-transition matrix* (STM)

$$\Phi(s, s_0) = \exp\left\{\int_{s_0}^{s} A(\eta)d\eta\right\} = \sum_{i=1}^{m} \exp\big(\mu_i(s - s_0)\big)u_i(s)v_i^T(s_0) \tag{D.3}$$

with the column vectors $u_i(s) : \mathbb{R} \to \mathbb{C}^{m\times 1}$ being the i'th *Floquet eigenvector*, the row vectors [2] $v_i^T(s) : \mathbb{R} \to \mathbb{C}^{1\times m}$ are the i'th *dual Floquet eigenvector* and μ_i is the i'th *Floquet characteristic exponent*. Both the u_i and the v_i vectors are 2π periodic in their arguments. Furthermore, according to Floquet theory, we can assume that these vectors form a complete *bi-orthogonal set* [3]

$$v_i^T(s)u_i(s) = \delta_{ij} \quad \text{for all } s \tag{D.4}$$

We then consider the *adjoint system*

$$\dot{w}(s) = -A^T(s)w(s) \tag{D.5}$$

and we define a STM for this system as

[1] here s is the instantaneous time $s = t+\alpha(t)$ and $m = \sum_{j=1}^{n} n_j$ with n being the number of oscillators in the coupling structure and n_i the state dimension of the i'th oscillator.

[2] in this report x^T refers to the *transposed vector*. So if $x(s) : \mathbb{R} \to \mathbb{C}^{m\times 1}$ then we have that $x^T(s) : \mathbb{R} \to \mathbb{C}^{1\times m}$.

[3] besides the condition in (D.4) this means that $\{u_i\}_{i=1}^{m}$ span the vector space $\mathbb{R}^m$ while the row vectors $\{v_i^T\}_{i=1}^{m}$ span the *dual vector space* $\mathbb{R}^{m*}$.

$$\Psi(s,s_0)=\exp\left\{-\int_{s_0}^{s}A^T(\eta)d\eta\right\}=\left[\exp\left\{\int_{s}^{s_0}A(\eta)d\eta\right\}\right]^T \tag{D.6}$$

where we have used that $\int_a^b f(x)dx=-\int_b^a f(x)dx$ and furthermore that the exponential of a transposed matrix is equal to the transpose of the exponential itself. Comparing (D.6) and (D.3) we can make the following identification

$$\Psi(s,s_0)=\Phi(s_0,s)^T \tag{D.7}$$

With the initial conditions $w(s_0)$ we then find

$$w(s)=\Psi(s,s_0)w(s_0)=\Phi(s_0,s)^Tw(s_0)=\sum_{i=1}^{m}\exp\big(\mu_i(s_0-s)\big)v_i(s)u_i^T(s_0)w(s_0) \tag{D.8}$$

Using (D.2) and (D.8) and the bi-orthogonality in (D.4) we find the special solutions

$$z(s_0)=u_i(s_0)\Rightarrow z(s)=\exp(\mu_i(s-s_0))u_i(s) \tag{D.9}$$
$$w(s_0)=v_i(s_0)\Rightarrow w(s)=\exp(\mu_i(s_0-s))v_i(s) \tag{D.10}$$

Which is also written

$$\exp(\mu_i(s-s_0))u_i(s)=\Phi(s,s_0)u_i(s_0) \tag{D.11}$$
$$\exp(\mu_i(s_0-s))v_i(s)=\Psi(s,s_0)v_i(s_0) \tag{D.12}$$

From (D.11)-(D.12) we see that u_i and v_i are *eigen-modes* of the STM's Φ and Ψ, respectively. Furthermore, since u_i and v_i are periodic, with period 2π, we see from (D.11)-(D.12) that $u_i(s)$ is an *eigenvector* of $\Phi(s+2\pi,s)$ while $v_i(s)$ is an eigenvector of $\Psi(s+2\pi,s)$

$$\Phi(s+2\pi,s)u_i(s)=\lambda_iu_i(s) \tag{D.13}$$
$$\Psi(s+2\pi,s)v_i(s)=\Phi(s,s+2\pi)^Tv_i(s)=\lambda_i^{-1}v_i(s) \tag{D.14}$$

where

$$\lambda_i=\exp(\mu_iT)=\exp(\mu_i2\pi) \tag{D.15}$$

are the so-called *Floquet characteristic multipliers*. The special STM $\Phi(s+2\pi,s)$ is known as the *monodromy matrix*.

Using the definitions in (D.4), (D.7) and (D.11)-(D.12) we can then derive the following important relationship

$$\begin{gathered}v_i^T(s)u_i(s)=1\Rightarrow\\ \exp\big(-\mu_i(s_0-s)\big)\Big[\Psi(s,s_0)v_i(s_0)\Big]^T\exp\big(-\mu_i(s-s_0)\big)\Phi(s,s_0)u_i(s_0)=\\ v_i^T(s)\Psi(s,s_0)^T\Phi(s,s_0)u_i(s_0)=1\Rightarrow\Psi(s,s_0)^T\Phi(s,s_0)=\Phi(s_0,s)\Phi(s,s_0)=I\Leftrightarrow\\ \Phi(s_0,s)=\Phi(s,s_0)^{-1}\end{gathered} \tag{D.16}$$

Using the above derivation we can write (D.8) as

$$w(s) = \left[\Phi(s, s_0)^{-1}\right]^T w(s_0) \Leftrightarrow w(s_0) = \Phi(s, s_0)^T w(s) = \Psi(s_0, s) w(s) \tag{D.17}$$

Assume now that we consider a 2π periodic steady state solution of some autonomous ODE and that (D.1) represents the linear response; how should we interpret the STM eigen-modes u_i, v_i?

note D.1 *The solution to the linear response system in* (D.1) *is written* $z(s) = \Phi(s, s_0)z(s_0)$ *where* $s > s_0$. *This should be interpreted as the STM or the Forward Time Map (FTM) taking the initial condition* $z(s_0)$ *and bringing it forward in time to the solution* $z(s)$. *The solution to the dual system in* (D.5) *is written* $w(s_0) = \Psi(s_0, s)w(s) = \Phi(s, s_0)^T w(s)$ $s > s_0$. *This should interpreted as the transposed STM or Backward Time Map (BTM) taking the initial solution* $w(s)$ *and bringing in backward in time to the solution* $w(s_0)$.

Consider and arbitrary initial condition $z(s_0)$ to the system in (D.1). Since u_i span the space $\mathbb{R}^m$ (see footnote 3) we can write

$$z(s_0) = \sum_{i=1}^{m} a_i u_i(s_0) \tag{D.18}$$

where a_i are the expansion coefficients. Inserting this expansion into (D.3) and using the bi-orthogonality condition in (D.4) we find the following solution at time $s_0 + 2\pi$

$$z(s_0 + 2\pi) = \Phi(s_0 + 2\pi, s_0)z(s_0) = \sum_{i=1}^{m} \lambda_i a_i u_i(s_0) \tag{D.19}$$

where we have used the formulations from (D.13)-(D.14). We see that the operator in (D.3) picks out the components in the different state-space directions, $u_i(s_0)$, in the initial condition and then brings them forward in time 2π to $u_i(s_0 + 2\pi) = u_i(s_0)$ by multiplying by a factor $\exp(\mu_i 2\pi)$. The selection operation is done by the terms $u_i(s_0 + 2\pi)v_i^T(s_0) = u_i(s_0)v_i^T(s_0)$. These terms then define a set of *orthogonal projection operators* (see footnote 6, on page 41)

$$P_i(s_0) = u_i(s_0)v_i^T(s_0) \tag{D.20}$$

This set is orthogonal since (see footnote 12 on page 42)

$$P_i P_j = u_i(s_0)v_i^T(s_0)u_j(s_0)v_j^T(s_0) = \delta_{ij} P_i \tag{D.21}$$

where we have used the bi-orthogonality condition in (D.4). We then see that we can write the monodromy matrix $\Phi(s_0 + 2\pi, s_0)$ as a series of orthogonal projection operators

$$\Phi(s_0 + 2\pi, s_0) = \sum_{i=1}^{m} \exp\big(\mu_i 2\pi\big) P_i(s_0) = \sum_{i=1}^{m} \lambda_i P_i(s_0) \tag{D.22}$$

Since s_0 is chosen arbitrarily we can set $s_0 = 0$

$$\Phi(2\pi,0)=\sum_{i=1}^{m}\lambda_i P_i(0)=\sum_{i=1}^{m}\lambda_i P_i \tag{D.23}$$

We see that Monodromy Matrix $\Phi(2\pi,0)$ constitutes a return-map which bring the solutions one period forward in time.

note D.2 *the monodromy matrix* $\Phi(2\pi,0)=\sum_{i=1}^{m}\lambda_i P_i$ *constitutes a return-map which bring the linear response solutions one period forward in time. The perturbations outside the null-space, as determined by* $v_i^T(0)$*, of the orthogonal projection operator* $P_i=u_i(0)v_i^T(0)$*, will be multiplied by a factor* λ_i *and projected onto the range* $u_i(0)$*.*

Finally, we consider the linear inhomogeneous ODE

$$\dot{z}(s)=A(s)z(s)+b(s) \tag{D.24}$$

where $b(s):\mathbb{R}\to\mathbb{R}^m$ is the forcing function. From standard analysis we known that the complete solution can be written as the sum of a homogenous and an inhomogeneous part. Furthermore, the inhomogeneous solution can be expressed as a folding integral with the homogeneous solution. This follows by writing the forcing function as

$$b(s)=\int b(s_i)\delta(s-s_i)ds_i \tag{D.25}$$

At each time, s_j, the forcing function *resets* the initial condition

$$z(s_j)=z(s_{j-})+b(s_j) \tag{D.26}$$

where $s_{j-}=\lim_{x\to 0}s_j-x$. The complete solution then reads

$$\begin{gathered}z(s)=\Phi(s,s_j)\big\{z(s_{j-})+b(s_j)\big\}=\\ \Phi(s,s_j)\Phi(s_{j-},s_0)z(s_0)+\Phi(s,s_j)b(s_j)=\Phi(s,s_0)z(s_0)+\Phi(s,s_j)b(s_j)\end{gathered} \tag{D.27}$$

Including the complete forcing function (D.25), and using the *superposition principle* which holds for linear ODE's, we can write the complete solution as

$$z(s)=\Phi(s,s_0)z(s_0)+\int_{s_0}^{s}\Phi(s,\eta)b(\eta)d\eta \tag{D.28}$$

D.1 Deriving the Monodromy Matrix $\Phi(2\pi, 0)$

Averaging techniques were discussed in section 1.2, on page 28, and applied in chapter 4 to the analysis of oscillators coupled in a unilateral ring. The averaged state equations work on a time scale $t = T = 2\pi$ and inside this time frame we have no information about the solution; we only receive stroboscopic signals at times $t = T, 2T, 3T, \cdots$. If we compare this with the description of the monodromy matrix in note D.2 we recognize an immediate similarity.

Using (D.3) we can write the monodromy matrix as

$$\Phi(2\pi, 0) = \exp\left\{ \int_0^{2\pi} J(\eta) d\eta \right\} \tag{D.29}$$

where we denote the Jacobian matrix $A(\cdot)$, in (D.3), as $J(\cdot)$, since we shall use A to symbolize the oscillator amplitude. If we write the Jacobian of the averaged system as J_{av}, we could suggest that

$$J_{av} = \frac{1}{2\pi} \int_0^{2\pi} J(\eta) d\eta \tag{D.30}$$

This simply follows from switching the order of differentiation and averaging (integration) [4].

A mathematical proof of (D.30) could thus probably be derived relatively painlessly; however, we shall prefer to consider a simple illustrative example. The van der Pol oscillator unit has been used throughout this report as a simple prototype oscillator. The state equations read

$$L \frac{\partial i_L}{\partial t} = -v_C \tag{D.31}$$

$$C \frac{\partial v_C}{\partial t} = i_L - \frac{v_C}{R} + G_M(v_C) \tag{D.32}$$

where $G_M(v_C) = g_1 v_C + g_2 v_C^2 + g_3 v_C^3$. We start by deriving the monodromy matrix for this system which is then compared with the expression for the Jacobian of the averaged equations. In section 1.1.1 we wrote (D.31)-(D.32) on the equivalent complex form, as shown in (1.29) on page 17. Then in (1.43) and (1.44), on page 20 of section 1.1.1, it was explained how we could transform this to the polar form

$$2A\dot{A} = \dot{z}\overline{z} + z\dot{\overline{z}} \tag{D.33}$$

$$\dot{\phi} = \frac{-j}{2z\overline{z}} (\dot{z}\overline{z} - z\dot{\overline{z}}) \tag{D.34}$$

where we have used the notation $z(t) = Ae^{j(t+\phi)}$. From (1.29) we find

$$\begin{aligned} \dot{z}\overline{z} = \lambda A^2 + \frac{c_2 - jc_1}{2c_2} \Big(& \frac{g_1}{C} \big(A^3 e^{j(t+\phi)} + A^3 e^{-3j(t+\phi)} - 2A^3 e^{-j(t+\phi)} \big) - \\ & \frac{g_2}{C} \big(A^4 e^{2j(t+\phi)} - A^4 e^{-4j(t+\phi)} + 3A^4 e^{-2j(t+\phi)} - 3A^4 \big) \Big) \end{aligned} \tag{D.35}$$

[4] the linear response averaged system is derived by first averaging and then differentiating while the monodromy matrix is found by first differentiating the state equations, to obtain the linear response equation in (D.1), and then integrating (averaging) the resulting Jacobian.

The parameters in the above expression are defined in (1.24)-(1.25), on page 16. Inserting (D.35), and it's complex conjugate, into (D.33)-(D.34), we obtain the equivalent amplitude/phase state equations of the van der Pol oscillator in (D.31)-(D.32). We can find the Jacobian, $J(t)$, of this ODE by differentiating with respect to the state variables A and ϕ (see (2.4) on page 38). What results is a complicated expression, involving various time varying terms as seen from (D.35). However, from the definition in (D.29) we see that all time varying terms, being periodic with period 2π, are removed by the integration. We can hence derive the monodromy matrix by inspection from (D.35) and (D.33)-(D.34)

$$\Phi(2\pi,0)=\exp\left[\int_0^{2\pi}J(\eta)d\eta\right]=\exp\left(\begin{bmatrix}\Re\{\lambda\}-\frac{9}{4}\frac{g_2}{C}\hat{A}^2 & 0\\ -\frac{c_1}{c_2}\frac{6}{2}\frac{g_2}{C}\hat{A} & 0\end{bmatrix}\times 2\pi\right)= \exp\left(\frac{2\pi}{C}\begin{bmatrix}\frac{(g_0-G_L)}{2}\left[1-\frac{9g_2}{2(g_0-G_L)}\hat{A}^2\right] & 0\\ -\frac{3(g_0-G_L)g_2}{\sqrt{\omega_0^2-\left(\frac{g_0-G_L}{C}\right)^2}}\hat{A} & 0\end{bmatrix}\right) \tag{D.36}$$

where $\hat{A}$ refers to the steady-state amplitude of the limit cycle, about which the Jacobian is formed. The averaged state equations are easily found as

$$\dot{A}=\Re\{\lambda\}A-3\frac{g_2}{2C}A^3 \tag{D.37}$$

$$\dot{\phi}=-3\frac{c_1}{2c_2}\frac{g_2}{C}A^2 \tag{D.38}$$

Deriving the Jacobian of the above vector field, and comparing with the expression in (D.36), we see that we can write the monodromy matrix in (D.29) as

$$\Phi(2\pi,0)=\exp\big(2\pi J_{av}\big) \tag{D.39}$$

We can decompose J_{av} as

$$J_{av}=\sum_i \rho_i x_i y_i^T \tag{D.40}$$

where ρ_i is the i'th eigenvalue, x_i is the i'th left eigenvector and y_i is the i'th right eigenvector. Since these vectors form a complete bi-orthogonal set we can write the monodromy matrix (D.39) as

$$\Phi(2\pi,0)=\sum_i \exp(2\pi\rho_i)x_i y_i^T \tag{D.41}$$

A comparison of this expression with (D.23) and (D.20) leads to the identifications $\rho_i=\mu_i$, $x_i=u_i(0)$ and $y_i^T=v_i^T(0)$. We summarize as follows

note D.3 *The monodromy matrix can be written as* $\Phi(2\pi,0)=\exp\big(2\pi J_{av}\big)$*, where* J_{av} *is the Jacobian of the averaged state equations. The left and right eigenvectors of* J_{av} *are then identified with the Floquet and dual Floquet eigenvectors* $u_i(0)$ *and* $v_i^T(0)$*, respectively. The eigenvalues of* J_{av} *are identified with the characteristic exponents* μ_i*.*

Bibliography

[1] "John Harrison." online Wikipedia article.

[2] M. Bennet, M. F. Schatz, H. Rockwood, and K. Wiesenfeld, "Huygens's clocks," *Proceedings of the Royal Society of London*, vol. 458, pp. 563–579, January 2002.

[3] "Millennium Bridge." online Wikipedia article.

[4] J. Vidkjaer, "Modulation." Class Notes for the Course : RF-Communication, 2000.

[5] A. Rofougaran, J. Rael, M. Rofougaran, and A. Abidi, "A 900MHz CMOS LC-oscillator," in *Digest of Tech. Papers. 43rd ISSCC., 1996 IEEE International Solid-State Circuits Conference*, pp. 392–393, 1996.

[6] T. Djurhuus, V. Krozer, J. Vidkjær, and T. Johansen, "Nonlinear analysis of a cross-coupled quadrature harmonic oscillator," *IEEE Trans. Circuits & Syst. - I : Fundamental Theory and Applications*, vol. 52, pp. 2276–2285, November 2005.

[7] J. van der Tang, P. van de Ven, D. Kasperkovitz, and A. van Roermund, "Analysis and design of an optimally coupled 5-GHz quadrature oscillator," *IEEE J. of Solid-State*, vol. 37, pp. 657–661, May 2002.

[8] L. Romano, S. Levantino, C. Samori, and A. L. Lacaita, "Multiphase LC oscillators," *IEEE Trans. Circuits & Syst. - I : Fundamental Theory and Applications*, vol. 53, pp. 1579–1588, JULY 2006.

[9] L. Dussopt and J.-M. Laheurte, "Phase noise improvement in a loop configuration of oscillating antennas," *IEEE Microwave and Guided Wave Letters*, vol. 10, pp. 111–113, Narch 2000.

[10] J. J. L. Robert A. York, Peter Liao, "Oscillator array dynamics with broadband n port coupling networks," *IEEE Trans. Microwave Theory & Tech.*, vol. 42, pp. 2040–2045, November 1994.

[11] C.-H. Park, O. Kim, and B. Kim, "A 1.8 GHz self-calibrated phase-locked loop with precise I/Q matching," *IEEE J. Solid-State Circuits*, vol. 36, pp. 777–783, May 2001.

[12] H. R. R. Shwetabh Verma and T. H. Lee, "A unified model for injection-locked frequency dividers," *IEEE J. of Solid-State Circuits*, vol. 38, pp. 1015–1027, June 2003.

[13] H.-C. Chang, X. Cao, U. Mishra, and R. A. York, "Phase noise in coupled oscillators : theory and experiment," *IEEE Trans. Microwave Theory & Tech.*, vol. 45, pp. 604–615, May 1997.

[14] A. Demir, A. Mehrotra, and J. Roychowdhury, "Phase noise in oscillators: A unifying theory and numerical methods for characterization.," *IEEE Trans. Circuits & Systems*, vol. 47, pp. 655–674, May 2000.

[15] A. Demir, "Phase noise and timing jitter in oscillators with colored-noise sources," *IEEE Trans. Circuits & Syst. I : Fundamental Theory and Applications*, vol. 49, pp. 1782–1791, December 2002.

[16] A. Demir and J. Roychowdhury, "A reliable and efficient procedure for oscillator PPV computation, with phase noise macromodeling applications," *IEEE Transactions on Computer-Aided Design of Integrated Circuits & System*, vol. 22, pp. 188 –197, February 2003.

[17] F. X. Kaertner, "Determination of the correlation spectrum of oscillators with low noise," *IEEE Trans. Microwave Theory Tech.*, vol. 37, pp. 90–101, January 1989.

[18] W. Anzill and P. Russer, "A general method to simulate noise in oscillator based on frequency domain techniques," *IEEE J. Microwave Theory & Tech.*, vol. 41, pp. 2256– 2262, December 1993.

[19] T. Djurhuus, V. Krozer, J. Vidkjær, and T. Johansen, "AM to PM noise conversion in a cross-coupled quadrature harmonic oscillator," *International J. of RF and Microwave Computer-Aided Engineering*, vol. 16, pp. 34–41, November 2005.

[20] T. Djurhuus, V. Krozer, J. Vidkjær, and T. Johansen, "Trade-off between phase-noise and signal quadrature in unilaterally coupled oscillators," in *Microwave Symp. Digest, 2005 IEEE MTT-S International*, pp. 883–886, 2005.

[21] S. Wiggins, *Introduction to Applied Nonlinear Dynamical Systems and Chaos*. Springer-Verlag, 2003.

[22] D. K. Arrowsmith and C. M. Place, *an Introduction to Dynamical Systems*. Cambridge University Press, 1994.

[23] J. D. Crawford, "Introduction to bifurcation theory," *Reviews of Modern Physics*, vol. 63, pp. 991–1037, October 1991.

[24] M. Golubitsky and D. G. Schaeffer, *Singularities and Groups in Bifurcation Theory - Volume I*. Applied Mathematical Science 69, Springer-Verlag, 1988.

[25] M. Golubitsky, I. Stewart, and D. G. Schaeffer, *Singularities and Groups in Bifurcation Theory - Volume II*. Applied Mathematical Science 69, Springer-Verlag, 1988.

[26] F. C. Hoppensteadt and E. M. Izhikevich, *Weakly Connected Neural Networks*. Springer Verlag, 1997.

[27] J. A. Acebron, L. L. Bonilla, C. J. P. Vicente, F. Ritort, and R. Spigler, "The kuramoto model: A simple paradigm for synchronization phenomena," *Review of Modern Physics*, vol. 77, pp. 137–185, January 2005.

[28] P. Vanassche, G. Gielen, and W. Sansen, "Behavioral modeling of (coupled) harmonic oscillators," *IEEE Trans. Computer-Aided Design*, vol. 22, pp. 1017–1026, August 2003.

[29] P. Ashwin and J. W. Swift, "The dynamics of n weakly coupled identical oscillators," *J. Nonlinear Science*, vol. 2, pp. 69–108, 1992.

[30] P. Ashwin, "Weak coupling of strongly nonlinear, weakly dissipative identical oscillators," *Dynamics and Stabillity of Systems*, vol. 10, no. 3, pp. 203–218, 1995.

[31] P. Ashwin and G. DangelMayr, "Reduced dynamics and symmetric solutions for globally coupled weakly dissipative oscillators," *Dynamical Systems*, vol. 20, no. 3, pp. 333–367, 2005.

[32] K. Kurokawa, "Noise in synchronized oscillators.," *IEEE Transactions on Microwave Theory and Tech.*, vol. MTT-16, pp. 234–240, April 1968.

[33] K. Kurokawa, "Injection locking of microwave solid-state oscillator," *Proc. IEEE*, vol. 61, pp. 1386–1410, October 1973.

[34] P. Vanassche, G. Gielen, and W. Sansen, "Behavioral modeling of (coupled) harmonic oscillators," *IEEE Trans. Computer-Aided Design*, vol. 22, pp. 1017–1026, August 2003.

[35] P. Vanassche, G. Gielen, and W. Sansen, "Efficient analysis of slow-varying oscillator dynamics," *IEEE Trans. Circuits & Syst. I : Regular Papers*, vol. 51, pp. 1457–1467, August 2004.

[36] J. Vidkjaer, "Mixers." Class Notes for the Course : RF-Communication, 2000.

[37] M. Golubitsky and I. Stewart, *The Symmetry Perspective - From Equilibrium to Chaos in Phase Space and Physical Space*. Birkhauser Verlag, 2003.

[38] T. Djurhuus, "IC quadrature oscillator," Master Thesis, Technical University of Denmark,2003.

[39] H. Risken, *Fokker-Planck Equation - Methods of Solution and Applications*. Springer, 1989.

[40] D. Ham and A. Hajimiri, "Virtual damping and Einstein relation in oscillators.," *IEEE J. of Solid-State Circuits*, vol. 38, pp. 407–418, March 2003.

[41] B. Razavi, "The study of phase noise in CMOS oscillators.," *IEEE J. of Solid-State Circuits*, vol. 31, pp. 331–343, March 1996.

[42] W. C. Lindsey, *Synchronization Systems in Communication and Control*. Prentice-Hall, 1973.

[43] T. Djurhuus, V. Krozer, J. Vidkjær, and T. Johansen, "A free-running oscillator perturbed by delta-correlated noise - inhomogeneous phase diffusion," *IEEE Trans. Circuits & Syst. - II : Express Briefs*. to be submitted.

[44] W. A. Edson, "Noise in oscillators.," *Proceedings of the IRE*, vol. 48, pp. 1454–1466, August 1960.

[45] M. Lax, "Clasical noise. v. noise in self-sustained oscillators," *Phys. Review*, vol. 160, pp. 290–307, August 1967.

[46] A. Hajimiri and T. H. Lee, "Design issues in CMOS differential LC oscillators," *IEEE J. of Solid-State Circuits*, vol. 34, pp. 717–724, May 1999.

[47] A. Demir, "Computing timing jitter from phase noise spectra for oscillators and phase-locked loops with white and 1/f noise," *IEEE Trans. Circuits & Syst. - I : Regular Papers*, vol. 53, pp. 1869–1884, September 2006.

[48] T. J. Aprille and T. N. Trick, "A computer algorithm to determine the steady-state respose of nonlinear oscillators," *IEEE Trans. Circuit Theory*, vol. CT-19, pp. 354–360, July 1972.

[49] A. Mehrotra, "Noise analysis of phase-locked loops," *IEEE Trans. Circuits & Syst. - I : Fundamental Theory and Applications*, vol. 49, pp. 1309–1316, September 2002.

[50] X. Lai and J. Roychowdhury, "Capturing oscillator injection locking via nonlinear phase-domain macromodels," *IEEE Trans. Microwave Theory & Tech.*, vol. 52, pp. 2251–2261, September 2004.

[51] T. Djurhuus, V. Krozer, J. Vidkjær, and T. Johansen, "A phase macro model of a subharmonic injection locked oscillator with application to phase noise characterization," *IEEE Trans. Circuits & Syst. - I : Fundamental Theory and Applications.* submitted.

[52] T. Djurhuus, V. Krozer, J. Vidkjær, and T. Johansen, "A projection formalism for phase-noise characterization of coupled oscillators," *IEEE Trans. Circuits & Syst. - I : Fundamental Theory and Applications.* to be submitted.

[53] K. Kamogawa, T. Tokumitsu, and M. Aikawa, "Injection-locked oscillator chain: A possible solution to milimeter-wave MMIC synthesizers," *IEEE Trans. Microwave & Tech.*, vol. 45, pp. 1578–1584, September 1997.

[54] K. F. Tsang and C. M. Yuen, "Phase noise measurement of free-running microwave oscillators at 5.8 GHz using 1/3-subharmonic injection locking," *IEEE Microwave and Wireless Components Letters*, vol. 15, pp. 217–219, April 2005.

[55] X. Zhang, X. Zhou, and A. Daryoush, "A study of subharmonic injection locking for local oscillators .," *IEEE Microwave and Guided Wave Letters*, vol. 2, pp. 97 –99, March 1992.

[56] E. Shumakher and G. Eisenstein, "On the noise properties of injection-locked oscillators," *IEEE Trans. Microwave Theory & Tech.*, vol. 52, pp. 1523–1537, May 2004.

[57] B. Razavi, "A study of injection locking and pulling in oscillators," *IEEE J. of Solid State Circuits*, vol. 39, pp. 1415–1424, September 2004.

[58] D. Leeson, "A simple model of feedback oscillator noise," *Proc. IEEE*, vol. 54, pp. 429–430, February 1966.

[59] A. Demir, E. W. Y. Liu, and A. L. Sangiovanni-Vincentelli, "Time-domain non-monte carlo noise simulation for nonlinear dynamic circuits with arbitrary excitations," *IEEE Trans. Computer Aided Design of Intgrated Circuits & Syst.*, vol. 15, pp. 493–505, May 1996.

[60] A. Demir, "Simulation and modeling of phase noise in open-loop oscillators," pp. 453–456, 1996.

[61] T. Djurhuus, "ashm." a small C-program.

[62] T. Endo and S. Mori, "Mode analysis of a multimode ladder oscillator," *IEEE Trans. Circuits and Syst.*, vol. Cas-23, pp. 7–18, February 1976.

[63] T. Endo and S. Mori, "Mode analysis of a ring of a large number of mutully coupled van der Pol oscillators," *IEEE Trans. Circuits & Syst.*, vol. Cas-25, pp. 7–18, January 1978.

[64] J. A. A. Rogge, "Stability of phase locking in a ring of unidirectionally coupled oscillators," *J. of Physics A : Mathematical and General*, vol. 37, 2004.

[65] J. A. A. Rogge, *Dynamic Behavior of Oscillator Networks.* PhD thesis, University of Gent, 2006.

[66] P. Ashwin and G. DangelMayr, "Isochronicity-induced bifurcations in systems of weakly dissipative coupled oscillators," *Dynamics and Stabillity of Systems*, vol. 15, no. 3, pp. 263–286, 2000.

[67] P. van de Ven, J. van der Tang, D. Kasperkovitzt, and A. van Roermundi, "An optimally coupled 5 GHz quadrature LC oscillator," in *2001 Symp. on VLSI Circuits Digest of Tech. Papers.*, pp. 115–118, 2001.

[68] L. Romano, S. Levantino, A. Bonfanti, C. Samori, and A. L. Lacaita, "Phase noise and accuracy in quadrature oscillators," vol. 1, pp. 161–164, ISCAS 2004, 2004.

[69] A. Mazzanti, F. Svelto, and P. Andreani, "On the amplitude and phase errors of quadrature LC-tank CMOS oscillators," *IEEE J. of Solid-State Circuits*, vol. 41, pp. 1305–1313, July 2006.

[70] P. Andreani, A. Bonfanti, L. Romano, and C. Samori, "Analysis and design of a 1.8-GHz CMOS LC quadrature VCO," *IEEE J. Solid State Circuits*, vol. 37, pp. 1737–1747, December 2002.

[71] P. Andreani and X. Wang, "On the phase-noise and phase-error performances of multiphase LC CMOS VCOs," *IEEE J. Solid State Circuits*, vol. 39, pp. 1883–1893, November 2004.

[72] J. Wang, J. Tan, and O. Wing, "Theory of cross-coupled RF oscillator for multi- and quadrature-phase signal generation," in *5th International Conf. on ASIC*, pp. 1014–1017, 2003.

[73] C. Boon, M. Do, K. Yeo, J. Ma, and R. Zhao, "Parasitic-compensated quadrature lc oscillator," in *IEE Proceedings on Circuits, Devices and Systems*, pp. 45–48, 2004.

[74] D. Cordeau, J.-M. Paillot, H. Cam, G. D. Astis, and L. Dascalescu, "A fully monolithic SiGe quadrature voltage controlled oscillator design for GSM/DCS-PCS applications," in *2002 IEEE Radio Frequency Integrated Circuits (RFIC) Symp.*, pp. 455–458, 2002.

[75] P. Vancorenland and M. S. J. Steyaert, "A 1.57GHz fully integrated very low-phase-noise quadrature VCO," in *2001 Symp. on VLSI Circuits Digest of Tech. Papers.*, pp. 111–114, 2001.

[76] P. Vancorenland and M. S. J. Steyaert, "A 1.57GHz fully integrated very low-phase-noise quadrature VCO," *IEEE J. of Solid State Circuits*, vol. 37, pp. 653 –656, May 2002.

[77] S. Hackl, J. Bock, G. Ritzberger, M. Wurzer, and A. L. Scholtz, "A 28-GHz monolithic integrated quadrature oscillator in SiGe technology.," *IEEE J. of Solid-State Circuits*, vol. 38, pp. 135 –137, January 2003.

[78] R. Aparicio and A. Hajimiri, "A noise-shifting differential Colpitts VCO," *IEEE J. Solid State Circuits*, vol. 37, pp. 1728–1736, December 2002.

[79] M. Tiebout, "Low-power low-phase-noise differentially tuned quadrature VCO design in standard CMOS," *IEEE J. of Solid-State Circuits*, vol. 36, no. 7, pp. 1018–1024, 2001.

[80] S. B. Shin, H. C. Choi, and S.-G. Lee, "Source-injection parallel coupled LC-QVCO," *IEEE Electronic Letters*, vol. 41, pp. 1059–1060, July 2003.

[81] B. Chi and B. Shi, "Integrated 2.4GHz CMOS quadrature VCO with symmetrical spiral inductors and differential varactors," in *2002 IEEE Radio Frequency Integrated Circuits Symp.*, pp. 451–454, 2002.

[82] M. A. Chu and D. J. Allstot, "A 6 GHz low-noise quadrature Colpitts VCO," in *Proceedings of the 2004 11th IEEE International Conference on Electronics, Circuits and Systems, 2004. ICECS 2004.*, pp. 21–24, 2004.

[83] D. Leenaerts, C. Dijkmans, and M. Thompson, "A 0.18μm CMOS 2.45 GHz low-power quadrature VCO with 15% tuning range.," in *2002 IEEE Radio Frequency Integrated Circuits Symp.*, pp. 67–70, 2002.

[84] T. Wakimoto and S. Konaka, "A 1.9GHz Si bipolar quadrature VCO with fully-integrated LC tank," *1998 Symp. on VLSI Circuits Digest of Tech. Papers*, pp. 30–31, 1998.

[85] F. Behbahani, Y. Kishigami, J. Leete, and A. A. Abidi, "Cmos mixers and polyphase filters for large image rejection," *IEEE J. of Solid-State Circuits*, vol. 36, pp. 873–887, June 2001.

[86] M. S. J. Steyaert, B. D. Muer, P. Leroux, M. Borremans, and K. Mertens, "Low-voltage low-power CMOS-RF transceiver design," *IEEE Trans. Microwave Theory Tech.*, vol. 50, pp. 281–287, January 2002.

[87] S. J. Fang, A. Bellaouar, S. T. Lee, and D. J. Allstot, "An image-rejection down-converter for low-if receivers," *IEEE Trans. Microwave & Tech.*, vol. 53, pp. 478–487, February 2005.

[88] A. Mazzanti, P. Uggetti, and F. Svelto, "Analysis and design of injection-locked lc dividers for quadrature generation," *IEEE J. of Solid-State Circuits*, vol. 39, pp. 1425–1433, September 2004.

[89] A. Bonfanti, A. Tedesco, C. Samori, and A. L. Lacaita, "A 15-GHz broad-band $\div$ 2 frequency divider in 0.13-μm CMOS for quadrature generation," *IEEE Microwave & Wireless Components Letters*, vol. 15, pp. 724–726, November 2005.

[90] P. Kinget, R. Melville, D. Long, and V. Gopinathan, "Injection-locking scheme for precision quadrature generation.," *IEEE J. of Solid-State Circuits*, vol. 37, pp. 845–851, July 2002.

[91] S. L. J. Gierkink, S. Levantino, R. C. Frye, C. Samori, and V. Boccuzzi, "A low-phase-noise 5GHz CMOS quadrature VCO using superharmonic coupling," *IEEE J. Solid State Circuits*, vol. 38, pp. 1148–1154, July 2003.

[92] T. M. Hancock and G. M. Rebeiz, "A novel superharmonic coupling topology for quadrature oscillator design at 6 GHz," in *Radio Frequency Integrated Circuits (RFIC) Symp., 2004. Digest of Papers. 2004 IEEE*, pp. 285–288, 2004.

[93] L. Dussopt and J.-M. Laheurte, "Coupled oscillator array generating circular polarization," *IEEE Microwave and Guided Wave Letters*, vol. 9, pp. 160–162, April 1999.

[94] J. Vidkjaer, "RF-circuits." Class Notes for the Course : RF-Communication, 2000.

[95] G. H. Golub and C. F. van Loan, *Matrix Computations*. The John Hopkins University Press, 1989.

[96] C. Samori, A. L. Lacaita, F. Villa, and F. Zappa, "Spectrum folding and phase noise in LC tuned oscillators," *IEEE Transactions on Circuits & Syst. II: Analog and Digital Signal Processing*, vol. 45, pp. 781–790, July 1998.

[97] A. B. Carlson, *Communication Systems*. McGraw-Hill, 3 ed., 1986.

[98] T. Djurhuus, V. Krozer, J. Vidkjær, and T. Johansen, "A new definition of single and coupled oscillator Q based on normal form state equations," *IEEE Trans. Circuits & Syst. - I : Fundamental Theory and Applications*. to be submitted.

[99] G. V. Klimovitch, "Optimization of tunable oscillators with AM to FM conversion for near carrier phase noise," pp. 207–210, RAWCON 2000, 2000.

[100] A. Takaoka and K. Ura, "Noise analysis of nonlinear feedback oscillator with AM-PM conversion coefficient," *IEEE Trans. Microwave Theory & Tech.*, vol. MTT-28, pp. 654–662, June 1980.

[101] T. Djurhuus, V. Krozer, J. Vidkjær, and T. Johansen, "Nonlinear analysis of a cross-coupled quadrature harmonic oscillator," in *Intern. Workshop on NonLinear Microwaves and Millimetre waves INMMIC, Roma, Italy*, 2004.

[102] J. Vidkjaer, "Linear, active two-ports noise and distortion." Class Notes for the Course : RF-Communication, 2000.